UNIVERSITAT DE BARCELONA

Identification and Preclinical Evaluation of Asenapine Maleate as a Direct Survivin Inhibitor for Lung Cancer Therapy and Sensitization to Proapoptotic Treatments

Cristina Benítez García

Identification and Preclinical Evaluation of Asenapine Maleate as a Direct Survivin Inhibitor for Lung Cancer Therapy and Sensitization to Proapoptotic Treatments

Doctoral thesis dissertation presented by Cristina Benítez García to apply for the degree of doctor at the University of Barcelona.

Director and tutor: Vanessa Soto Cerrato[a, b]

[a] Department of Pathology and Experimental Therapeutics, Faculty of Medicine and Health Sciences, Universitat de Barcelona, Barcelona, Spain.

[b] Molecular Signaling, Oncobell Program, Institut d'Investigació Biomèdica de Bellvitge (IDIBELL), L'Hospitalet de Llobregat, Spain.

Doctoral Program in Medicine and Translational Research.

School of Medicine and Health Sciences. University of Barcelona.

December 2024.

1 ACKNOWLEDGMENTS

Ahora que se acerca el final de mi etapa predoctoral, me gustaría dar las gracias a todas las personas que han formado parte de ella y sin las cuales esta tesis no habría sido posible.

En primer lugar, quisiera expresar mi más sincero agradecimiento a la Dra. Vanessa Soto Cerrato, investigadora principal del laboratorio de Biología Celular del Cáncer y directora de esta tesis, por haberme guiado a lo largo de todo este proceso. Su enfoque perfeccionista, su dedicación, su pragmatismo y su rigor científico han sido toda una inspiración para mí. Además de sus cualidades como investigadora, Vanessa es consciente de la importancia de fomentar un ambiente de trabajo positivo, lo cual se refleja en el gran valor, tanto profesional como personal, del equipo que lidera. Por todas estas razones, estoy convencida de que no podría haber contado con una mejor directora de tesis.

En segundo lugar, me gustaría agradecer al Dr. Ricardo Pérez Tomás, investigador principal del grupo de Biología Celular del Cáncer, todo su apoyo y confianza. De Ricardo quisiera destacar sus habilidades como docente, ya que el entusiasmo con el que nos hablaba a mis compañeras de universidad y a mí sobre biología celular contribuyó a que yo quisiera investigar el cáncer. Además, le estoy muy agradecida de que me haya dejado formar parte de este grupo de investigación.

También me gustaría darle las gracias a David Martínez García. Aunque solo hemos coincidido un par de veces, él fue quien empezó este proyecto, asentando las bases para que yo pudiera continuarlo. Gracias también a Ignasi Modolell Farré y Miriam Núñez Fernández por darnos acceso al equipo de radioterapia y ayudarnos con el diseño de los experimentos, y a Tyler Jacks y Laura Soucek por el modelo de ratón transgénico KRasG12D. También me gustaría agradecer a todo el equipo de servicios científico-técnicos de Bellvitge por su ayuda.

Sin duda, lo que realmente ha hecho tan especial esta etapa de mi vida, ha sido la gente que me ha acompañado a lo largo de esta aventura. Cuando entré en el laboratorio, empecé aprendiendo de Marta, a la que le tengo que agradecer la paciencia y todo lo

que aprendí de procedimientos con animales, incluidos la humanidad y el respeto con los que se han de tratar.

De mi compañero y amigo Alain, todo lo que pueda decir se queda corto. Empezamos este viaje prácticamente a la vez y para mí has sido un apoyo incondicional, tanto a nivel profesional como personal. Gracias por animarme a hacer las cosas que no me atrevía y que me han permitido crecer. Ojalá algún día vuelvas para quedarte y podamos tenerte cerca, te echamos mucho de menos.

Pere, podría decir muchas cosas sobre ti, pero creo que el resumen es que eres muy buena persona. Parece poco porque se suele decir muy a la ligera, pero es que eres buena persona de verdad, la mejor persona que conozco; el desinterés con el que ayudas a la gente, la sensibilidad, el cariño. Además, es inspiradora la ilusión con la que vives tu trabajo. Me alegro mucho de haberte conocido, Júlia va a tener unos padres increíbles.

Ana, mi sucesora en el lab y experta en cultura pop. En tus manos queda la organización de todos los eventos. No se me ocurre nadie mejor para heredar el puesto: responsable, sensata, trabajadora y dedicada 100% a cualquier cosa que haces, ya sea un doctorado o disfrazar a una nevera de muñeco de nieve. Y todo eso sólo como compañera de laboratorio, como amiga eres increíble. Gracias por alegrarme la jornada laboral siendo tan divertida y por seguirme el rollo en todos los planes, y, sobre todo, gracias por todos los consejos y por estar siempre ahí. Te deseo que esta etapa de tu vida la disfrutes tanto como la he disfrutado yo. Aquí me tienes para lo que necesites.

Quiero darle las gracias también a Celia por la energía tan positiva que transmite, y a Laura, que ha sido la última en llegar, pero se ha ganado la simpatía de todas en tiempo récord. Muchas gracias por tus consejos y por ser tan dulce.

También me gustaría dar las gracias a dos personas que formaron parte del laboratorio durante un tiempo. Adri, me lo pasé genial el tiempo que estuviste, habría sido *de locos* que te hubieras podido quedar unos años más, aunque seguro que también estás *espectacular* donde estás. Sea como sea, gracias por los buenos momentos, siempre serás mi *influencer* gastronómico de confianza.

Gracias también a Mar, fue un placer ayudarnos mutuamente con nuestros proyectos (tú con tu TFM y yo con mi tesis). Recuerdo con cariño las conversaciones tan interesantes que teníamos, me hiciste reflexionar mucho.

Aunque no forman parte de mi grupo de investigación, no puedo no mencionar al resto del laboratorio 5101, ya que me han acompañado diariamente a lo largo de esta etapa. Pep, gracias por los ratos que pasábamos debatiendo y por el chisme que hemos compartido, te echamos mucho de menos. Gisele, siempre tan sensata y dispuesta, eres la persona más trabajadora que conozco y te mereces todos los éxitos que vendrán. Marta, otra que también trabaja muchísimo, gracias por toda la energía que aportas al laboratorio, siempre con una sonrisa.

Sole y Alberto, creo que todos los correos que os he enviado han sido pidiéndoos dinero para los regalos de cumpleaños. Gracias por participar en todas las cosas que se me han ocurrido, he estado muy a gusto compartiendo laboratorio con vuestro equipo todos estos años.

Además, quisiera agradecer a Eric, Eva y Emilio su ayuda, tanto en el procesamiento de los tejidos de los experimentos *in vivo* como en el trabajo que hacen diariamente para que todo funcione bien.

No me pueden faltar en los agradecimientos mis compañeras de piso, Ana y Amàlia, que me han tenido ahí, siempre presente con mi ordenador, ocupando la mitad de la mesa del comedor con mis papeles, y que me han ayudado a distraerme cuando estaba más agobiada. Quiero mencionar también a mis amigas Ana, Andrea y Miguel, ya que no sólo me han acompañado desde la distancia en esta aventura, sino también en muchas otras que vinieron antes.

En estos agradecimientos no puede faltar Ivan, que ha sido quien más tiempo ha pasado conmigo en esta última etapa de escritura. Gracias por ayudarme a organizarme cuando estaba más agobiada, por hacerme compañía las noches que tenía que trabajar hasta tarde y por animarme cuando me costaba ver el final. En definitiva, gracias Ivan por el cariño y la paciencia. Por último, gracias también a mis padres y a mi hermana, que me han apoyado en todo lo que he hecho y que me han dado las herramientas y el motivo para seguir trabajando día a día en este proyecto. Esta tesis os la dedico a vosotros,

tomadla como muestra de agradecimiento por todo lo que me habéis dado a lo largo de mi vida.

2 FUNDING

This research has been funded by Universitat de Barcelona – Banco Santander (Grant PREDOCS-UB), Instituto de Salud Carlos III (Grant PI22/00256 and PI18/00441) and co-funded by the European Regional Development Fund ERDF. Additional institutional support was provided by the CERCA Program, Generalitat de Catalunya. This work has also been partially funded by Consejería de Educación de la Junta de Castilla y León.

3 TABLE OF CONTENT

4 ARTICLE

Thesis in classic format with 1 article annexed.

The thesis consists of 3 objectives and 1 article:

Cristina Benítez-García, David Martínez-García, Martin Kotev, Marta Pérez-Hernández, Yvonne Westermaier, Lucía Díaz, Luis Korrodi-Gregório, Pere Fontova, Ana Aurora Torres, Ricardo Pérez-Tomás, María García-Valverde, Roberto Quesada, Robert Soliva, Vanessa Soto-Cerrato. *Identification of the atypical antipsychotic Asenapine as a direct survivin inhibitor with anticancer properties and sensitizing effects to conventional therapies.* Biomedicine & Pharmacotherapy, 2025, 182, 117756.

Impact factor 6.9, Q1

5 ABBREVIATIONS

A

7-AAD	7-Aminoactinomycin
ABC	ATP-binding cassette
ABC	ATP-Binding Cassette
ABCB-1	ATP Binding Cassette Subfamily B Member 1
ACD	Accidental Cell Death
ACSL4	Acyl-CoA Synthetase Long Chain Family Member 4
AICAR	5-Aminoimidazole-4-carboxamide Ribonucleotide
AIF	Apoptosis-inducing Factor
AIFM1	Apoptosis-Inducing Factor M1
AIM2	Absent in Melanoma 2
AKAP149	PKA/A-kinase Anchoring Protein
AKT/PKB	Activating Protein Kinase B
ALDH	Aldehyde Dehydrogenase
ALK	Anaplastic Lymphoma Kinase
ALOX15	Arachidonate 15-Lipoxygenase
ALT	Alanine Aminotransferase
ANXA1	Annexin A1
APAF1	Apoptotic Protease Activating Factor 1
APC	Adenomatous Polyposis Coli
AR	Androgen Receptor
ASR	Age-Standardized Rate
ATCC	American Type Culture Collection
ATM	Ataxia Telangiectasia Mutated
ATP	Adenosine-5’-Triphosphate
ATP7A/B	Copper-transporting ATPase 1/2
AVPI	Alanine-Valine-Proline-Isoleucine

B

Bad	BCL-2 Associated Agonist of Cell Death

BAK	Bcl-2 Antagonist Killer 1
BAX	Bcl-2-associated X protein
BBB	Blood-Brain Barrier
BCA	Bicinchoninic Acid
BCL-2	B-Cell Leukemia/Lymphoma 2 Protein
BCL2A1	BCL2 Related Protein A1
BCL-W	B-Cell Lymphoma-W
BCL-X_L	B-Cell Lymphoma-Extra Large
BER	Base Excision Repair
BGP	β- Glycerolphosphate
BH	BCL-2 homology
Bid	BH3 Interacting Domain Death Agonist
Bim	Bis(indolyl)methanes
BIR	Baculovirus IAP Repeat
BOK	Bcl-2-related Ovarian Killer
BRAF	V-Raf Murine Sarcoma Viral Oncogene Homolog B
BRUCE	Bir-Ubiquitin Conjugating Enzyme
BSA	Bobine Serum Albumin

C

CA9	Carbonic Anhydrase 9
CAF	Cancer-Associated Fibroblast
CALR	Calreticulin
CAM	Chorioallantoic Membrane
CARD	Caspase Recruitment Domain
CARD	Caspase Recruitment Domain
CASP1	Caspase 1
CASP11	Caspase 11
CBP	CREB-binding Protein
CbPt	Carboplatin
CCT	Chaperonin-containing TCP-1
CDDP	Cisplatin

CDE/CHR	Cycle-Dependent Element/ Cell Cycle Genes Homology Region
CDK1	Cyclin-Dependent Kinase 1
CI	Combination Index
c-IAP1	Cellular IAP1
c-IAP2	Cellular IAP2
CIP	Cysteine Protease Inhibition Cocktail Tablet
COX-2	Cyclooxygenase-2
CPC	Chromosomal Passenger Complex
Crm1/Xpo1	Chromosome Region Maintenance 1
CSL	CBF1/Su(H)/Lag1
CT	Computational Tomography
CTC	Circulating Tumor Cell
CTL	Control
CTLA-4	Cytotoxic T-lymphocyte antigen 4
CTR1	Copper transporter 1
CXCL10	CXC-chemokine ligand 10
CYP1A2	Cytochrome P450 Family 1 Subfamily A Member 2

D

DAB	3,3’-Diaminobenzidine
DAI	Z-DNA-Binding Protein 1
DAMP	Damage-Associated Molecular Patterns
DAPI	4’,6-Diamidine-2’-Phenylindole Dihydrochloride
DC	Dendritic Cell
DCLK1	Doublecortin-like kinase 1
DDX5	DEAD-Box Helicase 5
dFdCDP	Gemcitabine Diphosphate
dFdCTP	Gemcitabine Triphosphate
dH_2O	Distilled H_2O
DIABLO	Direct Inhibitor of Apoptosis Protein (IAP)-Binding Protein with Low Pi
DISC	Death-Inducing Signaling Complex

DMEM	Dulbecco's Modified Eagle's Medium
DMSO	Dimethyl Sulfoxide
DNMT1	DNA methyltransferase 1
DR	Death Receptor
DSB	Double-Strand Breaks
DTT	Dithiothreitol

E

EBUS	Endobronchial ultrasound
ECACC	European Collection of Authenticated Cell Cultures
EDC	1-Ethyl-3-(3-Dimethylaminopropyl)-Carbodiimide
EF2	Elongation Factor 2
EGFR	Epidermal Growth Factor Receptor
Egr-1	Early Growth Response 1
ELISA	Enzyme-Linked Immunosorbent Assay
EMT	Epithelial-Mesenchymal Transition
ERCC1	Excision Repair Cross-Complementing 1
ERK	Extracellular Signal-Regulated Kinase
ESCAT	ESMO Scale for Clinical Actionability of Molecular Targets
ESMO	European Society for Medical Oncology
ES-SCLC	Extensive Stage-Small-Cell Lung Cancer
EUS	Endoscopic ultrasound

F

FA	Fraction Affected
FADD	Fas-associated Death Domain
Fas	Death receptor CD96
FasL	Fas ligand
FBS	Fetal Bovine Serum
FDA	Food and Drug Administration
FOXC1	Forkhead box C1 protein
FOXO1	Forkhead Box Protein O1

FOXO3a	Forkhead Box Protein O3a

G

GAPDH	Glyceraldehyde-3-Phosphate Dehydrogenase
Gem	Gemcitabine
GLUT1	Glucose Transporter 1
GPX4	Glutathione Peroxidase 4
GSDMD	Gasdermin D
GSK-3β	Glycogen Synthase Kinase 3 Beta
GTP	Guanosine Triphosphate

H

H3T3	Histone 3 on Thr3
HBS-P	4-(2-hydroxyethyl)-1-Piperazineethanesulfonic Acid (HEPES)-Buffered Saline 0.005% P20
HBXIP	Hepatitis B X-Interacting Protein
HDAC	TRIB1/histone deacetylase
HDAC6	Histone Deacetylase 6
H-E	Hematoxylin-Eosin
HEPES	4-(2-Hydroxyethyl)-1-Piperazineethanesulfonic Acid
HER2	Human Epidermal Growth Factor Receptor 2
hFAM	Ubiquitin Carboxyl-Terminal Hydrolase 9X
HIF-1α	Hypoxia-Inducing Factor 1A
HIV	Human Immunodeficiency Virus
HLA	Human Leukocyte Antigen
HMGB1	High-Mobility Group Box 1
HNSCC	Head And Neck Squamous Cell Carcinoma
HPC	Hematopoietic Progenitor Cells
Hrk	Activator of Apoptosis Harakiri
HRP	Horseradish Peroxidase
hsp	Heat Shock Protein
HTS	High Throughput Screening

HTVS	High-Throughput Virtual Screening
HUVEC	Human Umbilical Vein Endothelial Cell

I

IAP	Inhibitor Of Apoptosis Protein
IC50	Half-Maximal Inhibitory Concentration
ICAD	Inhibitor Of Caspase-Activated Deoxyribonuclease
ICB	Immune Checkpoint Blockers
ICI	Immune-Checkpoint Inhibitor
IFN	Interferon
IgG	Immunoglobulin G
IKBKB	Inhibitor Of Nuclear Factor Kappa B Kinase Subunit B
IKK	Inhibitor of NF-κB Kinase
ILP2	IAP-like protein 2
IMB	IAP Binding Motif
INCENP	Inner Centromere Protein
IR	Irradiation

J

JAK	Janus Kinase

K

K_D	Binding Constant
KEAP1	Kelch-like ECH-associated protein 1
KRAS	Kirsten Rat Sarcoma Viral Oncogene

L

LAC	Latin America and the Caribbean
LAP	Laryngeal Adductor Paralysis
LEF	Lymphoid Enhancer-Binding Factor
LLC	Lewis Lung Carcinoma
LMP	Lysosomal Membrane Permeabilization
LPCAT3	Lysophosphatidylcholine Acyltransferase 3

LPS	Lipopolysaccharide
LRP	Lung Resistance Proteins
LRR	Leucine-Rich Repeat

M

MACC1	Metastasis Associated in Colon Cancer 1
MAPK	Mitogen-Activated Protein Kinase
MAPKK	MAPK Kinase
MAPKKK	MAPK Kinase Kinase
MCBS	Medicare Current Beneficiary Survey
MCL-1	Myeloid Cell Leukemia 1
MDM2	Mouse Double Minute 2 Homolog
MDR	Multi-Drug Resistance
MET	MET proto-oncogene
MGMT	O^6-methylguanine-DNA methyltransferase
MIF	Macrophage Migration Inhibitory Factor
miRNA	micro-RNA
MKK3	Mitogen-activated Protein Kinase Kinase 3
MKK6	Mitogen-activated Protein Kinase Kinase 6
MLC	Myosin Light Chain
ML-IAP	Melanoma IAP
MLKL	Mixed-Lineage Kinase Domain-Like
MOMP	Mitochondrial Outer Membrane Permeabilization
mRNA	Messenger RNA
MRP	Multidrug Resistance Proteins
MTT	3-(4,5-Dimethylthiazol-2-Yl)-2,5-Diphenyltetrazolium Bromide

N

NADPH	Nicotinamide Adenine Dinucleotide Phosphate
NaF	Sodium Fluoride
NAPDH	Nicotinamide Adenine Dinucleotide Phosphate
NaVO4	Sodium Orthovanadate

NCCD	Nomenclature Committee on Cell Death
NEAA	Non-Essential Amino Acids Solution
NFE2L2	NFE2 like bZIP Transcription Factor 2
NF-κB	Nuclear Factor-Kappa B
NHS	N-Hydroxy Succinimide
NIAP	Neuronal IAP
NICD	Notch Intracellular Domain
NLR	Nod-like receptor
NLR	Nod-like Receptor
NMR	Nuclear Magnetic Resonance
Noxa	Oxidase Activator
NSCLC	Non-Small-Cell Lung Cancer
NSG	NOD Scid Gamma
NTRK	Neurotrophic Tyrosine Receptor Kinase

O

OS	Overall Survival

P

P	Phosphate
p70S6K	Ribosomal Protein S6 Kinase Beta-1
Pac	Paclitaxel
PAGE	Polyacrylamide Gel Electrophoresis
PAMP	Pathogen-Associated Molecular Patterns
PARP	Poly [ADP-Ribose] polymerase
PARP	Poly(ADP-Ribose) Polymerase
PBS	Phosphate-Buffered Saline
PCI	Prophylactic Cranial Irradiation
PD-1	Programmed Cell Death Protein 1
PDAC	Pancreatic Ductal Adenocarcinoma
PDB	Protein Data Bank
PD-L1	Programmed Cell Death Ligand 1

PE	Phycoerythrin
PECAM	Platelet Endothelial Cell Adhesion Molecule
PET	Positron Emission Tomography
PFA	Paraformaldehyde
PFS	Progression-Free Survival
PFU	Plaque-Forming Units
PGAM5	Phosphoglycerate Mutase Family Member 5
PI3K	Phosphatidylinositol-4,5-bisphosphate 3-kinase
PIK3CA	Phosphatidylinositol-4,5-biphosphate 3-kinase catalytic subunit alpha
PKA	Protein Kinase A
PLK1	Polo-like Kinase 1
PLOOH	Phospholipid Hydroperoxides
PMN	Polymorphonuclear
PMSF	Phenylmethylsulfonyl Fluoride
PP2A	Protein Phosphatase 2A
PRR	Pattern Recognition Receptors
PS	Performance Status
PS	Phosphatidylserine
PUMA	p53 Upregulated Modulator of Apoptosis
PVDF	Immobilon-P Polyvinylidene Difluoride

R

Ran	Ras-Related Nuclear Protein
RARRES3/RIG1	Retinoic Acid Receptor Responder 3
RAS	Rat Sarcoma
RATS	Robotic-Assisted Thoracoscopic Surgery
Rb	Tumor Suppressor Protein Retinoblastoma
RCD	Regulated Cell Death
RET	RET proto-oncogene
RHOA	Ras Homolog Family Member A
RING	Really Interesting New Gene

RIPK1	Receptor Interacting Serine/Threonine Kinase 1
RIPK3	Receptor-Interacting Serine/Threonine-Protein Kinase 3
RLR	RIG-like Receptor
R_{max}	Maximal Response
ROCK	Rho-Associated Protein Kinase
ROCK-1	Rho-Associated Coiled-Coil Forming Kinase-1
ROS	Reactive Oxygen Species
ROS1	ROS proto-oncogene 1
RT	Room Temperature
RU	Response Units

S

S	Sequential
SASP	Senescence-Associated Secretory Phenotype
SCLC	Small-Cell Lung Cancer
SD	Standard Deviation
SDS	Sodium Dodecyl Sulfate
SEM	Standard Error of The Mean
shRNA	Short Hairpin Rna
SLC7A11	Solute Carrier Family 7 Member 11
SMAC	Second Mitochondrial-Derived Activators of Caspases
SNP	Single Nucleotide Polymorphism
Sp1	Specificity Protein 1
SPR	Surface Plasmon Resonance
SQCLC	Squamous Cell Lung Carcinoma
SSB	Single-Strand Breaks
STAT	Signal Transducer and Activator of Transcription

T

TAM	Tumor-Associated Macrophages
TBS-T	TRIS-Buffered Saline-Tween 20
TCF	T-cell Factor

TGF-β	Transforming Growth Factor Beta
TICAM1	TIR Domain Containing Adaptor Molecule 1
TIGIT	T cell immunoreceptor with immunoglobulin and ITIM domain
TIL	Tumor-Infiltrating Lymphocyte
TKI	Tyrosine-Kinase Inhibitors
TLR	Toll-like receptor
TMEM173/STING	Transmembrane protein 173
TNF	Tumor Necrosis Factor
TNFR1	Tumor Necrosis Receptor
TOP	Topoisomerase
TP53	Tumor Protein 53
TRADD	TNF Receptor 1 Associated-death Domain
TRAF-2	Tumor Necrosis Factor Receptor Associated Factor 2
TRAIL	TNF-Related Apoptosis-inducing Ligand
TRIS	Tris(Hydroxymethyl)Aminomethane
TβRII	TGF-β receptor II

U

Ub	Ubiquitin
UBA	Ubiquitin-Associated Domain
UBC	Ubiquitin Conjugating Domain
Ufd1	Ubiquitin Fusion Degradation Protein 1
UGT1A4	UDP-glucuronosyltransferase 1A4
UICC	Union For International Cancer Control
UTR	Untranslated Regions
UV	Ultraviolet Radiation

V

V	Vehicle
VATS	Video-Assisted Thoracoscopic Surgery
VDAC2	Voltage-Dependent Anion Channel 2
VEGF	Vascular Endothelial Growth Factor

W

WT	Wild Type

X

XAF1	XIAP-associated factor 1
XIAP	X-linked IAP
XPF	Xeroderma Pigmentosum Group C
XRCC1	X-Ray Repair Cross-Complementing Gene 1

6 ABSTRACT

Identification and preclinical evaluation of asenapine maleate as a direct survivin inhibitor for lung cancer therapy and sensitization to proapoptotic treatments

A major challenge in cancer treatment is the ability of cancer cells to evade cell death, a hallmark of cancer that drives both disease progression and treatment resistance. Overexpression of anti-apoptotic proteins, such as survivin, is a pivotal factor in this process, since survivin promotes cell cycle progression and inhibits apoptosis. Its dual role makes survivin a compelling therapeutic target, and numerous strategies aimed at inhibiting its expression or function have shown promise in preclinical and early clinical studies. However, these approaches often fall short as standalone treatments, likely due to incomplete survivin inhibition. Previous investigations in our laboratory were focused on the development of a survivin inhibitor with a different mechanism of action than those evaluated in clinical trials. This led to the identification of asenapine maleate (AM), a known antipsychotic, as a direct inhibitor of survivin that binds to the homodimerization domain. Preliminary studies revealed that AM exhibits potent anticancer activity, positioning it as a promising candidate for further development in cancer therapy.

The aim of this project is the preclinical development of the novel direct survivin inhibitor AM for the treatment of lung cancer, as well as the evaluation of AM in combination with conventional pro-apoptotic therapies to sensitize cancer cells to conventional treatments.

For this purpose, the cytotoxic effects of AM were evaluated in various lung cancer cell lines, 3D lung cancer cell cultures and primary cultures derived from mice. The mechanism of action of AM predicted by computational methods was validated by investigating the impact of AM on survivin homodimers. The effects of AM on the two primary functions of survivin—regulation of cell cycle progression and inhibition of apoptosis—were further analyzed using flow cytometry and Western blotting, providing comprehensive insights into its anticancer potential.

We further explored the potential of combining AM with chemotherapy, radiotherapy and immunotherapy. The interaction between AM and commonly used

chemotherapeutic agents was assessed by analyzing the cytotoxic effects of these combinations by using specialized software. Additionally, the most effective combination was further evaluated for its impact on cell cycle progression and apoptosis, providing deeper insights into its mechanism of action.

The induction of DNA damage following treatment with AM and radiation was analyzed, along with its subsequent cellular effects on apoptosis, cell cycle progression and proliferation. Flow cytometry was employed to examine changes in cell cycle progression and apoptosis, which was further confirmed by Western blot analysis. Additionally, the clonogenic potential of cells after the combined treatment was evaluated, providing a comprehensive assessment of the impact of therapy on long-term cellular survival and behavior.

To determine whether AM could sensitize tumor cells to immunotherapy and thereby enhance the efficacy of immune-based treatments, we investigated whether AM could trigger and enhance a potential adaptive immune response *in vivo* against dying or stressed cells. To evaluate this, the release of specific damage-associated molecular patterns was analyzed, providing insights into the immunomodulatory potential of AM.

The preclinical *in vivo* evaluation of AM, and its combination with cisplatin, was conducted in various mouse models. Safety assessments of AM were carried out in C57BL/6J mice. To evaluate its anticancer efficacy, a subcutaneous tumor model was developed in C57BL/6J mice, where the effects of AM, and its combination with cisplatin, were tested. Additionally, the AM and cisplatin combination was studied in immunodeficient NSG mice, in which human lung cancer cells were inoculated to induce a subcutaneous tumor. Finally, this combination was also tested in KRASG12D transgenic mice, which develops lung cancer following inhalation of Cre recombinase-expressing viruses, providing a genetically relevant model for evaluation.

AM demonstrates cytotoxic activity across a range of human lung cancer cell lines, including lung adenocarcinoma (A549), squamous cell carcinoma (SW900), and small cell lung carcinoma (DMS53), as well as the murine Lewis lung carcinoma cell line (LLC1) and primary lung cancer mouse cultures. Its effectiveness extends to lung adenocarcinoma spheroids, highlighting its potential in more complex cellular models. AM disrupts

survivin homodimerization, destabilizing this key anti-apoptotic protein, and selectively decreases survivin levels in A549 lung adenocarcinoma and U87 MG glioblastoma cells, without affecting XIAP protein, another member of the inhibitor of apoptosis proteins family.

The anticancer effects of AM are driven by cell cycle arrest at the G_0/G_1 phase and the induction of apoptosis. When combined with cisplatin, carboplatin or gemcitabine, AM acts synergistically, sensitizing A549 cells to these chemotherapeutic agents. In particular, AM potentiates cisplatin-induced apoptosis in lung cancer cells. Additionally, pretreatment with AM before irradiation induces senescence-like morphological changes, as well as an increase in the cell cycle blockade induced by irradiation. Furthermore, AM enhances radiation-induced impairment of clonogenic potential in lung adenocarcinoma cells.

In addition, AM induces the release of damage-associated molecular patterns, suggesting it may potentially activate an immune response against tumor cells *in vivo*.

Preclinical studies in mice have shown that AM has a favorable safety profile at doses below 20 mg/kg and impairs tumor growth in mouse models. Furthermore, the combination of AM and cisplatin significantly reduces tumor growth in different syngeneic as well as immunocompromised mouse models, providing strong evidence of its therapeutic potential and paving the way for a potential repositioning of this drug and /or the development of novel analogs.

In conclusion, AM demonstrates significant anticancer potential by selectively targeting survivin, inducing cell cycle arrest and apoptosis, and enhancing the efficacy of chemotherapy and radiotherapy. Its ability to induce the release of damage-associated molecular patterns demonstrates AM potential to promote immune responses, further highlighting its therapeutic promise. Preclinical studies confirm the safety and effectiveness of AM in reducing tumor growth when combined with cisplatin, positioning it as a promising candidate for combination therapies in lung cancer treatment.

Keywords: cancer, apoptosis, survivin, asenapine, chemotherapy.

Identificación y evaluación preclínica del maleato de asenapina como inhibidor directo de survivina para la terapia del cáncer de pulmón y la sensibilización a tratamientos proapoptóticos

Uno de los principales retos en el tratamiento del cáncer es la evasión de la muerte celular por parte de las células cancerosas, que conlleva la progresión de la enfermedad y la posible resistencia al tratamiento. La sobreexpresión de proteínas inhibidoras de la apoptosis como survivina es fundamental en este proceso, ya que survivina promueve la progresión del ciclo celular e inhibe la apoptosis. Su doble función hace de survivina una buena diana terapéutica, y numerosas estrategias dirigidas a inhibir su expresión o función han resultado prometedoras en estudios preclínicos y en los primeros estudios clínicos. Sin embargo, estos enfoques no han sido eficaces como tratamientos independientes, probablemente debido a una inhibición incompleta de survivina. Investigaciones previas en nuestro laboratorio se enfocaron en el desarrollo de un inhibidor de survivina con un mecanismo de acción distinto que los hasta ahora evaluados en ensayos clínicos. Esto condujo a la identificación del maleato de asenapina (AM), un conocido antipsicótico, como inhibidor directo de survivina que se une al dominio de homodimerización. Los estudios preliminares revelaron que AM presenta una potente actividad anticancerosa, lo que lo sitúa como un prometedor candidato para el desarrollo en la terapia del cáncer.

El objetivo de este proyecto es el desarrollo preclínico del novedoso inhibidor directo de survivina AM para el tratamiento del cáncer de pulmón, así como la evaluación de AM en combinación con terapias proapoptóticas convencionales con el objetivo sensibilizar las células cancerosas a estos tratamientos.

Para ello, se evaluaron los efectos citotóxicos de AM en diversas líneas celulares de cáncer de pulmón, cultivos celulares tridimensionales de cáncer de pulmón y cultivos primarios derivados de tumores de ratones. El mecanismo de acción de AM predicho por métodos computacionales se validó evaluando el impacto de AM sobre los homodímeros de survivina. Los efectos de AM sobre las dos funciones principales de survivina -regulación de la progresión del ciclo celular e inhibición de la apoptosis- se analizaron mediante citometría de flujo y Western blot, proporcionando una visión completa de su potencial anticanceroso.

Además, exploramos el potencial de la combinación de AM con quimioterapia, radioterapia e inmunoterapia. La interacción entre AM y los agentes quimioterapéuticos de uso común se evaluó analizando los efectos citotóxicos de estas combinaciones mediante un software especializado. También se evaluó el impacto de la combinación más eficaz en la progresión del ciclo celular y la apoptosis.

Se analizó la inducción de daños en el ADN tras el tratamiento con AM y radiación, como también los consecuentes efectos sobre la apoptosis, la progresión del ciclo celular y la proliferación. La citometría de flujo permitió examinar los cambios en la progresión del ciclo celular y la apoptosis, confirmada esta última mediante la técnica de Western blot. Además, se evaluó el potencial clonogénico de las células tras el tratamiento combinado.

Para determinar si AM podría sensibilizar las células tumorales a la inmunoterapia y mejorar así la eficacia de los tratamientos basados en la inmunidad, investigamos si AM podría desencadenar y potenciar una posible respuesta inmune adaptativa *in vivo* contra células apoptóticas o dañadas. Para ello, se analizó la liberación de patrones moleculares asociados a daños.

La evaluación preclínica *in vivo* de AM y su combinación con cisplatino se llevó a cabo en varios modelos de ratón. La seguridad de AM se evaluó en un modelo de ratón C57BL/6J. Para analizar la eficacia de AM y su combinación con cisplatino, se desarrolló un modelo de tumor subcutáneo en ratones C57BL/6J. Además, la combinación se estudió en ratones NSG inmunodeficientes, en los que se inocularon células humanas de cáncer de pulmón para inducir un tumor subcutáneo. Por último, esta combinación también se probó en ratones transgénicos KRASG12D, que desarrollan cáncer de pulmón tras la inhalación de virus que expresan la Cre recombinasa.

AM demuestra actividad citotóxica en varias líneas celulares humanas de cáncer de pulmón, como el adenocarcinoma de pulmón (A549), el carcinoma de células escamosas (SW900) y el carcinoma pulmonar de células pequeñas (DMS53), así como en la línea celular de carcinoma pulmonar murino de Lewis (LLC1) y en cultivos primarios de cáncer de pulmón en ratones. Su eficacia se extiende a los esferoides de adenocarcinoma de pulmón, lo que pone de relieve su potencial en modelos celulares más complejos.

AM interrumpe la homodimerización de survivina, desestabilizando la proteína e inhibiéndola selectivamente en células de adenocarcinoma de pulmón A549 y de glioblastoma U87 MG, sin afectar a la expresión de XIAP, otro miembro de la familia de las proteínas inhibidoras de la apoptosis.

Los efectos anticancerosos de AM se deben a la detención del ciclo celular en la fase G_0/G_1 y a la inducción de la apoptosis. Cuando se combina con cisplatino, carboplatino o gemcitabina, AM actúa de forma sinérgica, sensibilizando las células A549 a estos agentes quimioterapéuticos. En particular, AM potencia la apoptosis inducida por cisplatino en células de cáncer de pulmón. Además, el pretratamiento con AM antes de la irradiación induce cambios morfológicos similares a los que se dan en el proceso de senescencia, así como un aumento en el bloqueo del ciclo celular inducido por la irradiación. Además, AM potencia la reducción de la capacidad clonogénica inducida por la radiación en células cancerosas.

AM induce la liberación de patrones moleculares asociados a daño, lo que sugiere la potencial capacidad de AM para estimular la respuesta inmunitaria contra el tumor *in vivo*.

Los estudios preclínicos en ratones han demostrado que AM tiene un perfil de seguridad favorable en dosis inferiores a 20 mg/kg y reduce el crecimiento tumoral en modelos de ratón. Además, AM combinado con cisplatino reduce significativamente el crecimiento tumoral en modelos de ratón.

En conclusión, AM demuestra un importante potencial anticanceroso al dirigirse selectivamente contra survivina, inducir la detención del ciclo celular y la apoptosis, y aumentar la eficacia de la quimioterapia y la radioterapia. Su capacidad para inducir la liberación de patrones moleculares asociados al daño demuestra el potencial de AM para promover respuestas inmunes, destacando aún más su promesa terapéutica. Los estudios preclínicos confirman la seguridad y eficacia de AM en la reducción del crecimiento tumoral cuando se combina con cisplatino, lo que lo sitúa como un candidato prometedor para las terapias combinadas en el tratamiento del cáncer de pulmón.

Palabras clave: cáncer, apoptosis, survivina, asenapina, quimioterapia.

Identificació i avaluació preclínica de l'asenapina maleat com a inhibidor directe de survivina per al tractament del càncer de pulmó i la sensibilització a tractaments proapoptòtics

Un dels principals reptes en el tractament del càncer és l'evitació de la mort cel·lular per part de les cèl·lules canceroses, fet que comporta la progressió de la malaltia i una possible resistència al tractament. La sobreexpressió de proteïnes inhibidores de l'apoptosi com la survivina és fonamental en aquest procés, ja que la survivina promou la progressió del cicle cel·lular i inhibeix l'apoptosi. La seva doble funció fa de la survivina una bona diana terapèutica, i nombroses estratègies dirigides a inhibir-ne l'expressió o la funció han resultat prometedores en estudis preclínics i en els primers estudis clínics. No obstant això, aquests enfocaments no han estat eficaços com a tractaments independents, probablement a causa d'una inhibició incompleta de la survivina.

Investigacions prèvies en el nostre laboratori es van centrar en el desenvolupament d'un inhibidor de la survivina amb un mecanisme d'acció diferent dels fins ara avaluats en assajos clínics. Això va conduir a la identificació de l'asenapina maleat (AM), un conegut antipsicòtic, com un inhibidor directe de la survivina que actua sobre el domini d'homodimerització. Els estudis preliminars van revelar que AM presenta una potent activitat anticancerosa, fet que el situa com un candidat prometedor per al desenvolupament en la teràpia del càncer.

L'objectiu d'aquest projecte és el desenvolupament preclínic del nou inhibidor directe de la survivina, AM, per al tractament del càncer de pulmó, així com l'avaluació de AM en combinació amb teràpies proapoptòtiques convencionals amb l'objectiu de sensibilitzar les cèl·lules canceroses a aquests tractaments.

Es van avaluar els efectes citotòxics de AM en diverses línies cel·lulars de càncer de pulmó, cultius cel·lulars tridimensionals de càncer de pulmó i cultius primaris derivats de tumors de ratolins. El mecanisme d'acció d'AM predit mitjançant mètodes computacionals es va validar avaluant l'impacte d'AM sobre els homodímers de la survivina. Els efectes d'AM sobre les dues funcions principals de la survivina —la regulació de la progressió del cicle cel·lular i la inhibició de l'apoptosi— es van analitzar mitjançant citometria de flux i Western blot, proporcionant una visió completa del seu potencial anticancerós.

A més, vam explorar el potencial de la combinació d'AM amb quimioteràpia, radioteràpia i immunoteràpia. La interacció entre AM i els agents quimioterapèutics d'ús comú es va avaluar analitzant els efectes citotòxics d'aquestes combinacions mitjançant un programari especialitzat. També es va avaluar l'impacte de la combinació més eficaç en la progressió del cicle cel·lular i l'apoptosi.

Es va analitzar la inducció de danys a l'ADN després del tractament amb AM i radiació, així com els conseqüents efectes sobre l'apoptosi, la progressió del cicle cel·lular i la proliferació. La citometria de flux va permetre examinar els canvis en la progressió del cicle cel·lular i l'apoptosi, confirmada aquesta última mitjançant la tècnica de Western blot. A més, es va avaluar el potencial clonogènic de les cèl·lules després del tractament combinat.

Per determinar si AM podria sensibilitzar les cèl·lules tumorals a la immunoteràpia i millorar així l'eficàcia dels tractaments basats en la immunitat, vam investigar si AM podria desencadenar i potenciar una possible resposta immune adaptativa *in vivo* contra cèl·lules apoptòtiques o danyades. Per a això, es va analitzar l'alliberament de patrons moleculars associats a danys.

L'avaluació preclínica *in vivo* d'AM i la seva combinació amb cisplatí es va dur a terme en diversos models de ratolí. La seguretat d'AM es va avaluar en un model de ratolí C57BL/6J. Per analitzar l'eficàcia d'AM i la seva combinació amb cisplatí, es va desenvolupar un model de tumor subcutani en ratolins C57BL/6J. A més, la combinació es va estudiar en ratolins NSG immunodeficients, als quals es van inocular cèl·lules humanes de càncer de pulmó per induir un tumor subcutani. Finalment, aquesta combinació també es va provar en ratolins transgènics KRASG12D, que desenvolupen càncer de pulmó després de la inhalació de virus que expressen la Cre recombinasa.

AM demostra activitat citotòxica en diverses línies cel·lulars humanes de càncer de pulmó, com l'adenocarcinoma de pulmó (A549), el carcinoma de cèl·lules escatoses (SW900) i el carcinoma pulmonar de cèl·lules petites (DMS53), així com en la línia cel·lular de carcinoma pulmonar murí de Lewis (LLC1) i en cultius primaris de ratolí. La seva eficàcia s'estén als esferoides d'adenocarcinoma de pulmó, fet que posa de manifest el seu potencial en models cel·lulars més complexos.

AM interromp la homodimerització de la survivina, desestabilitzant la proteïna i inhibint-la selectivament en cèl·lules d'adenocarcinoma de pulmó A549 i de glioblastoma U87 MG, sense afectar l'expressió de XIAP, un altre membre de la família de proteïnes inhibidores de l'apoptosi.

Els efectes anticancerosos de AM es deuen a la detenció del cicle cel·lular en la fase G0/G1 i a la inducció de l'apoptosi. Quan es combina amb cisplatí, carboplatí o gemcitabina, AM actua de manera sinèrgica, sensibilitzant les cèl·lules A549 a aquests agents quimioterapèutics. En particular, AM potencia l'apoptosi induïda per cisplatí en cèl·lules de càncer de pulmó. A més, el pretractament amb AM abans de la irradiació indueix canvis morfològics similars als que es donen en el procés de senescència. Així mateix, AM potencia la reducció de la capacitat clonogènica induïda per la radiació en cèl·lules canceroses.

AM augmenta l'alliberament de patrons moleculars associats a danys, fet que pot suggerir una potencial capacitat de AM per estimular la resposta immunitària contra el tumor *in vivo*.

Els estudis preclínics en ratolins han demostrat que AM té un perfil de seguretat favorable en dosis inferiors a 20 mg/kg. A més, AM combinat amb cisplatí redueix significativament el creixement tumoral en models de ratolí.

En conclusió, AM demostra un important potencial anticancerós dirigint-se selectivament contra la survivina, induint la detenció del cicle cel·lular i l'apoptosi, i augmentant l'eficàcia de la quimioteràpia i la radioteràpia. La seva capacitat per induir l'alliberament de patrons moleculars associats a danys demostra el potencial d'AM per promoure respostes immunitàries, destacant encara més la seva promesa terapèutica. Els estudis preclínics confirmen la seguretat i eficàcia de AM en la reducció del creixement tumoral quan es combina amb cisplatí, fet que el situa com un candidat prometedor per a les teràpies combinades en el tractament del càncer de pulmó.

Paraules clau: càncer, apoptosi, survivina, asenapina, quimioteràpia.

7 INTRODUCTION

7.1 Cancer

7.1.1 Definition and carcinogenesis

Cancer is a disease in which cells of an organism grow uncontrollably and spread to other parts of the body, a process known as metastasis. Cancers are usually named according to the organ or tissue where they were formed (e.g., lung cancer starts in the lung). Moreover, depending on which specific type of cell gives rise to cancer, we can distinguish multiple types of cancer. The most common is carcinoma, a cancer formed by epithelial cells. We can find different types of carcinoma depending on the epithelial cell type: adenocarcinoma (formed by epithelial cells that produce mucus or fluids), basal cell carcinoma (originated on the basal layer of the epidermis), squamous cell carcinoma (originated in epithelial cells just beneath the outer surface of the skin as well as in the stomach, intestines, lungs, bladder and kidneys) and transitional cell carcinoma (originated in transitional epithelium: in the linings of bladder, ureters and kidneys mostly). Those cancers originating in bones and soft tissues (muscle, fat, blood vessels and fibrous tissue) are called sarcomas. When cancer originates in bone marrow, it is called leukemia. Lymphoma is a cancer that begins in lymphocytes, while if it originates in plasma cells (another type of immune cells), it is named multiple myeloma. Melanoma begins in the precursors of melanocytes. Finally, in the case of brain and spinal cord tumors, the cancer name is based on the type of cell in which they are formed (e.g. astrocytic tumors)(1).

There are different theories about how cancer arises (Figure 1). The first theory, named **Somatic Mutation Theory,** explains that proliferating cells, without necessitating external stimulus, acquire factors (now believed to be DNA mutations) during life (2), which lead to uncontrolled proliferation and cancer. The major risk factor is age. Hence, the larger the age, the higher the number of mutations. However, age dependency is not true for all cancers and not all carcinogens damage DNA (3). Later, the **Tissue Organization Field Theory** was proposed, which states that carcinogens target the entire tissue, altering communication between the parenchyma and the mesenchyme or stroma. Then, tissue loses restraints on proliferation and motility, which results in the

induction of metaplasia, dysplasia and carcinoma (4). Another hypothesis is the **Bad Luck Theory**, in which random mistakes in DNA replication of stem cells (named R-mutations) generate mutant clones that propagate and lead to cancer. Apart from the R-mutations, there are also heritable (H-mutations) and others caused by environmental carcinogens (E-mutations) (5). However, there are variables not contemplated in this theory (temporal and geographical variations) that affect cancer risk. Moreover, it does not consider cell intrinsic (epigenetic states) and extrinsic (immune microenvironment) factors that also affect cancer susceptibility and that are independent of cell division. In fact, many carcinogens are not mutagenic (3). Finally, the **Ground State Theory** unites elements from the previous theories. It is based on the fact that every cell in the body has arisen from a single zygote. Hence, the cells of the body are clones. Physiological genomic changes depend on the organ system, for example, rearrangement and mutation of immunoglobulins in lymphocytes. However, the huge variability among cells in humans is due to the epigenome, transcriptome and proteome of the cells. Hence, referring to the genome, there is a "ground state" of a cell. This "ground state" strongly influences how a somatic mutation will affect the cell. This theory suggests that cancer originates from mutations in stem cells in a cancer-susceptible state that depends on age, damage and location in the body. It also suggests that cancer is the result of cell-intrinsic (changes in cell identity, epigenetic changes and DNA mutations) and cell-extrinsic factors (tumor microenvironment, infections and carcinogens) (6,7).

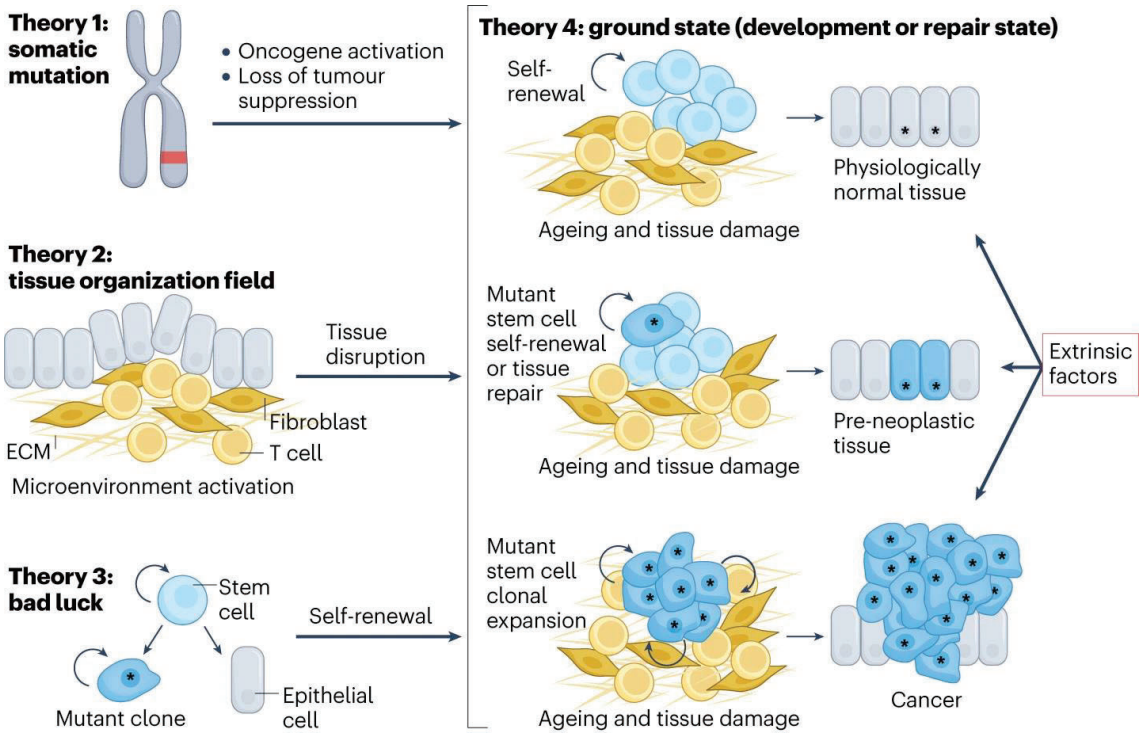

Figure 1. Principal theories of cancer origins. Figure from Jassim et al., 2023 (7).

7.1.2 Hallmarks of cancer

Cancer cells do not have the same characteristics as normal cells. The capabilities that acquire human cells when they transform from a normal to a neoplastic state (specifically capabilities that are essential for malignant tumor formation) are known as the hallmarks of cancer (8) (Figure 2).

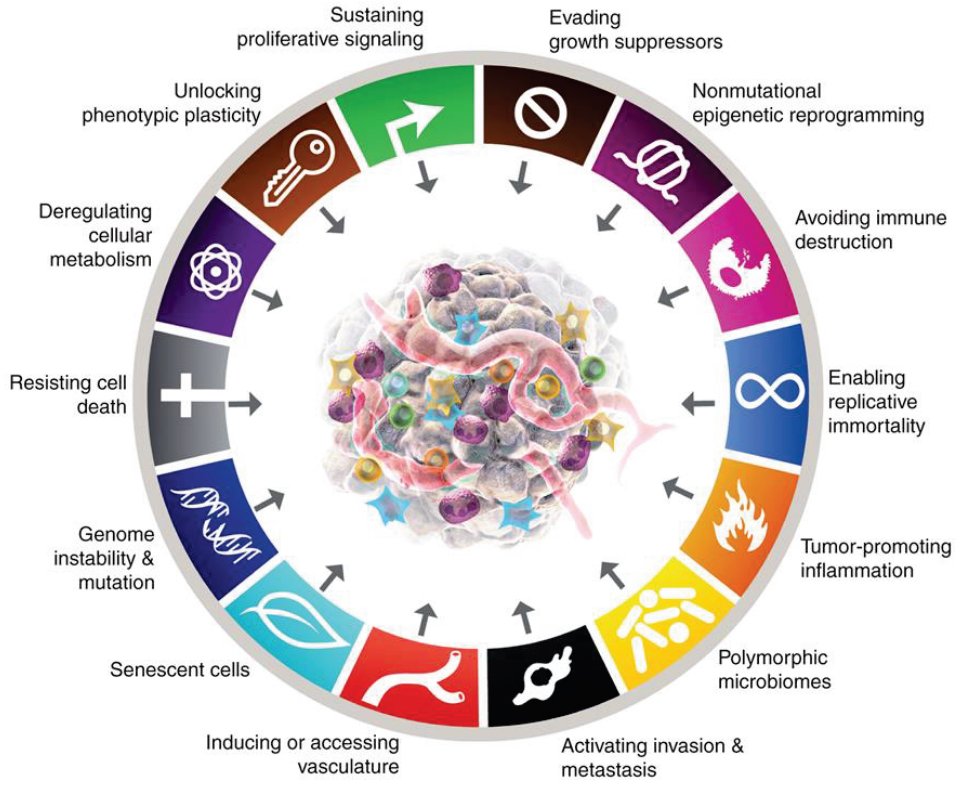

Figure 2. Hallmarks of cancer figure from Hanahan, 2022 (8).

Firstly, cancer cells can **constantly induce and sustain growth stimulatory signals** (by producing growth factors themselves, stimulating normal cells to produce them or maintaining signaling pathways constitutively activated) (9–11) and to **evade growth suppressors** (e.g., by inactivating tumor suppressors, such as RB and TP53 proteins) (12,13). Conversely to normal cells, cancer cell proliferation is not inhibited by contact. One mechanism that can cause this evasion of contact inhibition is the loss of the tumor suppressor gene NF2 in some cells (14).

Another hallmark of cancer cells is the **resistance to cell death**. Apoptosis, a programmed cell death that is considered a barrier to cancer pathogenesis, is attenuated in cancer. The most common mechanism to evade apoptosis is the loss of TP53 tumor suppressor function, a crucial damage sensor that induces apoptosis (13).

Moreover, cancer cells have replicative immortality, which means they have an unlimited number of successive cell divisions. Telomeres are regions of nucleotide repeats that are essential for chromosome protection and genome stability. They shorten progressively with age. Consequently, the cell loses the protection of the ends of chromosomal DNA

from end-to-end fusion, which threatens cell viability. Telomerase counteracts the telomere loss that would occur in its absence. The activity of this enzyme is downregulated during human development. However, telomerase is expressed at significant levels in cancer cells (15). Hence, cancer cells have unlimited proliferation (16).

Another hallmark of cancer is **induction or access to vasculature**. In tumor progression, there is an activation of the "angiogenic switch", in which vasculature that in normal tissue is quiescent, continues to sprout new vessels in tumoral tissues, helping to sustain tumor growth (17).

Invasion and metastasis are multistep processes consisting on local invasion, intravasation of cancer cells into nearby blood and lymphatic vessels, transit of cancer cells through lymphatic and hematogenous systems, escape of cancer cells from vessels to distant tissues (extravasation), formation of nodules of cancer cells (micrometastases) and, finally, growth of micrometastasis into macroscopic tumors (colonization) (18). Cancer cells develop alterations in their shape and in their attachment to other cells and to the extracellular matrix, which makes the cells more capable to invade other tissues and metastasize. A common alteration is the loss of E-cadherin (a cell-to-cell adhesion molecule), which in normal cells helps to assemble cell sheets maintaining cells in a quiescent state. When its expression is reduced, it potentiates invasive phenotypes, although it has been proved that, in some conditions, E-cadherin can function as a survival factor and promoter of metastasis (19). Adhesion molecules associated with cell migration in processes such as embryogenesis or inflammation in normal tissues are often upregulated in tumors. An example is N-cadherin, normally expressed in migrating neurons and mesenchymal cells in organogenesis and upregulated in carcinoma cells (20,21).

Another hallmark of cancer cells is the ability to **reprogram cellular metabolism**. Cancer cells have to adjust their metabolism to obtain enough energy to be constantly proliferating. Cancer cells limit their metabolism mainly to glycolysis even in the presence of oxygen, leading to a state called "aerobic glycolysis". This is called the Warburg effect and is a less efficient method to obtain energy compared to mitochondrial oxidative phosphorylation. To compensate for this lower adenosine-5'-

triphosphate (ATP) production, cancer cells have glucose transporters upregulated, especially Glucose Transporter 1 (GLUT1), which increases glucose import into the cytoplasm. This dependence of cancer cells on glycolysis may be exacerbated by the hypoxic conditions present in many tumors. As a response to hypoxia, there is an upregulation of glucose transporters and enzymes of the glycolytic pathway. This metabolic switch has been also associated with activated oncogenes (e.g. Rat Sarcoma, RAS) and mutated tumor suppressors (e.g. Tumor Protein 53, TP53) (22,23). Some tumors present two subpopulations, one subpopulation is formed by cells that are glucose-dependent (Warburg effect) and secrete lactate. The other population uses lactate produced by the first subpopulation as the main source of energy (24).

Another ability of cancer cells is to **avoid immune detection** and destruction. CD8 T cells are the primary mediators of anticancer immunity. These lymphocytes recognize antigens on tumor cells, become activated and kill tumor cells. However, in tumors, there are inhibitory signals. Then, T cells become dysfunctional, which means the immune system is not able to kill cancer cells (25).

Cancer cells have the capability of **unlocking phenotypic plasticity**. Differentiation is a cellular process that, in normal conditions, occurs in organogenesis. It consists of the transformation of a progenitor cell into a more specialized cell. At the end of this process, cells stop their proliferation. In cancer, though, there is evidence that suggests cancer cells can unlock the capability of phenotypic plasticity to evade the terminal state of cell differentiation and, therefore, overcome the blockade of the proliferation capability (26).

Finally, **senescence** is an irreversible form of proliferative arrest and it helps to maintain tissue homeostasis, producing the inactivation cells that are dysfunctional or unnecessary. Apart from cell cycle arrest, senescence also includes changes in cell morphology and metabolism, as well as the activation of senescence-associated secretory phenotype (SASP) (27). Senescence is induced by multiple conditions, e.g. nutrient deprivation or DNA damage, damage to organelles and cellular infrastructure and imbalance in signaling networks, which are associated with aging. In some contexts, senescent cells stimulate tumor development and malignant progression, since SASP includes pro-inflammatory factors that potentiate proliferation, metastasis and immunosuppression (28).

Apart from the hallmarks of cancer, we can distinguish enabling characteristics, which are consequences of the neoplastic conditions that provide means by which cancer and tumor cells can adopt the hallmarks.

One of these enabling characteristics is **genome instability**. Acquisition of hallmarks depends, in large part, on alterations in the genomes of neoplastic cells. There are mutant genotypes that confer an advantage to subclones of cells by enabling outgrowth and dominance in the tissue, hence orchestrating tumorigenesis. In the process of acquiring these mutations, cancer cells often increase the rates of mutation. This can occur due to an increase in sensitivity to mutagenic agents, disruption of the genome maintenance machinery or both. Moreover, the accumulation of mutations can overtake the capability of the surveillance system of the genome, forcing damaged cells to senescence or apoptosis (29,30). Defects in the DNA-maintenance machinery lead to cancer development (31,32). Another source of genomic instability is the loss of telomeric DNA, which leads to the amplification or loss of segments of chromosomes and karyotypic instability (33).

Another important enabling characteristic is **tumor-associated inflammatory response**, which enhances tumorigenesis and tumor progression, helping to acquire hallmark capabilities. Inflammation supplies bioactive molecules to the tumor microenvironment, such as growth factors (to sustain proliferative signaling), survival factors (to limit cell death), proangiogenic factors, factors that modify extracellular matrix (facilitating angiogenesis and metastasis) and signals that activate epithelial-mesenchymal transition (EMT) (34,35). Moreover, inflammatory cells release chemicals such as reactive oxygen species, which are mutagenic (36).

Non-mutational **epigenetic regulation** of gene expression is an important mechanism in embryonic development, differentiation and organogenesis (37,38). In cancer, abnormal physical properties of the tumor microenvironment can cause changes in the epigenome. Those changes can make cancer cells to obtain the hallmark capabilities that can result in the outgrowth of clonal cancer cells with enhanced capabilities of proliferation.

Finally, a recently described enabling characteristic of cancer is polymorphic microbiomes, since human cancer has been associated with microbiome alterations. The microbiome can exert an effect on cancer development, malignant progression and response to therapy. Microbials may promote cancer at a community level (when the microbiome is altered, named “dysbiosis”) (39), at an individual level (direct interaction of one member of the microbiome) (40) and via secreted or modulated metabolites (41).

Overall, the hallmarks of cancer highlight the complexity of cancer disease and allow us to understand mechanisms of cancer development and malignancy that help us to progress in cancer medicine.

7.1.3 Cancer statistics

Regarding the epidemiology of cancer, in 2022, it was estimated that nearly 19 million people were diagnosed with cancer and almost 10 million died of the disease globally. The annual cancer burden is expected to rise to more than 30 million cases globally in 2050 (42). Hence, we need to find new therapeutic strategies to halt the increase in cancer mortality.

By stratifying the incidence of cancer by organ of origin, we find that lung cancer presented the highest number of new cases in 2022 (12.4% of new cases of cancer in 2022 were lung cancer), followed by breast cancer (11.5%) and colorectum cancer (9.6%). As for mortality, 18.7% of cancer-related deaths are due to lung cancer, followed by colorectum (9.3%) and liver (7.8%) in 2022 (Figure 3).

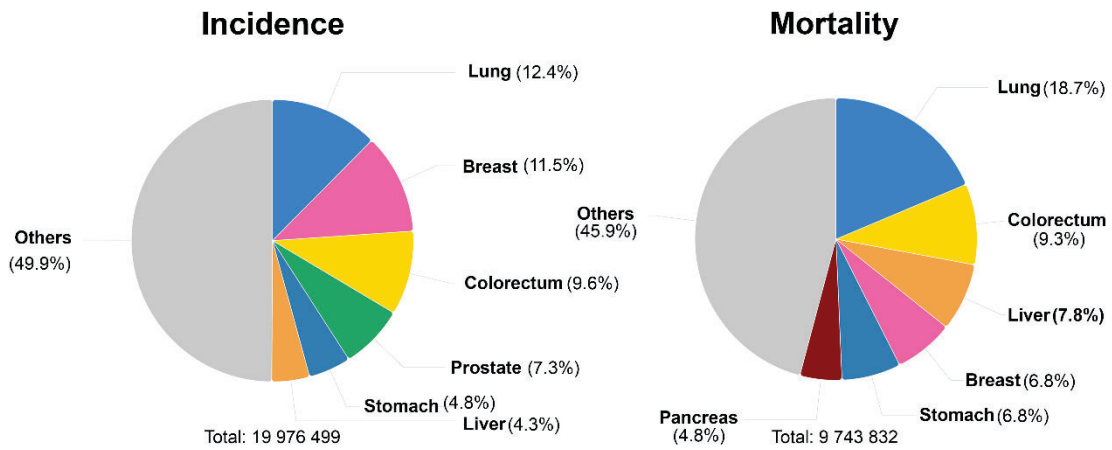

Figure 3. Epidemiology of cancer depending on organ of origin. Estimated number of new cases and estimated number of deaths in 2022, world, both sexes and all ages. Figure from Global Cancer Observatory (42).

In female population, the cancer with the highest incidence and mortality is breast cancer, followed by lung cancer. In male population, though, the cancer with the highest incidence and mortality is lung cancer (42) (Figure 4).

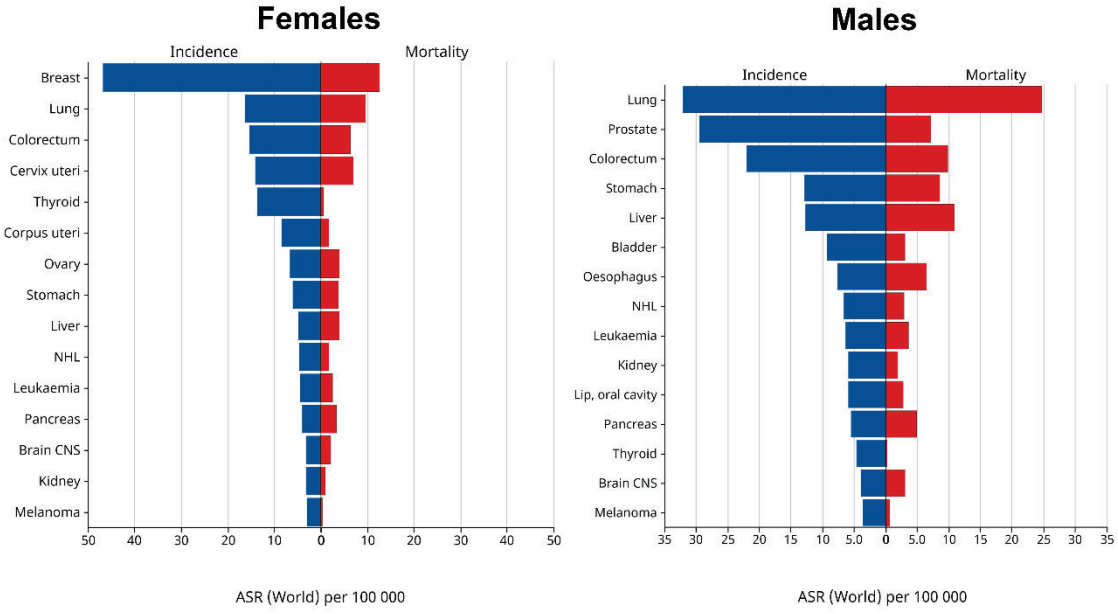

Figure 4. Incidence and mortality of different types of cancer in females and males in 2022, world population. ASR, age-standardized rate. Diagram from Global Cancer Observatory (42).

7.2 Lung cancer

7.2.1 Epidemiology and risk factors

As mentioned before, in 2022, 18.7% of cancer-related deaths were due to lung cancer (42) and it is the type of cancer with the highest incidence (2,480,675 new cases, 12.4%).

The variations in lung cancer incidence and mortality among ages, sexes and regions (Figure 5) can be attributable to differences in tobacco consumption and related population-based policy since tobacco consumption is the main risk factor of lung cancer. 80% of lung cancer mortality is estimated to be due to tobacco consumption. It is considered a high-risk population people who are 50-80 years old, with a minimum smoking history of 20 pack-years (pack-years = number of cigarette packs smoked per day x number of years smoked), currently smoking or have quit in the past 15 years, including healthy and asymptomatic subjects (43). Advances in genomics have allowed the identification of transcriptional signatures in lung cancer patients to define the high-risk population (44).

In the population of 50 years old or older, there is an overall decreasing trend in lung cancer incidence in males. There is, though, an increasing trend in females over the past decade. Delayed incidence and mortality in females may be associated with the later uptake of the smoking habit, since most females started smoking during or after World War II, while males started smoking in the early 20th century, reaching the peak during World War II, in the United States (45). Moreover, females have a much higher number of deaths due to second-hand smoke (46,47).

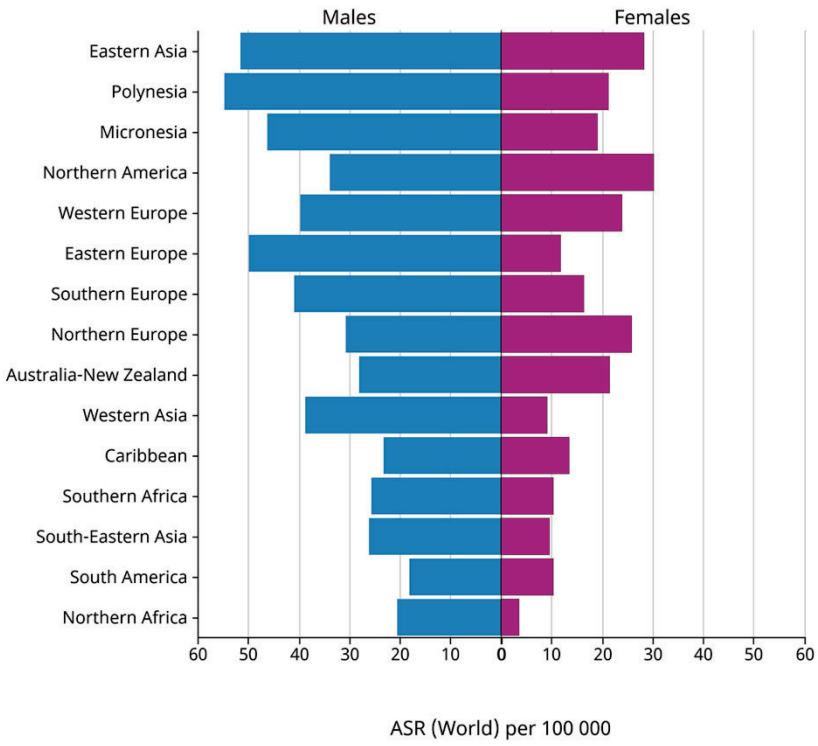

Figure 5. Age-standardized incidence rates of trachea, bronchus and lung cancer, by sex, in United Nations regions. Figure from Global Cancer Observatory (42).

People younger than 50 years had a declining incidence trend in most countries for both sexes. There are also differences in smoking cessation rates. It increased in 1980 and 2010 among young people (16-40) in Europe. In middle-aged and older populations, it only increased in North Europe. One of the reasons for the differences in incidence by age is tobacco control policy; the higher the tobacco control level, the lower the prevalence of smoking in Europe, especially among young adults (48).

In high-income countries, people began smoking earlier than in low- and middle-income countries, so the tobacco epidemic has already peaked in those countries. After that peak, lung cancer incidence and mortality tend to plateau or decrease. In contrast, in low- and middle-income countries it has just peaked or is still increasing, so lung cancer incidence and mortality are more likely to increase (49) (Figure 6).

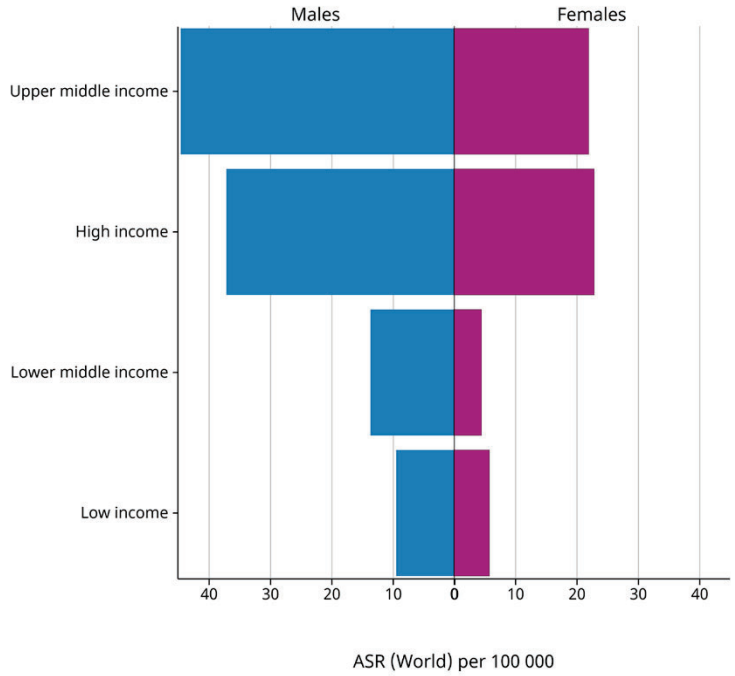

Figure 6. Age-standardized rate per 100000 incidences of trachea, bronchus and lung cancer according to World Bank classification. Diagram from Global Cancer Observatory (42). ASR, age-standardized rate.

It is in Asia where we can find the highest lung cancer incidence and mortality, and it is associated with the human development index, gross domestic products and prevalence of smoking (Figure 7). Other risk factors of lung cancer include exposure to radon, asbestos, chromium, cadmium arsenic, radioactivity and coal products (50).

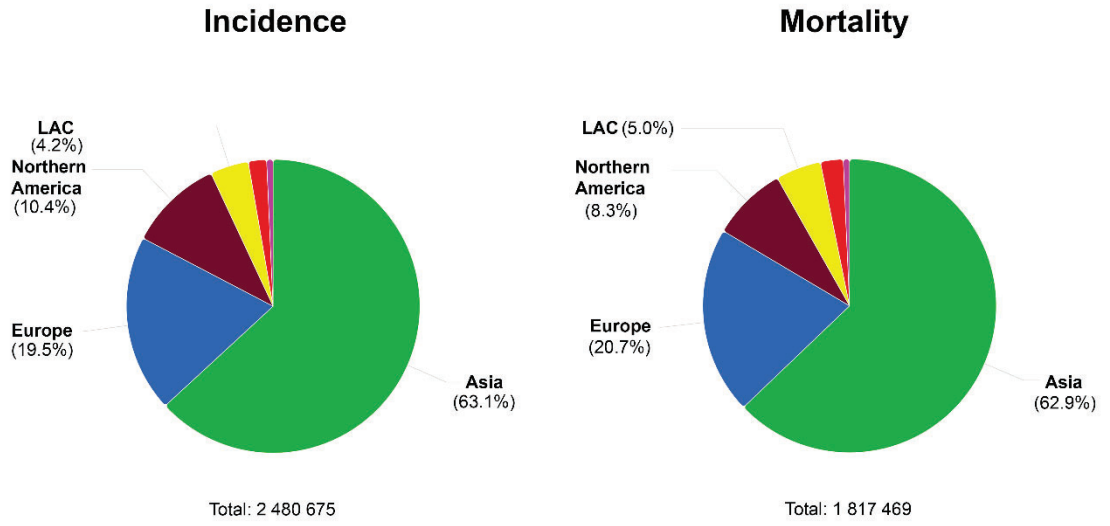

Figure 7. Incidence and mortality of trachea, bronchus and lung cancer by region. LAC, Latin America and the Caribbean. Figure from Global Cancer Observatory (42).

Recent improvements in lung cancer mortality rates are due in part to treatment advances in some high-income countries, such as the United States, the United Kingdom and Australia (51–53). However, mortality rates in lung cancer are still high, and this is mainly due to diagnosis at late stages, hence, cancer may have already spread to other organs, being more difficult to treat (57% of lung cancer cases diagnosed in the United States shows distant metastasis, based on data from 2010-2016) (54). Moreover, 25-75% of patients with resected non-small cell lung cancer (NSCLC) (stages I-III) develop recurrence within 5 years (55).

7.2.2 Diagnosis

The main challenge in lung cancer is that it is diagnosed at an advanced stage, meaning a poor prognosis. More than 75% of patients have stage III or IV disease at diagnosis. This data indicates a lack of effective early detection strategies. Moreover, lung cancer is commonly resistant to standard therapeutic strategies, such as chemotherapy and radiotherapy (RDT). This fact, and the lack of successful treatments for metastasis, result in bad outcomes (56).

The symptoms that can suggest the presence of lung cancer are cough (the most common, present in 50-75% of patients), hemoptysis, chest pain and dyspnea.

In lung cancer diagnosis, it is mandatory to consider medical history and carry out physical examination, as well as assess comorbidity and performance status. Smoking history, complete blood count, liver enzymes, sodium, potassium, calcium, glucose, lactate dehydrogenase (LDH), creatinine and lung function tests are mandatory for correct diagnosis of lung cancer.

The most common diagnostic test for lung cancer is fiber optic bronchoscopy, which is normally accompanied by the evaluation of regional lymph nodes by endobronchial ultrasound (EBUS) and/or endoscopic ultrasound (EUS). Computational tomography (CT) and positron emission tomography (PET) are also essential in the diagnosis of lung cancer since they help to distinguish between limited and extensive stages and have a potential role in adapting target volume for RDT, apart from identifying lymph node involvement and metastasis. However, treatment decisions should be taken after histological confirmation of PET and CT findings. Hence, it is important to obtain enough samples from the tumor to classify the cancer, identify mutations and select the most tailored treatment (57).

Moreover, the diagnosis of lung cancer requires the determination of the TNM stage, where T is the size of the primary tumor (T1-T4), N is the spread of the cancer to the lymph nodes (N0-N3) and M is the presence of metastasis (M0 or M1). When tumor size is <3 cm, it is considered T1. If it is >3 cm, it can be T2a (3-5 cm) or T2b (5-7 cm), and atelectasis or incomplete lung inflation can be seen in part of the lung, as well as invasion of the visceral pleura and the main bronchus more than 2 cm from the lung carina. If the tumor is >7 cm, it is considered T3. In this stage, we find atelectasis to the whole lung, invasion of the phrenic nerve, diaphragm, chest wall, mediastinal pleura and closer approach to the main bronchus (less than 2 cm from the carina). When a tumor invades mediastinal organs, vertebral bodies and lung carina, it is T4. As for lymph node infiltration, no lymph node involvement corresponds to N0. N1 and N2 indicate ipsilateral lymph node involvement (bronchopulmonary/hilar lymph nodes or mediastinal/subcarinal lymph nodes respectively). Contralateral lymph node infiltration is considered N3. Finally, M0 and M1 indicate the absence or presence of metastasis, respectively (58).

7.2.3 Classification

Lung cancer classification is based on morphology, supported by immunohistochemistry and molecular techniques (58,59). The two main groups in which lung cancer is classified are small-cell lung cancer (SCLC) and non-small-cell lung cancer (NSCLC).

SCLC represents 10-15% of all lung cancer and it consists of a mass that arises from the airway submucosa and surrounds the pulmonary hilum. It originates in the neuroendocrine cells of the basal bronchial epithelium. SCLC cells are characterized by their small size and spindle or round shape. They also present poor cytoplasm and granular chromatin. Necrosis is common in this type of tumor. SCLC can be pure or combined with NSCLC. SCLC presents an aggressive clinical course, with rapid tumor growth and early metastatic spread. It may metastasize to the brain, liver and bone.

From a molecular perspective, SCLC is characterized by mutations in tumor suppressor genes, transcriptional addiction and epigenetic dysregulation. It frequently presents biallelic inactivation of TP53 and RB1. Gene amplification of transcription factor MYC is also common (60). We can distinguish two stages of SCLC, limited and extensive. More than two-thirds of patients have extensive stage-small-cell lung cancer (ES-SCLC), which means tumor with distant metastasis or that exceeds an area that can be treated with a radiation field (61). The standard therapy for SCLC is platinum-based chemotherapy and chest RDT. For ES-SCLC, platinum-based chemotherapy plus etoposide is usually used. Therapeutic resistance is a common problem in ES-SCLC treatment. Although the combination of platinum-based chemotherapy and Programmed Cell Death Protein 1 (PD-1) axis inhibitors have improved survival in ES-SCLC, it only occurred in a small number of unidentified patients.

NSCLC can be histologically subclassified into three main histological subtypes adenocarcinoma, large-cell carcinoma and squamous cell carcinoma (Figure 8). Adenocarcinoma is the most prevalent NSCLC, representing 50-60% of total cases. This histological type is frequent in non-smoker females. The tumor presents a glandular pattern (58). Squamous cell carcinoma represents 20-30% of NSCLC cases and large cell carcinoma and other subtypes (such as transitional cell carcinoma, sarcomatoid carcinoma and mixed subtypes) represent 10-20%.

Regarding the molecular characteristics of NSCLC, it may present activating mutations that affect driver genes. In adenocarcinoma, 11% of these mutations alter the function of epidermal growth factor receptor (EGFR), 13% are Kirsten rat sarcoma viral oncogene (KRAS) G12C mutations, 5% mutations are in MET, 3.9% in anaplastic lymphoma kinase (ALK), 1% in human epidermal growth factor receptor 2 (HER2), 1% in V-Raf Murine Sarcoma Viral Oncogene Homolog B (BRAF), 1% in ROS Proto-Oncogene 1 (ROS1) and 1% in ret proto-oncogene (RET). In squamous carcinoma, few driver mutations have been described, being 1% of mutations affecting driver genes located in EGFR (62,63).

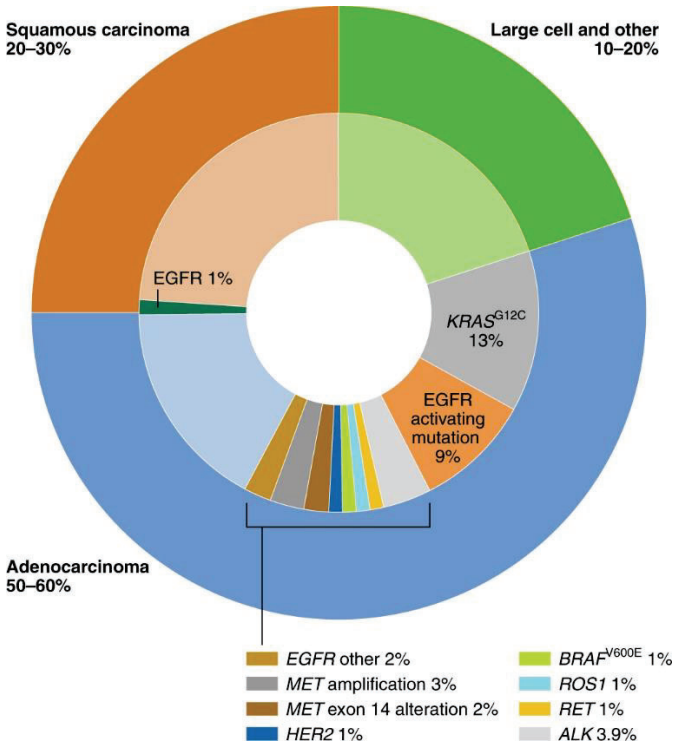

Figure 8. Molecular landscape of NSCLC. EGFR, epidermal growth factor receptor; KRAS, Kirsten rat sarcoma viral oncogene; MET, MET proto-oncogene; HER2, human epidermal growth factor receptor 2; BRAF, V-Raf Murine Sarcoma Viral Oncogene Homolog B; ROS1, ROS proto-oncogene 1; RET, RET proto-oncogene; ALK, anaplastic lymphoma kinase. Figure from Wang et al., 2021 (62).

7.2.4 Treatment options

7.2.4.1 Surgery

Complete surgical resection of the tumor is recommended in local lung cancer cases. Surgical techniques for lung cancer are wedge resection (small non-anatomic fragment of the lung), segmentectomy (resection of a segment of the lung), lobectomy (resection

of a single lobe with regional lymph nodes) and pneumonectomy (removal of the entire lung and lymph nodes). Wedge resection and segmentectomy have the advantage that are typically done via video-assisted thoracoscopic surgery (VATS) or robotic-assisted thoracoscopic surgery (RATS), which are minimally invasive assisted techniques (64). Patients must be diagnosed with high-resolution CT and PET (or combined PET-CT) to discard lymph node infiltration, in which case chemoradiotherapy treatment would be required (65).

7.2.4.2 Radiotherapy

RDT can be used as a curative or palliative strategy in all stages of lung cancer (66). In the case of concurrent chemoradiotherapy, 60-66 Gy in 30-33 daily fractions of 1.8-2.0 Gy is the conventional regime. In the case of preoperative radiotherapy, 40-50 Gy in conventional fractionation (1.8-2.0 Gy per day) or 40-45 Gy in accelerated hyper-fractionation (1.5 Gy twice daily) are sufficient (65).

7.2.4.3 Chemotherapy

Platinum-based cancer therapy is the standard chemotherapy for lung cancer patients (67), cisplatin being the most used in clinics (68). The treatment regimen for concomitant chemotherapy is 2-4 cycles. For perioperative cisplatin-based chemotherapy, 3-4 cycles are recommended, with a total accumulative minimum dose of 300 mg/m^2 of cisplatin (65). In treatment for metastatic lung cancer, the standard of care for patients is 4-6 cycles of platinum doublet (69).

7.2.4.4 Targeted therapy

Inhibitors of EGFR, ALK, RET, BRAF, ROS1, neurotrophic tyrosine receptor kinase (NTRK), MET proto-oncogene (MET) and KRAS, known as tyrosine-kinase inhibitors (TKI), are available for their use in clinics, although less than 25% of patients benefit from targeted therapies and they usually develop resistance (70).

TKI studies show prolonged progression-free survival (PFS), whereas no effect is observed on overall survival (OS), compared to platinum-based therapy (71). Osimertinib, a third-generation TKI, was approved by Food and Drug Administration

(FDA) for first-line treatment in EGFR mutated cases of NSCLC (72). Dacomotib was also approved in the US, but with more adverse effects (73).

Crizotinib showed good results in cases with translocation in ALK and ROS-1 genes, especially in ROS-1 positive NSCLC, as well as ceritinib (2nd generation). Alectinib is FDA-approved for ALK-positive NSCLC. In cases of resistance to alectinib, lorlatinib is an alternative option. Crizotinib is the preferred option in ROS1-positive NSCLC.

7.2.4.5 Immunotherapy

Immunotherapy disrupts the inhibitory signaling between tumor cells and immune cells. In lung cancer, programmed cell death ligand 1 (PD-L1) (on tumor cells) and PD-1 (the receptor of PD-L1, on T cells) interaction inhibits T cell response to the tumor. This interaction can be blocked by immune checkpoint blockers (ICB), which would increase the immune response against the tumor. Immunomodulatory therapy is approved as a secondary-line treatment in advanced lung cancer cases, as well as first-line treatment in patients with high levels of PD-L1 expression (>50%) and absence of oncogenic-driver mutations (74).

In 2017, pembrolizumab, an ICB anti-PD-1, was added to the platinum-based frontline chemotherapy and showed improvement of OS (75,76).

Although there are multiple clinical studies about immunotherapy combinations, most of them show disappointing results. One of the most effective combinations is anti-cytotoxic T-lymphocyte antigen 4 (CTLA-4) (CTLA-4 presents an inhibitory immune function) with anti-PD-L1. However, the addition of anti-CTLA-4 to anti-PD-L1 therapy did not show a meaningful improvement but increased toxicity (77). Another studied combination is anti-T cell immunoreceptor with immunoglobulin and ITIM domain (TIGIT) (TIGIT inhibits immunity through multiple mechanisms) and anti-PD-1. Blockade of both pathways increases CD8 T cells expansion and function. This strategy showed important improvement in tumors with high PD-L1 expression (78).

7.2.5 Clinical management

7.2.5.1 SCLC

As a first-line treatment, the European Society for Medical Oncology recommends a surgical approach for patients with T1-2 N0-1. Before the surgery, it is important to carry out mediastinal node exploration, since it is not indicated if there is mediastinal involvement. Moreover, resection should be followed by chemotherapy and postoperative RDT should be considered for N1 or unforeseen N2 cases. In metastatic SCLC, chemotherapy is the best option as a first-line treatment. In limited-stage patients with good performance status (PS), consider concomitant chemoradiotherapy. In case of brain involvement, it is recommended prophylactic cranial irradiation (PCI) for patients with tumor response. In these cases, though, clinicians should consider the risk of neurocognitive impairment before this treatment in patients ≥65 years old.

There are cases of SCLC in which second-line treatment is required. In the case of resistant disease (with recurrence in less than 90 days of completing therapy), oral or intravenous topotecan treatment is recommended. If the patient never responded to first-line therapy (refractory disease), the recommended treatment is a chemotherapy agent not previously used. In platinum-refractory and resistant patients, outcomes are poor. In these cases, participation in clinical trials or best supportive care is recommended. Patients with symptomatic recurrence in mediastinum that have not been irradiated before can be subjected to thoracic RDT. Finally, in case of recurrence in the brain, radiotherapy may be implemented newly if no systemic therapies are available.

Response to treatment may differ depending on the molecular traits of the tumor. We can distinguish 4 main subtypes of SCLC depending on the differential expression of transcriptional regulators. Those transcriptional regulators are: ASCL1 (subtype SCLC-A), NEUROD1 (subtype SCLC-N) and POU2F2 (subtype SCLC-P). There is another subtype characterized by being triple negative for the three transcriptional regulators (subtype SCLC-I) (79,80).

SCLC relapses can be categorized depending on the response of the tumor to the first-line therapy. It is called sensitive disease when there are ≥90 days of response to platinum-based chemotherapy. It is a resistant disease when there are <90 days of response and refractory disease when the best response is progressive disease (61).

Until June 2020, topotecan was the only second-line treatment for SCLC (81). Nowadays, a common strategy for second-line treatment after a sensitive relapse is retreatment with platinum-based chemotherapy (82). Lurbinectedin is also a common strategy. It binds to guanines in GC-rich areas of gene promoters, impairing transcription in tumor cells and leading to DNA breaks that trigger apoptosis (83).

Other chemotherapeutics for second and further line treatment are irinotecan (84), paclitaxel (85) and temozolomide (86), that have better tolerability than topotecan.

7.2.5.2 NSCLC

7.2.5.2.1 Local NSCLC (Stage I and II)

For stage I and II NSCLC, complete surgical resection is recommended. In cases where surgical intervention is contraindicated, RDT should be used. Lobectomy is the best option for early-stage disease (87,88). However, clinical studies showed good results after wedge resection or segmentectomy in patients with peripheral N0 lung cancer (2 cm or less), especially when it is bronchoalveolar carcinoma (89).

7.2.5.2.2 Locally advanced NSCLC (stage III)

In the case of patients diagnosed with stage I or II but during surgery it is observed N2 disease, adjuvant chemotherapy after surgery is recommended. If NSCLC stage III is diagnosed before the surgical intervention, there are multiple strategies: induction chemotherapy followed by surgery, induction chemoradiotherapy followed by surgery or concurrent chemoradiotherapy. The most appropriate strategy for each patient should be decided by a multimodality team. Finally, if the tumor is non-resectable, concurrent chemoradiotherapy is the best option.

Cisplatin is the optimal chemotherapy for stage III NSCLC. Most clinical studies use cisplatin plus etoposide or cisplatin plus vinca alkaloid for concurrent

chemoradiotherapy. The treatment regimen for concomitant chemotherapy is 2-4 cycles. For perioperative cisplatin-based chemotherapy, 3-4 cycles are recommended, with a total accumulative dose of 300 mg/m2 of cisplatin minimum.

After therapy, it is recommended to follow up with a CT scan (thoracic and upper abdominal), every 6 months for 2 years and, then, yearly for 3 years. In patients with a high risk of brain relapse, it is recommended to follow up the case with imaging methods. Apart from all these clinical measures, the patient is strongly encouraged to quit smoking (65).

7.2.5.2.3 Non-oncogene-addicted metastatic NSCLC

In oligometastatic disease, limited metastatic lesions in one or two organ systems can be treated locally by surgery or radiation in conjunction with the primary tumor. The treatment depends on the systems affected. In the case of brain lesions, surgical resection or stereotactic radiosurgery are the optimal strategies. Adrenal lesions are also resected in patients responding to therapy (90).

In metastatic NSCLC, the standard of care for patients is 4-6 cycles of platinum doublet. The best tolerated combination is pemetrexed + cisplatin. If the patient does not improve after 4 cycles of treatment, it is recommended to continue with the administration of pemetrexed monotherapy.

In cases of advanced or metastatic NSCLC without driver alterations, an immunochemotherapeutic combination is available. With this strategy, 15% of advanced NSCLC patients responded, improving OS for up to 5 years or more (70). However, in metastatic cases of NSCLC, the OS remains less than 3 years (91).

Potential biomarkers that could predict response to immunotherapy are PD-L1 expression (92), presence of tumor-infiltrating lymphocytes (TILs) (93) and tumor mutational burden (if there are more mutations, more different antigens could be presented to the T cells) (94). Hence, tumors with high tumor mutational burden or high PD-L1 expression may respond when treated with single-agent ICB (95).

7.2.5.2.4 Oncogene-addicted metastatic NSCLC

Detection of biomarkers is crucial to identify subgroups of NSCLC, which helps to select the most adequate treatment for patients and achieve better clinical outcomes than traditional chemotherapy (96).

One of the most frequently altered genes in NSCLC is EGFR, especially in women and non-smokers (97). EGFR mutations include substitutions, deletions and insertions in exons 18-21 that activate the tyrosine kinase. The most common alterations are the exon 21 L858R substitution and exon 19 deletion mutations. In these cases, TKIs are available and studies show prolonged PFS with no effect on overall OS, compared to platinum-based therapy (71). Osimertinib, a third-generation TKI, was approved by FDA for first-line treatment (72). Dacomotib was also approved in the US, but with more adverse effects (73). Treatment resistance can appear after 6-12 months of treatment with EGFR TKI due to secondary alterations in EGFR, developed in 40-60% of patients. Concretely, these secondary alterations comprise a large group of exon 20 insertions. Then, treatment is switched to osimertinib, which targets this mutation and the primary ones (98). Other cases of resistance are due to amplification of the MET oncogene as well as amplifications of phosphatidylinositol-4,5-biphosphate 3-kinase catalytic subunit alpha (PIK3CA) and HER-2 (99,100).

Translocation in the ALK gene is also commonly found in NSCLC, as well as ROS1 translocation, BRAF V600 mutation and other alterations in driver oncogenes that are shown in Figure 9, where the most adequate treatments for each case can be seen.

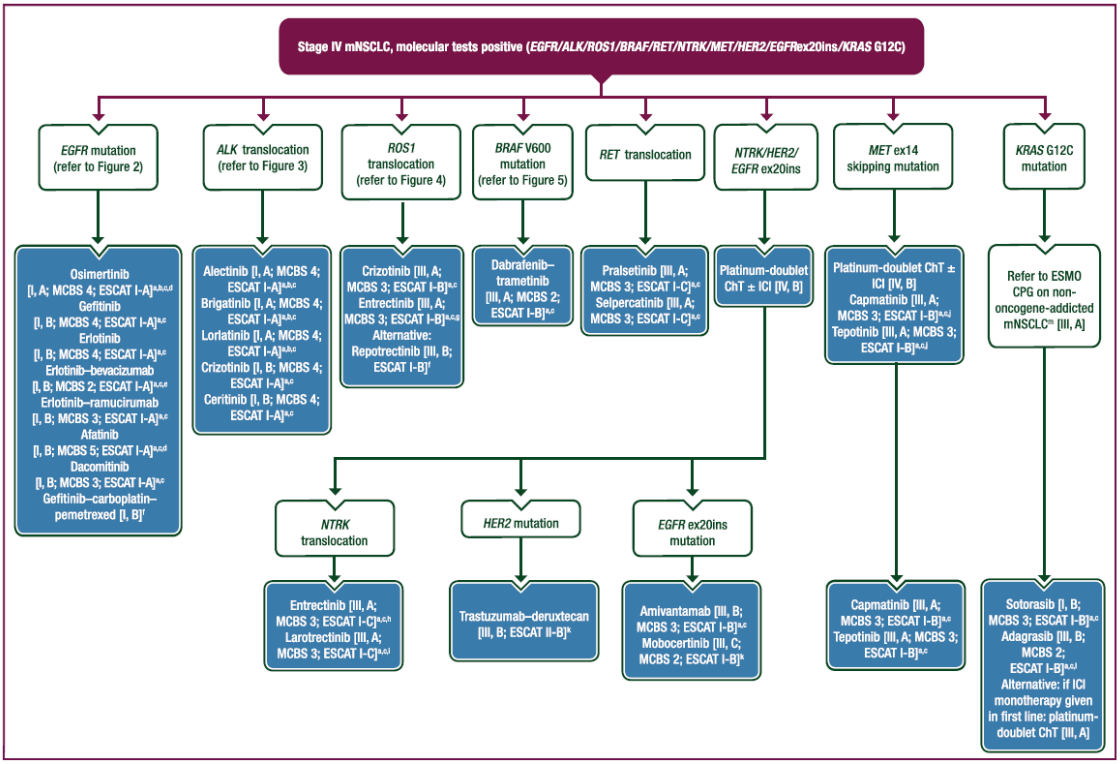

Figure 9. Treatment algorithm for oncogene-addicted metastatic NSCLC. NSCLC, non-small-cell lung cancer; EGFR, epidermal growth factor receptor; ALK, anaplastic lymphoma kinase; ROS1, ROS Proto-Oncogene 1; BRAF, V-Raf Murine Sarcoma Viral Oncogene Homolog B; RET, RET proto-oncogene; NTRK, neurotrophic tyrosine receptor kinase; HER2, human epidermal growth factor receptor 2; MET, MET proto-oncogene; MCBS, Medicare Current Beneficiary Survey; ESCAT, ESMO Scale for Clinical Actionability of molecular Targets; ICI, immune-checkpoint inhibitor. Diagram from European Society for Medical Oncology (ESMO), (101).

7.3 Treatment resistance

Cancer therapy can be considered as a three-component system. There is a **therapy** that targets a **population of cancer cells,** which is in a specific **host environment**. Hence, the clinical response of the patient depends on the pharmacological properties of the therapy, the characteristics of the cancer cells (intrinsic and acquired) and the environmental factors. Treatment resistance is an important obstacle in cancer treatment. Traditionally, resistance mechanisms have been grouped into intrinsic and acquired resistance (Figure 10). In intrinsic resistance, the factors that reduce drug effectiveness are present in cancer cells or tissues itself before the therapy, making it ineffective. Conversely, acquired resistance develops during the treatment of tumors that were initially sensitive to the therapy. It can be caused by mutations that arise during

the treatment or adaptive responses that compensate for the therapeutic effect, e.g. increased expression of the therapeutic target or activation of compensatory signaling pathways. The key determinants of drug resistance include tumor burden, growth kinetics, tumor heterogeneity, physical barriers, immune system and microenvironment, undruggable cancer drivers and the consequences of applying selective therapeutic pressures (102,103).

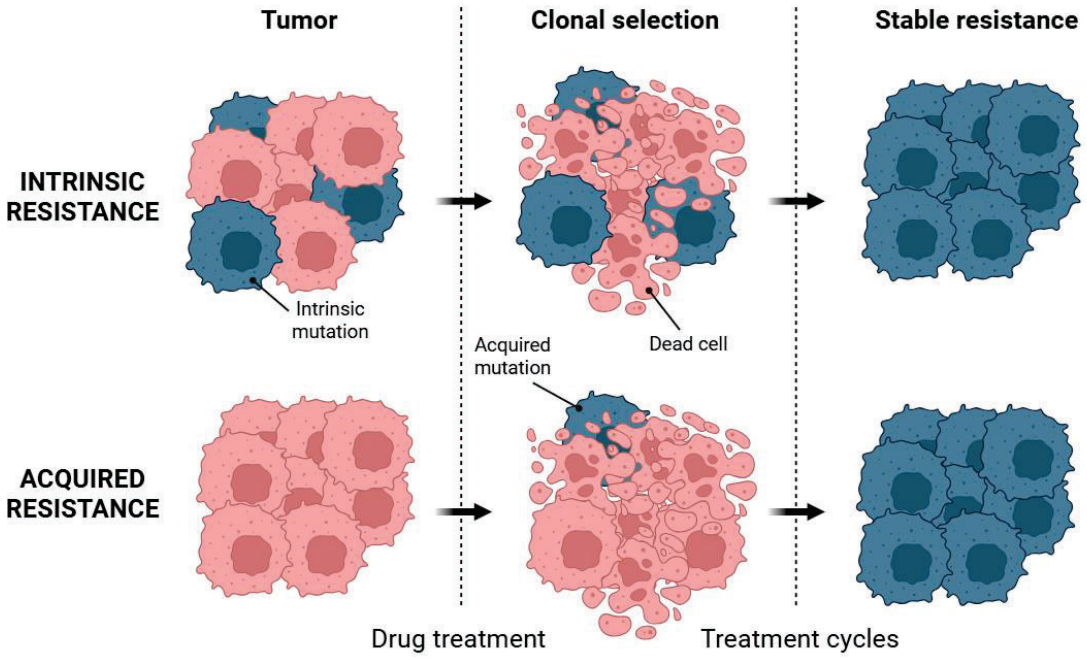

Figure 10. Intrinsic and acquired chemoresistance in cancer. Diagram adapted from Ramos et al., 2021 (104,105). Created in https://BioRender.com.

7.3.1 Major mechanisms of resistance

7.3.1.1 Decrease of drug accumulation inside the cell

Drug concentration in the cell can be reduced by increasing drug efflux or by decreasing drug uptake. The first condition can be produced by overexpression of membrane efflux pumps. ATP-binding cassette (ABC) is a superfamily of efflux pumps, that is, transmembrane proteins capable of regulating the flux of different chemotherapeutic agents across the plasma membrane. An example is the copper-transporting ATPase 1/2 (ATP7A/B) (105), which regulates the efflux of platinum. High expression of ATP7A/B is correlated with poor response to platinum treatment in NSCLC (106). Other transporters

involved in drug resistance are multidrug resistance proteins (MRP) and lung resistance proteins (LRP) (107).

On the other hand, drugs can enter the cells via receptors/transporters, endocytosis or diffusion across the cell membrane (108). Alterations in the receptors or transporters of the drug can reduce the intake of this one. Platinum compounds enter the cells by passive diffusion or transporters. Copper transporter 1 (CTR1) not only controls the acquisition of copper ions respectively but also of platinum-based agents (109). High CTR1 expression is related to longer patient survival, since it means the increase of cisplatin concentration in the cancer cell, while low expression of CTR1 indicates less drug uptake and, hence, worse response to chemotherapy (110).

7.3.1.2 Drug inactivation

In some cases, the drug may not be properly activated or inactivated by certain molecules inside the cell. For example, platinum drugs are inactivated by thiol glutathione (GSH) (111). Irinotecan, a topoisomerase (TOP) I inhibitor, must be activated by carboxylesterase enzymes, since the product SN-38 is the active anticancer metabolite (112).

7.3.1.3 Tumor heterogeneity

Cancer cells acquire genomic alterations, not only age-related mutations but also those produced by genomic instability, which generates genetic diversity in the tumor. Some of the mutations can be resistance mutations and produce a change in tumor phenotype (102).

Intra-tumor heterogeneity includes factors related to disease progression and treatment failure, such as phenotypic diversity (e.g. cell surface markers), epigenetic or genetic abnormality, growth rate or apoptosis.

Another determining factor of intra-tumor heterogeneity is the presence of cancer stem cells (CSC). Lung cancer stem cells (LCSC) can self-renew and differentiate into different cancer cell lines in different circumstances, such as under the effect of platinum, and are a main factor in lung cancer recurrence (113). Multiple molecules such as Forkhead box C1 protein (FOXC1), circular RNAs, TRIB1/histone deacetylase (HDAC), doublecortin-like

kinase 1 (DCLK1), gap junctions and heat shock protein 27 (hsp27) are responsible for CSCs-like properties in lung cancer, generating resistance. Moreover, LCSCs have an increased expression of CD133+/CD44+ and Nanog, Oct-4, SOX-2 and Aldehyde dehydrogenase (ALDH), which are significantly upregulated in platinum-induced resistance (107).

7.3.1.4 Increase in DNA repair

Resistant cells have a stronger DNA repair ability to fix DNA damage induced by drugs. In the case of platinum resistance, the most important pathways are nucleotide excision repair (NER) and base excision repair (BER) pathways. There are multiple proteins involved in NER pathway, among them excision repair cross-complementing 1 (ERCC1)/ xeroderma pigmentosum group C (XPF), an endonuclease that is used as a predictive biomarker of platinum-based treatment. On the other hand, X-ray repair cross-complementing gene 1 (XRCC1)/ metastasis associated in colon cancer 1 (MACC1) is a key component in BER mechanism that induces platinum resistance by activating protein kinase B (AKT) pathway (107).

7.3.1.5 Microenvironment

Hypoxia is a common trait in tumor microenvironment (107). It induces genomic and proteomic changes mainly coordinated by hypoxia induced factor 1 (HIF-1). The response to hypoxia includes regulation of genes involved in glucose metabolism, cell proliferation, angiogenesis, macrophage polarization into tumor-associated macrophages (TAM), apoptosis, DNA damage, metastasis and drug efflux (114,115). In the case of platinum resistance, there are two pathways related to hypoxia. Firstly, hypoxia inhibits cell apoptosis pathway (116,117) and, secondly, it promotes survival signaling pathways such as nuclear factor-kappa B (NF-κB) (117).

EMT refers to the process of trans-differentiation of cells from epithelial to mesenchymal features. It alters cell-cell adhesion and extracellular matrix, leading to invasion of tumor cells (118). Cisplatin treatment induces autophagy, NF-κB, TAMs and ataxia telangiectasia mutated (ATM) activation, which in turn induces EMT, promoting treatment resistance (119).

On the other hand, cancer has multiple mechanisms to evade immune responses. Those mechanisms can lead to the development of resistance to immunotherapy. Firstly, signals induced by tumor and non-tumor cells recruit suppressive immune cells and stroma cells, such as cancer-associated fibroblasts (CAFs). Secondly, inhibition of one immune checkpoint by ICBs can increase the expression of other immune checkpoints, generating acquired resistance. Thirdly, the increased levels of immunosuppressive cells and molecules can reduce tumor sensitivity to immunotherapy. Finally, cancer cells are constantly evolving. They suffer epigenetic and genetic changes that can cause impairment of neoantigen formation, which leads to impairment of recognition of tumor antigens by cytotoxic tumor cells (120).

7.3.1.6 Apoptosis inactivation

Alterations in cell death by apoptosis are often found in tumors. Apart from being responsible for tumor development and progression, they are also responsible for tumor resistance to therapies. The reason is that most anticancer drugs take advantage of the intact apoptotic signaling pathways to trigger cancer cell death. Thus, defects in the death pathways can lead to drug resistance, limiting the efficacy of cancer therapies. Apoptotic pathways can be altered through multiple mechanisms, such as impaired death receptor signaling, impaired p53 function (which is a tumor suppressor gene), unbalance of B-cell leukemia/lymphoma 2 protein (BCL-2) family members (the proteins that regulate apoptosis), overexpression of inhibitor of apoptosis proteins (IAPs) or downregulation of caspases, resulting in reduction of apoptosis or acquisition of treatment resistance (108,121).

7.4 Cell death

Cell death is a crucial physiological process in organisms, having roles during embryonic development, organ maintenance, aging and immune response, among others. It can occur in multiple forms, in response to different kinds of stress. Loss of control of cell death processes can lead to multiple diseases, such as neurodegeneration, autoimmune diseases, infectious diseases and cancer (122). According to the Nomenclature Committee on Cell Death (NCCD), cell death can be divided into two groups: accidental cell death (ACD) and regulated cell death (RCD).

7.4.1 Accidental cell death (ACD)

ACD consists of an uncontrolled process in which the cell spills its contents into the surrounding tissue and it is triggered by an injury that overwhelms control mechanisms.

Necrosis. Necrosis is the most studied ACD and is triggered by an external injury, for example, prolonged hypoxia and inflammation (123). It involves the upregulation of proinflammatory compounds (e.g. NF-κB) that leads to breakage of the cell membrane and leakage of cell content in the surrounding area, causing a cascade of inflammation and tissue damage. It is characterized by being an energy-independent process in which a sudden shock (e.g. heat, irradiation, chemicals, hypoxia) seriously damages the cell and it is not viable anymore.

Oncosis. Oncosis is an ACD mainly induced by the depletion of intracellular ATP that leads to the inactivation of Na+/K+-ATPase, causing the increase of sodium and calcium ions. Some drugs that induce oncosis by increasing cellular reactive oxygen species (ROS) and depleting ATP are aspirin, Kahalalide F and Fluopsin C (124). Oncosis is characterized by swelling of the cell and the organelles, as well as an increase in membrane permeability. In oncosis, there is a depletion of intracellular energy stores and failure of ionic pumps. This kind of cell death produces leakage of cellular debris into surrounding tissues, inducing damage to the surrounding cells, which generates inflammation. Oncosis can lead to oncotic necrosis which is characterized by cellular swelling, karyolysis, vacuolation and lysis (123).

7.4.2 Regulated cell death (RCD)

RCD is a controlled process that involves biochemical and molecular events in order to remove cells in a tissue. The best studied form is apoptosis, which will be extensively explained in the following sections. However, a brief explanation of the key events of other non-apoptotic regulated cell death mechanisms is found below (Figure 11).

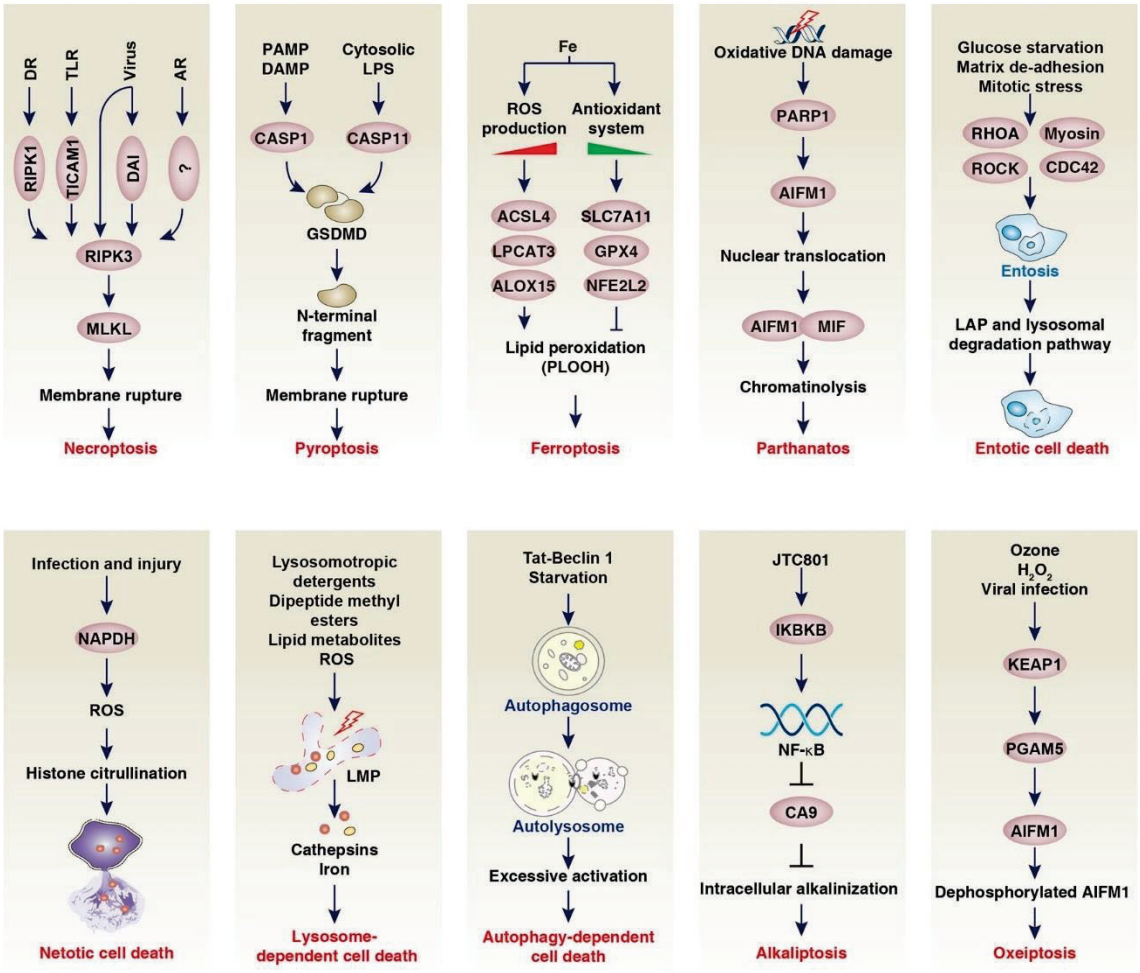

Figure 11. Molecular mechanism of non-apoptotic regulated cell death. DR, death receptor; TLR, toll-like receptor; AR, androgen receptor; RIPK1, receptor interacting serine/threonine kinase 1; TICAM1, TIR domain containing adaptor molecule 1; DAI, Z-DNA-binding protein 1; RIPK3, Receptor-interacting serine/threonine-protein kinase 3; MLKL, mixed-lineage kinase domain-like; PAMP, pathogen-associated molecular patterns; DAMP, damage-associated molecular patterns; LPS, lipopolysaccharide; CASP1, caspase 1; CASP11, caspase 11; GSDMD, gasdermin D; ROS, reactive oxygen species; ACSL4, acyl-CoA synthetase long chain family member 4; LPCAT3, lysophosphatidylcholine acyltransferase 3; ALOX15, arachidonate 15-lipoxygenase; SLC7A11, solute carrier family 7 member 11; GPX4, glutathione peroxidase 4; NFE2L2, NFE2 like bZIP transcription factor 2; PLOOH, phospholipid hydroperoxides; PARP1, poly [ADP-Ribose] polymerase 1; AIFM1, apoptosis-inducing factor M1; MIF, macrophage migration inhibitory factor; RHOA, ras homolog family member A; ROCK, Rho-associated protein kinase; CDC42, cell division cycle 42; LAP, laryngeal adductor paralysis; NAPDH, nicotinamide adenine dinucleotide phosphate; LMP, lysosomal membrane permeabilization; IKBKB, inhibitor of nuclear factor kappa B kinase subunit B; NFκB, nuclear factor-kappa B; CA9, carbonic anhydrase 9; KEAP1, Kelch-like ECH-associated protein 1; PGAM5, phosphoglycerate mutase family member 5. Diagram adapted from Tang et al., 2019 (122).

Necroptosis. Necroptosis occurs following the activation of tumor necrosis receptor (TNFR1) by tumor necrosis factor-α (TNFα). However, there are other receptors that trigger necroptosis: activation of death receptors (e.g. death receptor CD96 (FAS)), toll-like receptors (e.g. toll-like receptor 3 (TLR3) and toll like receptor 4 (TLR4), nucleic acid sensors (Z-DNA binding protein 1, ZBP1), retinoic acid receptor responder 3 (RARRES3, also named RIG1), transmembrane protein 173 (TMEM173, also named STING) and adhesion receptors (122). The main difference with necrosis is that necroptosis follows signal regulation and has characteristics of active energy consumption (125).

Pyroptosis. Pyroptosis is induced by the activation of inflammasome sensors, such as Nod-like receptor (NLR) family, DNA receptor Absent in Melanoma 2 (AIM2) and the Pyrin receptor. The inflammasome sensors detect pathogen-associated molecular patterns (PAMPs) and damage associated molecular patterns (DAMPs) released by microbes or dysregulated pathways (122,125).

Ferroptosis. Ferroptosis is a type of cell death induced by iron-dependent lipid peroxide injury in the mitochondria, as well as by deficiency of activity of glutathione peroxidase 4 (GPX4) (125).

Parthanathos. Parthanatos is a poly [ADP-Ribose] polymerase 1 (PARP)-dependent RCD. It is activated by DNA damage and chromatinolysis induced by oxidative stress (122).

Entosis. Entosis consists in cell cannibalism (one cell kills and engulfs another cell). It occurs when there is an aberrant proliferation of cells, glucose starvation, matrix deadhesion or mitotic stress (122). Cell adhesion and cytoskeletal rearrangement pathways play a central role in entosis (126).

Netosis. NETs are extracellular net-like DNA structures released by the cells in response to infection or injury. Netosis is a type of RCD driven by NET release (127).

Lysosome-dependent cell death. Lysosomotropic detergents, dipeptide methyl esters, lipid metabolites and ROS generate the permeabilization of **the** lysosomal membrane and, thus, the release into the cytosol of hydrolytic enzymes, causing cell death (128).

Autophagy. Autophagy-induced cell death is a type of cell death driven by the molecular machinery of autophagy. It is characterized by enhanced adherence to the cell substrate,

fragmented or vanished endoplasmic reticulum, focal swelling of the perinuclear space and mild chromatin condensation. During macroautophagy, the most described form of autophagy, different membrane structures are formed: phagophore, autophagosome and autolysosome. In this process, regions of the cell are enclosed in vesicles known as autophagosomes. Autophagosomes can fuse with lysosomes and become autophagolysosomes, and their content is degraded by proteases (123).

Alkaliptosis. Alkaliptosis is a type of RCD driven by intracellular alkalinization. It is only triggered by the small molecule compound JTC801 (129,130).

Oxeiptosis. Oxeiptosis is induced by ROS, non-inflammatory and caspase-independent cell death. Involves interaction among Kelch-like ECH-associated protein 1 (KEAP1, ROS sensor and antioxidant factor), phosphoglycerate mutase family member 5 (PGAM5) and apoptosis-inducing factor M1 (AIFM1, a proapoptotic factor) (131).

Immunogenic cell death (ICD). This is a type of RCD that generates an immune response (132). DAMPs are molecules that are secreted, released or exposed on the surface by stressed, injured or dying cells and that interact with the immune system (133). It is called ICD when the dying cell generates these DAMPs and potentiates the immune system's effect.

Release of DAMPs involves alterations on the cell surface, for example, because of the translocation of intracellular proteins to the plasma membrane. It also involves changes in the extracellular microenvironment, since some proteins and metabolites that are normally secluded in live cells are released (134).

In chemotherapy-driven ICD, malignant cells expose calreticulin (CALR) on the surface, as well as other endoplasmic reticulum chaperones. Malignant cells also secrete ATP and initiate type I interferon (IFN) response, culminating in the production of CXC-chemokine ligand 10 (CXCL10) and release of high-mobility group box 1 (HMGB1) and annexin A1 (ANXA1). These DAMPs bind to receptors on the surface of myeloid and lymphoid cells favoring the uptake of cell corpses and debris, which leads to higher antigen presentation and, thus, immunological memory and eradication of cancer cells that survived chemotherapy (134).

It is the primary mode of action of two approved anticancer drugs, belantamab mafodotin (135) and lurbinectedin (136). Conventional cancer treatments, such as some chemotherapeutics (e.g. cyclophosphamide, anthracyclines and oxaliplatin), RDT and some targeted therapies (such as bortezomib and crizotinib) also induce ICD (132). This engages the immune response against the tumor, enhancing treatment efficacy.

7.4.2.1 Apoptosis

Apoptosis is the most evolutionary conserved type of RCD, as well as the most studied. It is characterized by membrane blebbing, cell shrinkage, nuclear disassembling, pyknosis (chromatin condensation), DNA fragmentation, exposure of phosphatidylserine on the surface of the plasma membrane and changes in mitochondrial membrane permeability. It culminates with the formation of small vesicles, known as apoptotic bodies, that are phagocytized by neighboring cells. It is an essential process in the development and functioning of multicellular organisms, since it eliminates undesired cells, including those that are infected, damaged or mutated. Caspases, a class of cysteine proteases that cause proteolysis of cellular proteins, play a crucial role in apoptosis.

Extracellular or intracellular perturbations can induce the activation of apoptosis by two different pathways: the extrinsic pathway or the intrinsic pathway, respectively (125,137) (Figure 12).

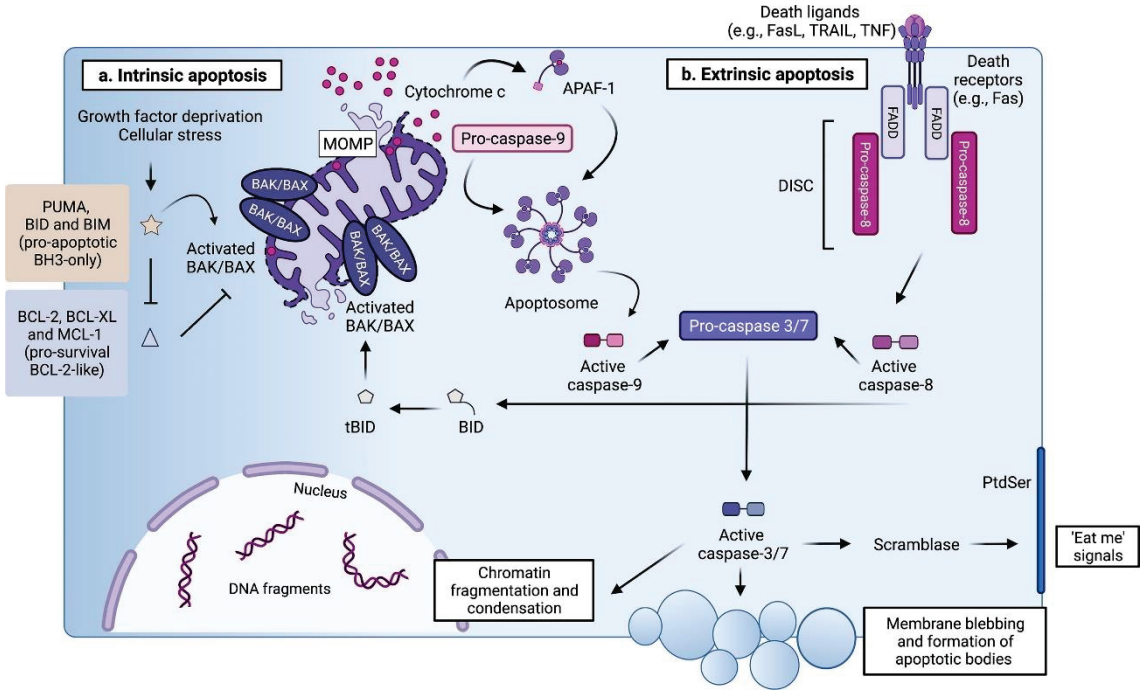

Figure 12. Molecular mechanisms of apoptosis. MOMP, mitochondrial outer membrane permeabilization; APAF-1, apoptotic protease activating factor 1; BAK, Bcl-2 antagonist killer 1; BAX, Bcl-2-associated X protein; PUMA, p53 upregulated modulator of apoptosis; BID, BH3 interacting domain death agonist; BIM, bis(indolyl)methanes; BCL-2, B-cell leukemia/lymphoma 2 protein; BCL-XL, B-cell lymphoma-extra large, MCL-1, myeloid cell leukemia 1; FasL, Fas ligand; TRAIL, TNF-related apoptosis-inducing ligand; TNF, tumor necrosis factor; FADD, Fas-associated death domain; DISC, death-inducing signaling complex; PtdSer, phosphatidylserine. Image from Ketelut-Carneiro et al., 2021 (138).

7.4.2.1.1 Extrinsic pathway

In the extrinsic pathway, extracellular perturbations initiate apoptosis, such as natural killer cells or macrophages that produce death ligands (123). It is initiated by the activation of cell surface death receptors. This includes TNFR1/2, Fas and the TNF-related apoptosis-inducing ligand (TRAIL) receptors DR4 and DR5. When activated by their ligands (TNFα, Fas ligand (FasL)L or TRAIL respectively), receptors oligomerize and form platforms in the cell surface, which induce the recruitment of adapter proteins (TNF receptor 1 associated-death domain (TRADD) and Fas-associated death domain (FADD)). ProCaspase-8 and -10 are also recruited to form the death-inducing signaling complex (DISC). Caspase-8 and -10 are activated by cleavage. Caspase-8 directly cleaves effector caspases caspase-3, -6 and -7, which execute cell death. Moreover, caspase-8 can indirectly cleave effector caspases-3, -6 and -7 by activating BID, a BCL-2 protein family

member, which generates feedback into the intrinsic pathway and promotes mitochondrial outer membrane permeabilization (MOMP) (139).

7.4.2.1.2 Intrinsic pathway

The activation of the intrinsic pathway depends on factors released by mitochondria. It is initiated by positive (hypoxia, toxins, radiation, ROS and viruses) or negative signals (absence of cytokines, hormones and growth factors in the cell environment) (140).

When apoptosis is induced, MOMP occurs and leads to the release of proapoptotic proteins, including cytochrome c, second mitochondria-derived activator of caspases (SMAC)/ direct IAP-binding protein with low pI (DIABLO) and HtrA2/Omi. Cytochrome c binds to adapter protein apoptotic protease activating factor 1 (Apaf1) (141), which undergoes a conformational change. This change exposes the caspase recruitment domain (CARD) and oligomerization domains, which make several Apaf1 assemble and the multiple CARD domains recruit procaspase-9, forming the apoptosome (142). Within the apoptosome, caspase-9 is activated and it activates the executor Caspase-3 and -7, inducing apoptosis (143). SMAC/DIABLO and HtrA2/Omi inhibit IAPs (123,138,139).

7.4.2.1.2.1 BCL-2 family members

The BCL-2 family is a heterogeneous group of proteins that regulates apoptotic mitochondrial events (Figure 13). The proteins of this family share one to four BCL-2 homology (BH) domains and are categorized into three functional and structural groups: initiators (pro-apoptotic), guardians (pro-survival) and executioners (pro-apoptotic).

Initiators. Initiators are traditionally known as BH3-only pro-apoptotic group and include bis(indolyl)methanes (Bim), Nicotinamide adenine dinucleotide phosphate (NADPH) oxidase activator (Noxa), BCL-2 associated agonist of cell death (Bad), BH3 interacting domain death agonist (Bid), p53 upregulated modulator of apoptosis (PUMA) and activator of apoptosis harakiri (Hrk). They are the first responders to cellular stress and their function is to interact with other members of the BCL-2 family regulating their activity: they disable the activity of guardian family members and activate executioners (144).

When there is an apoptotic signal, initiators respond through transcriptional upregulation and post-translational modifications. Initiators may have a degree of specificity for some guardians. In the case of Bim, PUMA and BID, they possess a broad specificity, that is, they inhibit all guardians. On the contrary, BAD specifically blocks BCL-2, B-cell lymphoma-extra large (BCL-X_L) and BCL-W and NOXA inhibits myeloid cell leukemia sequence 1 (MCL1) and BCL2 related protein A1 (BCL2A1).

BID is a special initiator, since it contains a BH4 domain (145). BID is activated by cleavage (for example, by caspase 8), which produces tBID. tBID translocates to the mitochondrial outer membrane, where it interacts with guardians and executioners (146).

We can distinguish two categories of initiators: activators (Bim and tBid) and sensitizers (Bad). Other proteins of this group are more difficult to classify, for example, NOXA, which has a less clear classification since it is considered a sensitizer but can directly activate Bak (147).

Guardians. This is considered the multidomain anti-apoptotic group. Guardians have four BH domains (BH1-BH4) and include BCL-2, BCL-X_L, BCL-W, MCL-1 (myeloid cell leukemia 1), and BCL2A1. Their overexpression inhibits cell death, so they must be neutralized for apoptosis undergoing. Guardians are commonly upregulated in cancer, as a mechanism of cancer cells to avoid apoptosis (144). They sequester activators and executioners by binding their BH3 domain with high affinity. Moreover, as a consequence of interacting with executioners, guardians promote the translocation of BAX and BAK from the mitochondria to the cytosol (148).

Executioners. They form the multidomain pro-apoptotic group. They have four BH domains (BH1-BH4) and include BCL-2 antagonist killer (BAK), BCL-2 associated X protein (BAX) and BCL-2-related ovarian killer (BOK). BAK and BAX are the most studied executioners. The most crucial event for apoptosis is MOMP. BAK and BAX are labile and easily undergo conformational changes. Hence, when they are activated, they accumulate in the mitochondrial outer membrane, undergo conformational changes and oligomerize, forming membrane pores that lead to MOMP (149).

BAX is mainly localized in the cytosol, while BAK is mostly found in the mitochondrial membrane and is maintained inactive due to the association of the protein voltage-

dependent anion channel 2 (VDAC2) (150,151). The activity of BAK and BAX can be regulated by post-translational modifications. There are multiple mechanisms of activation of BAK and BAX: direct interaction with activator family members, autoactivation (because of their inherent instability) or direct interaction with activated BAK and BAX (144).

Both extrinsic and intrinsic pathways are not totally independent, there is a cross-talk of both pathways. Caspase 8 can activate BID (an initiator protein), which results in the truncated form of tBID. This engages BAX/BAX-dependent MOMP-driven and cytochrome release (138).

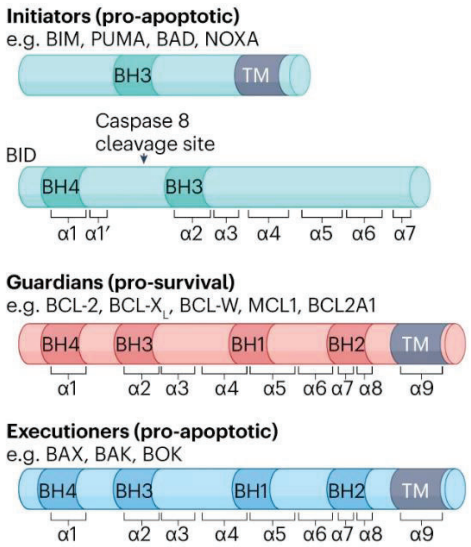

Figure 13. The BCL-2 family. BIM, bis(indolyl)methanes; PUMA, p53 upregulated modulator of apoptosis; BAD, BCL-2 associated agonist of cell death; NOXA, oxidase activator; BH, BCL-2 homology; TM, transmembrane; BID, BH3 interacting domain death agonist; BCL-2, B-cell leukemia/lymphoma 2 protein; BCL-X_L, B-cell lymphoma-extra large; BCL-W, B-cell lymphoma-w; MCL-1, myeloid cell leukemia sequence 1; BCL2A1, BCL2 Related Protein A1; BAX, Bcl-2-associated X protein; BAK, Bcl-2 antagonist killer 1; BOK, Bcl-2-related ovarian killer. Image from Czabotar et al., 2023 (144).

7.4.2.1.3 Execution pathway

The execution pathway is the final step of apoptosis. Executioner caspases -3, -6 and -7 (activated by caspases -8, -9 and -10) trigger morphological and biochemical changes in the apoptotic cell by cleaving multiple substrates, such as cytokeratins, inhibitor of caspase-activated deoxyribonuclease (ICAD), PARP, Rho-associated coiled-coil forming kinase-1 (ROCK-1), gelsolin and foldrin.

Caspase-3 is considered the most important executioner caspase. Catalyzes the inhibitory cleavage of ICAD, the inhibitor of the endonuclease CAD. When CAD is released, it degrades chromosomal DNA and causes chromosomal condensation (152). Caspase-3 and -7 promote phosphatidylserine (PS) exposure in the outer surface of the plasma membrane by activating proteins that externalize PS or inactivating factors involved in its internalization. The exposure of PS allows noninflammatory phagocytic recognition and the uptake of apoptotic cells (153). Caspase -3 is also required for plasma membrane blebbing, regulated by ROCK1. ROCK1 phosphorylates the myosin light chain (MLC), which induces actomyosin contraction, delamination of cortical cytoskeleton and cell shrinkage (154). Moreover, caspase-3 and 7 activate several pro-caspases (e.g. 2, 6, 8 and 10) triggering the amplification of the apoptotic signal (155).

7.4.2.1.4 Inhibitors of apoptosis

The IAP family is a group of proteins that share functional and structural characteristics and that can inhibit apoptosis. The eight human IAPs that have been identified until now are neuronal IAP (NAIP), cellular IAP1 (c-IAP1), cellular IAP2 (c-IAP2), X-linked IAP (XIAP), survivin, Bir-ubiquitin conjugating enzyme (BRUCE, also known as Apollon), melanoma IAP (ML-IAP, also known as Livin) and IAP-like protein 2 (ILP2) (156) (Figure 14).

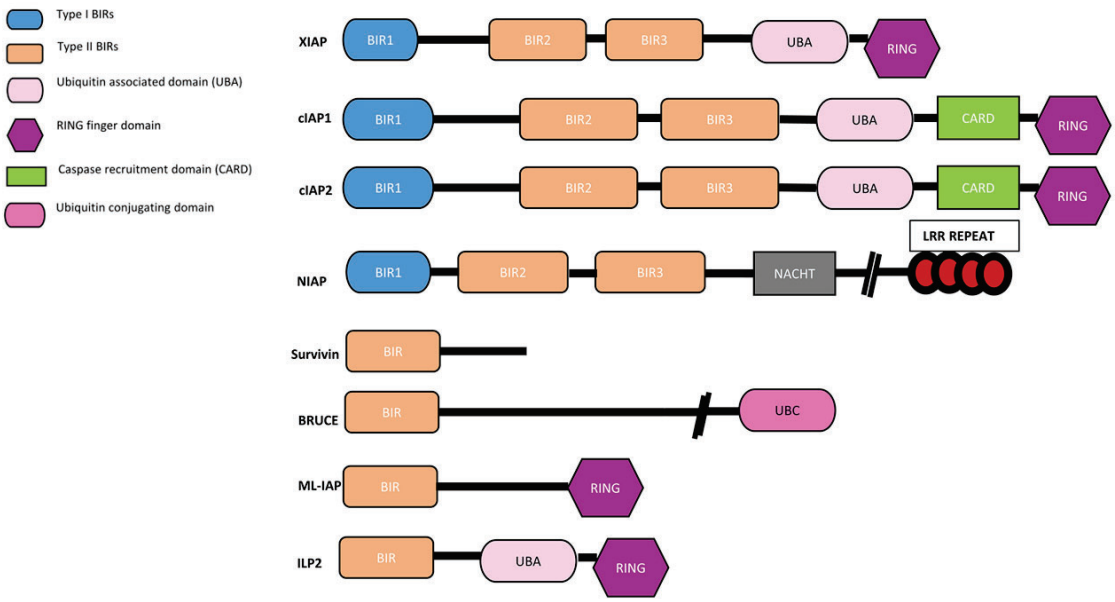

Figure 14. Structure of the IAP family of proteins. BIR, baculovirus IAP repeat; RING, Really Interesting New Gene; LRR, leucine-rich. Image from Kumar et al., 2020 (156).

The main common structural characteristic of IAPs is the baculovirus IAP repeat (BIR) domain. The 8 mammalian IAPs contain one to three copies of BIR domain. Common features of the BIR domains include the presence of three conserved cysteine residues and one histidine residue. They coordinate a zinc ion, which is required to stabilize the BIR fold (156). There are 2 types of BIR domains. Type II contains a hydrophobic cleft that allows it to bind to IAP binding motifs (IBMs) present in caspases and IAP antagonists. Type I BIR domain has a shallow pocket instead of a deep peptide binding groove. Hence, type I BIR domains do not interact with caspases or IAP antagonists, but with other proteins. For instance, the type I BIRs of cIAP1 and cIAP2 interact with Tumor Necrosis Factor Receptor Associated Factor 2 (TRAF-2), which is an adaptor protein involved in the signal transduction from the TNF receptor family (157).

BIR domains confer the inhibitory properties of IAPs, since they prevent the conversion of pro-caspases to caspases. However, it is essential but not sufficient for antiapoptotic activity because not all BIR-containing proteins can inhibit apoptosis. The BIR domain can also mediate protein recognition and protein-protein interactions.

Several IAP family members also contain a zinc finger domain called really interesting new gene (RING). The **RING domain** allows IAP to recruit ubiquitin conjugating enzymes (E2), which transfer ubiquitin onto lysine residues of target proteins. If the residue of lysine polyubiquitinated is lysine 48 (K48), the chain of ubiquitin is recognized by the proteasome and typically degraded (158).

Some IAPs also contain a **ubiquitin-associated domain (UBA)** and a **ubiquitin conjugating domain (UBC)**. XIAP, cIAP1, cIAP2 and Ts-IAP have UBA domains, which allows them to bind to polyubiquitylated proteins and substrates (159). The only IAP with a UBC domain is Apollon. The UBC domain confers to Apollon the function of a ubiquitin conjugating enzyme (E2), which is able to transfer ubiquitin to substrates directly (160).

cIAP1 and cIAP2 also contain a **caspase recruitment domain (CARD)** (161). The CARD is also present in procaspase-9 and apaf1 and is important for the formation of the apoptosome. The function of CARD in cIAP/2 is not clear but it has been suggested that it plays a role in stabilizing cIAP1 by inhibiting auto-ubiquitination by the RING domain (162).

IAPs are upregulated in different cancer types and this is correlated with treatment response and prognosis (156). For instance, cIAP1 is overexpressed in esophageal squamous cell carcinoma cell lines and is associated with resistance of esophageal squamous cell carcinomas to drug-induced apoptosis (163). In addition, Imoto et al. demonstrated that the expression of cIAP1 correlates with resistance to RDT in cervical cancers (164). Another study found a subset of CD133+ glioblastoma stem cells with higher expression of all IAP family members that presented resistance to temozolomide, carboplatin and paclitaxel (165).

SMAC is an endogenous IAP inhibitor whose N terminus contains a mitochondrial targeting sequence that is cleaved to expose a sequence of four amino acids Ala-Val-Pro-Ile (AVPI) required for binding to IAP proteins. The discovery of SMAC led to the synthesis of SMAC peptides derived from this sequence. These SMAC peptides were able to bind to IAP proteins and abrogate their activity, as well as sensitize cancer cells to chemotherapy (166,167). SMAC peptides did not have the pharmacological properties to its use in clinics, so small molecules that mimicked the IAP binding motif were developed, with better cell permeability and potency (168). A third generation of these compounds named bivalent SMAC mimetic was developed, consisting of two linked IAP binding tetrapeptides. Bivalent SMAC mimetic compounds can inhibit not only BIR3 (like the previous SMAC mimetic compounds) but also BIR2 domain, which also plays an important role in inhibiting caspases (169).

Apart from the evasion of apoptosis, the IAP family also plays a role in other processes related to the hallmarks of cancer, such as the evasion of the immune system response. PAMPs and DAMPs activate pattern recognition receptors (PRRs) such as TLRs, nod-like receptor (NLR) family and RIG-like receptor (RLR) family. These receptors lead to the activation of NF-κB, resulting in the transcription of proinflammatory cytokines, chemokines and interferons. IAPs interact with TRAF-2 and -3, regulating PRRs activation with IAPs' E3-ligase ubiquitylation activity (170). IAPs are also negative regulators of B lymphocytes due to their role in the noncanonical NF-κB pathway (171). The role of IAP in regulating immune system responses makes the members of this protein family good targets for developing immunotherapy-based treatments for cancer. In fact, some

studies show IAP antagonists have co-stimulatory effects on T-cells (172). What is more, these compounds have shown synergism with immune checkpoint inhibitors (173).

Overall, the overexpression of IAPs in multiple cancer types makes the IAP family an attractive target. A great effort is being made to develop specific IAP inhibitors, such as SMAC mimetic compounds, in order to induce apoptosis or sensitize cancer cells to conventional therapies.

7.4.2.1.5 Survivin

7.4.2.1.5.1 Survivin structure and isoforms

Survivin is a protein encoded by BIRC5 gene (baculoviral inhibitor of apoptosis repeat-containing 5). It has four exons, three introns and three cryptic exons, which are exons that, when included in RNA transcripts, introduce premature translation stop codons into the mRNA, helping to control the abundance of the protein (174) formed by 14,796 nucleotides in the chromosome 17q25. The molecular weight of survivin is 16.5 kDa, being the smallest member of the IAP family, since it only contains a single N-terminus BIR domain linked to a C-terminal α-helical coiled-coil domain (Figure 15).

The **BIR domain** is formed by 70-80 residues, made of antiparallel beta sheets with 3 strands and surrounded by 4 alpha helices. At the carboxyl terminus, BIR domain forms a ring finger motif containing a zinc anion, coordinated by the residues C57, C60, H77 and C84.

Survivin has a 65 Å amphipathic alpha helix in the C-terminal of survivin, comprising residues 100-140. This **helical domain** is crucial for the formation of the chromosomal passenger complex (CPC), which assures the correct segregation of chromosomes and cytokinesis during cell division (175,176). There is a **homodimerization domain** located at two different areas in the linear sequence of survivin. The residues through which interact both monomers are 90-102. This homodimerization allows the formation of a stable homodimer that carries out the mitotic activity, while the monomeric form of survivin is associated with antiapoptotic activity (177,178)

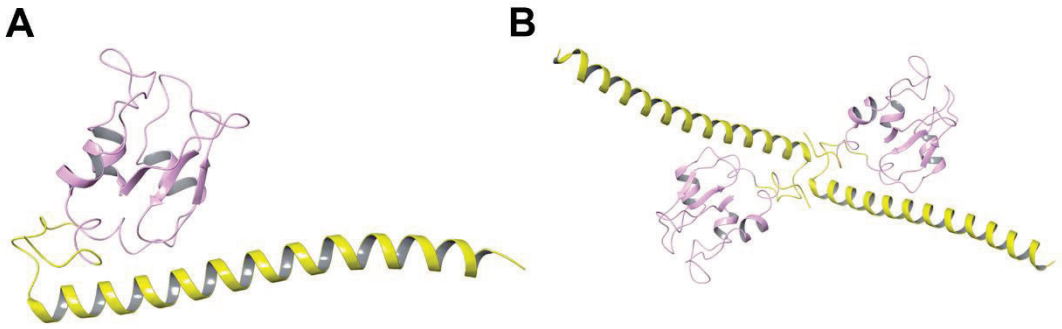

Figure 15. 3D structure of survivin as a monomer (A) and as a dimer (B). Figure from Martínez-García et al., 2018 (179).

Alternative splicing of survivin pre-messenger RNA (mRNA) can give rise to five more splice variants (Figure 16), which are distributed in the nucleus, mitochondria and cytoplasm, and interact with wild type (WT) survivin to exert anti-apoptotic activity. The splice variants are ΔEx3 (survivin with deletion of exon 3, which allows its interaction with mitochondrial WT survivin), 2B (survivin with exons 1-4 and an additional -69bp fragment from intron 2), 3B (survivin with an additional 165 bp sequence from intron 3), 2α (with only exons 1 and 2) and 3α (2 exons) (180). All isoforms share a complete sequence in the N-terminus region and differ in the carboxyl end. They have different expression patterns and subcellular localization compared to WT survivin form (181). Some splice variants present tumor-specific expression and are correlated with tumor progression and response to therapy (180).

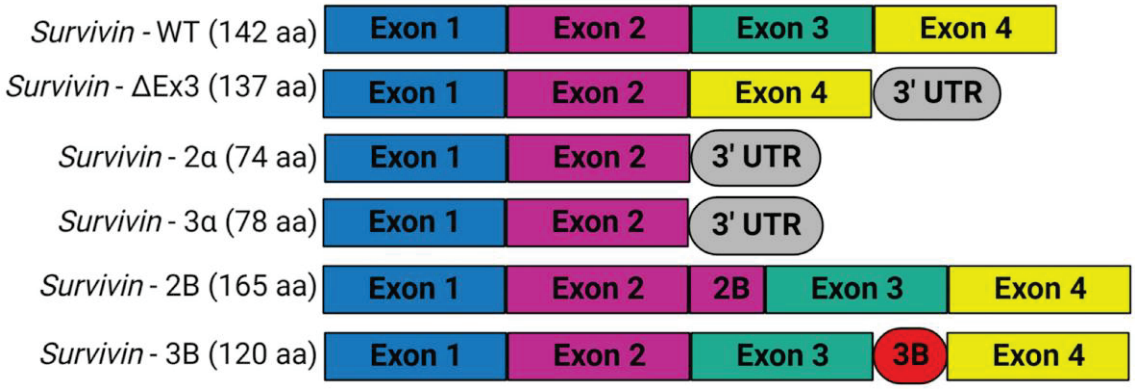

Figure 16. Schematic representation of splice variants of survivin encoded by BIRC5 gene. WT, wild type; aa, amino acids; UTR, untranslated regions. Figure from Albadari et al., 2023 (182).

7.4.2.1.5.2 Survivin expression pattern and subcellular localization

Survivin is highly expressed during embryonic and fetal development, and almost undetectable in most normal differentiated tissues. The differentiated tissues and cells that express survivin during the cell cycle are hematopoietic progenitor cells, T lymphocytes, endothelial cells and testes (183). In cancer cells, survivin is re-expressed in vast amounts, participating in signaling cascades crucial for carcinogenesis (184).

Survivin can be found in different subcellular localizations, which, in turn, are associated with different functions. Cytosolic survivin is associated with an apoptotic suppressor role, while nuclear survivin has been related to cell division regulation (185). In the mitochondria, there is a small pool of survivin, released to the cytosol in response to cell death stimulation, which confers resistance to apoptosis (186). There is also extracellular survivin originated from exosomes secreted by tumor cells. These exosomes are taken by neighboring cells, which increase their proliferation and resistance to therapy (187).

7.4.2.1.5.3 Survivin functions

7.4.2.1.5.3.1 Cell division

During cell division, survivin is transported to the nucleus. Survivin is essential to complete mitosis and cell division, and it is a key mitotic regulator. The expression peak of survivin is in the G_2/M phase, and rapidly declines in the G_1 phase. However, in cancer, survivin is ubiquitously expressed in all the phases of the cycle (188). Moreover, the survivin gene may be regulated by the cell cycle, since the BIRC5 gene contains cycle-dependent element/ cell cycle genes homology region (CDE/CHR) (189).

Survivin is part of the CPC. The CPC regulates key events in cell division: chromosome-microtubule attachment, spindle assembly checkpoint and occurrence of cytokinesis. It is formed by Aurora B (the enzymatic component), inner centromere protein (INCENP) (the scaffold protein, that stabilizes the complex) and borealin, which promotes attachment of survivin to the complex (190). Survivin binds to the CPC through the dimerization domain, hence, survivin functions as a monomer in the CPC (191). Kinase haspin phosphorylates histone 3 on Thr3 (H3T3), and this is recognized by a pocket in the BIR domain of survivin. This phosphorylation, together with the phosphorylation of

histone 2A at threonine 120T, that recruits Shugoshin1 (an adaptor for borealin), are responsible for the CPC recruitment (Figure 17). CPC is localized in the centromere during prophase, prometaphase and metaphase (190). In anaphase, CPC re-localizes to the anti-parallel microtubules of the central spindle and the equatorial cortex. Finally, CPC is concentrated at the midbody during telophase and cytokinesis (192). The mislocalization of the CPC at some phases of mitosis causes fatal mitotic defects.

Survivin is also involved in microtubule formation during cell division, since it can alter microtubule dynamics and nucleation (193). Grodini et al. 2002 suggest one of the mechanisms survivin may promote resistance to chemotherapy is by promoting microtubule stability (194).

Survivin also regulates cytokinesis. It has been shown that survivin homodimer interacts with myosin II, which impairs myosin II assembly into filaments. Before anaphase, cyclin-dependent kinase 1 (CDK1) is highly active and phosphorylates survivin in Thr34. This prevents interaction of survivin with myosin II. At telophase, survivin is dephosphorylated by a phosphatase and forms a complex with myosin II, regulating the number of molecules that form the contractile ring. It also regulates the size of the ring. Disruptions of this interaction lead to unregulated myosin II filament assembly and mitosis defects (195).

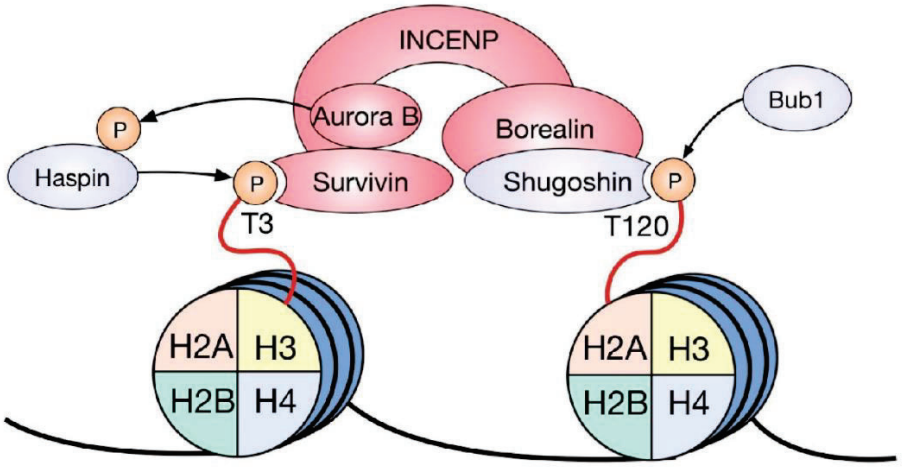

Figure 17. Chromosomal passenger complex (CPC) recruitment. P, phosphate. Figure from Andonegui-Elguera et al., 2022 (196).

7.4.2.1.5.3.2 Inhibition of apoptosis

In case of a cell death stimulus, survivin is released from mitochondria to the cytosol. There, survivin directly binds to caspases -3 and -7 and, consequently, inhibits caspase-9-mediated apoptosis (197–199). Moreover, once survivin is released to the cytosol, it can also form a complex with XIAP (186,200). This increases XIAP stability since it avoids ubiquitin-dependent degradation, leading to an increase in the ability of XIAP to inhibit caspases -3, -7 and -9 (186). At the same time, it enhances survivin stability, because its binding avoids the formation of the complex XIAP- XIAP-associated factor 1 (XAF1), which induces polyubiquitination and proteasomal degradation of survivin (201). Survivin-XIAP complex also induces the translocation of NF-kB to the nucleus, where it upregulates the expression of genes involved in cell invasion and metastasis (202).

When survivin is released from mitochondria to the cytosol upon cell death stimuli, survivin can form a complex with hepatitis B X-interacting protein (HBXIP), which binds to procaspase 9, preventing its recruitment to form the apoptosome, as well as its activation. Thr34 phosphorylation is required for optimal association with HBXIP (203).

Furthermore, survivin can indirectly disrupt caspase activation by interacting with proapoptotic proteins. An example is SMAC/DIABLO, a proapoptotic protein released by the mitochondria upon apoptotic stimuli, that antagonizes IAPs, promoting cytochrome c-dependent apoptosis. SMAC/DIABLO binds to XIAP, releasing caspase-9 from the complex and inducing apoptosis. Cytosolic survivin can bind SMAC/DIABLO through the AVPI peptide binding region, inhibiting the proapoptotic functions of SMAC/DIABLO (204). In the mitochondria, survivin can delay the release of SMAC/DIABLO by direct binding after apoptotic stimuli (205).

Survivin can also prevent apoptosis in a caspase-independent manner, by interfering with mitochondrial apoptosis-inducing factor (AIF) (206). Upon apoptotic stimuli, AIF translocates from the mitochondrial intermembrane space to the nucleus and produces DNA fragmentation.

Moreover, survivin can suppress the attack by immune cells on cancer cells, since survivin can inhibit Fas-mediated apoptotic signaling (involved in the extrinsic apoptotic pathway), as well as induce FasL on the cancer cell surface, to counterattack immune

cells. Survivin increases specificity protein 1 (Sp1) phosphorylation, which enhances the ability of DNA-binding of Sp1 to the FasL promoter (207). It is suggested that this increment of Sp1 phosphorylation may be induced by survivin activation of Aurora B kinase (208).

Moreover, survivin can also intervene in the extrinsic pathway of apoptosis by weakening TRAIL-induced cell apoptosis, when survivin is phosphorylated in Thr34 by CDK15 (209).

7.4.2.1.5.4 Survivin regulation

7.4.2.1.5.4.1 Transcriptional regulation

The promoter of survivin has binding sites for multiple **regulatory proteins**, e.g. Sp1, p53 and tumor suppressor protein retinoblastoma (Rb)/elongation factor 2 (EF2). Binding sites for transcription factors are principally concentrated in a proximal region of the promoter: -250 to +70 nt relative to the transcriptional initiation point (176,210). Two main transcriptional start sites were confirmed: at position -72 and within the range -57/-61 from the initiation codon (176,211).

Sp1 is a transcription factor that enhances transcription of genes lacking a functional TATA box, such as BIRC5. Hence, Sp1 enhances survivin transcription (212). p53 is a survivin repressor. It promotes DNA methyltransferase 1 (DNMT1), which hypermethylates BIRC5 promoter (213). It has been shown that there is an increase of survivin expression in tumors with p53 mutated (compared to WT) in NSCLC patients (213,214). This study also shows survivin can be negatively regulated by p53 by avoiding the binding of hypoxia-inducing factor 1α (HIF-1α). p53 can also prevent the binding of Sp1 factor to the survivin promoter, suppressing its activity (213). Moreover, survivin can regulate p53 expression and degradation through the caspase-3/mouse double minute 2 homolog (MDM2) complex (215). Downregulation of survivin stabilizes p53, which leads to the amplification of survivin reduction signal. Conversely, overexpression of survivin in tumor cells may reduce p53 levels, which means blocking the p53-dependent apoptosis pathway (216).

Survivin expression can also be regulated through p53 independent pathways, for example by HER2 through interactions with the transcription factors NF-κB and c-MYC

(217). Early growth response 1 (Egr-1) also represses survivin promoters. Egr-1 is crucial in the regulation of cell growth, differentiation and apoptosis (218). On the one hand, Egr-1 stimulates the synthesis of growth and differentiation factors by direct promoter activation (219). On the other hand, Egr-1 induces transcription of p53 and that leads to p53-dependent apoptosis (220). Moreover, Egr-1 binds to the transcription factor c-Jun, increasing the activity of c-Jun to promote cell death (221). The pathway Rb/EF2 can also regulate survivin expression, which is induced by E2F and this induction is abolished by Rb (222).

There are micro-RNAs (miRNA) that bind to the 3'-untranslated region (UTR) of survivin mRNA and downregulate survivin expression. E.g., miR-34a binds directly to a specific sequence of survivin mRNA, reducing survivin expression (223). Moreover, upregulation of miR-34a can indirectly reduce survivin levels by repressing upstream activators or transcriptional factors (224). MiRNA-335 is a tumor suppressor miRNA that directly targets survivin and induces its degradation, promoting apoptosis and inhibiting cancer cell growth (225). MiRNA-182 can also downregulate survivin expression in some cancers (226).

The aberrant activation of some signaling pathways alters survivin expression. E.g. phosphatidylinositol-4,5-bisphosphate 3-kinase (PI3K)/protein kinase B (PKB or AKT), Janus kinase (JAK)/ signal transducer and activator of transcription (STAT) and Mitogen-activated protein kinase (MAPK)/extracellular signal-regulated kinase (ERK)(227).

Several factors influence the activity of the survivin promoter, such as cell type and microenvironment. For example, promoter activity is inherently high in established tumor cell lines and primary melanoma cells (228). Moreover, the activity of survivin promoter is upregulated by hypoxia in tumor cells (229).

7.4.2.1.5.4.2 Post-translational regulation

Survivin can be regulated through protein modifications, such as phosphorylation, acetylation and ubiquitination.

Phosphorylation. As mentioned above, survivin can be phosphorylated at Thr34 by CDK1 (also known as CDC2) and CDK15 (230), which stabilizes survivin at metaphase and

allows it to exert its anti-apoptotic activity (203). Phosphorylation at Thr48 by CK2 is crucial for maintaining survivin in the cytoplasm during interphase, where survivin may perform antiapoptotic activity (230). Phosphorylation of Thr117 by Aurora B regulates the activity of the CPC. The dephosphorylation of Thr117 is important for stabilizing the association between survivin and the centromere, resulting in a proper chromosome progression into anaphase (231).

Phosphorylation on Ser20 catalyzed by protein kinase A (PKA) and polo-like kinase 1 (PLK1) avoids interaction with XIAP, which evades apoptosis inhibition. PKA phosphorylates Ser20 of survivin released by mitochondria into the cytosol when there are apoptotic stimuli (232). Phosphorylation of survivin decreases its stability, confining the apoptotic roles of survivin to the mitochondria (223). Ser20 can be dephosphorylated by purified protein phosphatase 2A (PP2A), which allows interaction with XIAP and, consequently, inhibition of apoptosis. In the mitochondrial intermembrane space, there is a pool of PP2A. Moreover, in the mitochondria, there is no PKA, so survivin is maintained dephosphorylated in Ser20. PLK1 phosphorylation has been shown to catalyze Aurora B activation, allowing microtubule attachment and CPC formation (233).

Acetylation. Survivin can be acetylated in multiple lysine residues (23, 90, 110, 112, 115, 120, 121, 122, 129 and 130), mostly clustered in the COOH-terminal α-helical coil (234). For example, CREB-binding protein (CBP) acetylates survivin on Lys129, which promotes survivin homodimerization and subsequent nuclear accumulation. Acetylated survivin binds to STAT3 (N-terminal) and represses its oncogenic activity. Deacetylation of survivin is catalyzed by histone deacetylase 6 (HDAC6) and produces the inhibition of homodimerization and promotion of heterodimerization with chromosome region maintenance 1 (Crm1/Xpo1). Crm1 is a nuclear export receptor that shuttles survivin from the nucleus to the cytoplasm, where survivin does its antiapoptotic activity (235).

Ubiquitination. Survivin can be ubiquitinated in multiple lysine residues (e.g. Lys23, 62, 78 and 79) (236). Lys63 mono-ubiquitination by ubiquitin fusion degradation protein 1 (Ufd1) promotes CPC binding to the centromere. Deubiquitination by ubiquitin carboxyl-terminal hydrolase 9X (hFAM) leads to the dissociation of survivin and centromeres (237).

XAF1, a physiological inhibitor of XIAP, promotes indirect ubiquitination of survivin (201) because it activates the RING E3 ligase of XIAP, which ubiquitinates survivin. Then, survivin is degraded by the ubiquitin-proteasome pathway.

7.4.2.1.5.5 Survivin as a therapeutic target in oncology

Survivin is associated with drug resistance to chemotherapy, poor patient prognosis, irradiation insensitivity and tumor angiogenesis (238). Abnormally high expression of survivin in tumors and its strong association with worse prognosis turns survivin into a good biomarker for cancer diagnosis (239–241).

7.4.2.1.5.5.1 Survivin expression in healthy and cancer tissues

Survivin is highly expressed in embryonic and fetal tissues, but negligible in normal differentiated cells. In fact, it is absent in terminally differentiated cells (242,243). In adult tissues, we can find survivin expression in the thymus, endothelial tissue during angiogenesis and basal epithelial cells of the colon. Other cells where it has been suggested survivin plays an important role are polymorphonuclear cells (PMN), vascular endothelial cells, T cells, hematopoietic progenitor cells (HPC) and erythroid cells. Survivin expression is also found in the gastrointestinal mucosa, adult hepatocytes and ovarian granulosa (238). Despite its presence in normal tissues associated with self-renewal and growth, survivin is significantly higher expressed in transformed cells.

In normal adult cells, the activity of the survivin promoter is usually silent, while it is remarkably higher in most tumor cells. Survivin expression has been found in more than sixty types of human cancer, breast and lung cancer being the ones with higher survivin expression and renal cancer with the lowest (238). Moreover, upregulation of survivin is the fourth-most significant transcriptome in multiple hematological malignancies (244).

7.4.2.1.5.5.2 Role of survivin in cancer

Disruption of the natural expression of survivin in cancer is primarily caused by de-repression of its transcription, which results in continuous synthesis of survivin along the cell cycle, and altered splicing (245,246). Pathways that hinder survivin regulation in tumor cells are enhanced promoter activity, epigenetic modification of survivin exons

and amplification of survivin locus (17q25) (238). As mentioned above, survivin can be used as a biomarker in cancer, helping to determine the prognosis of the disease. Furthermore, some single nucleotide polymorphisms (SNPs) that have been identified in survivin are linked to cancer risk. SNPs are single-base pair differences in the DNA sequence at a specific position in the genome, where the only change is that one nucleotide is substituted for another. SNPs are implicated in the understanding of disease susceptibility, genetic diversity and response to treatment. Some of the SNPs identified in survivin linked to cancer risk are -31 G/C, -625 G/C and +9194 A/G (223). The most studied SNP is -31 G/C. Several studies have demonstrated a correlation between -31 G/C SNP and cancer risk, the level of correlation depending on specific sub-populations. On the one hand, there is a strong association between -31 G/C and urothelial carcinoma risk in the Serbian population (247) and oral cancer risk in the Taiwanese population (248). On the other hand, there is a weak association between -31 G/C and head and neck cancer risk in the Serbian population (249), as well as between this SNP and hepatocellular carcinoma risk in the Turkish population (250).

In cancer cells, survivin tends to accumulate in the mitochondria, generating resistance to cell death mechanisms by altering the energy production mechanisms of the mitochondria (251). Survivin is also accumulated in the nucleus and cytoplasm, where it can be used as a prognostic biomarker, since overexpression of survivin is associated with enhanced anti-apoptotic effect (survival of cancer cells). Moreover, increased survivin expression is associated with metastasis, cancer recurrence, invasion of lymph nodes and drug resistance (252). Survivin promotes these processes by intervening in cell division, inhibition of apoptosis, migration, angiogenesis and autophagy through multiple mechanisms.

One of the cancer hallmarks in which survivin plays a role is in angiogenesis, since it promotes the proliferation of vascular endothelial cells and secretion of vascular endothelial growth factor (VEGF) (253). Furthermore, high expression of survivin results in decreased autophagy, which is a crucial process for cancer development and disease progression. In fact, in osteosarcoma cells, overexpression of survivin leads to the formation of smaller autophagosomes, enlarged lysosomes and a reduction in

autophagic flux (254). Moreover, inhibition of survivin induces cell death through apoptotic and autophagic pathways in *in vivo* mouse models (255).

7.4.2.1.5.5.3 Role of survivin in cancer treatment resistance

Many anticancer therapies induce cell death through apoptosis. Therefore, survivin is an important determinant of chemo and radiosensitivity of tumor cells. Upregulation of survivin contributes to treatment resistance by promoting tumor cell survival (238). The ability of survivin to promote resistance could also be related to its function in mitotic spindle fibers assembly to microtubules (256). Multiple studies have shown that overexpression of survivin protects from apoptosis caused by taxol, a chemotherapeutic agent that stabilizes microtubules (194,257,258). What is more, Zaffaroni et al. revealed that the stabilization of microtubules and mitosis arrest induced by taxol increases survivin expression (257). It has been shown that the role of survivin in resistance to taxol is due to the induction of PI3K/Akt signaling pathway (259).

Angiogenic growth factors such as VEGF promote the survival of endothelial cells by activating PI3K survival pathway (260), making the cells less susceptible to apoptosis. VEGF also induces the expression of several antiapoptotic effectors molecules, including survivin (261). Survivin induction by VEGF helps to protect endothelial cells from chemotherapy, since it ensures the integrity of microtubules (262).

It has also been observed an increased survivin expression in thyroid and prostate cancer cells with permanent resistance to cisplatin, as well as colorectal cancer resistant to TRAIL (263–265). Moreover, survivin is also involved in resistance to adriamycin (266) and flutamide, an anti-androgen therapeutic. In this case, resistance may be carried on via insulin-like growth factor-1/Akt signaling during androgen blockade (267).

Survivin also affects the sensitivity of cancer cells to ionizing irradiation. A negative correlation between survivin mRNA expression and sensitivity to ionizing X-ray irradiation has been demonstrated in several cancer cell lines. In fact, sublethal doses of irradiation increased the expression of survivin mRNA (268).

High survivin expression is not only linked to therapeutic resistance but also to an increased risk of tumor recurrence (269). In tumorigenesis, accumulation of β-catenin in

the cytoplasm leads to activation of the Wnt pathway. Then, β-catenin translocates into the nucleus, where it forms a transcriptional activator complex with T-cell factor (TCF). This complex upregulates the expression of genes such as survivin, c-Myc and VEGF. This upregulation of survivin induces protection against apoptosis (227).

7.4.2.1.5.6 Therapeutic options targeting survivin

Survivin has a dual role in the cell, since it is involved in cell cycle promotion and apoptosis inhibition. This, together with the expression pattern of survivin, which provides selectivity over tumor cells, makes survivin an ideal target for anticancer therapy. In addition, survivin is considered a biomarker with a negative correlation on patient clinical outcome and a positive correlation on drug resistance (223)The emergence of survivin as an ideal therapeutic target has led to the development of different approaches to targeting survivin. These treatments aim to augment apoptosis and impede tumor cell proliferation. Among these new therapeutic strategies, we can find specific direct inhibitors (Figure 18) and other molecules that reduce survivin expression by indirect pathways. Moreover, vaccines and immunotherapy directed against survivin are also being investigated.

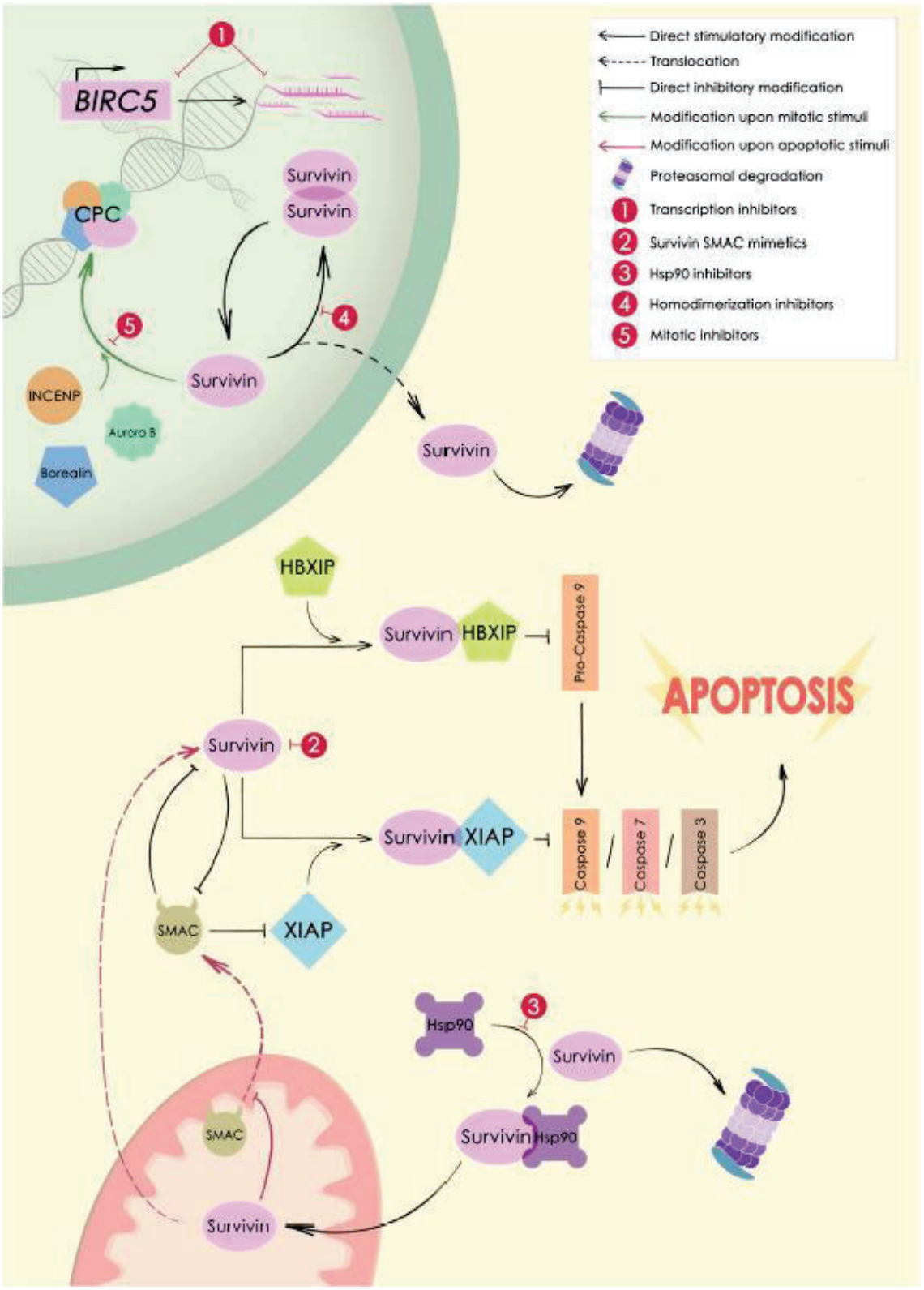

Figure 18. Survivin subcellular functions and direct survivin inhibitors. CPC, chromosomal passenger complex; INCENP, inner centromere protein; HBXIP, hepatitis B X-interacting protein; XIAP, X-linked inhibitor of apoptosis protein; SMAC, second mitochondrial-derived activators of caspases; Hsp90, heat shock protein 90. Diagram from Martínez-García et al., 2018 (179).

7.4.2.1.5.6.1 Survivin direct inhibitors: targeting survivin gene or protein

7.4.2.1.5.6.1.1 Transcriptional inhibition of survivin

Inhibiting survivin gene expression aims to counteract survivin overexpression in tumor cells. Several small molecules inhibiting survivin gene promoter or mRNA have been studied.

YM155 was first defined as a small-molecule inhibitor that suppresses the activity of survivin promoter, regardless of p53 status (270). It was discovered through high throughput screening (HTS) of potential compounds that could bind to the survivin promoter and inhibit its transcription (238). In prostate cancer cells, it suppressed the survivin gene promoter, induced apoptosis and promoted tumor regression in prostate ectopic xenograft tumors (270). Other studies have shown an average inhibitory concentration (IC_{50}) of 15 nM against 119 human cancer cell lines. In *in vivo* experiments, continuous 3- or 7-day infusion (1-10 mg/kg) in xenograft model had a significant antitumor activity without significant toxicity (measured through weight loss) (271). In phase I clinical assay, YM155 is a well-tolerated anticancer drug, with some efficacy against blood cancer (272). In phase II studies, however, modest single-agent activity against NSCLC has been shown, but the disease control rate is similar to other second-line agents for advanced NSCLC (273). The combination with carboplatin and paclitaxel showed a good safety profile but did not demonstrate improvement in response rate in advanced NSCLC (274).

Several studies reported that the effect of YM155 could be due to off-target effects, apart from its effects on survivin expression. For example, YM155 can inhibit Mcl-1 expression in D37, PC-3, H28 and U251 cancer cells (182,275). Furthermore, some data support that YM155 damages the DNA and survivin suppression is a secondary event (probably the consequence of transcriptional repression) (276). Another study suggests that the inhibition of survivin is via suppression of EGFR signaling pathway (277), which means YM155 is not a specific inhibitor of survivin. In fact, recent studies suggest TOP is the molecular target of YM155, instead of survivin (278,279).

FL118 is a non-selective small molecule that has been identified by HTS of chemical libraries. It is structurally similar to TOP I inhibitor (irinotecan) and inhibits survivin promoter activity as well as survivin gene expression. It also downregulates the expression of Mcl-1 and some IAPs (e.g. XIAP and c-IAP2) (280).

Recently, it has been suggested that the direct target of FL118 is DEAD-Box Helicase 5 (DDX5). FL188 binds and inhibits phosphorylation and expression of DDX5 in colorectal cancer and pancreatic ductal adenocarcinoma (281). DDX5 is an upstream regulator in cancer that positively regulates the expression of survivin, Mcl-1, XIAP and cIAP2 (282).

FL118 inhibits cancer cell growth at concentrations lower than 1 nM (p53-status independent). In *in vivo* studies, FL118 had greater antitumor efficacy without significant toxicity compared to first-line chemotherapeutics (280). The good results obtained in preclinical *in vivo* studies have allowed clinical trials to proceed in patients with colorectal and pancreatic cancer (NCT06206876) (182).

LY2181308 is a single-strand antisense oligonucleotide that binds and degrades survivin mRNA. LY2181308 treatment showed a decrease in survivin mRNA and protein levels, cell cycle arrest, cell-death induction and tumor growth inhibition in several cell lines and human tumor xenografts (283). It has a good safety profile with some clinical benefit (238). LY2181308 presents mixed clinical outcomes, since it shows synergistic benefits in combination with cytarabine and idarubicin for treatment in refractory or relapsed acute myeloid leukemia (284,285) but no benefit against solid tumors if used as a single agent or combined with docetaxel/prednisone (285).

SPC3042 (EZN-3042) is an antisense oligonucleotide with higher potency for survivin mRNA inhibition than former antisense agents (286). SPC3042 not only targets survivin mRNA, but also BCL-2 mRNA. It produces cell cycle arrest, cellular apoptosis and sensitization of prostate cancer cells to taxol treatment, *in vitro* and *in vivo*. As a single agent, it can downregulate 60% survivin mRNA in A549 tumors and Calu-6 lung xenografts models. It also showed 37-45% tumor growth inhibition. Combined with paclitaxel, tumor growth was inhibited in an 83% (287). Despite its anti-tumor effect, the phase I trial was terminated because of dose-limiting toxicity (288).

Other gene therapy-based approaches are, for instance, **Small interfering (si) RNA** against survivin, which combined with temozolomide or etoposide has a synergistic cytotoxic effect in glioblastoma cells (289). Another strategy to inhibit survivin is the combination of **miR-542-3-3p** and paclitaxel, which inhibits tumor growth of HER2-overexpressing breast cancer cells, overcoming chemoresistance (290).

7.4.2.1.5.6.1.2 Protein-protein interaction abrogation

7.4.2.1.5.6.1.2.1 SMAC/DIABLO binding site

SMAC mimetics are small molecules that mimic the binding site of SMAC/DIABLO to IAP proteins, that is, competitors of SMAC/DIABLO for its binding site in IAPs, such as survivin. Hence, SMAC mimetics inhibit IAPs, allowing caspase activation and the consequent apoptotic process. Moreover, as a result of the absence of binding for SMAC/DIABLO in the presence of SMAC mimetics, survivin cannot inhibit the proapoptotic function of SMAC/DIABLO (291).

PZ-6-QN is the first small molecule developed to inhibit the interaction between survivin and SMAC protein in the mitochondria. It was discovered by screening a library of compounds containing phenothiazine derivatives, by fluorescence anisotropy assay. It has been shown to be an effective anticancer agent against leukemia, lymphoma and solid tumors, with an IC_{50} between 2 and 4 µM (292).

GDC-0152 is a SMAC mimetic that inhibits tumor growth in an MDA-MB-231 breast cancer xenograft model. It has been tested in phase I studies for solid tumors in advanced or metastatic stage and no toxicity data was reported, but it presented linear pharmacokinetics in doses ranging from 0.049 to 1.48 mg/kg (293).

LCL161 is a SMAC mimetic that strongly antagonizes IAPs, with antineoplastic activity and good oral bioavailability. It interacts with XIAP, cIAP1, cIAP2 and survivin. Although in previous phase I/II clinical studies for the treatment of multiple types of cancer (myeloma, breast cancer, leukemia, neoplasms, ovarian cancer, colorectal cancer, NSCLC, myelofibrosis and metastatic pancreatic cancer among others) LCL161 (alone or in combination) has shown tolerable toxicity (294), the most recent study, a phase Ib clinical trial with patients with relapsed/refractory SCLC and gynecologic malignancies

treated with LCL161 and topotecan combination revealed more myelosuppression in the combination than alone. Furthermore, the combination did not improve the outcomes. Thus, the study was early terminated (295).

Withanone is a natural product derived from the roots of *Withania somnifera*. It binds to the survivin BIR domain in the same hydrophobic cavity as Smac/DIABLO, interfering with survivin inhibition of caspases (296). Its anticancer properties have been studied in multiple cell lines (297), but we need experimental analysis to confirm that withanone specifically binds and inhibits survivin.

Analogs of **Piperine**, a phenolic component of black pepper, bind to the hydrophobic cavity of BIR domain (298). It inhibits cell growth and induces apoptosis in several cancer cell types (e.g. colon cancer cells) (299). In mouse models, it suppresses tumor growth and metastasis. Studies are needed to determine if the anticancer effect of analogs of piperine is mediated by survivin inhibition.

UC-112 is a potent and selective survivin inhibitor discovered using similarity-based virtual screening for the AVPI peptide in survivin-SMAC crystal complex (300). It presents a potent cell growth inhibition in human melanoma and prostate cancer cell lines. In melanoma xenografts models, UC-112 presented antitumor activity, with little reduction in tumor weight. There was also a strong downregulation of survivin after UC-112 treatment.

New survivin inhibitors have been developed based on UC-112 scaffold, e.g. **MX-106**. It is four times more active than UC-112, with increased selectivity. In *in vivo* experiments, it has shown inhibition of tumor growth and induction of apoptosis in human melanoma xenografts as well as in orthotopic ovarian cancer mouse model (182,301).

Multi-drug resistance (MDR) in colorectal cancer is one of the major reasons for therapy failure (302). ATP-binding cassette (ABC) transporters are involved in drug efflux, which is the major cause of cancer MDR (303). **MX106-4C** (an MX-106 analog) can kill the ATP Binding Cassette Subfamily B Member 1 (ABCB-1)-overexpressing MCR colorectal cancer cells selectively by interacting with these transporters. Zi-Ning Lei et al. suggest there is a functional inhibition of survivin dependent on ABCB-1 transporters and this survivin inhibition induces cell cycle arrest and apoptosis. Further studies are needed to know

the interaction between ABCB-1 and survivin, but these results reveal a great potential of MX106-4C to combine it with conventional anticancer drugs to have a synergistic effect, as well as to re-sensitize tumors to ABCB-1 substrate drugs (304).

7.4.2.1.5.6.1.2.2 HSP-90 (survivin interacting partner)

Hsp90 binds to the BIR domain of survivin through the N domain (305). Hsp90 contributes to the transportation of survivin to mitochondria and preserves survivin stability *in vivo*. **Hsp90-survivin inhibitors** induce proteasomal degradation of survivin. Moreover, blockage of Hsp90-survivin complex formation promotes apoptosis and mitotic defects in cultured cells.

Shepherdin was the first small peptidomimetic that was designed to inhibit Hsp90-survivin complex formation (306). Shepherdin contacts with the N domain of Hsp90. This destabilizes survivin and, as a result, there is a massive death of tumor cells by apoptotic and nonapoptotic mechanisms. Shepherdin not only affects survivin but also destabilizes other proteins that form a complex with Hsp90. However, it does not affect normal cells while it maintains antitumor activity. It also inhibits the interaction of other proteins with HSP60. In *in vivo* experiments, shepherdin inhibited tumor growth without significant toxicity (307).

AICAR (5-aminoimidazole-4-carboxamide ribonucleotide) is a non-peptidic small molecule based on shepherdin. It was produced through structure- and dynamics-based rational design. AICAR directly binds to the N-terminal domain of Hsp90, destabilizing its client proteins, including survivin. It presents antiproliferative and proapoptotic activity in melanoma, prostate and cervical cancer cell lines, and does not affect normal human fibroblasts (308).

7.4.2.1.5.6.1.2.3 Dimerization interface

Monomeric and dimeric forms of survivin coexist in the cell. The homodimeric form is more related to the promotion of mitosis by enhancing tubulin stability (178). The exposition of the hydrophobic interface of dimeric protein causes conformational changes which lead to the destabilization and degradation of the survivin (309). The inhibition of homodimerization by **survivin homodimerization inhibitors** is an interesting strategy to treat cancer, since the homodimerization interface of survivin is

not shared with other IAPs, which means inhibitors of this site may be more selective for survivin.

Abbot 8 is a small soluble compound identified by NMR (Nuclear Magnetic Resonance) and affinity-based screening (310). It allowed the design of **LLP3** and **LLP9**, analogs of Abbot 8 that modulate cell cycle progression and cause mitotic defects, such as impairment of CPC organization and prolonged mitosis in proliferating human umbilical vein endothelial cells (HUVECs) and prostate cancer PC-3 cells, at low nanomolar concentrations. LLP3 also disrupts the complex formed by survivin and the guanosine triphosphate (GTP)ase Ran (Ras-related nuclear protein) (311). Ran is implicated in microtubule stability and mitotic spindle assembly in tumor cells (312). The inhibition of this complex formation leads to survival and growth inhibition of glioma stem cells *in vitro* and *in vivo* (313). A study showed that LLP3 could sensitize colorectal cancer cells to irinotecan (depending on XAF1 proficiency in p53-mutated context). It also showed good efficacy as a monotherapy in a subgroup of colorectal cancer p53-proficient cells and some p53-mutated cells (314).

LQZ-7 is a molecule identified using *in silico* screening. It dissociates survivin dimer *in vitro* and promotes its proteasome-dependent degradation. **LQZ-7F** is an analog that effectively disrupts dimerization, leading to proteasome-dependent degradation, mitotic arrest, induction of spontaneous apoptosis and, consequently, inhibition of cancer cell survival (0.4-4.4 µM). In *in vivo* experiments, LQZ-7F suppressed tumor growth in PC3 xenografts, reduced survivin levels and no significant toxicity was observed in mice (315).

With a similar structure to LQZ-7F, **LQZ-7I** has been recently developed as a specific survivin homodimer inhibitor (316). LQZ-7I induces survivin degradation in a proteasome-dependent way as well as apoptosis in prostate cancer cell lines (C4-2 and PC-3). In *in vivo* experiments, LQZ-7I suppressed tumor growth with little toxicity in a PC-3 xenograft mouse model (316). Moreover, *in vivo* administration of LQZ-7I using the chorioallantoic membrane (CAM) assay reduced tumor size and proliferation of SK-N-AS neuroblastoma cells without discernible toxicity (317).

From LQZ-7F, **LQZ-7F1** was derived, which is more potent than its predecessors and induces spontaneous apoptosis in prostate cancer cells. It inhibits more efficiently

survivin dimerization and induces more survivin degradation through proteasome than LQZ-7F. Moreover, LQZ-7F1 strongly synergizes with docetaxel in inhibiting survival of prostate cancer cells (318).

7.4.2.1.5.6.1.3 Mitosis-related protein inhibitors

Depletion of survivin leads to cell proliferation arrest, sustained prometaphase blockade, chromosomal defects and failure in cytokinesis (319). Moreover, another pool of survivin sustains microtubule stability, contributing to the bipolar spindle assembly. Hotspot residues related to protein-protein interaction were found in survivin (including CPC complex interface) (320) by using *in silico* analysis, resulting in the creation of a pharmacophore model used to virtually screen a database of compounds. Using this model, it was found that **indinavir**, a protease inhibitor used in the treatment of human immunodeficiency virus (HIV), inhibits the interaction of survivin with binding partners (e.g., the CPC complex). Indinavir showed anti-proliferative and apoptotic activity in breast cancer cells by downregulating Aurora B and XIAP and inducing caspase-3 activation. Further investigation is needed to understand the antiproliferative mechanism of action of indinavir (320).

S12 is a small molecule that targets a specific cavity adjacent to survivin dimerization surface. It was identified in an *in silico* study and was designed to inhibit survivin homodimerization (321), although it may also inhibit heterodimerization (322). The binding of S12 to survivin induces conformational changes that disrupt protein function (321). This small molecule alters spindle formation and cell cycle progression, causing the accumulation of cells in the G_2/M phase (321). It has been shown to inhibit growth of hedgehog-driven medulloblastoma cancer cells *in vitro*, as well as of pancreatic xenografts tumors (323).

7.4.2.1.5.6.2 Survivin indirect inhibitors

Dysregulation of survivin expression can be triggered by multiple signaling pathways. The most described are discussed below.

7.4.2.1.5.6.2.1 Cell growth, proliferation and survival

PI3K/AKT pathway is involved in several cellular functions such as cell proliferation, growth and survival. External signals activate tyrosine receptor and class I PI3K is recruited to the plasma membrane. Consequently, it is activated and triggers a cascade of phosphorylation, which activates AKT. AKT pathway have multiple downstream components that control several processes in the cell and is improperly activated in cancer.

One of the mechanisms of the PI3K/AKT pathway to regulate protein expression is by activation of mTOR/Ribosomal protein S6 kinase beta-1 (p70S6K) axis, which induces translation of oncogenic proteins (e.g. HIF-1α) that control cell survival-related genes (including upregulation of survivin) (324). Another mechanism is by MDM2, since MDM2 negatively regulates p53, which is a tumor suppressor that binds to survivin promoter, consequently decreasing survivin expression (216).

Furthermore, AKT negatively regulates the transcription factors forkhead box protein O1 (FOXO1) and O3a (FOXO3a). These transcription factors associate with the survivin promoter, repressing its expression (325).

Finally, NF-κB, upstream regulated by the AKT/inhibitor of NF-κB kinase (IKK) axis, is also associated with transcriptional upregulation of survivin (326,327).

Due to the multiple mechanisms of the PI3K/AKT pathway to induce survivin expression, its inhibition is an important strategy in cancer treatment. In breast cancer, we can find **Herceptin**, **lapatinib** (HER-2 inhibitors) and **AG1478** (EGFR inhibitor) that inhibit survivin expression (328–330). In ovarian cancer, **gefitinib** and **PD153035** are two EGFR inhibitors (331,332) that have also shown to have similar effects. **LY294002** and **wortmannin** inhibit PI3K and have been studied in multiple types of cancer: breast, colon, liver, ovary, lung and leukemia (325,328,331,333–337). **PI-3065** is a small-molecule inhibitor of PI3K delta (PI3K δ) that inhibits growth and metastasis of solid breast cancers (338). It also has anti-tumor effects on hepatocarcinoma cells (339). **SP101** is a novel EGFR inhibitor that suppresses survivin in gefitinib-resistant NSCLC (340).

Other molecules inhibit AKT are **MK-2206**, that blocks survivin in glioma and colon cancer (341); **SH5 inhibitor**, that reduces survivin levels in lung cancer (333) and **AKT inhibitor X**, that reduces survivin levels in prostate cancer (334). mTOR inhibitors, specifically rapamycin, downregulate survivin in glioblastoma, multiple myeloma and prostate cancer (324,342). As inhibitors of NF-κB, we can find **SN50** and **BAY 11-7082**, which inhibit the induction of survivin in endothelial cells (326,343). Cyclooxygenase-2 (COX-2) induces survivin expression through AKT activation in several cancers (e.g. glioblastoma, lymphoma, breast, colon, myeloma and prostate). Thus, inhibitors of COX-2, **celecoxib** and **etodolac**, can revert this survivin induction (344).

Other indirect inhibitors of survivin that affect the PI3K/AKT pathway are **LY294002** (328), **dihidromyricetin** (345), **simvastatin** (synergistic effect with LY294002) (346), **SHP2** (347), **deguelin** (348), **metformin** (349) and **chaperonin-containing TCP-1 (CCT)** (350)**.**

JAK/STAT pathway has a critical role in cell proliferation, differentiation, migration, apoptosis and immunity. It is stimulated by a wide range of cytokines, hormones and growth factors (351). JAK1 can phosphorylate STAT3 on Try705 residue. Then, STAT3 homodimerizes and translocates to the nucleus, where it regulates target genes such as survivin (352).

Dysregulation of JAK/STAT pathway collaborates in cancer development and metastasis (351). In fact, persistent activation of STAT3 increases survivin expression, consequently avoiding apoptosis and inducing resistance to chemotherapy (353).

TG101209 is a JAK2 kinase inhibitor that induces a decrease in survivin expression in leukemia (354). **AG490** (355,356) is another JAK2 inhibitor that downregulates survivin in lymphoma as well as leukemia. We can also find **SD-1029**, another JAK2 inhibitor that downregulates survivin in breast and ovary cancers (357). Other indirect inhibitors of survivin that affect the JAK/STAT pathway are **arctigenin** (358), **ritonavir** (359) and **T21** (360).

MAPK/ERK pathway mediates cellular proliferation, differentiation, survival, development, migration and apoptosis. When the ligand binds to the tyrosine kinase receptor, its cytoplasmic domains dimerize and phosphorylate. Then, adaptor proteins bind to the receptor, which triggers Ras GTPase and, as a result, a cascade of kinases is

activated: MAPK kinase kinase (MAPKKK) Raf (rapid accelerated fibrosarcoma), MAPKK MEK (mitogen-activated protein kinase kinase) and MAPK ERK. Activated ERK is transported to the nucleus where it phosphorylates transcription factors that regulate several target genes such as survivin (361).

MAPK/ERK pathway is involved in cancer progression, especially in proliferation and immune escape (362). Multiple mutations in MAPK/ERK pathway have been identified in tumors, for example in RAS genes (361). EGF, one of the ligands that activate MAPK/ERK signaling pathway, increases survivin levels (363). Therapeutic strategies to reduce survivin levels through the regulation of this pathway are **PD98059** in breast cancer and leukemia (328), **CI1040** in leukemia (364), **PD0325901**, which is derived from CI1040 and prevents the induction of survivin produced by the placental lactogen (332), **U0126**, which strongly blocks MAPK induction of survivin in leukemia (364), breast cancer (335) and keratinocytes (337) and **imatinib**, which inhibits BCR-ABL, hindering MAPK/ERK-induced survivin expression in leukemia (364).

7.4.2.1.5.6.2.2 Cell cycle regulation

In the cell cycle, CDK2/4, which is active in the G_1 and S cell cycle phases, phosphorylates Rb. Then, Rb is relieved from E2F transcription factors, allowing cell cycle transcription. Survivin is positively regulated by E2F1, E2F2, and E2F3 through CDE/CHR dependent mechanism and negatively regulated by E2F4 and E2F5 repressors (222). Another CDK protein important in the regulation of survivin is CDK1/cyclin-B1, which phosphorylates Survivin on Thr34, favoring survivin stability and association with caspases (365).

Some CDK inhibitors can arrest the cell cycle, induce apoptosis and abrogate survivin phosphorylation on Thr34, inducing survivin degradation (366). One example is **purvalanol A**, a specific CDK inhibitor that downregulates survivin through JAK/STAT inhibition in gastric cancer (353,367). **Flavopiridol** is a broad-spectrum CDK inhibitor that impedes Thr34 phosphorylation of survivin, reducing protein levels in cervical cancer. Flavopiridol has shown antitumor activity in phase II clinical trials (368,369). Furthermore, **NU6140** is a CDK2 inhibitor that decreases survivin expression in cervical and ovary cancers (365,370). **Cephalochromin** is a bacterial inhibitor of CDK2/cyclin-E and CDK4/cyclin-D1 pairs, inducing cell cycle arrest in the G_0/G_1 phase and consequently

decreasing survivin expression and inducing apoptosis (371). Finally, **fascaplysin** is a CDK4 inhibitor that downregulates survivin (372).

7.4.2.1.5.6.2.3 Cellular stress: p38MAPK

P38MAPK signaling is involved in inflammation, cell cycle, cell death, development, differentiation and senescence. Environmental stresses, such as ultraviolet radiation (UV) and heat, and inflammatory cytokines produce the phosphorylation of MAPKKKs and the consequent induction of mitogen-activated protein kinase kinase 3 (MKK3), mitogen-activated protein kinase kinase 6 (MKK6) and finally p38MAPK, that activates transcription factors such as p53. Then, p53 regulates several target genes (373), such as survivin.

Celecoxib is a COX-2 inhibitor that can activate p38MAPK route, inducing survivin downregulation in colon cancer cells (371) and glioma cells (374). We can also find **oxaliplatin,** a chemotherapeutic drug that triggers p38MAPK pathway, downregulates survivin and induces proteasomal degradation (375,376).

7.4.2.1.5.6.2.4 Development and differentiation

Transforming growth factor beta (TGF-β) pathway is involved in several cellular functions such as cell growth, proliferation, differentiation, development and migration. Ligand binding to constitutively active TGF-β receptor II (TβRII) induces the recruitment and activates TβRI by phosphorylation. Thus, Smad2 and Smad3 are phosphorylated and form a complex with co-Smad (Smad4) in the cytoplasm. The complex is translocated to the nucleus, where it regulates gene expression, including survivin (377).

TGF-β is an important tumor suppressor, but cancer cells can disrupt this pathway and potentiate the tumor-promoting effects. TGF-β is overexpressed in multiple types of cancer, while inactivating mutations in Smad2 and Smad4 are reported in hepatocellular, colorectal and lung cancer (377). In colon cancer, activation of TGF-β causes the hypophosphorylation of Rb via a Smad3-dependent mechanism, which induces the association of Rb/E2F4, a complex that represses CDE/CHR elements of survivin gene. This promotes survivin downregulation (336,378). Moreover, PKA/A-kinase anchoring protein (AKAP149)/ PP2A produces TGF-β inhibition of PI3K/AKT signaling, reducing

survivin levels (336,378). Furthermore, PKA activates TGF-β, which phosphorylates survivin in Ser20. Consequently, survivin is degraded (378).

Pirfenidone, an approved drug used for the treatment of lung fibrosis, is an example of TGF-β inhibitor that downregulates survivin (379).

Wnt/β-Catenin signaling pathway regulates stem cell pluripotency, differentiation and embryonic development. The activation of Wnt signaling disrupts adenomatous polyposis coli (APC)/Axin/glycogen synthase kinase 3 beta (GSK-3β) inhibitory complex, which ubiquitinates β-catenin. Thus, β-catenin accumulates in the cytoplasm, causing its translocation to the nucleus, where it binds to the lymphoid enhancer-binding factor (LEF)/TCF transcription factors and co-activators (e.g. CBP). These transcription factors regulate multiple genes, including survivin (380).

Wnt and APC are frequently mutated in cancer (380). It has been shown that TCF/β-catenin induces survivin expression in lung, colorectal and breast cancers (380–382).

The drugs that bind to HER-2 receptor (e.g., **herceptin (trastuzumab**) in breast cancer) compromise β-catenin stabilization. As a result, they decrease survivin expression (382). Another example of a drug that affects the Wnt/β-Catenin signaling pathway is **Wnt-2 Ab**, which is an antibody against Wnt2 protein that has been reported to inhibit this pathway in lung cancer (380). **ICG-001** is a β-catenin/CBP disruptor and it downregulates β-catenin and survivin expression in colon cancer (383). Suppression of the Wnt/β-catenin signaling pathway is also induced by **obatoclax**, a pan-BCL-2 inhibitor, which downregulates survivin, inducing apoptosis in human colorectal carcinoma cells (384).

Notch signaling is involved in proliferation, development, differentiation and homeostasis (385). Notch mediates communication between cells through interaction with transmembrane ligands on adjacent cells. Once the ligand binds, γ-secretase produces the cleavage of Notch receptor. Consequently, the notch intracellular domain (NICD) is released and translocated to the nucleus, where it associates with CBF1/Su(H)/Lag1 (CSL) transcription factor and activates Notch target genes, which include survivin (385,386). Hypoxia and Jagged-1 are ligands that activate Notch signaling, increasing survivin expression in lung cancer (387). Aberrant Notch signaling is

associated with tumorigenesis and cancer progression in lung, pancreas and breast cancer (385).

The HIF-1α inhibitor **echinomycin** and inhibitors of γ-secretase (**MRK-003,** a specific peptide inhibitor) decrease survivin expression in lung and breast cancers under hypoxia conditions (386).

7.4.2.1.5.6.3 Survivin vaccines and immunotherapy

The objective of immunotherapy is to produce a direct response of the immune system against the tumor by targeting survivin. Survivin is considered a good target for this therapy due to its high expression in tumor cells (in contrast to protein expression in non-tumor cells) and because it is immunogenic (388). The first survivin vaccine was described by Hirohashi et al. who assessed **survivin-2B80-88**, an 8-amino acid peptide derived from the splice variant 2B that binds to human leukocyte antigen (HLA)-A24 and is recognized by CD8+ cytotoxic T lymphocytes (389). Moreover, *ex vivo*, the lymphocytes from peripheral blood that were stimulated by survivin-2B80-88-pulsed antigen-presenting cells showed cytotoxicity against tumor cells that expressed HLA-A24 and presented endogenously processed survivin-2B peptide. Phase I clinical trial showed good tolerability, but clinical response was limited (390). The good tolerability of this peptide encouraged researchers to optimize this therapeutic strategy.

Nowadays, survivin-targeted immunotherapy refers to different types of cancer vaccines: dendritic cell (DC)-based vaccines, DNA vaccines and peptide vaccines. They induce an immune response against survivin antigen. The good results in preclinical studies lead to perform phase I/II clinical assays, where these vaccines showed good safety profile but moderate effectiveness when used alone (223).

Among them, **SurVaxM** is a conjugated survivin peptide-mimic formed by amino acids 53-67 of the survivin protein. It induced an antitumor immune response against glioma *in vivo* and *ex vivo*. SurVaxM safety and efficacy have been evaluated on eight patients with glioma. Six of them developed well-tolerated cellular and humoral responses. Currently, multiple phase I/II are being carried on using SurVaxM for cancer therapy (glioblastoma, pancreatic neuroendocrine tumor, lung atypical carcinoid tumor, etc.) alone or in combination with pembrolizumab (238).

DPX-Survivac is a survivin-based peptide vaccine tested in multiple phase I/II clinical studies alone or in combination and in several types of cancer (e.g., ovarian cancer, breast cancer, hepatocellular carcinoma and non-small cell lung cancer). DPX-Survivac is approved by the FDA for fast-track evaluation as a maintenance therapy for advanced ovarian cancer (391).

CVD908ssb-TXSNV is a DCs vaccine against survivin. It is a weakened form of a live strain (CVD908ssb strain) of salmonella genetically modified to produce survivin. It presented a strong anticancer activity in mouse models of lymphoma and neuroblastoma. A phase I clinical trial is currently being performed in patients with multiple myeloma (NCT03762291) (392).

Moreover, other survivin-based peptide vaccines are under clinical trials, such as IDO/survivin or hTERT/survivin/CVM multi-peptide vaccine (393). Overall, the outcomes of these studies are encouraging, but there is still work to do before using survivin-based vaccine approaches in the clinics.

7.5 Preliminary results

In order to find therapeutic targets for squamous cell lung carcinoma (SQCLC) treatment, David Martínez-García, a former PhD student of our research group, performed a lung cancer-related gene profiler array to look for gene expression alterations in SQCLC patient samples. The analysis was focused on overexpressed genes that played a role in biological processes that contribute to cancer transformation, mainly dysregulated proliferation and cell death. The proteins of the candidate genes were also assessed for druggability, which includes structure availability, druggable structure features and specific available drugs. The most promising therapeutic target was the BIRC5 gene, which encodes survivin, because it is involved in cell death and mitosis regulation, its crystallographic structure was available, it is a druggable protein, and there are few drug inhibitors available (179).

To develop a new anti-cancer strategy based on survivin inhibition targeting the homodimerization domain, computational methods were used. The anticancer effect of the selected survivin inhibitors was evaluated and the best candidate was chosen to

deeply study its anticancer properties, including the mechanism of action and the assessment of safety and efficacy profiles *in vivo*.

7.5.1 Identification of survivin inhibitors by high-throughput virtual screening (HTVS)

Drug repositioning, also called drug repurposing, consists of identifying new uses for approved or investigational drugs that are not included in the original medical indication. One of the advantages of this strategy is the lower cost (in terms of time and money) to develop a new drug, since most preclinical testing, safety assessment and formulation development is already done. The previous safety data also lowers the failure risk of clinical trials. Hence, the drug can be introduced in the market as soon as enough antitumor effect is established (394,395). There are two different approaches to drug repositioning: experimental and computational approaches. There are two main **experimental approaches**: the identification of relevant target interactions by binding assays (**target-based screening**) or the identification of compounds that produce relevant effects in model systems (without knowing the target), known as **phenotypic screening**. **Computational approaches** consist of selecting potential candidate drugs from chemical libraries and performing *in silico* screening for pre-defined parameters related to structural, pharmacological and toxicological properties (396). There are multiple strategies to undertake the computational approach. One of these strategies is molecular docking, which predicts interactions between the target and the ligand based on the chemical structure (395).

To identify suitable molecules targeting survivin, two high throughput virtual screenings (HTVSs) were run on two publicly available survivin structures focusing on the homodimerization interface. The druggability analysis revealed that the homodimerization site changes its druggability score due to the flipping of one single residue, namely, Phe93. When this change occurs, a deeper cavity is created on the surface, increasing its susceptibility to binding small molecules.

The databases used for the screening were both catalog compounds (Zinc database (397)) and also FDA-approved and experimental drugs (as found in DrugBank version 2015 (398)).

Biological testing revealed promising results for some molecules, especially for asenapine. SPR and cell viability experiments (see below) confirmed its binding to survivin and anticancer activity, prompting a closer look at its binding mode and careful study of its potential interactions with the target (Figure 19).

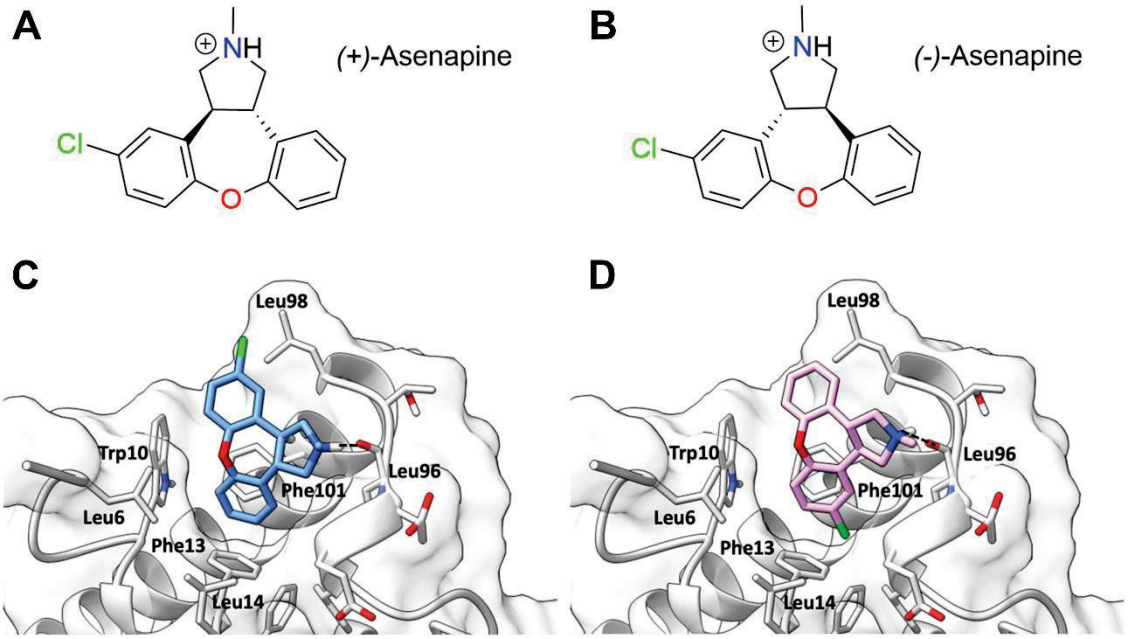

Figure 19. Structures and docking poses of (+)-Asenapine (A and C) and (-)-Asenapine (B and D) at the dimerization interface of survivin (apo X-ray structure of the chromosome passenger complex; PDB identifier: 2QFA).

7.5.2 Evaluation of *in vitro* cytotoxic effect

From more than 8 M compounds screened *in silico*, 7 FDA-approved drugs and 9 small molecules from commercial catalogs were selected for *in vitro* testing, all of them highly ranked. In order to evaluate the potential inhibitory effect of the selected lead compounds on tumor cell proliferation, cell viability 3-(4,5-dimethylthiazol-2-yl)-2,5-diphenyltetrazolium bromide (MTT) assay was performed at different concentrations (5 and 20 µM for FDA-approved molecules; 5 and 50 µM for small-molecules from chemical libraries) in cell lines representative of the cancers with the highest incidence (lung adenocarcinoma A549 and colorectal cancer cells SW620) (Figure 20 and 21).

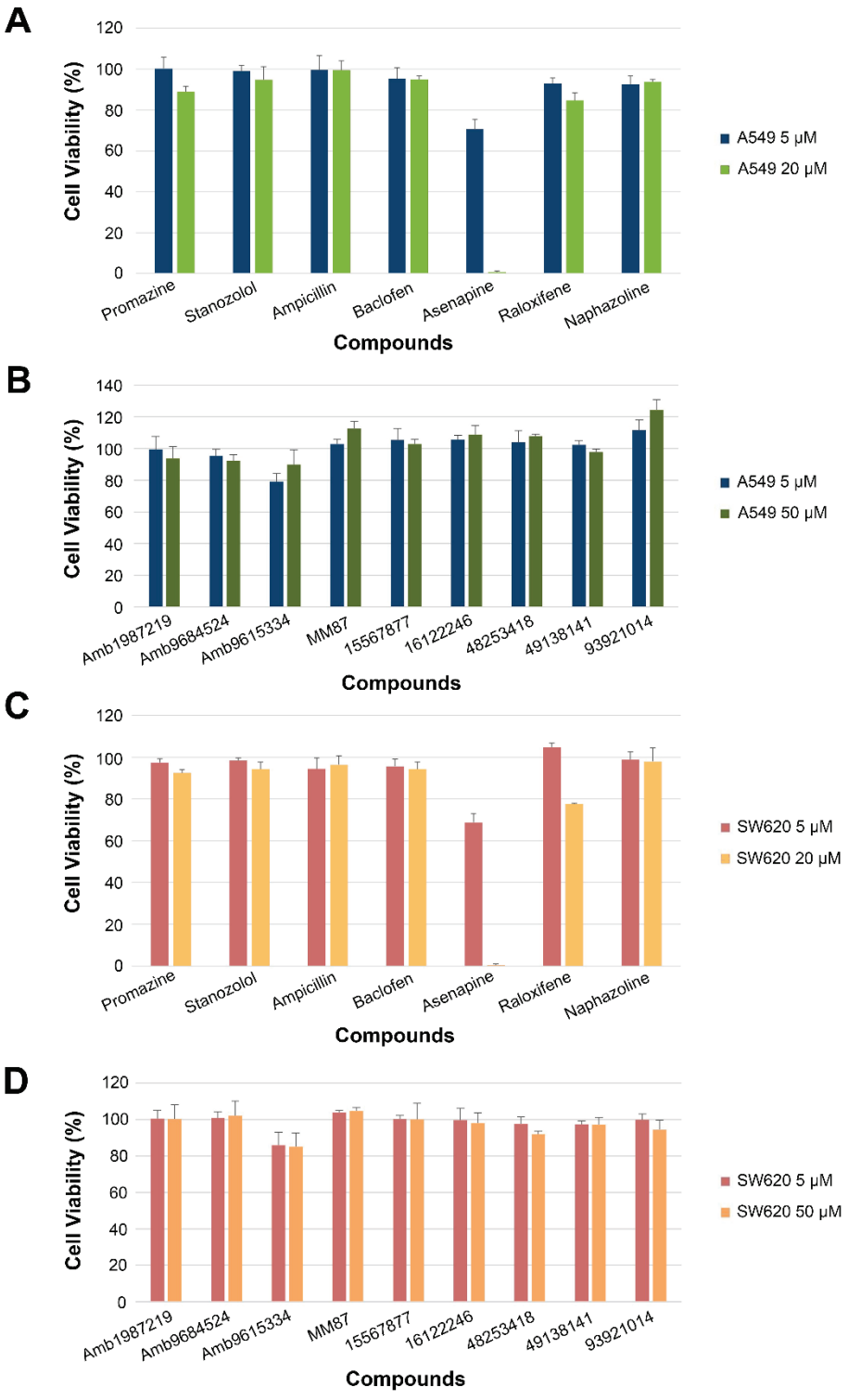

Figure 20. Single point MTT cell viability assay was performed in A549 (A, B) and SW620 (C, D) cancer cells after 24 h of treatment with selected FDA-approved drugs (5 and 20 µM) (A, C) and commercially available small molecules (5 and 50 µM) (B, D) that showed potential binding with survivin in the high-throughput virtual screening and docking studies. Promazine, stanozolol, ampicillin, baclofen, asenapine, raloxifene and naphazoline were supplied by MedChem Express. Amb1987219, Amb9684524 and Amb9615334 were

from Ambinter. MM87 (Abbott 23b) is an in-house re-synthesized compound. 15567877, 16122246, 48253418, 49138141 and 93921014 were supplied by Chembridge.

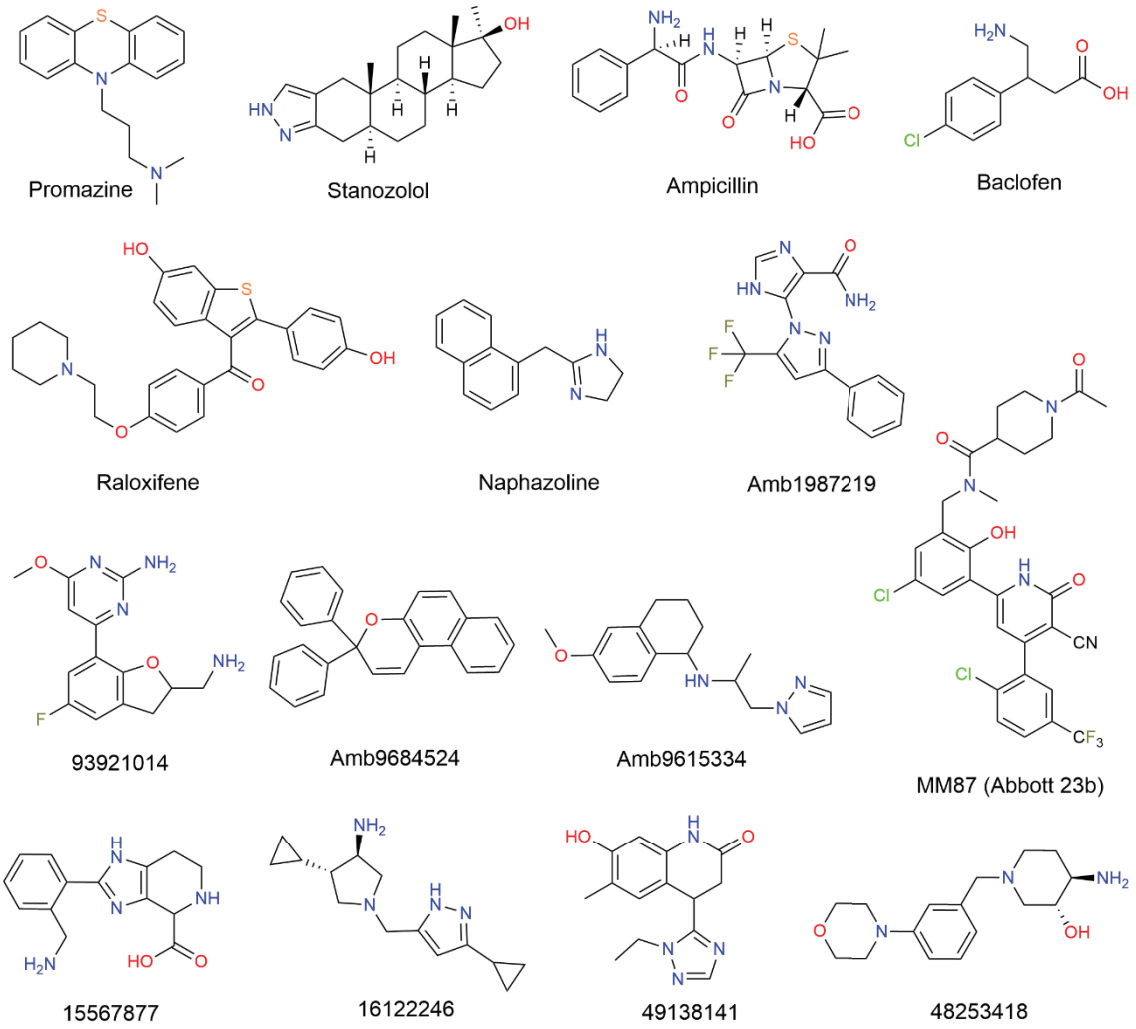

Figure 21. Structures of explored compounds: Promazine, stanozolol, ampicillin, baclofen, asenapine, raloxifene, and naphazoline were supplied by MedChem Express. Amb1987219, Amb9684524, and Amb9615334 were supplied from Ambinter. MM87 (Abbott 23b) was re-synthesized in-house. 15567877, 16122246, 48253418, 49138141, and 93921014 were supplied by Chembridge.

Asenapine was the compound with the most potent cytotoxic effect. To compare the cytotoxic effect of asenapine on healthy and cancer cells, non-tumor human lung fibroblasts HFL-1, as well as A549 and SW620 cells, were treated with different drug concentrations. The cancer cells were more sensitive to asenapine cytotoxic effects than the non-cancer cells (Figure 22).

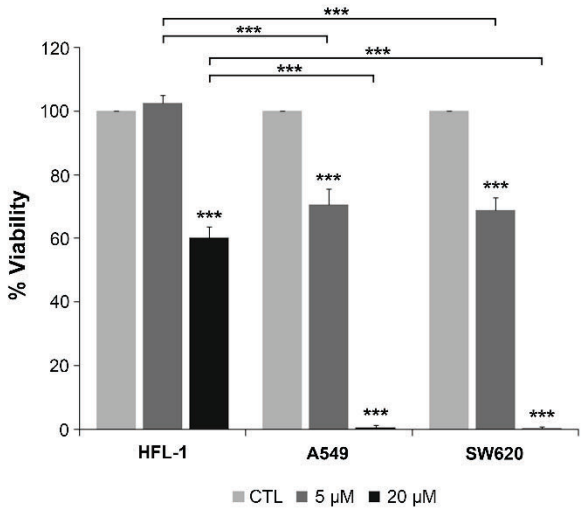

*Figure 22. Asenapine decreased cell viability especially in cancer cell lines. MTT cell viability assay was performed after 24 h of treatment with asenapine at 5 and 20 µM in HFL-1 (non-tumor human lung fibroblast), A549 (human lung adenocarcinoma) and SW620 (human colon adenocarcinoma) cell lines. Data are shown as mean ± Standard deviation (SD). Statistically significant results are indicated as ***, p-value < 0.001.*

To evaluate the potential repositioning of asenapine for cancer treatment, we tested the sensitivity of cancer cells to the formulated form, AM in A549 and SW620 cancer cell lines at concentrations ranging from 0.8 to 100 µM for 24 h (Figure 23). Moreover, since AM can cross the blood-brain barrier due to its tetracyclic structure, the cytotoxic effect of AM in glioblastoma cells U87 MG was assessed for the potential application in brain cancers or brain metastases treatment. Additionally, AM was also tested in two pediatric cancer cell lines (RD and LAN-1) with no current successful clinical treatment, as well as in LLC1 murine lung cancer cells, which are the cells inoculated in the *in vivo* lung cancer model for the assessment of therapeutic efficacy in this project (Figure 23). Altogether, although AM showed less anticancer effect than the active molecule alone, it still maintains a significant cytotoxic effect in all the evaluated cancer cell lines (Figure 23 and Table 1). This result suggests that AM may have potential use as a future anti-cancer drug beyond its antipsychotic properties.

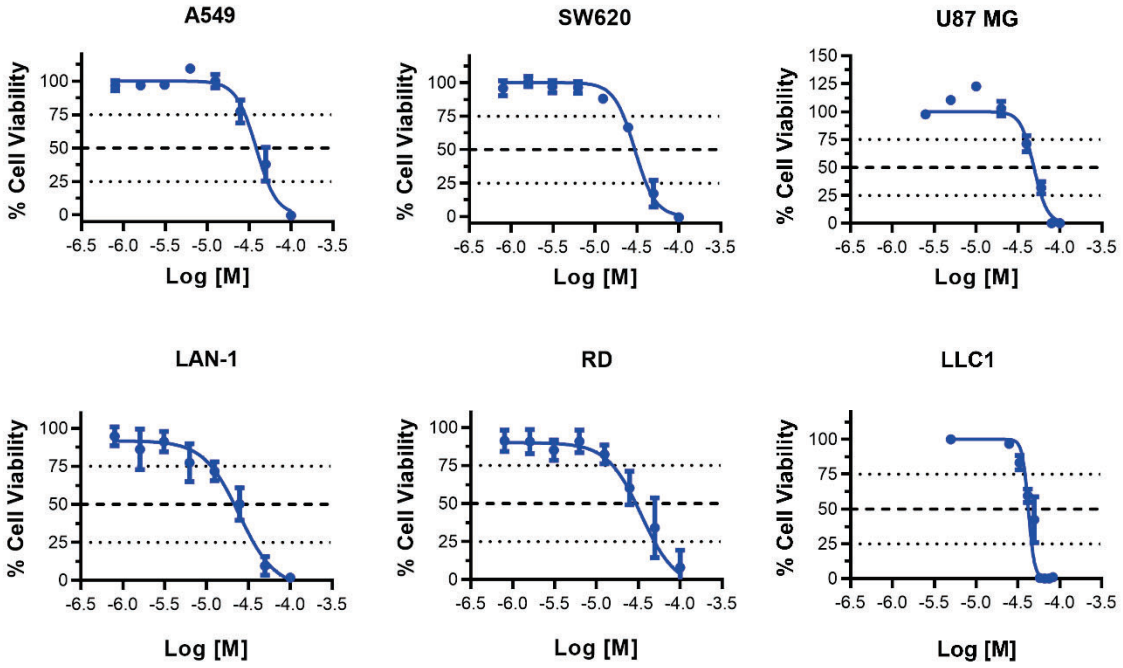

Figure 23. Effect of asenapine maleate (AM) on cell viability. Dose-response MTT cell viability assay after 24 h of treatment with AM at concentrations ranging from 0.8 to 100 µM in A549, SW620, U87 MG (glioblastoma), LAN-1 (pediatric neuroblastoma) and RD (pediatric sarcoma) human cancer cell lines, as well as in murine cancer cell line LLC1 (Lewis lung carcinoma). Data are shown as mean ± SD.

	A549	SW620	U87 MG	RD	LAN-1	LLC1
IC_{50} AM (µM)	40.43 ± 4.88	31.03 ± 2.46	49.52 ± 5.54	35.17 ± 7.74	22.85 ± 3.84	46.15 ± 7.43

Table 1. Half-maximal concentration (IC_{50}) of AM in lung adenocarcinoma (A549), colon adenocarcinoma (SW620), glioblastoma (U87 MG), pediatric neuroblastoma (LAN-1), pediatric sarcoma (RD) human cancer cell lines, and Lewis lung carcinoma (LLC1 murine cancer cells). Data are shown as mean ± SD in µM.

7.5.3 Validation of AM binding to survivin by Surface Plasmon Resonance assay (SPR)

In order to corroborate and characterize the binding of asenapine to survivin, SPR assays were used to monitor its direct interaction. SPR is a real-time interaction analysis that allows kinetics and affinity evaluation and determination of binding specificity between proteins and small molecules. Firstly, the recombinant protein survivin was immobilized on a sensor surface. Survivin ligand was tagged with calmodulin, which was also

immobilized on another sensor surface to use as a reference channel. Next, analytes AM and Abbott23b (the positive control, a survivin inhibitor that binds to the dimer surface of survivin but has bad physicochemical properties) (310) were injected over the sensor surface. Changes in SPR response, expressed in response units (RU), showed the association and dissociation curves of the interactions between survivin and the analytes AM or Abbott23b (Figure 24A), allowing in turn to obtain the affinity curves (Figure 24B). The values obtained reflect affinity of AM to the ligand, suggesting that the small molecule AM forms a complex with survivin.

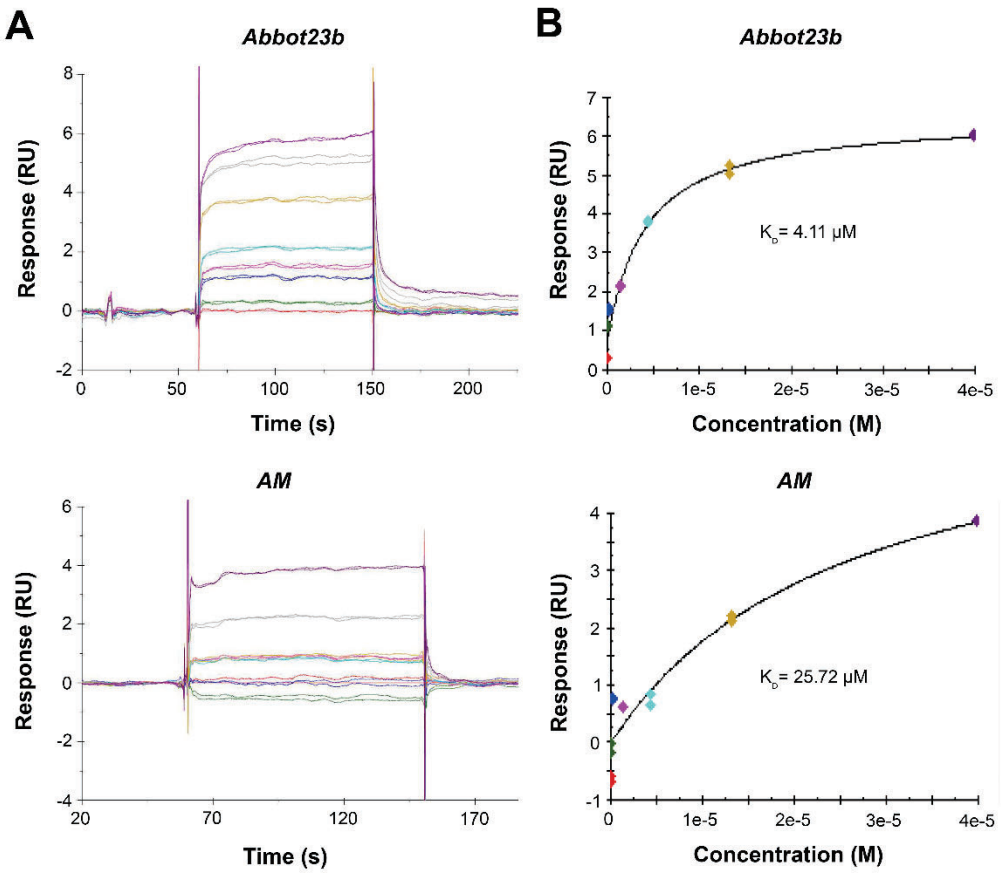

Figure 24. Asenapine maleate (AM) binds to survivin protein. Association and dissociation experimental curves for binding of Abbot23b and AM (concentrations ranging from 0.012 to 40 µM) to immobilized survivin (calmodulin tag) analyzed by SPR as described in methods (A). Affinity curves data (B). RU: Response units; (M): concentration in molar. (K_D): binding constant.

7.5.4 Asenapine maleate (AM)

The novel identified survivin inhibitor AM is an FDA-approved drug that is currently being used in clinics as an atypical antipsychotic for the treatment of psychosis, schizophrenia and schizoaffective disorders, maniac disorders and bipolar disorders as monotherapy or in combination. It is a diabenzo-oxepino pyrrole (Figure 25) that was approved by the FDA in 2009. In the clinics, it is used via sublingual administration.

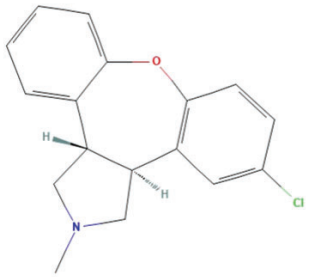

Figure 25. Chemical structure of asenapine. Figure from National Library of Medicine (399).

The most frequently reported adverse drug reactions associated with asenapine are somnolence and anxiety. Hypersensitivity has also been reported (400). Other adverse effects with lower incidence can be abnormal or decreased touch sensation, inability to move the eyes, restlessness, shakiness in legs, arms, hands or feet, trouble with breathing, speaking or swallowing, unusual facial expressions and weakness of arms and legs (401).

Asenapine is a strong antagonist of 5HT2A (serotonin) and D2 (dopamine) receptors. Sedation in patients is associated with the antagonist activity of asenapine at histamine receptors. The extrapyramidal effects that may cause asenapine are associated with the upregulation of D1 receptors, caused by the effects of asenapine on glutamate transmission in the brain.

The primary mode of metabolism of asenapine is direct glucuronidation, mediated by UDP-glucuronosyltransferase 1A4 (UGT1A4), and cytochrome P450 family 1 subfamily A member 2 (CYP1A2) mediated oxidation and demethylation. It is eliminated by urine and feces and has a half-life of 24 h (400,402).

Overall, asenapine is an FDA-approved drug that is currently being used for psychiatric disorders and our group has recently demonstrated that it is a direct survivin binder that possesses anticancer effects. The fact that the preclinical testing, safety assessment and formulation development is already done makes asenapine a good candidate for drug repositioning, since the development of this new anticancer drug would be faster and more economical. Additionally, a direct survivin inhibitor such as asenapine is also a suitable option to be evaluated in combination with other conventional therapeutic strategies, due to the antiapoptotic function of survivin. All these facts prompted us to perform all the preclinical studies needed to evaluate the potential repositioning of asenapine as a new anticancer treatment.

8 HYPOTHESIS

A major challenge in cancer treatment is the ability of cancer cells to evade cell death, a hallmark of cancer that also contributes to treatment resistance. One key factor in this process is the overexpression of anti-apoptotic proteins such as survivin, which has been implicated in multiple tumor types. Survivin plays a dual role in critical cellular processes, promoting cell cycle progression and inhibiting apoptosis. This makes survivin an attractive target for cancer therapies. Several approaches aimed at blocking survivin expression or function have shown promise as potential cancer treatments in preclinical studies. However, their efficacy as standalone treatments has been modest in clinical trials, likely due to incomplete inhibition of survivin. For this reason, we decided to develop a novel survivin inhibitor with a mechanism of action different from the ones previously tested in clinical trials. Thus, we focused on survivin homodimerization domain and identified, through HTVS, the antipsychotic drug asenapine maleate (AM), as a direct inhibitor of survivin, which efficiently binds to this domain. Based on these findings and the previously mentioned premises, we hypothesize that AM will be able to impair tumor growth by disrupting mitosis as well as inducing apoptosis, since the breakdown of survivin homodimerization will trigger its degradation, affecting all its cellular functions. Additionally, since survivin blocks apoptosis, we hypothesize that AM can sensitize cancer cells to conventional pro-apoptotic cancer therapies, such as RDT and chemotherapy.

9 OBJECTIVES

Main objective:

Preclinical development of the novel direct survivin inhibitor asenapine maleate for the treatment of lung cancer, especially in combination with conventional pro-apoptotic therapies.

Specific objectives:

1. **Evaluation of asenapine maleate for the treatment of cancer.**
    a. Extensive evaluation of drug anticancer effects in a wide panel of cellular models of lung and brain cancers.
    b. Characterization of the molecular mechanism of action.
2. **Assessment of combination therapies for tumor sensitization to pro-apoptotic conventional treatments and immunotherapy.**
    a. Evaluation of asenapine maleate combination with currently used chemotherapeutics.
    b. Evaluation of asenapine maleate combination with radiotherapy.
    c. Evaluation of the ability of asenapine maleate to induce immunogenic cell death.
3. **Preclinical evaluation of asenapine maleate as monotherapy and combined therapy for tumor sensitization to pro-apoptotic therapies *in vivo.***
    a. *In vivo* safety evaluation.
    b. *In vivo* efficacy evaluation

10 MATERIALS AND METHODS

10.1 High-throughput virtual screening

A druggability analysis was carried out on the Protein Data Bank (PDB) structures 2QFA (191) and 3UEC (403) using fpocket (404). The DrugBank database (version of 2015) and the ZINC database of 'lead' compounds, composed of 8 M ligands, were prepared using the default settings of LigPrep (Schrödinger Release 2018-1: LigPrep, Schrödinger, LLC, New York, NY, 2018). 2QFA and 3UED were prepared using the default settings of Maestro's PrepWizard (Schrödinger Release 2018-1: Maestro, Schrödinger, LLC, New York, NY, 2018). HTVS was carried out with Glide at the SP level on a grid centered around Phe13 for both crystal structures. The 200 top-scored docking poses from each database were visually inspected and prioritized according to favorable survivin-ligand contacts and electrostatic and shape complementarity.

10.2 Compounds

Asenapine (ref. HY-10121, MedChem Express, Monmouth Junction, NJ, USA) or its formulated form, asenapine maleate (AM) (ref. HY-11100, MedChemExpress), were dissolved in dimethyl sulfoxide (DMSO, ref. D5879, Sigma-Aldrich, STL, USA). Subsequent solutions for biological assays were made in medium for *in vitro* experiments (1% DMSO v/v, ref. D5879, Sigma Aldrich, St. Louis, MO, USA) or in 1X phosphate-buffered saline (PBS, ref. 02-023-5A, Biological Industries, Beit Haemek, Israel) with 7.5% DMSO and 0.8% Tween20 (ref. 28829.296, VWR Prolabo Chemicals, Fontenay-sous-Bois, France) for *in vivo* experiments. The chemotherapeutics used for the combination assays were cisplatin (1 mg/mL, Accord, London, UK), carboplatin (10 mg/mL, ref. C2043, TCI, Tokyo, Japan), paclitaxel (6 mg/mL, Accord, London, UK) and gemcitabine (SUN Pharmaceutical, Industries Europe B.V., Hoofddorp, Netherlands). The FDA-approved compounds used in the single-point cell viability assays were promazine (1032472060), stanozolol (1025149306), ampicillin (1025470147), baclofen (1032119993), raloxifene (1032471356), and naphazoline (1032472098), supplied by MedChemExpress. The small molecules evaluated in single-point cell viability assays were Amb1987219, Amb9684524, and Amb9615334, supplied by Ambinter (Orleans,

France), as well as 15567877, 16122246, 48253418, 49138141 and 93921014, supplied by Chembridge (San Diego, CA, USA).

1-acetyl-N-(5-chloro-3-(4-(2-chloro-5-(trifluoromethyl)phenyl)-5-cyano-6-oxo-1,6-dihydropyridin-2-yl)-2-hydroxybenzyl)-N-methylpiperidine-4-carboxamide (MM87 or compound Abbot 23b as described in (310)) is the compound that was used as a reference in the single-point cell viability assay and the SPR assay since it has a high capacity for interaction with the dimer interface of survivin. However, it presents difficulties reaching the intracellular space. Abbot 23b was re-synthesized in-house.

10.3 Cell lines and culture conditions

10.3.1 Cell lines

The cell lines used in this project are indicated in Table 2. A549, SW620, U87 MG, RD, HFL-1 and LLC1 cell lines were obtained from the American Type Culture Collection (ATCC, Manassas, VA, USA). LAN-1 cell line was obtained from the European Collection of Authenticated Cell Cultures (ECACC, Salisbury, UK).

A549, SW620, U87 MG, and LLC1 cell lines were maintained in Dulbecco's modified Eagle's medium (DMEM, ref. 01-055, Biological Industries) supplemented with 100 U/mL penicillin and 100 µg/mL streptomycin (ref. 03-031-1B), and 2 mM L-glutamine (ref. 03-020-1B), all from Biological Industries, and 10% fetal bovine serum (FBS, ref. A5256701, Gibco^{TM}, Paisley, UK). LAN-1 and RD cell lines were cultured in Roswell Park Memorial Institute (RPMI) (Biological Industries) with 100 U/mL penicillin, 100 ug/mL streptomycin, 2 mM L-glutamine, and 10% FBS. HFL-1 cells were cultured in HAM-F12 (HAM-F12: ref. 01-095, Biological Industries) with 100 U/mL penicillin, 100 ug/mL streptomycin, 2 mM L-glutamine, 1% non-essential amino acids solution (NEAA, ref. 01-340-1B, Biological Industries), and 10% FBS. All cell lines were maintained in 5% CO_2 and 37 ºC conditions. Cells were cultured between passages 10 and 25 and were routinely tested for mycoplasma contamination.

Cell line	Origin
A549	Human epithelial lung adenocarcinoma
U87 MG	Human glioblastoma
SW620	Human colon carcinoma
SW900	Human squamous cell lung carcinoma
DMS53	Human small cell lung carcinoma
RD	Pediatric human rhabdomyosarcoma
LAN-1	Human neuroblastoma bone marrow metastasis
HFL-1	Normal human lung fibroblasts
LLC1	Mouse Lewis lung carcinoma

Table 2. Cell lines used in this project.

10.3.2 3D cultures

In a 96-well plate with BIOMMIEMSYS® hydroscaffold, 2 x 10^4 A549 cells were seeded per well in a volume of 20 µL. Once the drop was diffused in the hydroscaffold, wells were completed at 200 µL with fresh medium. The plate was maintained in the incubator (37 ºC, 5% CO_2) for five days. On the fifth day, cells were treated with 10, 50 and 100 µg/mL of AM. After 24 h of treatment, 20 µL of MTT at 10 µM diluted in PBS 1X were added. The plate was incubated for 2 h at 37 ºC, 5% CO_2. Then, the medium was carefully removed and 100 µL of DMSO were added to each well to solubilize formazan produced by viable cells, as a result of MTT metabolism. Once formazan was solubilized, the absorbance was read at 570 nm. Three independent experiments were performed.

10.3.3 Primary cultures

Lungs were isolated from two transgenic mice that developed lung tumors. A cross-section of the lung of each mouse was done. The tumor sample was washed twice in PBS 1X and the tissue was disrupted mechanically by using forceps and bistouries. The sample was collected with 9 mL of RPMI supplemented with 1% Penicillin/Streptomycin solution. 1 mL of Collagenase Type II (2000 U/mL, C2-BIOC, Sigma-Aldrich) was added to the samples and they were incubated for 2 h at 37 ºC. Once the tumor was disaggregated, the samples were centrifuged at 300 g for 5 min. The supernatant was discarded and the pellet was washed with PBS 1X. The cell pellet was resuspended in 2-4 mL of fresh medium and seeded in a 6-well plate. 24 h later, to reduce the high

presence of erythrocytes, a protocol was followed to lyse those blood cells and allow tumor cells to attach. The content of the well (lung cells, tumor cells, erythrocytes and medium) was collected and washed with PBS. The PBS was also collected. The samples were centrifuged at 500 g for 6 min at 10 ºC. The supernatant was discarded and 500 µL of PBS were added to the cell pellet. Samples were placed on ice and 3 mL of NH_4Cl. Samples were thoroughly resuspended and, after 5 min, they were centrifuged again. The supernatant was removed and the cell pellet was washed with PBS. The cell pellet was resuspended in fresh medium and cells were seeded in a new 6-well plate. Two weeks after this procedure (in which the medium was changed once a week), to isolate tumor cells and to eliminate non-tumor cells, cells were trypsinized for only 30 s in the area where a group of tumor cells was found, and the detached cells were seeded into a new plate. This procedure was repeated once a week until the majority of cells on the plate were tumor cells.

10.4 Immunofluorescence in cell cultures

Primary culture cells were characterized as tumor cells by performing dual immunofluorescence of E-cadherin (a marker of epithelial cells) and vimentin (a marker of mesenchymal cells). To perform this experiment, a 15 mm coverslip previously sterilized was placed in each well of a 12-well plate. 300 µL of FBS were added to each well and the plate was incubated without the lid at room temperature (RT) overnight. Once FBS had dried, cells were trypsinized and seeded at 1 x 10^5 cells/mL. After 24 h, the culture medium was removed and washed with PBS 1X twice for 10 min in agitation. To fix the cells, 4% paraformaldehyde (PFA, previously tempered) was added. 20 min later, the samples were washed with PBS 1X twice in agitation for 5 min. Once cells were fixed, the samples were kept at 4 ºC.

To permeabilize cells, the 12-well plate was tempered and the cells were washed with PBS 1X for 5 min with agitation. Then, 0.2% Triton X-100 was added to each well for 10 min. Another wash of PBS was performed before the blocking, which was done with 3% bovine serum albumin (BSA) in PBS and 5 % goat serum for 2 h at RT with agitation.

The primary antibodies used were for E-cadherin (ref. SC-8426, Santa Cruz Biotechnology Inc., Dallas, TX, USA) and for vimentin (ref. 5741S, Cell Signaling Technology Inc., Danvers,

MA, USA), both used at 1:100 dilution. Drops of the corresponding antibodies were set in a humid chamber and the coverslips were placed on the top of each drop. Cells were incubated with the antibodies at 4 ºC overnight. Later, coverslips were replaced in the 12-well plate and cells were washed three times with PBS 1X for 10 min. Then, the coverslips were placed in the humid chamber again, with anti-mouse 647 (ref. A-21236, Invitrogen, Waltham, MA, USA) and anti-rabbit 488 (ref. 11008, Invitrogen) fluorophore-conjugated secondary antibodies diluted 1:750. After 1 h at RT. The samples were washed with PBS 1X three times for 5 min with agitation.

Fluoromount-G with 4',6-diamidine-2'-phenylindole dihydrochloride (DAPI) (ref. 00-4959-52, Invitrogen) was applied on glass microscope slides, and coverslips were carefully placed on the top of each drop. After 2 h, once the samples were dry, the borders of the coverslips were sealed with transparent nail polish. The slides were stored at 4 ºC until the observation with the optical microscope Carl Zeiss Axio Imager M2 Apotome (Zeiss, Oberkochen, Germany).

10.5 Cell viability assays

The effect of the compounds on cell viability was determined by the MTT colorimetric assay. This method is based on the reduction of the MTT, soluble in water, to insoluble purple formazan crystals by the action of the mitochondrial succinate dehydrogenase in living cells.

To perform these assays, cells (1 x 10^5 cells/well) were seeded in 96-well microtiter plates and incubated for 24 h to allow cell attaching. For single-point cell viability assays, A549 and SW620 cells were treated for 24 h with selected FDA-approved drugs (5 and 20 µM) and small molecules (5 and 50 µM) from available chemical libraries (Figure 20) that showed potential binding to survivin protein in the HTVS and docking studies. We also obtained dose-response curves of AM to calculate the IC_{25}, IC_{50} and IC_{75} of cell populations in different cell lines. For this purpose, cells were treated for 24 h with AM in a concentration range of 0.8-100 µM. Two different approaches were performed. For combination experiments, after 24 h of seeding, cells were treated with AM, cisplatin, carboplatin, paclitaxel or gemcitabine in monotherapy, or with AM plus cisplatin, carboplatin, paclitaxel or gemcitabine simultaneously. Secondly, the sequential

combination treatment was performed by adding cisplatin (to A549 and LLC1 cells) and, 24 h later, adding AM. The concentrations of chemotherapeutics were 0.013-0.1 mg/mL for cisplatin, 0.063-1 mg/mL for carboplatin, 0.005-0.6 mg/mL paclitaxel and 0.25-4 mg/mL for gemcitabine, combined with the corresponding IC_{50} of AM depending on the cell line used. DMSO was used as a negative control at a concentration of 1% (v/v).

In all experiments, 10 µM of MTT (ref. 1003478241, Sigma-Aldrich) diluted in 1x PBS was added to each well after treatment and incubated at 37 ºC for an additional 2 h. Then, we removed the medium and dissolved the MTT formazan precipitates in 100 µL of DMSO. Absorbance was read on a Multiskan™ multiwell plate reader (Thermo Fisher Scientific Inc., Waltham, MA, USA) at 570 nm. For each condition, at least three independent experiments were performed (in duplicate or triplicate). Cell viability was expressed as a percentage of control cells, and data are shown as the mean value ± SD. The IC_{25}, IC_{50}, and IC_{75} values were calculated with GraphPad Prism™ 8 software (Graph Pad Software, San Diego, CA, USA).

In the combination experiments, the Compusyn software was used to generate the combination index (CI), which is defined as the sum of the ratios of the dose of the combination (D1, D2) required to produce a determined percentage of efficacy (x) divided by the dose of the drug alone needed for the same effect (Dx1, Dx2) (Formula 1).

$$CI = \frac{D1}{Dx1} + \frac{D2}{Dx2}$$

Formula 1. Combination Index (CI) calculation. D1 and D2 correspond to the doses of drug 1 or drug 2 that produce x percentage of effect in combination. Dx1 and Dx2 are the doses of each drug alone required to produce x percentage of effect.

Depending on the value of CI, we distinguish different types of interaction: CI < 1 synergism, CI = 1 additive effect, and CI > 1 antagonism.

10.6 Surface Plasmon Resonance assay (SPR)

SPR assays were designed to monitor the interaction between survivin (Calmodulin tag; ref. Abcam87202, Abcam, Cambridge, UK) bound to the chip and the compounds AM and Abbot23b (as analytes). Abbott23b was used as a positive control. Survivin was

immobilized following the Biacore T200 protocol on a sensor chip CM5 (GE Healthcare BioSciences AB) coated with a carboxymethylated dextran matrix that allows a covalent protein attachment by amine coupling. Survivin is tagged with calmodulin; thus, we also immobilized the calmodulin (ref. Abcam78694) ligand alone in the reference channel. A pH scouting was performed before immobilization to determine the optimal pH to pre-concentrate the ligand on the matrix. The ligand was diluted to 1 µM in 10 mM acetate buffers pH 4 and 4.25, and injected during 180 s with a flow of 5 µL/min on an unmodified sensor chip. Then, the surface was regenerated with 50 mM NaOH to ensure no ligand remained bound to the surface. Once the optimum pH was selected, the surface of the sensor chip was activated with a 1:1 mixture of 1-ethyl-3-(3-dimethylaminopropyl)-carbodiimide (EDC) and N-hydroxy succinimide (NHS) to form reactive ester groups on the surface. Subsequently, survivin protein was diluted to 0.05 µg/µL in 10 mM acetate buffer pH 4.25 and immobilized in flow-cell 2 up to 1600 RU. Similarly, calmodulin protein was diluted to 0.05 µg/µL in 10 mM acetate buffer with pH 4 and immobilized in flow-cell 1 up to 1300 RU. The immobilized ligand level was previously calculated according to the relative molecular weights of survivin and the analytes and the maximum binding capacity of the surface with a theoretical R_{max} (maximal response) of 50 RU. Once the immobilization was performed, an ethanolamine solution was injected to deactivate the remaining reactive groups of the surface.

Compounds were stored as a stock solution in 100% DMSO at -20 ºC. The compounds were diluted with running buffer, 1X HBS-P (4-(2-hydroxyethyl)-1-piperazineethanesulfonic acid (HEPES)-buffered saline 0.005% P20) 5% DMSO, at concentrations ranging from 0.012 µM to 40 µM. Afterward, samples were injected in duplicates in both channels at 30 µL/min flow for 90 s and dissociated within 300 s. Moreover, a solvent correction with carefully prepared DMSO reference solutions ranging from 4.5% to 5.8% was run to adjust measured sample responses due to solvent effects on the bulk refractive index variations.

Experiments were performed with the instrument temperature (flow cell, sensor chip, and sample compartment temperature) set to 25 ºC. For affinity evaluation, the Biacore™ T200 evaluation software 2.0 was used to subtract the reference and blank data, correct the solvent, and fit the curve, using the 1:1 Langmuir model.

10.7 Immunoblot analysis

This technique was performed to detect protein modifications (dissociation of survivin dimer or cleavage of proteins) as well as expression of single proteins in cell lysates from cells exposed to different conditions. The immunoblot analysis has been divided into three steps: protein extract preparation, gel electrophoresis plus protein transfer and detection of proteins.

10.7.1 Protein extract preparation

The ability of AM to dissociate survivin dimers was evaluated with a non-denaturing electrophoresis, 1 µg of purified survivin (Abcam) was incubated in PBS with DMSO or with different concentrations of AM (50, 200 or 500 µM).

On the other hand, to determine the molecular mechanism of action of AM, A549 and U87 MG cells were seeded at 1 x 10^5 cells/mL. After 24 h, cells were treated with DMSO (control) or AM (IC_{50}) for 24 h. In the combination experiments, cisplatin (IC_{50}) was added after 24 h of seeding, whereas AM (IC_{50}) was incorporated on the next day for an additional 24 h. Dead cells from culture supernatants were collected and washed with PBS 1X twice. Dead cells were lysed with attached cells using ice-cold lysis buffer containing RIPA lysis buffer (sodium dodecyl sulfate (SDS) 10%, NP40 (IGEPAL®, ref. I8896, Sigma-Aldrich), 0.5% sodium deoxycholate (ref. D6750, Sigma-Aldrich)) with 40 mM β- glycerolphosphete (BGP, ref. 50020, Sigma-Aldrich), 50 mM sodium fluoride (NaF, ref. S1504, Sigma-Aldrich), 1 mM sodium orthovanadate (NaVO4, ref. S6508, Sigma-Aldrich), 1X cysteine protease inhibition cocktail tablet (CIP, ref. 4693159001, Sigma-Aldrich) and 1 mM phenylmethylsulfonyl fluoride (PMSF, ref. P7626, Sigma-Aldrich). Lysate was sonicated, followed by centrifugation at 16000 g for 15 min at 4 ºC. The supernatant was collected and the protein concentration was determined by bicinchoninic acid (BCA) protein assay (ref. 23227, Pierce™, Thermo Fisher Scientific) following the manufacturer's instructions and using BSA protein to create a standard curve that was taken as a reference to calculate protein concentration in our samples, based on their absorbance. The protocol was performed in 96 well plates in duplicate

and absorbance was read with a multi-well plate reader (Multiskan FC, Thermo Fisher Scientific Inc.) at 562 nm.

10.7.2 Gel electrophoresis plus protein transfer

For the non-denaturing electrophoresis, samples were mixed with an equal volume of sample buffer (0.5 M Tris(hydroxymethyl)aminomethane (Tris) pH 8 (ref. 28811.295, VWR), 20% glycerol (ref. 50020, Sigma-Aldrich), 0.005% bromophenol blue (ref. M6769, BioRad, Richmond, CA, USA), 2% Triton X-100 (ref. 9002-93-1, Sigma-Aldrich), 100 mM dithiothreitol (DTT) (ref. D9779, Sigma-Aldrich)) for 30 min at RT. Then, samples were centrifuged at 11000 g for 10 min and the supernatants were separated by electrophoresis in a non-denaturing polyacrylamide gel electrophoresis (PAGE) of 15% polyacrylamide except for the detection of ATM and γATM, in which case the gel was 8% polyacrylamide.

Laemli buffer containing Tris-HCl 250 mM pH 6.8, 10% SDS (ref. L3771-500G, Sigma-Aldrich), 50% glycerol, 0.01% Bromophenol Blue 25% 2-mercaptoethanol (ref. 805740, Merck, Darmstadt, Germany) was added to the samples and then they were boiled at 95 ºC for 5 min. Then, 40 µg of protein extracts were loaded in SDS-PAGE of 15% polyacrylamide. The gels were run at 80 V for 20 min and then, the voltage was changed to 120 V for 90 min approximately in Running Buffer (25 nM Tris, 192 nM Glycine (ref. 50046, Sigma-Aldrich), 0.1% SDS). After that, proteins were transferred to Immobilon-P polyvinylidene difluoride (PVDF) membranes (EMD Millipore, Merk KGaG) using Mini Trans-Blot Cell (Bio-Rad) wet/tank system in Transfer Buffer (25 mM Tris, 192 mM glycine, 20% methanol) at 100 V during 90 min.

10.7.3 Detection of proteins

Membranes were then incubated with the following primary antibodies overnight at 4 ºC (Table 3).

Antibody	Dilution	Produced in	Brand	Reference
GAPDH	1:1000	Rabbit	Cell Signaling	2118
Cleaved Caspase 3	1:500	Rabbit	Cell Signaling	9664
PARP	1:750	Rabbit	Cell Signaling	9542
Survivin	1:1000	Rabbit	Cell Signaling	2808
XIAP	1:500 in BSA	Mouse	Santa Cruz	SC-55550
P53	1:200 in BSA	Rabbit	Santa Cruz	SC-6243
γATM	1:1000	Rabbit	Cell Signaling	13050
ATM	1:1000	Rabbit	Cell Signaling	2873
γH2A.X	1:500	Rabbit	Cell Signaling	9718
H2A.X	1:1000	Rabbit	Cell Signaling	7631
Vinculin	1:200	Mouse	Santa Cruz	SC-25336

Table 3. List of primary antibodies used for Western blot analysis. GAPDH, glyceraldehyde-3-phosphate dehydrogenase; PARP, poly [ADP-Ribose] polymerase; XIAP, X-linked inhibitor of apoptosis protein; ATM, ataxia telangiectasia mutated; BSA, bovine serum albumin.

On the next day, after washing with Tris-buffered saline-Tween 20 0.1% (TBS-T), membranes were incubated with horseradish peroxidase (HRP) conjugated secondary antibodies for 1 h at RT, goat anti-mouse immunoglobulin G (IgG)-HRP (ref. 62-6520, Thermo Fisher Scientific) and goat anti-rabbit IgG-HRP (ref. 7074P2, Cell Signaling Technology Inc.). Images were captured on an Image Quant LAS 500 (GE Healthcare, Buckinghamshire, UK) using ECL™ Western blotting detection reagent (Amersham, GE Healthcare). Band densitometries were retrieved using the Image J software (v1.53t, National Institutes of Health, Bethesda, MD, USA) and Image Studio™ Lite software (v.5.2., LICOR Biosciences, Lincoln, NE, USA). Glyceraldehyde-3-phosphate dehydrogenase (GAPDH) was used as the gel loading control. The results shown are representative of Western blot data analysis obtained from at least three independent experiments except in the case of survivin evaluation after irradiation, where only one replicate was performed.

10.8 Flow cytometry

10.8.1 Cell cycle analysis

Quantification of DNA content by flow cytometry is the most used method to analyze the cell cycle because it allows differentiation of the different phases of the cell cycle. In this assay, cells are treated with a fluorescent dye that stains DNA quantitatively (7-aminoactinomycin D (7-AAD)). Thus, fluorescent intensity registered by flow cytometry corresponds to the amount of DNA that cells have in each phase.

To study the effect of AM on the cell cycle, 1.25 x 10^5 cells/mL were seeded in 6-well plates and, 24 h later, cells were treated with DMSO or AM (IC_{50}). Three independent experiments were performed to obtain the results.

For the cell cycle analysis of cells treated with AM and cisplatin combination, 1.25 x 10^5 cells/mL were seeded. 24 h later, cells were treated with DMSO, AM (IC_{50}), cisplatin (0.03 mg/mL), and the combination of AM (IC_{50}) plus cisplatin (0.03 mg/mL) for 24 h. The findings were obtained from four independent experiments.

In all experiments, cells were collected in a 15 mL tube and centrifuged at 300 g for 5 min. Supernatant was discarded and cell pellet was washed with PBS 1X. The sample was centrifuged again (300 g, 5 min) and the supernatant was discarded. Cell pellet was resuspended in residual PBS and added, drop by drop, into a 50 mL tube containing 1 mL of cold 70% ethanol while vortexing at medium speed to fix cells. Fixed cells were stored overnight at -20 ºC. 200 µL of fixed cells were centrifuged at 300 g for 5 min at RT. Supernatant was discarded and the cell pellet was washed with PBS 1X and centrifuged again (300 g, 5 min). Supernatant was discarded again and the cell pellet was resuspended in 200 µL of Muse™ Cell Cycle Reagent (ref. MCH100106, Luminex Corporation, Austin, TX, USA), which has 7-AAD, and incubated 30 min at RT, protected from light. The reagent forms part of the Muse™ Cell Cycle Kit (ref. MCH100105, Luminex Corporation). All analyses were performed using Muse™ Cell Analyzer and 10,000 events were acquired.

10.8.2 Cell death analysis

One of the physiological changes produced in cells once apoptosis is induced is the externalization of phosphatidylserine (PS) to the cell surface, a component of the cell membrane that is normally localized in the inner cell membrane. Annexin V is a calcium-dependent protein with high affinity for PS. When apoptosis is induced, PS is externalized and annexin V is able to bind to it. This is the principle in which is based the Muse™ Annexin V & Death Cell Assay (ref. MCH100105, Luminex Corporation), which also uses 7-AAD, a death cell marker, as an indicator of cell membrane integrity.

A549 cells at 1 x 105 cells/mL were seeded in 6-well plates to analyze combination therapy effects on apoptosis. After 24 h, cells were treated with DMSO, AM (IC_{50}), cisplatin (0.03 mg/mL) or the combination (cisplatin plus AM) for 48 h. Dead cells from the culture supernatants were collected into 15 mL tubes. The attached cells were washed twice with 1X PBS (retaining the PBS to collect any detached cells), trypsinized, and then combined with the dead cells in the same tube. Samples were centrifuged at 300 g for 5 min. The supernatant was discarded and the cell pellet was washed with PBS 1X. Then, samples were centrifuged again (300 g, 5 min). Once more, the supernatant was discarded. The cell pellet was resuspended in fresh medium with a final concentration of 1 x 10^6 cells/mL. 100 µL of cells in suspension were added to fresh 1.5 mL Eppendorf tubes, together with 100 µL of Muse™ Annexin V & Dead Cell Reagent. Then, samples were mixed and incubated for 20 min at RT in the dark. The analysis of the samples was performed using Muse™ Cell Analyzer (Merck) and 10,000 events were acquired. The findings were obtained from four independent experiments.

10.8.3 Calreticulin

CALR is an endoplasmic reticulum-resident chaperone exposed at the cell surface when the cell succumbs to ICD. CALR exposure promotes phagocyte uptake of cell corpses and the initiation of anticancer immunity. This makes CALR exposure an important hallmark of ICD.

In order to analyze CALR membrane exposure on AM-treated cells, A549 and LLC1 cells (1 x 10^5 cells/mL) were seeded in 6-well plates. After 24 h, cells were treated with AM at concentrations corresponding to AM IC_{25}, IC_{50} and IC_{75} for 24 h. On the next day, the

medium with dead cells was collected in a 15 mL tube. Attached cells were washed with PBS 1X, which was also added to the tube and cells were trypsinized. Detached cells were added to the tube containing the other cells with the same treatment. The wells were washed twice with PBS 1X to ensure all cells were collected. Samples were centrifuged at 500 g for 6 min. The supernatant was removed, and the pellet was resuspended in 600 µL of 1X PBS. The samples were then distributed into cytometry tubes. To recover the maximum number of cells, 1 mL of 1X PBS was added to the 15 mL tube, and these cells were also distributed into the cytometry tubes. All samples were vortexed and centrifuged at 500 g for 6 min. The supernatant was discarded and cells were incubated 1 h at RT with CALR phycoerythrin (PE)-conjugated monoclonal antibody (1:70, ref. ADI-SPA-601PE-F, Enzo Life Sciences Inc., Farmingdale, NY, USA). 1 mL of PBS-BSA 1% was added to each tube to wash cells. Then, samples were vortexed and centrifuged 6 min at 500 g, and the supernatant was discarded. Washing and centrifugation was repeated and then the secondary antibody was added (anti-rabbit 488, 1:1000 in PBS-BSA 1%, ref. A-11008, Invitrogen). Samples were vortexed and incubated 30 min at 4 ºC. Then, cells were washed twice with PBS-BSA 1%. 1 mL of PBS 1X was added to each tube for the analysis. Death cells were labeled with 7-AAD viability staining solution (ref. 00-6993-50 eBioscience™, Thermo Fisher Scientific). Flow cytometry was completed using a FACS Canto II™ (BD Biosciences, Franklin Lakes, NJ, USA) taking 10,000 events for each condition. The mean fluorescence intensity of PE-CALR was analyzed by BD FACSDiva™ Software. The findings were obtained from four independent experiments.

10.9 Radiotherapy

Cells were seeded at a density of 5 x 10^4 cells/mL (when the experiment included 24 h pretreatment conditions) or 1 x 10^5 cells/mL (when the pretreatment was performed just 1 h before irradiation), in p60 or p100 plates and incubated for 24 h to allow them to attach. Cells were then treated with AM for 1 h or 24 h before irradiation. Irradiation was repeatedly performed using an X-ray accelerator (TrueBeam 3320, Varian Medical Systems Inc., Palo Alto, CA, USA) at 2 Gy/fraction to achieve a total dose of 2 Gy, 4 Gy or 8 Gy. A non-irradiated control was also included in all the experiments. Afterwards, cells were incubated for 24 h and then handled differently according to each particular

experiment. At least three independent experiments were performed, except in the case of survivin expression evaluation 2 h and 24 h after the combination treatment, where the experiment was performed once.

10.10 Clonogenic assay

This assay is based on the ability of a single cell to form a colony by undergoing its division. In this project, the clonogenic assay was undertaken to study the effect of AM and RDT. For this purpose, cells were collected 24 h post-irradiation and plated into 6-well plates at a density of 200 and 400 viable cells/well. After 12 days of incubation at 37 ºC in a humidified incubator with a 5% CO_2 atmosphere, the medium was removed and colonies were carefully washed with PBS 1X. Cells were fixed and stained using a mixture of glutaraldehyde (6% v/v) and crystal violet (0.5% w/v) for 20 min at RT. Subsequently, the fixing solution was removed and colonies were washed carefully with distilled H_2O (dH_2O). Finally, colonies were counted and photographed. Three independent experiments were conducted.

10.11 HMGB1 release determination

When cancer cells undergo ICD, the permeabilization of the lamina and the plasma membrane enables the translocation of HMGB1 from the nucleus to the cytoplasm and its liberation to the extracellular space. Once HMGB1 is released, it binds to TLR4 on DCs and potentiates the presentation of tumor antigens from dying cancer cells. HMGB1 is used as a biomarker for plasma membrane permeabilization, since it is not only released in immunogenic but also non-immunogenic variants of cell death.

A549 (5×10^4 cells/mL) cells were seeded in a 6-well plate. After 48 h, we treated cells with AM for 24 h at concentrations corresponding to AM IC_{25}, IC_{50}, and IC_{75} in A549 cells. Cell culture supernatants were collected and stored at -80 ºC. On the one hand, HMGB1 release was quantified in cell culture supernatants with the HMGB1 express enzyme-linked immunosorbent assay (ELISA) (#30164033, TECAN, Hamburg, Germany). This is an enzyme immunoassay for the quantitative determination of HMGB1. The wells of the microtiter strips are coated with anti-HMGB1 antibody. HMGB1 of the samples binds

to the immobilized antibody and is recognized by a second enzyme-marked antibody. After the substrate reaction, HMGB1 concentration is determined by color intensity.

Firstly, to perform this assay, a standard curve was prepared. Samples were diluted (10 µL of sample and 400 µL of diluent) and 100 µL of the mix were pipetted into the wells of the microtiter plate. The plate was incubated for 2 h at 37 ºC. After that, the incubation solution was discarded and wells were washed five times with 400 µL of diluted Wash Buffer. Then, 100 µL of Enzyme conjugate was added into each well and samples were incubated 1 h at 25 ªC. The solution was discarded and 100 µL of Color solution was added with an 8-channel micropipette. The plate was incubated for 20 min at RT in the dark. The color reaction was stopped by adding 100 µL of Stop solution and mixing with gently shaking. Optical density was measured at 450 nm (within 60 min after pipetting stop solution) with Microplate reader FLUOstar® Omega (BMG Labtech, Mornington, VIC, Australia). Three experiments were carried out independently.

10.12 ATP release determination

During ICD, ATP is released through active exocytosis of ATP-containing vesicles via pannexin channels, which is a large pore formed by the proteins pannexins that facilitate the diffusion of a variety of substrates. Extracellular ATP works as a “find-me” signal for DC precursors and macrophages, leading to the recruitment of myeloid cells to the sites of active ICD. Extracellular ATP also mediates pro-inflammatory effects that culminate in the activation of T cells. Like HMGB1, ATP release can occur in both immunogenic and non-immunogenic variations of cell death.

ATP release was determined in cell culture supernatants with RealTime-Glo™ Extracellular ATP Assay (Promega, Madison, WI, USA). This assay is based on the following reaction:

ATP + D-luciferin + O_2 → Oxyluciferin + AMP + PPi + CO_2 + Light (560 nm)

The intensity of the emitted light is proportional to ATP concentration. To perform this experiment, an ATP standard curve was made on the same day. 100 µL of sample was mixed with 100 µL of rL/L Reagent and, rapidly, the ATP-derived luminescent signal was

detected on multi-mode microplate reader FLUOstar® Omega in five reading cycles of 1 min duration. Seven independent replicates were performed.

10.13 Histological analysis

This type of analysis allowed us to evaluate the expression of specific proteins on mice tumors obtained in the *in vivo* experiments.

10.13.1 Sample processing

Subcutaneous tumors were isolated and washed in PBS 1X. Then, they were fixed in formalin 10% (ref. HT501128, Sigma-Aldrich) for 24 h. Then samples were processed following the steps indicated in Table 4. To include the samples in paraffin, dehydrating cells was necessary because paraffin is hydrophobic. Then, ethanol should be removed, since ethanol and paraffin are not miscible.

Washing	PBS 1X	30 min
	PBS 1X	1 h
Dehydration	Ethanol 30%	1.5 h
	Ethanol 70%	1.5 h
	Ethanol 96%	1.5 h
	Ethanol 100%	1.5 h
	Ethanol 100%	2 h
Clearing	Xylene	1.5 h
	Xylene	2 h
Infiltration	Paraffin wax	3 h
	Paraffin wax	6 h

Table 4. Sample processing for paraffination. PBS, phosphate-buffered saline.

Then, samples were embedded into a plastic cassette by using a mold and adding paraffin. Once paraffin was solidified, the blocks were kept 1 h at 4 ºC to be able to remove the mold. Samples were stored at RT.

Finally, the blocks were sectioned with a microtome at 5 µm. The sections were placed in a water bath and then were placed in glass slides pre-treated with polylysine.

10.13.2 Sample staining

10.13.2.1 Immunohistochemical staining

10.13.2.1.1 Survivin Immunohistochemistry

Samples were deparaffinized in a drying oven for 30 min at 60 ºC. Then, they were immersed in xylene followed by a decreasing concentration of alcohol to rehydrate samples. Afterward, antigen retrieval was carried out using 10 mmol/L sodium citrate buffer with 0.05% Tween-20 in the microwave at sub-boiling temperature, 95–98 ºC, for 20 min and slides were washed twice with dH_2O for 5 min each time. Endogenous peroxidase was blocked by incubation in 3% H_2O_2 for 5 min at RT followed by two washing steps for 5 min, with dH_2O and PBS, respectively. Slides were blocked with normal goat serum in a 1:30 dilution for 1 h at RT and incubated with anti-survivin antibody (ref. 2808, Cell Signaling Technology Inc.) diluted 1:200 in PBS overnight at 4 ºC in a wet chamber. Afterward, slides were washed three times in PBS 0.1% Tween-20 for 5 min each and incubated with biotin-conjugated secondary antibody (ref. 711-066-15, The Jackson Laboratory, Bar Harbor, ME, USA) at 1:200 dilution in PBS 0.1% Tween-20 for 1 h at RT. Later, we added streptavidin coupled with HRP (ref. 016-030-084, The Jackson Laboratory) at 1:250 dilution in PBS for 20 min, at RT. Then, slides were washed three times with PBS for 5 min each and the signal was developed by incubation with DAB (3,3'-diaminobenzidine) (ref. D8001, Sigma-Aldrich) for 10 min at RT. Finally, slides were washed for 5 min with dH_2O, counterstained with Hematoxylin (ref. A3865, PanReac AppliChem, Glenview, IL, USA), dehydrated, and mounted with DPX (ref. 100579, Merck). Samples were observed in a Nikon Eclipse E800 microscope and images were taken.

10.13.2.1.2 CD3 and CD8

The Pathological Anatomy Services at Hospital de Bellvitge performed immunohistochemical staining for CD3 and CD8 to evaluate immune cell infiltration in mouse tumor samples.

The first step for immunohistochemistry for CD3 was the deparaffinization of the samples by heating the slides at 60°C for 8 min. Next, the slides were heated to 72°C. The following step was antigen retrieval, for which ULTRA Conditioner #1 (CC1) was used. Then, the samples were heated to 95°C and incubated with the reagent for 8 min. Subsequently, ULTRA CC1 treatment was continued at intervals of 20, 36, 52, and 64 min. Once antigen retrieval was completed, a drop of anti-CD3 (2GV6) antibody (Ref. 790-4341) was applied to each sample, and then they were covered with a coverslip and incubated for 32 min. After incubation, a wash was performed with ULTRA Wash.

To perform immunohistochemistry for CD8, first, samples were prepared by deparaffinizing the slides at 72°C. The following step was antigen retrieval, for which ULTRA Conditioner #1 (CC1) was applied. Then, samples were heated to 95°C and incubated with the reagent for 8 min. Furthermore, ULTRA CC1 treatment was continued at intervals of 20 and 36 min. Once conditioning was completed, each sample received a drop of anti-CD8 (SP57) antibody (Ref. 790-4460) and then covered with a coverslip for a 32-minute incubation. Afterward, a wash was performed with ULTRA Wash.

For counterstaining, a drop of Hematoxylin was applied to each sample and they were covered with a coverslip, leaving them incubating for 12 min. Finally, in the post-counterstaining stage, Bluing Reagent staining was performed for 4 min. This protocol was performed using BenchMark ULTRA PLUS equipment and reagents from Roche Diagnostics (Basel, Switzerland).

Finally, lymphocyte infiltration in these samples was evaluated using the optical microscope Carl Zeiss Axio Imager M2 Apotome.

10.13.2.2 Immunofluorescence staining

10.13.2.2.1 CD31

CD31, also named platelet endothelial cell adhesion molecule (PECAM), is a protein found on the surface of endothelial and immune cell membranes and is crucial for the interaction between vascular and immune systems. In this study, CD31 is used as a marker for angiogenesis and microvessel density.

Like in the immunohistochemistry staining, samples were deparaffinized in a drying oven for 30 min at 60 ºC. Then, they were immersed in xylene followed by a decreasing concentration of alcohol to rehydrate samples. Afterward, antigen retrieval was carried out using 10 mmol/L sodium citrate buffer with 0.05% Tween-20 in a pressure cooker. We turned off the heat once the pressure cooker started beeping and waited for 20 min to let the samples cool down. Slides were washed with PBS 1X for 5 min. Samples were incubated in 3% H_2O_2 for 15 min at RT followed by four washing steps for 5 min, one with dH_2O and three with PBS. Normal goat serum in PBS (1:30) was added and slides were incubated for 1 h at RT. Afterward, goat serum was discarded and an antibody for CD31 was added (ab28364, Abcam), diluted 1:30 in PBS. Samples were incubated overnight at 4 ºC. The next day, donkey anti-rabbit 555 (ref. A31572, Thermo Fisher Scientific) was added to the samples diluted 1:500 in PBS and the slides were incubated 2 h at RT in the dark. After the incubation, samples were washed three times in PBS 0.1% Tween-20 for 5 min each. Later, a drop of Fluoromount-G with DAPI (Invitrogen, ref. 00-4959-52) was applied on the sample and a coverslip was placed on the top. Once samples were dry, they were stored at 4 ºC until the observation with the optical microscope Carl Zeiss Axio Imager M2 Apotome.

10.14 *In vivo* experiments

All animal studies were carried out in accordance with EU Directive 2010/63/EU for animal experiments and protocols were approved by the Local Ethics Committee (Generalitat de Catalunya) under the protocol number 10928.

In order to estimate the minimum number of animals required to find significant differences among groups at a p-value of 0.05 and confidence interval of 95%, sample size was determined by using a Microsoft Excel spreadsheet “LaMorte’s Power Calculator” (405).

10.14.1 Safety evaluation of AM

For the AM safety evaluation assay, ten-week-old C57BL6 mice were separated into 4 different groups (4 mice/group): vehicle (V) (7.5% DMSO and 0.8% Tween-20 in PBS), 10, 15 and 20 mg/kg AM. The treatment was intraperitoneally injected once a day in a 5-days-on/2-days-off schedule. Body weight was recorded daily until the end of

the treatment. Once mice were sacrificed, blood, liver, kidneys, spleen and brain were extracted and weighed. Organs were fixed in formalin at 4 ºC for 24 h. Then, the samples were processed for hematoxylin-eosin (H-E) staining and were analyzed on the microscope (Nikon Europe BV, Badhoevedorp, The Netherlands).

10.14.1.1 ALT activity

On the day of the sacrifice, blood was extracted through cardiac puncture. Sodium citrate (3.2%, ratio of 9 parts of blood to 1 part of citrate) was used as an anticoagulant. The blood samples were used to evaluate ALT activity using the kit ALT Activity Assay (ref. MAK052, Sigma-Aldrich).

Samples were diluted 1:2 in ALT Assay Buffer and pyruvate standards were prepared according to manufacturer instructions. Samples, standards and positive controls were added to a 96-well plate (20 µL/well). Master Reaction Mix was added to each well. Wells were mixed using a horizontal shaker. After 2-3 min, an initial measurement was taken at 570 nm absorbance. Then, the plate was incubated at 37 ºC protected from light. Measurements were taken every 5 min until the value of the most active sample was higher than the value of the highest standard. The change in measurement was calculated following Formula 2.

$$\Delta A_{570} = (A_{570})_{final} - (A_{570})_{initial}$$

Formula 2. Calculation of change in measurement of ALT activity. A, absorbance.

The ΔA_{570} value of the samples was compared to the standard curve to determine the amount of pyruvate generated between initial and final measurements. The ALT activity of each sample was determined using Formula 3.

$$ALT\ Activity = \frac{B\ x\ Sample\ Dilution\ Factor}{\left(T_{final} - T_{initial}\right)\ x\ V}$$

Formula 3. Determination of ALT activity. $T_{initial}$, time of first reading (min); T_{final}, time of penultimate reading (min); B, amount of pyruvate generated between $T_{initial}$ and T_{final} (nmol); V, sample volume added to the well (mL).

10.14.2 Efficacy evaluation of AM

For the therapeutic efficacy evaluation of AM, a subcutaneous mouse model was used and 100 µL of 5 x 10^4 LLC1 cells in PBS:Corning® Matrigel® (Cultek, Spain) (1:1) were inoculated into the mice's right flank. We started the treatment when the tumors were palpable. For this experiment, tumor-bearing mice were separated into 2 groups and treated with V or 10 mg/kg of AM (n=6). The treatment was administered once a day on a 5-days-on/2-days-off schedule for 22 days (Figure 26).

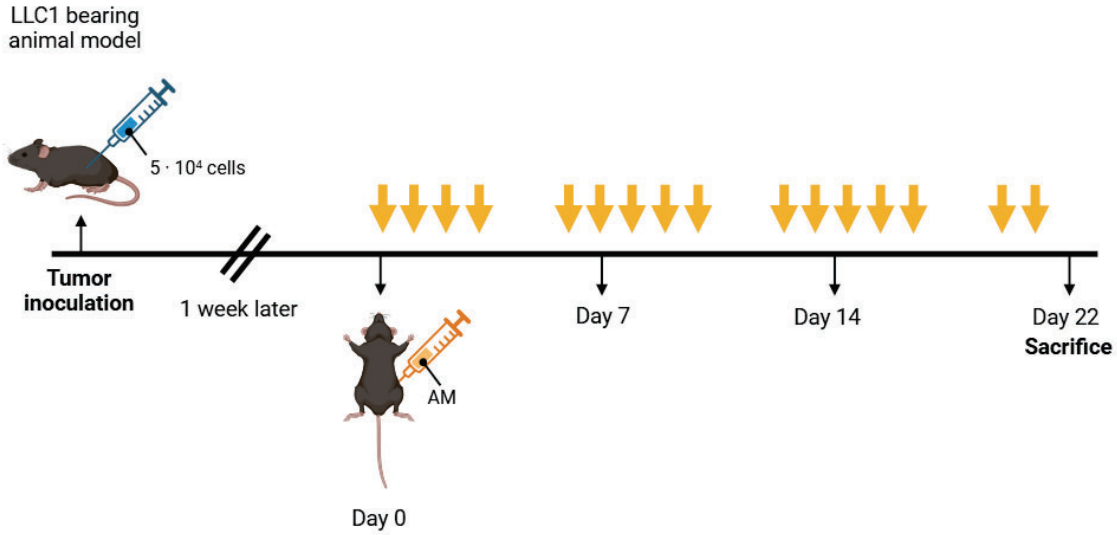

Figure 26. Diagram of the therapeutic efficacy experiment of asenapine maleate (AM). Orange arrows represent AM administrations (10 mg/kg). Created in https://BioRender.com.

Body weight and tumor volume were recorded daily. Tumor volume was evaluated every weekday using a caliper and calculated by Formula 4.

$$Tumor\ volume = \frac{(width^2\ x\ length)}{2}$$

Formula 4. Tumor volume calculation in in vivo *experiments.*

Mice were sacrificed and tumors were extracted and weighed. Tumors were kept in PBS until all of them were collected and then they were photographed. Tumors were fixed in formalin 10% at 4 ºC. After 24 h, samples were cut in 5 µm sections and were processed for H-E staining and immunohistochemistry.

10.14.3 Efficacy evaluation of AM and cisplatin combination in an ectopic model

In the case of the combination efficacy assay, there were 4 groups of treatment: V, 5 mg/kg of AM, 3 mg/kg of cisplatin and the combination of AM plus cisplatin (5 mg/kg and 3 mg/kg, respectively) (n=9). Cisplatin was administered on days 0, 3 and 6 of treatment. Once cisplatin administration was finished, we started with daily doses of AM (5-days-on/2-days-off schedule). This experiment finished 18 days after the first drug administration (Figure 27). As in the monotherapy experiment, body weight and tumor volume were recorded daily. Tumor volume evaluation and tumor processing methodologies were the same as in the AM monotherapy efficacy evaluation experiment.

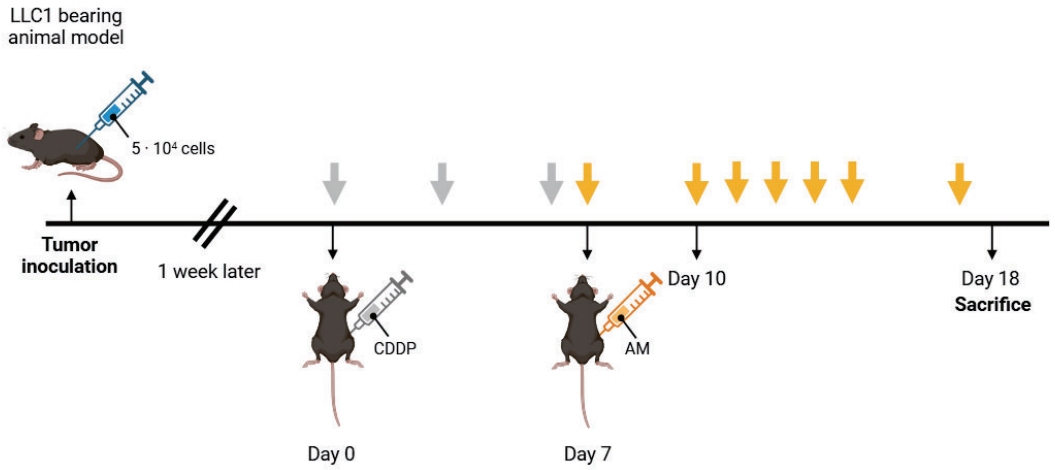

Figure 27. Diagram of the therapeutic efficacy assessment of asenapine maleate (AM) and cisplatin (CDDP) combination in C57BL/6J mice. Grey arrows correspond to CDDP administrations and orange arrows correspond to AM administrations. Created in https://BioRender.com.

10.14.4 Efficacy evaluation of AM and cisplatin combination in transgenic mice model

AM and cisplatin combination therapeutic efficacy was evaluated in a KRasG12D transgenic mice model, which was kindly provided by Tyler Jacks (MIT, Massachusetts Institute of Technology) and Laura Soucek (VHIO, Vall D'Hebron Institute of Oncology). This model presents an oncogenic mutation in KRAS (gly → asp in codon 12) and an LSL cassette (transcriptional and translational stop elements flaked by LoxP sites) into the first intron of KRAS gene. These elements prevent the expression of the mutant allele until the stop elements are removed by Cre recombinase. Thus, cancer may be initiated

after inhalation of viruses expressing Cre recombinase. The activation of the oncogenic KRAS allele initiates small lung tumors with no metastases, limited tumor progression and long survival. The virus system used in this experiment was provided by the Viral Vector Production Unit (UAB), Prep# UPV-757 23/10/2014.

5 x 10^7 plaque-forming units (PFU) were administered per mouse, resuspended in Eagle's minimum essential medium (EMEM) (ref. 30-2003, ATCC) with 12 mM $CaCl_2$, total volume administered being 30 µL/mouse. Once the virus was prepared, the mix was incubated for 20 min at RT to allow the formation of precipitates (of $CaCl_2$ with the virus).

Mice were anesthetized with a mixture of ketamine (80 mg/kg) and xylazine (10 mg/kg), diluted 1:2 in physiological serum. Anesthetics were administered by intraperitoneal injection. Once mice were anesthetized, the virus preparation was administered holding a pipette tip over one nostril and dispensing dropwise until the volume was inhaled. After 13 weeks, treatment administration started. 44 mice were divided into 4 groups. The treatment groups were V, 5 mg/kg of AM, 3 mg/kg of cisplatin and the combination of AM plus cisplatin (5 mg/kg and 3 mg/kg, respectively). Cisplatin was administered on days 0, 3 and 6 of treatment. Once cisplatin administration was finished, we started with daily doses of AM (5-days-on/2-days-off schedule). Mice weight was monitored every weekday until the end of the experiment. This experiment finished 36 days after the first drug administration. Then, animals were sacrificed and lungs were isolated, weighed, photographed and processed for H-E staining (Figure 28).

Microscopic images of complete lung slices at three different heights were taken with the optical microscope Carl Zeiss Axio Imager M2 Apotome. Then, the percentage of area with cells in the sample was calculated by adding a color threshold to select the specific area of the image by using Image J software (v1.53t).

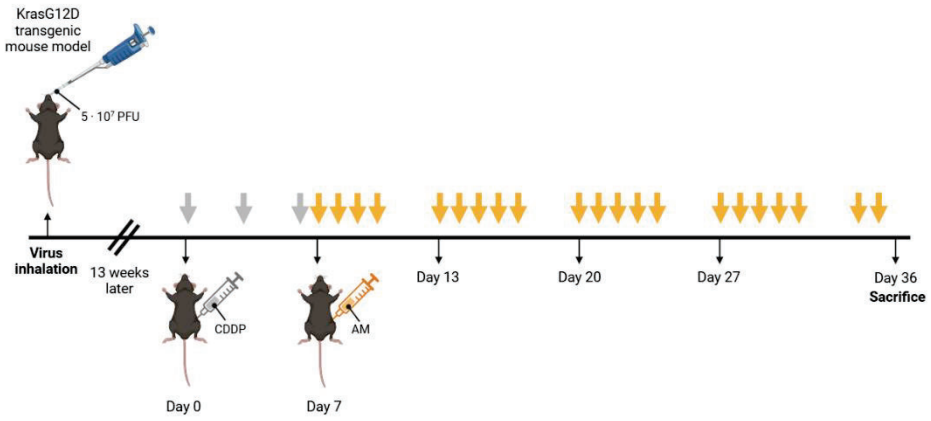

Figure 28. Diagram of the therapeutic efficacy assessment of asenapine maleate (AM) and cisplatin (CDDP) combination in KRAS mouse model. Grey arrows correspond to CDDP administrations and orange arrows correspond to AM administrations. Created in https://BioRender.com.

10.14.5 Efficacy evaluation of AM and cisplatin combination in NSG mice

The AM monotherapy efficacy assay was also conducted in NOD scid gamma (NSG) mice (Mouse Lab, Idibell, Barcelona, Spain). 4 x 10^6 A549 cells in PBS:Corning® Matrigel® (Corning Inc., Tewksbury, MA, USA) (1:1) were inoculated subcutaneously in each flank of the animals (n=5 mice/group, 8-12-week-old, both sexes). Tumor-bearing mice were separated into 4 groups and treated with V, 5 mg/kg of AM, 3 mg/kg cisplatin or the combination of AM plus cisplatin (n=10). CDDP treatment was administered on days 0, 3 and 6 of the experiment. Then, AM treatment was administered once daily on a 5-days-on/2-days-off schedule until day 25 of the experiment. At the end of the experiment, animals were sacrificed and tumors were isolated and weighed (Figure 29).

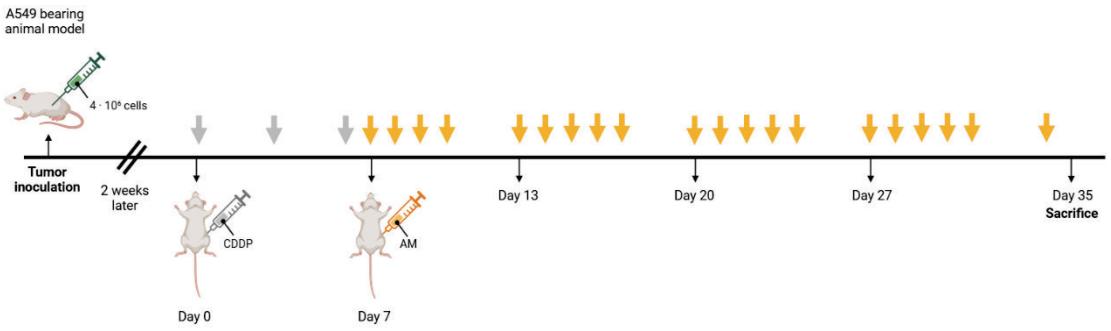

Figure 29. Diagram of the therapeutic efficacy assessment of asenapine maleate (AM) and cisplatin (CDDP) combination in NSG mice. Grey arrows correspond to CDDP administrations and orange arrows correspond to AM administrations. Created in https://BioRender.com.

10.15 Statistical and data mining analysis

For the statistical analysis of Western blot, cytometry, and MTT assay data, one-way ANOVA with *post-hoc* Tukey analysis were carried out using the GraphPad Prism 8 software when more than two groups were compared, whereas t-student analysis was performed when only two groups were compared. The *in vivo* results were analyzed with GraphPad Prism 8 using the nonparametric Mann-Whitney U-test when two groups were compared. When more than two groups were compared in the *in vivo* studies, the Kruskall-Wallis nonparametric test with Dunn's test for multiple comparisons were performed. Statistically significant differences, $p < 0.05$, $p < 0.01$, $p < 0.001$, and $p < 0.0001$, are represented by *, **, ***, **** respectively.

11 RESULTS

11.1 Extensive evaluation of drug anticancer effects in a wide panel of cellular models of lung

11.1.1 Evaluation of AM cytotoxic effect in several cell lines and 3D *in vitro* cultures

As previously described, we tested AM cytotoxic effects in some cancer cell lines, including the A549 lung adenocarcinoma cell line. In order to evaluate AM as a new treatment strategy for lung cancer, we also tested its cytotoxicity in lung cancer cell lines from other histological types. SW900 is a squamous cell carcinoma cell line, whereas DMS53 is a small cell carcinoma cell line. While in A549 the IC_{50} was 40 µM, SW900 and DMS53 cell lines required a higher concentration of AM to exert the same effect (53.14 ± 4.71 and 80.95 ± 5.68 µM, respectively) (Figure 30).

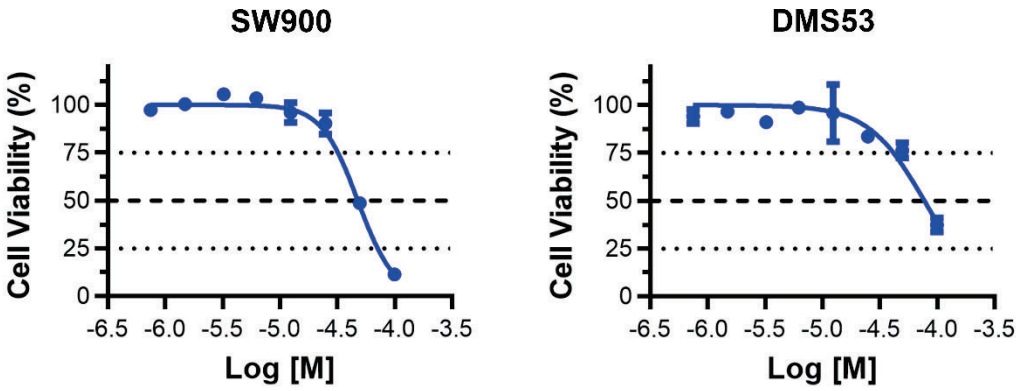

Figure 30. Effect of asenapine maleate (AM) on cell viability in lung cancer cell lines. Dose-response MTT cell viability assay after 24 h of treatment with AM at concentrations ranging from 0.8 to 100 µM in SW900 and DMS53 human cancer cell lines. Data are shown as mean ± SD.

In order to have an *in vitro* model more similar to tumors, we induced a spheroid morphology in A549 cells. We observed a substantial anticancer effect of AM in A549 spheroids (IC_{50}= 70 ± 13.43 µM), especially considering that the access of the drug to the cells is more limited and less uniform in a 3D structure than in a monolayer (Figure 31).

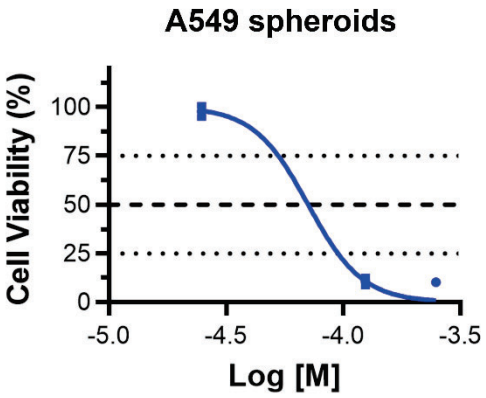

Figure 31. Effect of asenapine maleate (AM) on cell viability in A549 spheroids. Dose-response MTT cell viability assay after 24 h of treatment with AM at concentrations of 25, 125 and 250 µM in A549 3D culture. Data are shown as mean ± SD.

11.1.2 Evaluation of AM cytotoxicity in lung cancer primary cell cultures derived from a mouse model

The cytotoxicity of AM was also tested in primary cultures derived from the lung cancer transgenic KRASG12D mice model, which was later used in the therapeutic efficacy assay of AM. The lung cancer cells were characterized using the immunofluorescent markers E-cadherin (as an epithelial marker) and vimentin (as a marker of fibroblasts). The presence of E-cadherin confirmed that they are epithelial cells from lung carcinoma. Cells from mouse 2 had higher amounts of vimentin, but still, E-cadherin was also present in all the cells (Figure 32).

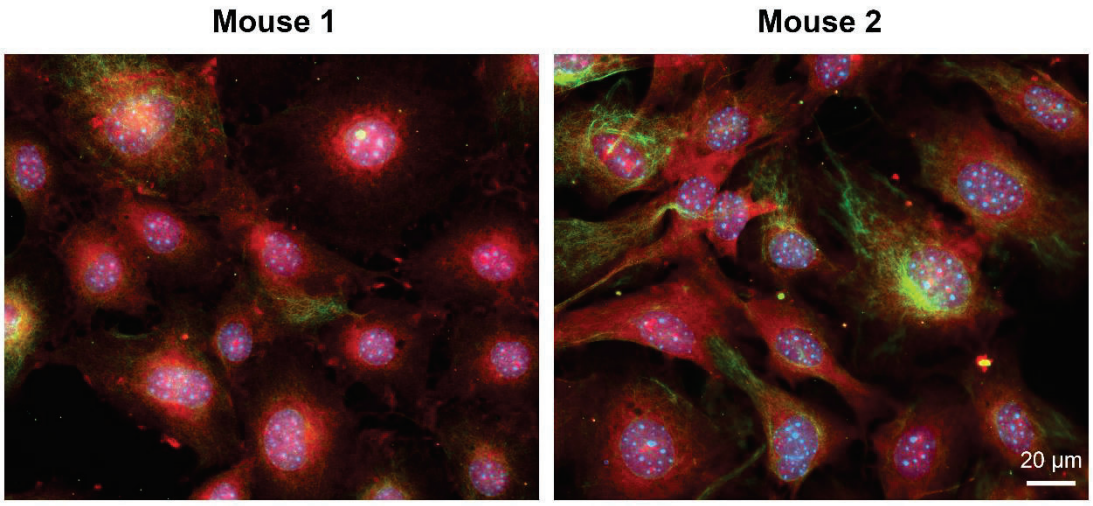

Figure 32. Characterization of cell cultures derived from a lung cancer transgenic Kras G12D mice model. E-cadherin (red) and vimentin (green) were marked by immunofluorescence. Original magnification: 400x. Scale bar: 20 µm.

Once the cells from the primary culture were characterized, we evaluated the cytotoxic effect of AM on these mouse primary cultures. The cells were sensitive to AM, since the IC_{50}s were in a low micromolar range (10 and 37 µM in cells from mice 1 and 2, respectively) (Figure 33).

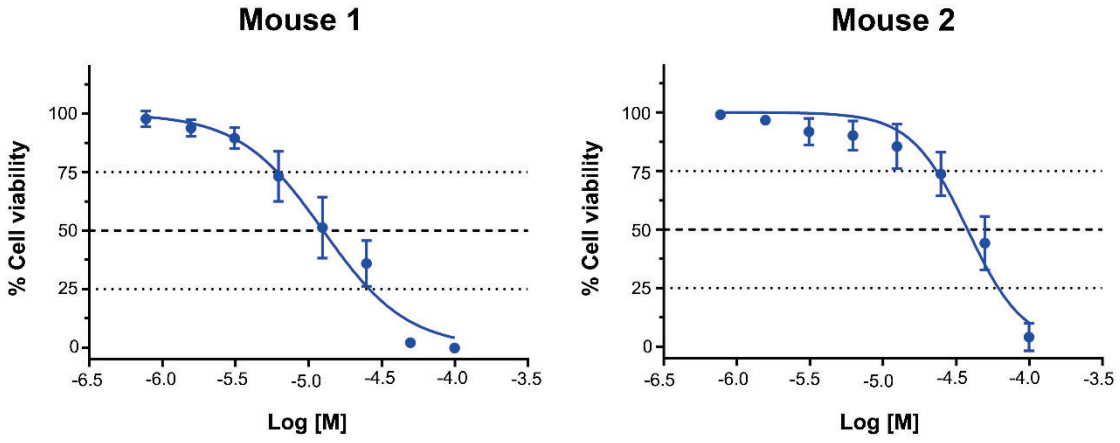

Figure 33. Effect of asenapine maleate (AM) on cell viability of mice lung carcinoma primary cultures. Dose-response MTT cell viability assay after 24 h of treatment with AM at concentrations ranging from 0.8 to 100 µM. Data are shown as mean ± SD.

11.2 Characterization of the molecular mechanism of action of AM

11.2.1 Assessment of the homodimerization domain binding mode of AM

As mentioned before, virtual studies identified AM as a potential survivin inhibitor that binds to its dimerization domain. Here, we evaluated the ability of AM to dissociate survivin homodimers. To do so, we assessed the effect of AM in purified survivin homodimers by non-denaturing gel electrophoresis. AM showed a significant ability to break the homodimer, thus compromising survivin stability (Figure 34).

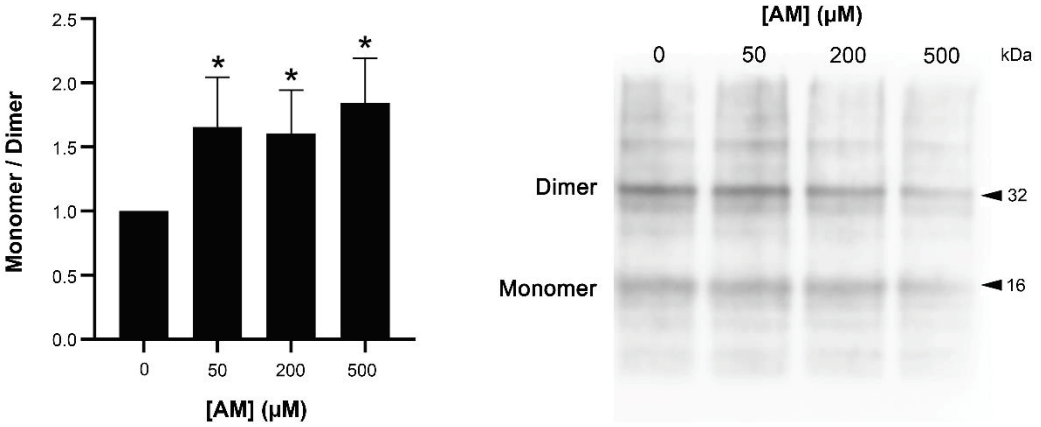

*Figure 34. Effect of asenapine maleate (AM) in survivin homodimerization. A non-denaturing gel electrophoresis was conducted to test the ability of AM to dissociate purified survivin homodimers at concentrations of 50, 200 and 500 µM). Bars represent the mean ± SD. Statistically significant results are indicated as *, p-value < 0.05.*

11.2.2 Comprehensive mechanism of action of AM

The lack of specificity of a survivin inhibitor can result in a lack of efficacy or non-desired toxicity when it is tested in clinical trials. Hence, AM specificity was evaluated *in vitro*. A549 and U87 MG cells were treated with AM at their IC_{50} for 24 h to investigate a possible cellular inhibitory effect on survivin as well as in XIAP, another IAP protein structurally closely related to survivin. AM was able to significantly decrease survivin at the protein level, while XIAP did not show significant differences between AM-treated and non-treated cells (Figure 35). Thus, AM specifically and efficiently downregulates survivin levels.

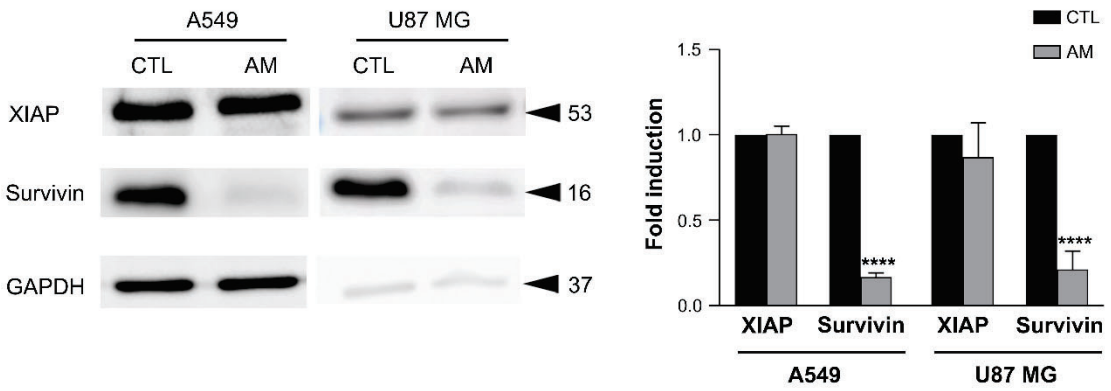

*Figure 35. Evaluation of asenapine maleate (AM) specificity for survivin in A549 lung adenocarcinoma and U87 MG glioblastoma cell lines. After 24 h of treatment with IC_{50} value of AM, the expression of survivin and XIAP was analyzed by Western blot analysis in A549 and U87 MG cell lines. Bars represent the mean ± SD. Statistically significant results are indicated as ****, p-value <0.0001. CTL, control.*

In preliminary results, we observed that AM decreased cell viability. Here, we evaluated whether this effect is due to cell cycle arrest and/or cell death induction. First, since survivin exerts promitotic activity, we assessed the AM effect on cell cycle progression in A549 cells. Treatment of A549 cells with AM for 24 h showed a clear and significant cell cycle arrest, compared to control cells (Figure 36). In particular, AM was able to decrease the percentage of cells in both S and G_2/M phases while increasing it in G_0/G_1.

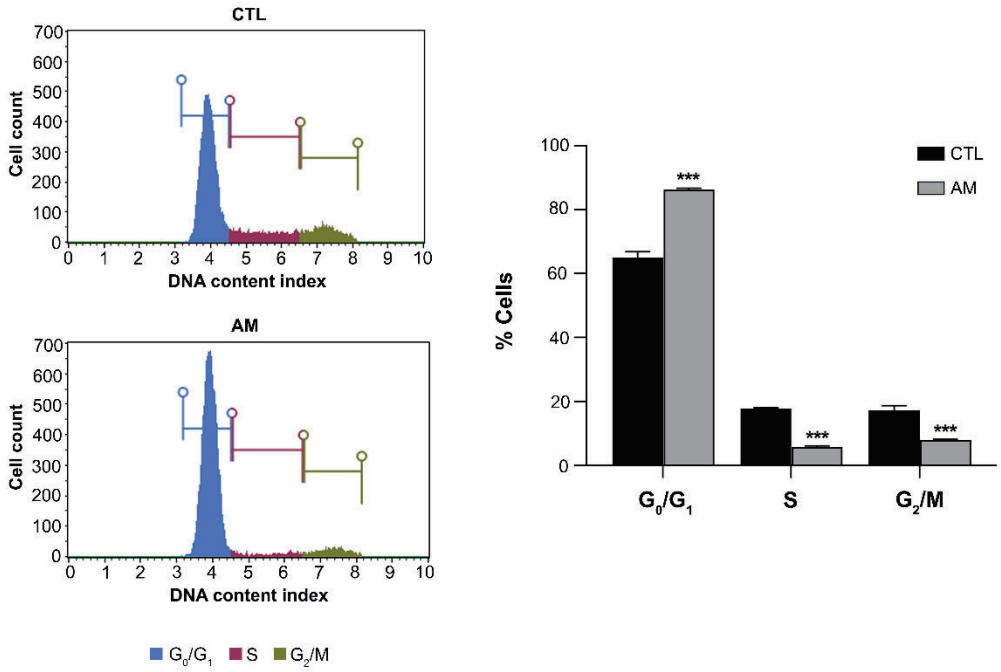

*Figure 36. Effect of asenapine maleate (AM) on cell cycle. AM effect on cell cycle was analyzed in A549 cell line after 24 h of treatment with AM at IC_{50} value. Quantification of different cell cycle phases was measured using the flow cytometry-based MUSE™ cell cycle assay kit. Bars represent the mean ± SD. Statistically significant results are indicated as ***, p-value < 0.001. CTL, control.*

On the other hand, as survivin also holds an antiapoptotic function, we evaluated whether AM was triggering apoptosis in A549 and U87 MG cells. Our results showed a significant cleavage of caspase-3, an important protease in the execution pathway of apoptosis, and of PARP, a substrate of caspase-3, after 24 h of AM treatment in both cell lines, corroborating an apoptotic induction triggered by AM (Figure 37).

Altogether, AM treatment was able to promote cell cycle arrest and apoptosis activation.

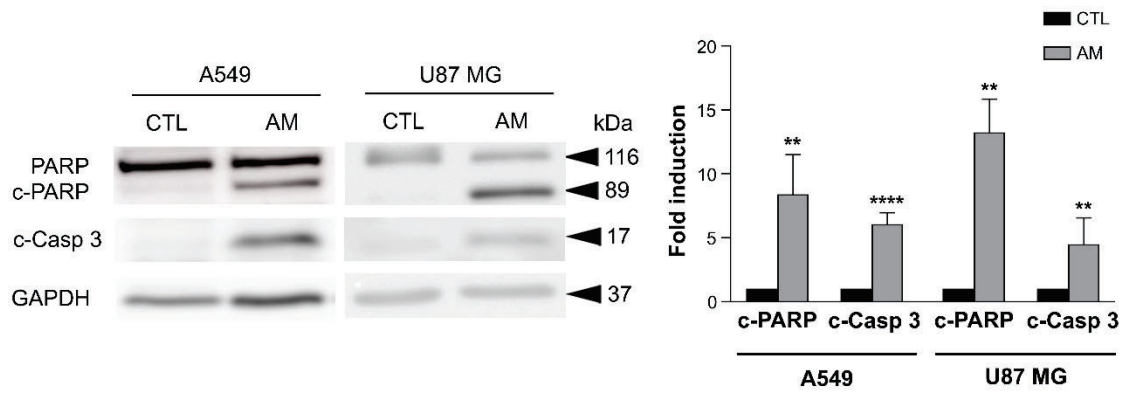

*Figure 37. Evaluation of apoptosis after asenapine maleate (AM) treatment in A549 lung adenocarcinoma and U87 MG glioblastoma cell lines. Expression of apoptotic proteins in A549 and U87 MG cells previously treated with the IC_{50} of AM for 24 h. Protein levels were normalized with their respective loading controls. Bars represent the mean ± SD. Statistically significant results are indicated as **, p-value < 0.01; ****, p-value <0.0001. c-PARP, cleaved PARP; c-Casp 3, cleaved caspase 3; CTL, control.*

11.3 Assessment of combination therapies for tumor sensitization to pro-apoptotic conventional treatments and immunotherapy

11.3.1 Combination of AM with currently used chemotherapeutics *in vitro*

11.3.1.1 Combination cell viability assays in A549 and LLC1 cells

Since survivin is a member of the IAP family, it is expected that AM improves the anticancer response in combination with therapies that induce apoptosis. Thus, we investigated whether AM could exert a possible higher effect sensitizing cancer cells to conventional chemotherapy. To test the effect of AM combined with chemotherapy, we treated A549 cells with the IC_{50} of AM and different concentrations of one of four currently used conventional lung cancer chemotherapeutics: cisplatin, carboplatin, paclitaxel and gemcitabine. Cell viability assays revealed that the IC_{50} of the combination of the chemotherapeutic plus AM was significantly lower compared to monotherapy in all cases except AM and paclitaxel combination (Figure 38).

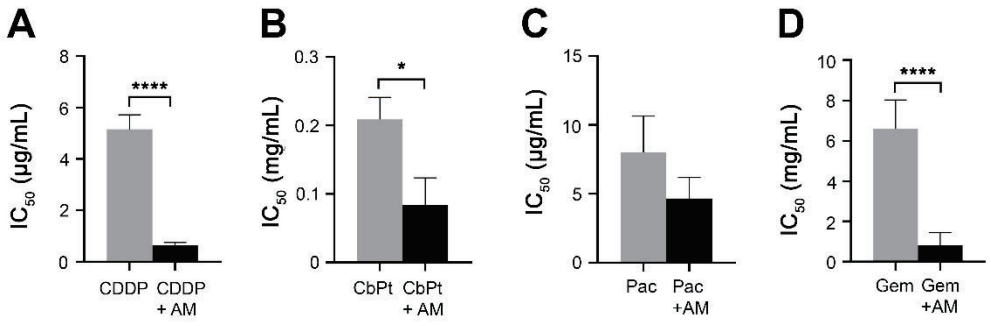

*Figure 38. Impact of asenapine maleate (AM) addition on the half-maximal inhibitory concentration (IC_{50}) of different chemotherapeutic agents in A549 cells. IC_{50} value of cisplatin, carboplatin and gemcitabine significantly decreases in combination with AM. The dose-response MTT cell viability assays were performed treating A549 cells for 24 h with IC_{50} of AM and one chemotherapeutic: CDDP (concentration range of 13-100 µg/mL), carboplatin (CbPt, concentration range of 0.063-1 mg/mL), paclitaxel (Pac, concentration range of 0.6-75 µg/mL) or gemcitabine (Gem, concentration range of 0.25-4 mg/mL). Data are shown as mean ± SD. Statistically significant results are indicated as *, p-value < 0.05; ****, p-value < 0.0001.*

We analyzed the data obtained in the viability assays with Compusyn software to elucidate the possible interactions between chemotherapeutics and AM. We obtained combination indexes (CIs) under 1 in all combinations except with paclitaxel (Table 5), which indicates paclitaxel does not present synergism with AM. In the case of carboplatin and gemcitabine, there is a moderate synergism when combined with AM (CI = 0.7-0.85), whereas there is a stronger synergistic effect when combining AM with cisplatin (CI = 0.48).

	CDDP (mg/mL)	**CI**	**CbPt (mg/mL)**	**CI**	**Gem (mg/mL)**	**CI**
IC_{50} AM	0.013	1.65	0.063	1.50	0.250	1.01
	0.025	1.01	0.125	**0.83**	0.500	1.00
	0.050	**0.85**	0.250	**0.87**	1.000	0.96
	0.100	**0.48**	0.500	1.09	2.000	**0.89**
			1.000	1.92	4.000	**0.74**

Table 5. Combination index (CI) of multiple doses of cisplatin (CDDP), carboplatin (CbPt), and gemcitabine (Gem) with AM (at a half maximal inhibitory concentration of the cell population, IC_{50}) for the A549 cell line.

In order to validate the parameter CI, we selected the dose of cisplatin, carboplatin and gemcitabine at which more synergism was observed with AM according to the CI, and compared cell viability at that dose in cells treated with the chemotherapeutic alone versus the combination with AM. At the same dose as the chemotherapeutic alone, the cell viability percentage was considerably inferior (50%) when cells were treated with the combination (Figure 39), confirming the synergy predicted by the analysis performed with Compusyn software.

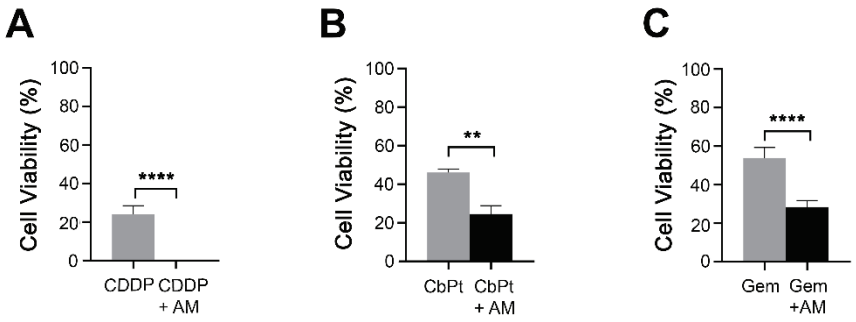

*Figure 39. Effect of chemotherapeutic agents and asenapine maleate (AM) combination treatment on A549 cell viability. Cell viability decreases when combining the chemotherapeutic plus AM. Cell viability of A549 cells at the dose at which more synergism is shown in cells treated with chemotherapeutic monotherapy (CDDP at 0.1 mg/mL; carboplatin, CbPt, at 0.25 mg/mL; gemcitabine, Gem, at 4 mg/mL) versus the combination with AM. Data are shown as mean ± SD. Statistically significant results are indicated as **, p-value < 0.01; ****, p-value < 0.0001.*

Moreover, the fraction of affected cells (FA) by the drugs predicted by Compusyn software was higher in the case of the combination with cisplatin, carboplatin and gemcitabine (Figure 40).

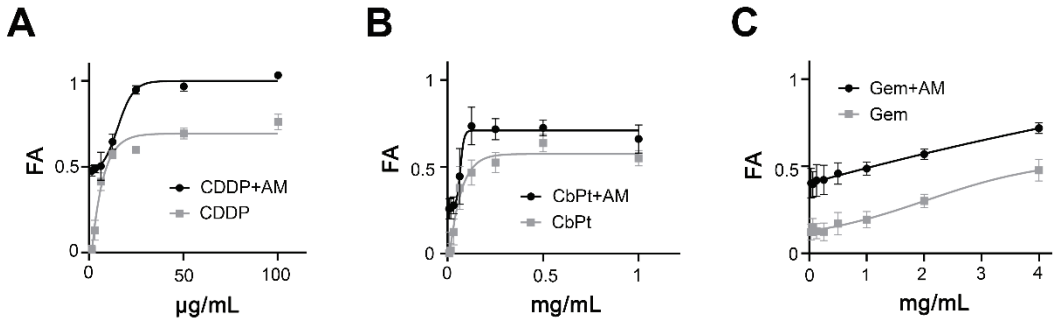

Figure 40. Fraction of affected (FA) after treatment with chemotherapeutic monotherapy and after treatment with asenapine maleate (AM) and chemotherapeutic combination. A549 cells were treated for 24 h with half-maximal inhibitory concentration (IC_{50}) of AM plus one chemotherapeutic: CDDP

(concentration range of 13-100 µg/mL) (A), carboplatin (CbPt, concentration range of 0.063-1 mg/mL) (B) or gemcitabine (Gem, concentration range of 0.25-4 mg/mL) (C). Data shows the mean ± SD.

Altogether, our data shows a synergistic effect of combining AM with cisplatin, carboplatin and gemcitabine in A549 cells. This effect is especially stronger when we combine AM with cisplatin. Hence, that combination was selected to test in further experiments, including the *in vivo* therapeutic effect assay. For the *in vivo* studies, the tumor is induced by inoculating LLC1 cells into the flank of the mouse. To determine whether LLC1 cells respond to the combination in a similar manner to A549 cells, the combination was tested in LLC1 cell culture prior to the *in vivo* experiment. Initially, the combination of cisplatin and AM in LLC1 cells showed antagonism instead of synergism (Figure 41).

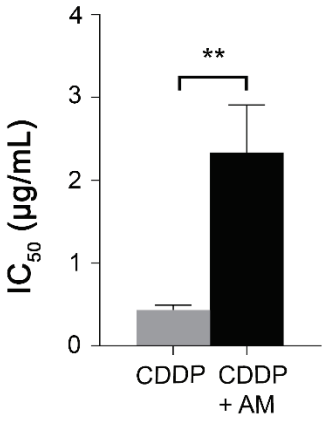

*Figure 41. Impact of asenapine maleate (AM) addition on the half-maximal inhibitory concentration (IC_{50}) of cisplatin (CDDP)-treated LLC1 cells. Graph representing the IC_{50} value of CDDP alone versus the IC_{50} of its combination with AM. Data are shown as mean ± SD. Statistically significant results are indicated as **, p-value < 0.01.*

However, the same experiment with a different treatment regimen (both treatments were added sequentially to the cells instead of simultaneously), resulted in CI < 1 (CI=0.65 at 0.003 mg/mL), indicating moderate synergism of the combination of CDDP and AM in LLC1 cells (Figure 42 and Table 6).

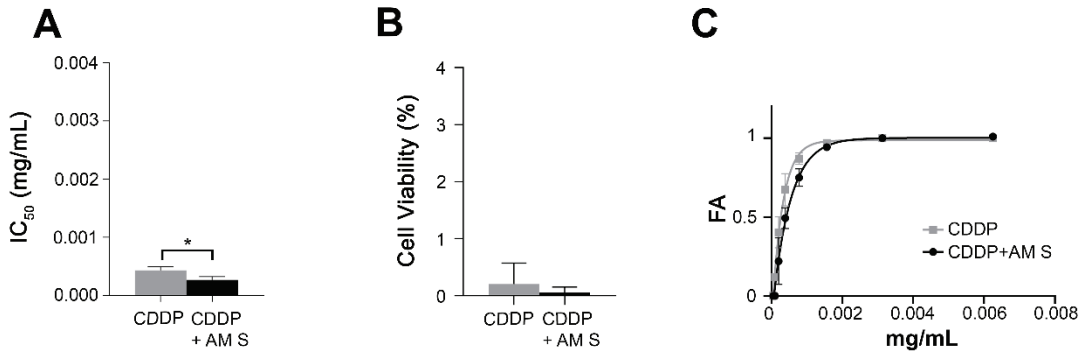

*Figure 42. Effect of sequential asenapine maleate (AM) plus cisplatin (CDDP) combination treatment on LLC1 cells. Graph representing the half-maximal inhibitory concentration (IC_{50}) value of CDDP alone versus the IC_{50} of its sequential combination with AM (A). Cell viability of LLC1 cells at the dose of CDDP at which more synergism is shown (0.003 mg/mL) when combined with AM (B). Dose-effect curve of CDDP and the sequential combination of CDDP and AM (C). Data are shown as mean ± SD. Statistically significant results are indicated as *, p-value < 0.05. FA, fraction affected; S, sequential.*

	CDDP (mg/mL)	**CI**
IC_{50} AM Sequential	0.0016	1.52
	0.003	**0.65**
	0.006	**0.86**

Table 6. Combination index (CI) of AM (IC_{50}) added 24 h after CDDP (different doses) for LLC1 cell line.

Overall, AM may sensitize LLC1 cells to cisplatin when administered in a sequential manner, although the effect is considerably inferior than that observed in A549 cells. Hence, the administration regimen selected for the *in vivo* study was a sequential administration of CDDP and, 24 h later, AM.

11.3.1.2 Molecular mechanism of action of AM and cisplatin combination

In order to elucidate the molecular mechanism of action of AM and cisplatin combination, A549 cells were treated with the IC_{50} of cisplatin and the IC_{50} of AM, the latter added after 24 h. Cytometry assays showed that AM induces slight apoptosis at this dose, but when it is combined with cisplatin, apoptosis is significantly enhanced in comparison to cells treated with cisplatin alone (Figure 43).

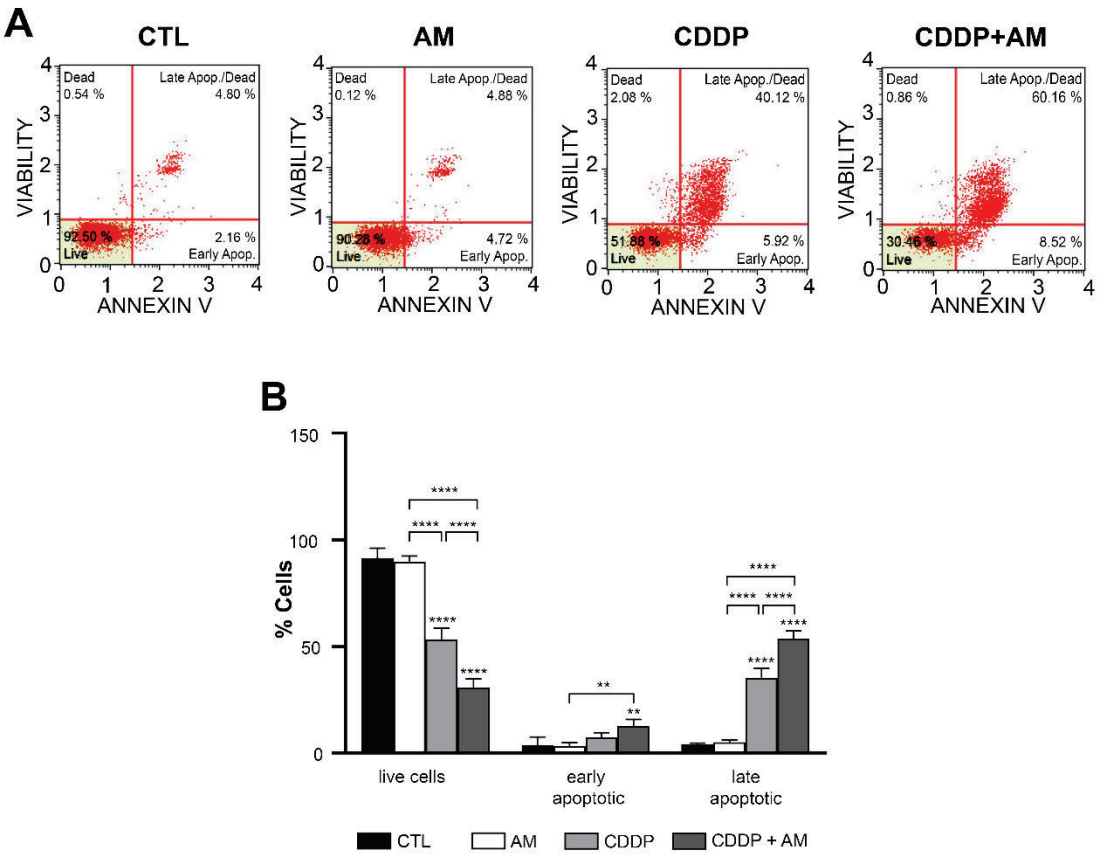

*Figure 43. Evaluation of apoptosis after asenapine maleate (AM) plus cisplatin (CDDP) treatment in A549 lung adenocarcinoma cells. A549 cells were treated with half-maximal inhibitory concentration (IC_{50}) of CDDP and, after 24 h, with the IC_{50} of AM. The percentage of apoptotic cells was measured using the flow cytometry-based MUSE™ dead cell assay kit. Representative cytometry graphs are shown (A). The graph represents the percentages of cells in each state (B). Bars represent the mean ± SD. Statistically significant results are indicated as **, p-value < 0.01; ****, p-value <0.0001. CTL, control.*

To further investigate the molecular mechanism, we evaluated the expression of proteins involved in apoptosis (PARP and caspase-3) (Figure 44) and observed that cells treated with the combination had significantly higher expression of both, cleaved PARP and cleaved caspase-3, compared to cisplatin monotherapy. p53 expression is induced in cells treated with cisplatin alone and in those treated with the combination. Survivin expression was also evaluated to corroborate the effects of AM on its target. Together, these results suggest that AM enhances cisplatin's ability to induce apoptosis in A549 cells.

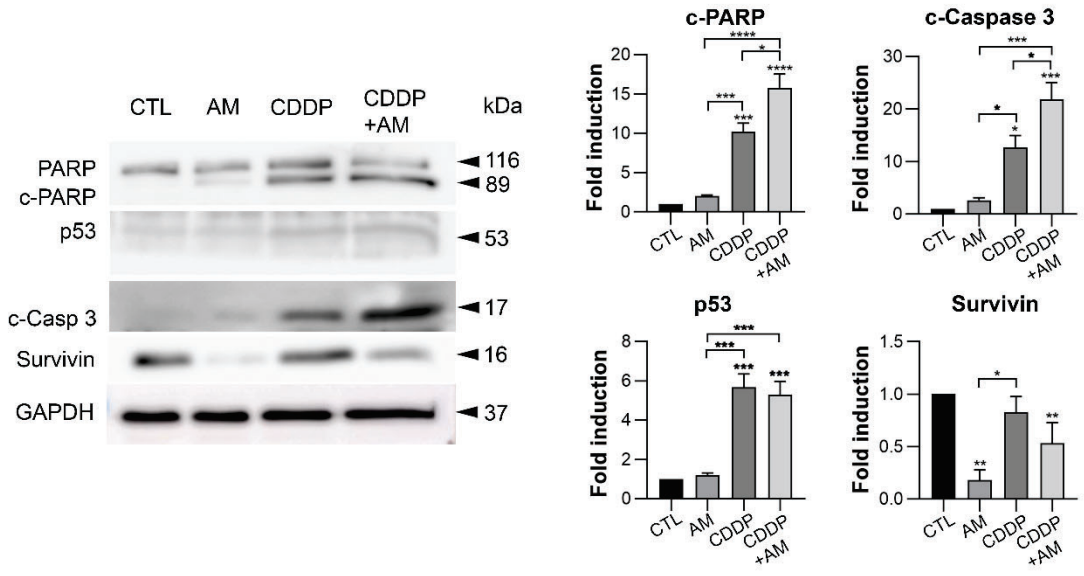

*Figure 44. Expression of apoptotic proteins in A549 cells after treatment with asenapine maleate (AM) plus cisplatin (CDDP) combination. A549 cells that were previously treated with the half-inhibitory inhibitory concentration (IC_{50}) of CDDP and AM. Protein levels were normalized with their respective loading controls. Statistically significant results are indicated as *, p-value < 0.05; **, p-value < 0.01; ***, p-value < 0.001; ****, p-value <0.0001. CTL, control; c-PARP, cleaved PARP, c-Casp 3, cleaved caspase 3.*

Furthermore, cytometry assays were also performed to evaluate the effect of the same treatment regimen in the cell cycle of A549 cells (Figure 45). The results confirmed what we observed in the evaluation of AM monotherapy, hence, AM arrests the cell cycle in G_1/G_0. This effect is not induced when AM is combined with cisplatin.

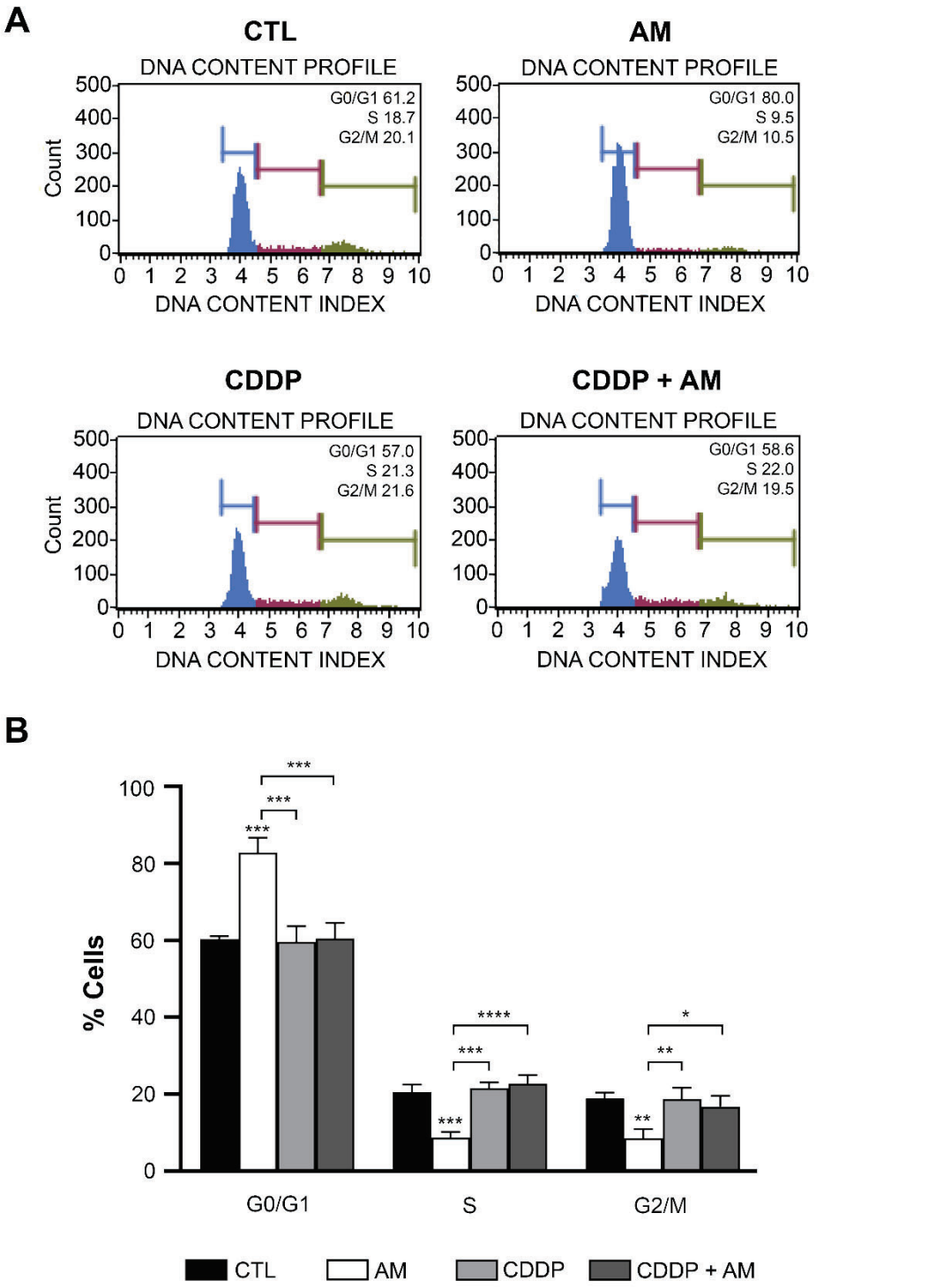

*Figure 45. Effect of asenapine maleate (AM) plus cisplatin (CDDP) combination on the cell cycle. A549 cells were treated with half-maximal inhibitory concentration (IC_{50}) of CDDP and, after 24 h, with the IC_{50} of AM. The percentage of cells in each cell cycle phase was measured using the flow cytometry-based MUSE™ cell cycle assay kit. Representative cytometry graphs are shown (A). The graph represents the percentages of cells in each cell cycle phase (B). Bars represent the mean ± SD. Statistically significant results are indicated as *, p-value <0.05; **, p-value < 0.01; ***, p-value < 0.001; ****, p-value <0.0001. CTL, control.*

11.3.2 Combination of AM with radiotherapy

11.3.2.1 Evaluation of DNA damage after treating cells with AM and radiotherapy

RDT induces DNA damage, either directly by the effect of ionizing radiation in DNA or indirectly by the effect of the free radicals generated. It often leads to the induction of different forms of cell death programs, such as senescence, apoptosis or mitotic catastrophe. Since our results have shown that AM promotes apoptosis, the combination of AM and RDT may result in a synergistic effect.

To study the potential synergistic effect of AM in combination with RDT, we initially tested different concentrations of the survivin inhibitor either alone or in combination with several doses of irradiation and analyzed DNA damage induction in each treatment condition (Figure 46). Concretely, the lung adenocarcinoma A549 cell line was treated with AM at its IC_{25} and IC_{50} with or without different irradiation doses (2 Gy, 4 Gy or 8 Gy). Western blot analysis was performed 24 h post-irradiation to evaluate the levels of DNA damage-related proteins, histone variant H2A.X and ATM, and their respective phosphorylated forms (γH2A.X and γATM). Higher expression of the phosphorylated forms corresponds to an increase in DNA damage, indicating the impact of each treatment condition on DNA integrity and subsequent activation of DNA damage signaling pathways.

Results show an irradiation-dependent phosphorylation of ATM, especially at higher irradiation doses (8 Gy), regardless of the AM treatment, which did not have a significant effect on γATM basal levels (Figure 46A, C and E).

Instead, total H2A.X progressively increases along with AM dosage, while irradiation dose does not significantly affect the expression of H2A.X (Figure 46B, D and E).

Altogether, these results suggest AM could induce a certain DNA damage in irradiated A549 cells. Therefore, we selected the highest doses of irradiation (8 Gy) and AM (IC_{50}) tested in this pilot study for further investigation of a possible interaction between both therapies.

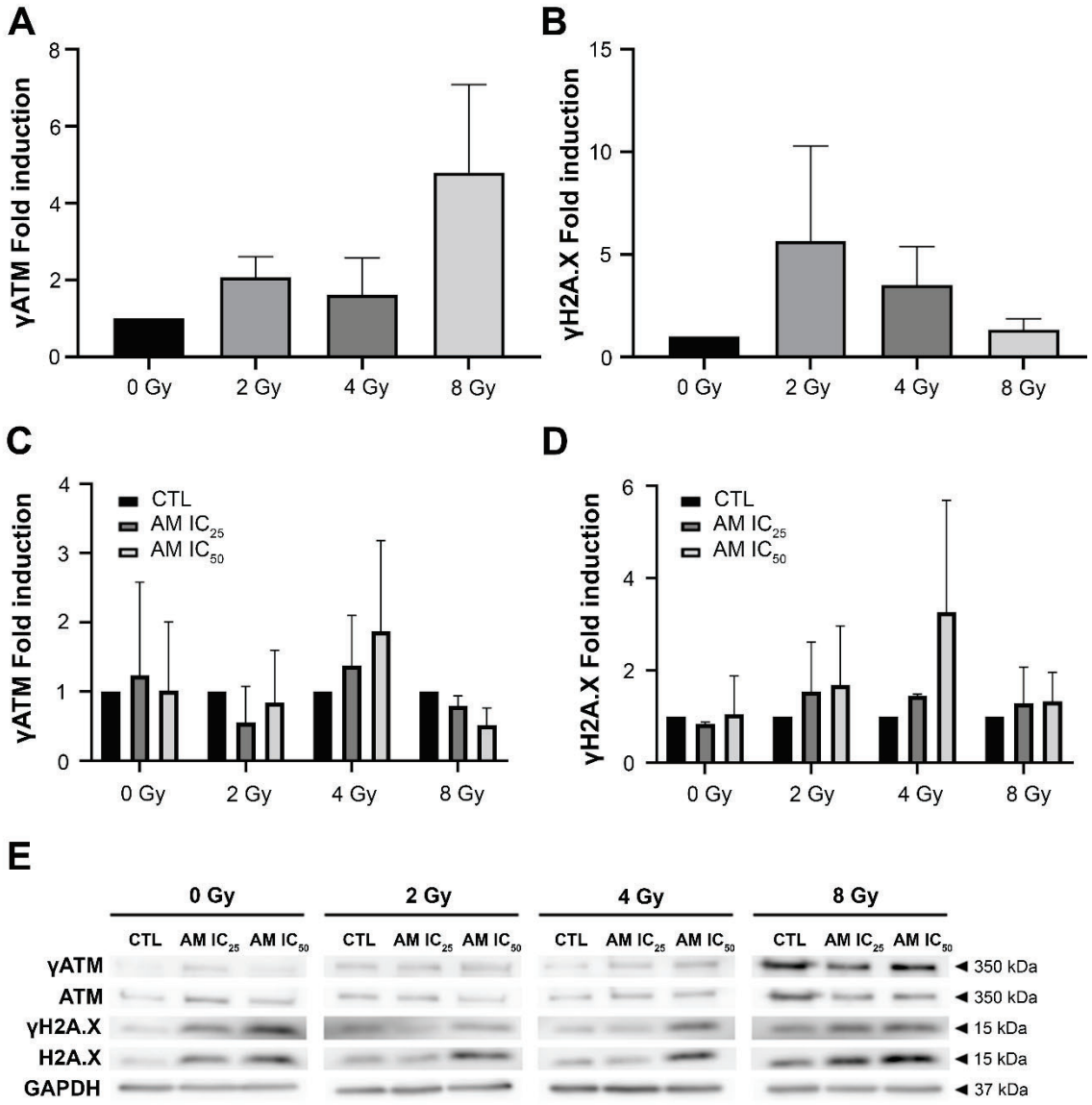

Figure 46. Effects on DNA damage of AM and irradiation combined treatment in A549 lung adenocarcinoma cells. γATM (A) and γH2A.X (B) expression in A549 cells were evaluated 24 h after irradiation (0 Gy, 2 Gy, 4 Gy or 8 Gy). γATM (C) and γH2A.X (D) expression was also evaluated after treatment with or without AM (IC_{25} or IC_{50}) added 1 h previous to irradiation (0 Gy, 2 Gy, 4 Gy or 8 Gy). Western blot showing H2A.X and ATM total and phosphorylated proteins (E). GAPDH was used as a loading control to normalize protein levels. Figures show mean ± standard error of the mean (SEM).

To study if the time of exposure to AM had an impact on sensitizing lung adenocarcinoma cells to RDT, the A549 cell line was pretreated with AM (IC_{50}) either 1 h or 24 h prior to irradiation (8 Gy). Western blot analysis was performed 24 h post-irradiation to study DNA damage induction (Figure 47). No significant differences were observed between 1

h and 24 h pretreatment. γATM levels increased with exposure to irradiation, being slightly higher in combination with AM treatment.

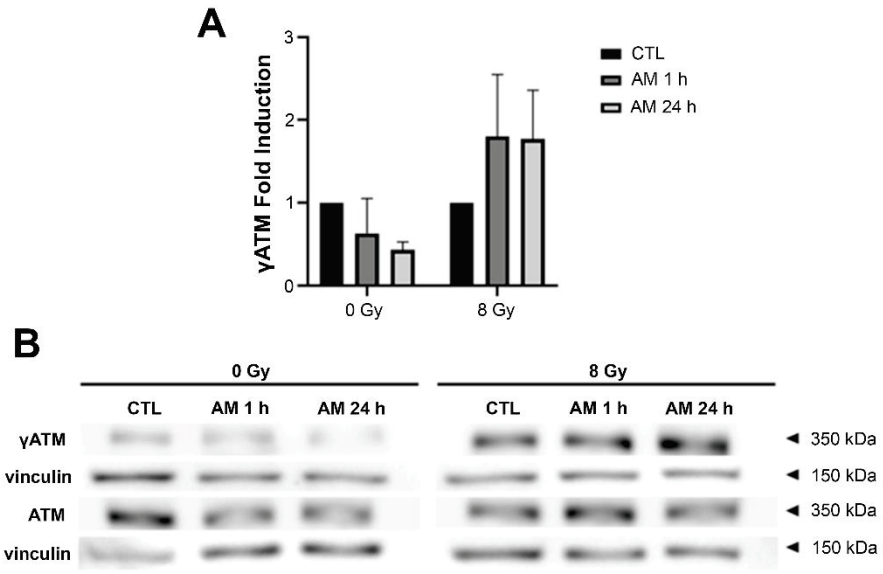

Figure 47. Impact of time exposure to asenapine maleate (AM) on the expression of γATM in A549 cells after irradiation. Protein fold induction values (A) and Western blot (B) show the total ATM and phosphorylated proteins of A549 cells under the above-mentioned treatment conditions. Vinculin was used as a loading control to normalize protein levels. Figure shows mean ± SEM. CTL, control.

On the other hand, H2A.X phosphorylation seems to be more dependent on AM addition, although no significant effects were observed (Figure 48).

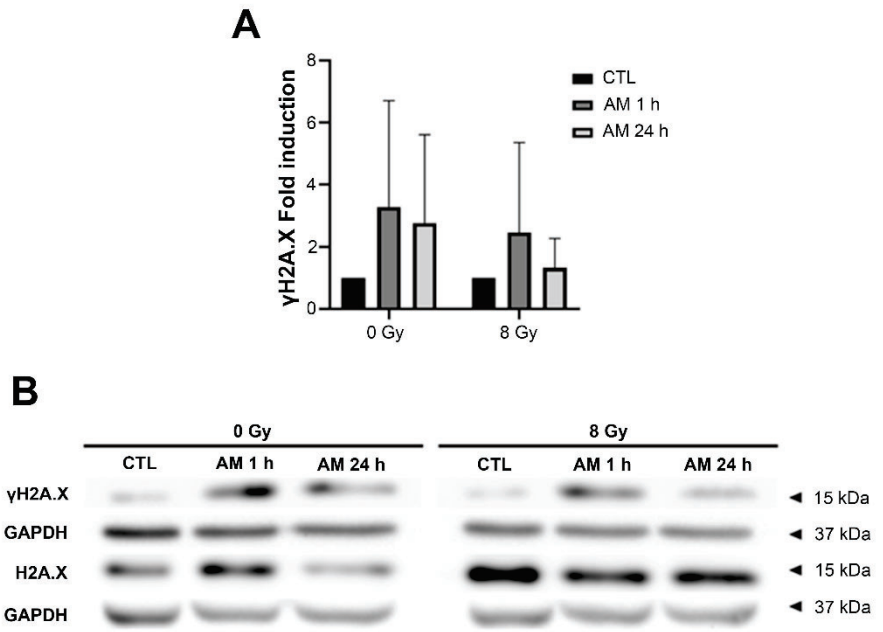

Figure 48. Impact of time exposure to asenapine maleate (AM) on γH2A.X expression in A549 after irradiation. Protein fold induction values (A) and Western blot (B) show the total H2A.X and phosphorylated proteins in A549 cells under the above-mentioned treatment conditions. GAPDH was used as a loading control to normalize protein levels. Figure shows mean ± SEM. CTL, control.

11.3.2.2 Alterations in cell morphology after AM treatment and radiotherapy

When observed by phase-contrast light microscopy, A549 AM-treated and untreated cells differed in morphology and confluence between conditions (Figure 49). Morphologically, cells showed many vacuolar structures, slightly lost their typical angular shape and showed higher size after combined treatment with irradiation and AM pretreatment at 24 h, which may be indicative of senescence. In addition, blebbing structures, characteristic of apoptotic cells, can also be observed in most conditions. Regarding confluence, there was an evident decrease in cell density when cells were treated with AM 24 h prior to irradiation. All in all, microscopy results suggest that the time of exposure to AM may have an impact on sensitizing NSCLC cells to RDT.

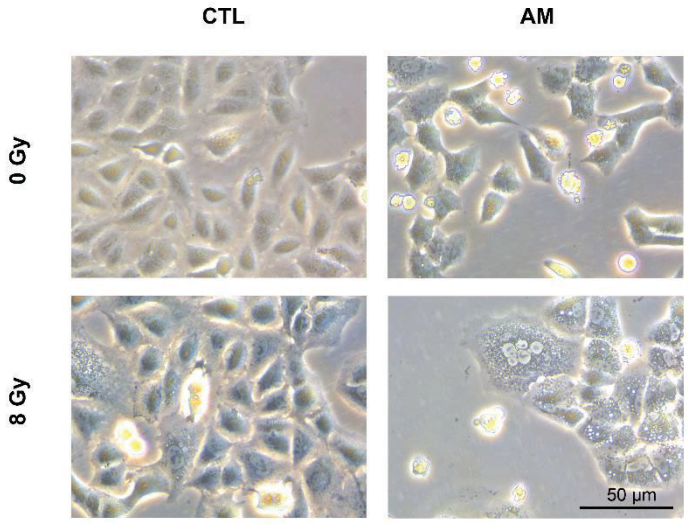

Figure 49. Alteration of morphological characteristics in irradiated A549 cells previously treated with asenapine maleate (AM). A549 cells morphology after treatment with or without AM added 24 h before irradiation (0 Gy or 8 Gy). Original magnification 400x. Scale bar: 50 µm.

11.3.2.3 Effect of AM and radiotherapy on survivin expression

To corroborate if AM inhibitory effects on survivin were affected by irradiation or were only dependent on time exposure to AM treatment, A549 cells were treated with AM (IC_{50}) monotherapy or in combination with irradiation (2 Gy, 4 Gy, 8 Gy). Western blot analysis was performed at both 2 h and 24 h post-irradiation to assess the expression of survivin (Figure 50). As expected, our results showed a decrease in survivin basal levels in correlation with the addition of AM, especially after 24 h treatment. Moreover, irradiation also seems to have a slight effect on survivin inhibition, which can be notably appreciated in the 8 Gy irradiated condition.

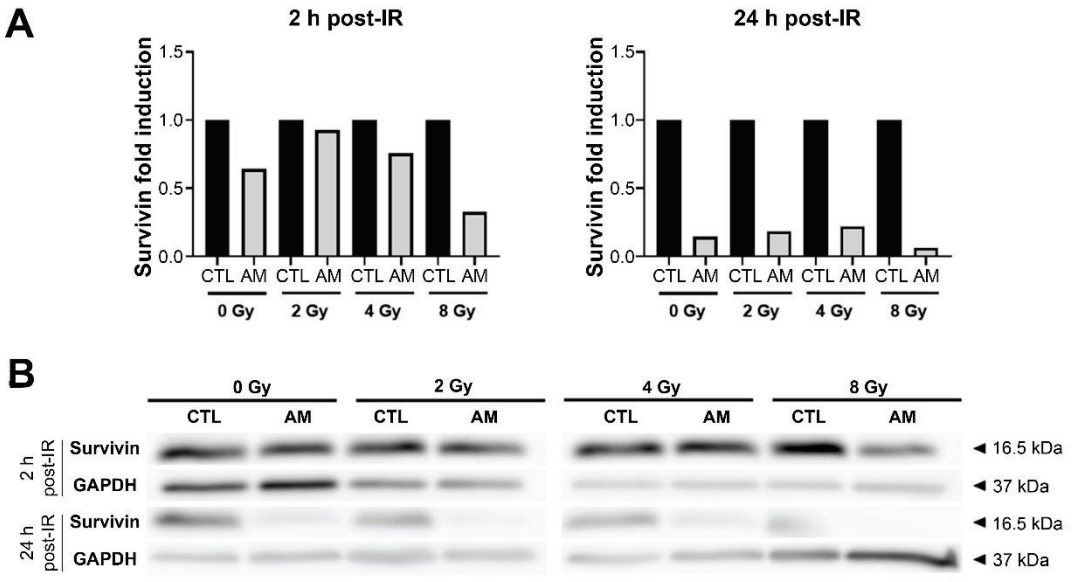

Figure 50. Evaluation of survivin inhibition after asenapine maleate (AM) treatment combined with irradiation. Fold induction ratios (A) and Western blot (B) show survivin inhibition of A549 cells treated with or without AM (half-maximal inhibitory concentration (IC_{50})) added 1 h prior to irradiation (0 Gy, 2 Gy, 4 Gy or 8 Gy). Protein expression was evaluated 2 or 24 h after irradiation. GAPDH was used as a loading control to normalize protein levels. CTL, control; IR, irradiation.

Overall, these results suggest that the molecular effects of AM on survivin inhibition increase with time exposure and irradiation dose, supporting the idea that longer exposure to AM may enhance its potential radiosensitizing effect.

11.3.2.4 Effect of AM treatment and radiotherapy over cell death induction

To evaluate the cellular effects induced by the treatments, we evaluated the effects of AM in combination with irradiation over cell death induction in NSCLC cells, as survivin has a main role in apoptosis inhibition. For this purpose, we performed cell death analyses through flow cytometry, testing differences among single and combined treatment with AM and irradiation (Figure 51). Apoptosis induction, especially early apoptosis, significantly increased when A549 cells were exposed to AM for 24 h in contrast to those exposed for 1 h, independently of irradiation. However, there are no significant global apoptosis changes between single and combined treatment, which leads to the conclusion that the AM compound does not have a synergistic effect with RDT regarding cell death induction.

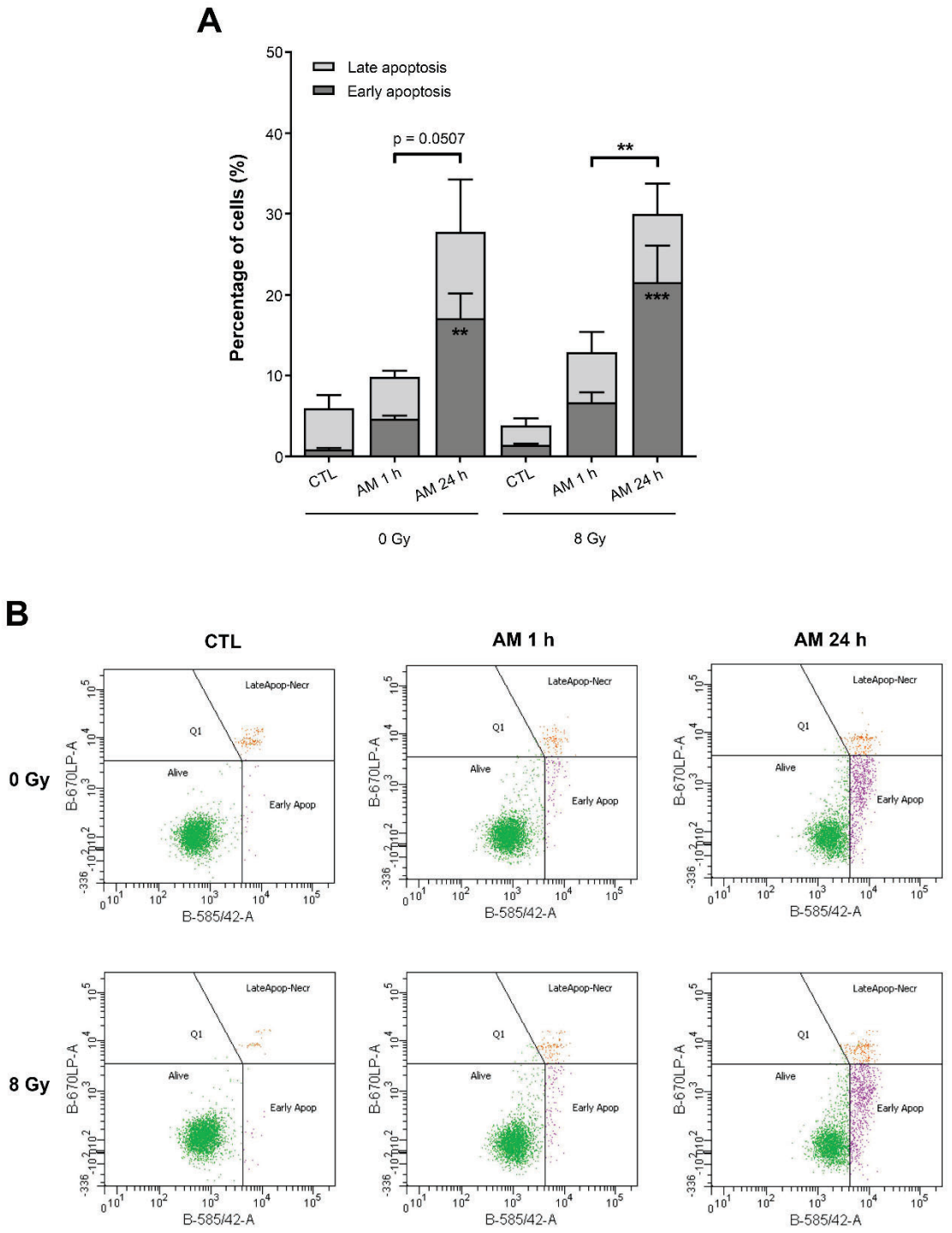

Figure 51. Evaluation of apoptosis after the combination of asenapine maleate (AM) treatment plus radiotherapy. Quantification of apoptotic cells was assessed by Annexin V/7-aminoactinomycin D flow cytometry analysis. Early and late apoptosis were quantified in A549 cells treated with AM (half-maximal inhibitory concentration (IC_{50})) 1 h or 24 h alone or in combination with irradiation (8 Gy) (A). Representative flow cytometry plots show alive, early apoptotic and late apoptotic/necrotic populations of the A549 cell line treated as above mentioned (B). Figure shows mean ± SEM. Early apoptosis statistical

*differences against control and among conditions are indicated as ** p < 0.01 and *** p < 0.001. Apop, apoptosis; Necr, necrosis; CTL, control.*

11.3.2.5 Effect of AM treatment and radiotherapy on the cell cycle

Cytometry assay was also used to study the effect of the treatments in the cell cycle of A549 cells and our results showed that AM alone significantly induced G_0/G_1 phase arrest while diminishing the percentage of cells on S and G_2/M phase, compared to the non-treated condition (Figure 52). Besides, no changes could be observed when comparing single AM treatment at different exposition times. In addition, irradiation provoked an increase in the G_2/M phase, leading to a significant decrease in the S phase.

Regarding the combination of both treatments, when cells were irradiated after 1 h AM pretreatment, the G_0/G_1 phase significantly decreased compared to single 1 h AM exposure, whereas G_2/M augmented compared both to AM and irradiation alone. In contrast, cells exposed to AM for 24 h before irradiation were mainly arrested at G_0/G_1 phase compared to those exposed only for 1 h. This increase in G_0/G_1 also led to the almost disappearance of cells at the S phase. All in all, results indicate an evident G_0/G_1 arrest due to AM treatment and a slight G_2/M phase arrest induced by irradiation. In combined treatment, irradiated cells that were exposed to AM for 1 h showed an irradiation-induced G_2/M arrest, while those exposed to 24 h AM pretreatment showed a higher arrest at G_0/G_1 compared to AM-treated cells.

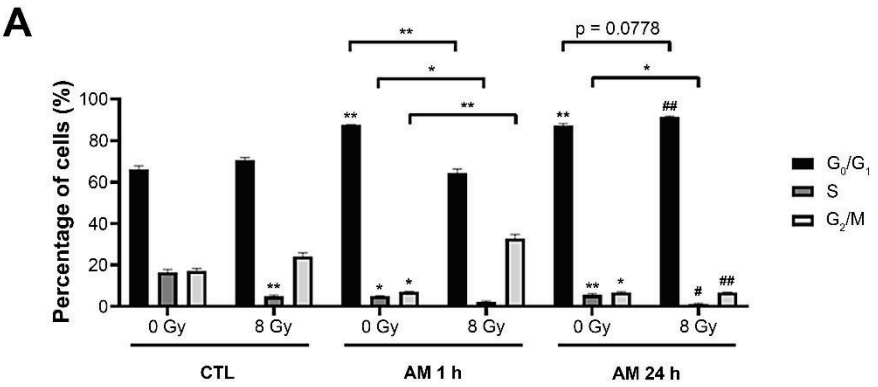

B

	0 Gy			8 Gy		
	CTL	AM 1 h	AM 24 h	CTL	AM 1 h	AM 24 h
G_0/G_1	66.0	87.6	87.3	70.6	64.4	91.5
S	16.4	4.9	4.0	4.8	2.3	1.3
G_2/M	17.0	7.0	6.7	24.2	32.7	6.7

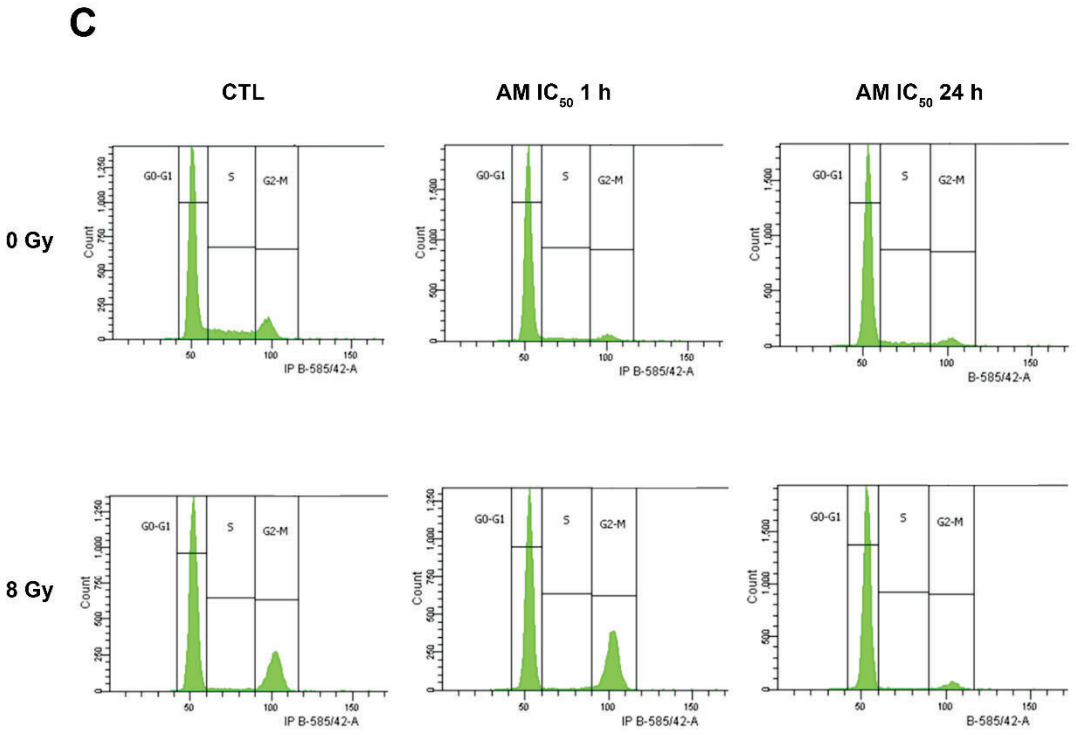

*Figure 52. Effect of asenapine maleate (AM) treatment plus radiotherapy on cell cycle of A549 cells. Cell cycle arrest was evaluated through flow cytometry. The percentage of A549 cells pretreated with AM and irradiated at G_0/G_1, S and G_2/M was quantified (A, B). Data is shown as a plot (A), total percentages (B) and representative flow cytometry graphs (C). Figure shows mean ± SEM. Statistical differences are indicated as * $p < 0.05$ and ** $p < 0.01$, against non-treated control and among conditions; and as # $p < 0.05$ and ## $p < 0.01$, against 8 Gy irradiated non-treated control. CTL, control; IC_{50}, half-maximal inhibitory concentration.*

11.3.2.6 Assessment of the ability of AM and radiotherapy combination to impair clonogenicity

Altogether, confluence differences observed through phase contrast light microscopy (Figure 49), along with the results from cell cycle analysis with flow cytometry (Figure 52), evidenced how AM had an impact on cell proliferation capacity in the A549 cell line. Thus, we performed clonogenic assays to evaluate long-term proliferation effects. For this experiment, A549 cells were treated as in previous experiments and were grown for 12 days, when colony formation was analyzed.

Results showed a significant decrease in colony formation after AM single treatment, although irradiation alone had a higher impact on long-term proliferation (Figure 53). Moreover, when irradiation was combined with 1 h AM pretreatment, the clonogenic potential of A549 cells did not change regarding the single-irradiation condition. However, when cells were exposed to AM for 24 h before irradiation, there was an evident reduction in the number of colonies, which suggests that survivin inhibition slightly enhances the effects of RDT on NSCLC cells.

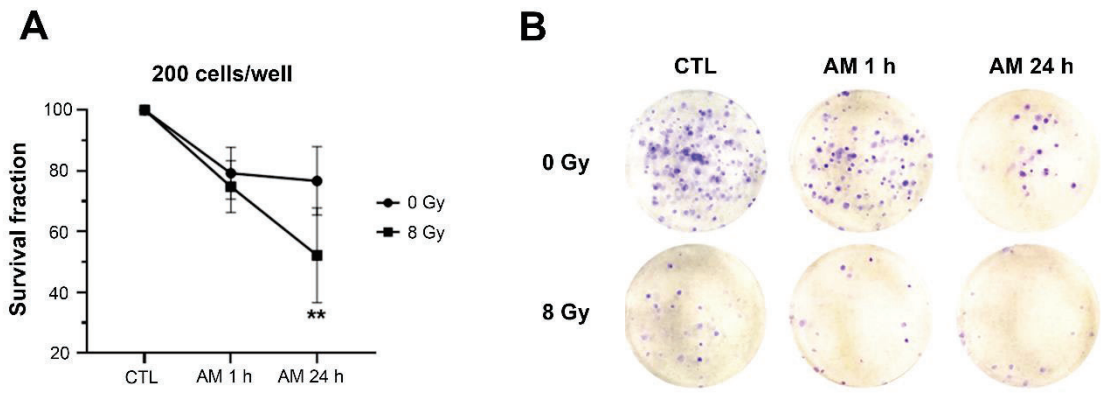

*Figure 53. Effect of asenapine maleate (AM) and irradiation in combination on the clonogenic ability of A549 lung adenocarcinoma cell line. Colony formation percentages (%) are shown (A), as well as representative images of the different conditions of the clonogenic assay (treatment with or without AM (half-maximal inhibitory concentration (IC_{50})) added either 1 h or 24 h previous to irradiation (8 Gy) in A549 cells). Figure shows mean ± SEM. Statistical differences against control (CTL, 0 Gy) and among conditions are indicated as ** p < 0.01. CTL, control.*

11.3.3 Combination of AM with immunotherapy

11.3.3.1 Evaluation of DAMPs production after AM treatment

ICD was analyzed to evaluate whether AM could induce and activate a potential adaptive immune response *in vivo* against dying or stressed cells, which release DAMPs. Therefore, we measured the exposure and release of DAMPs (CALR, ATP, HMGB1) in cells treated with AM to evaluate the induction of ICD by this compound (Figure 54). AM significantly increased CALR exposure -the most characteristic signal of ICD- in A549 cells treated with the IC_{25} of AM for 24 h. In LLC1 cells (used in further *in vivo* experiments), we observed a significant increase in CALR exposure at IC_{75}.

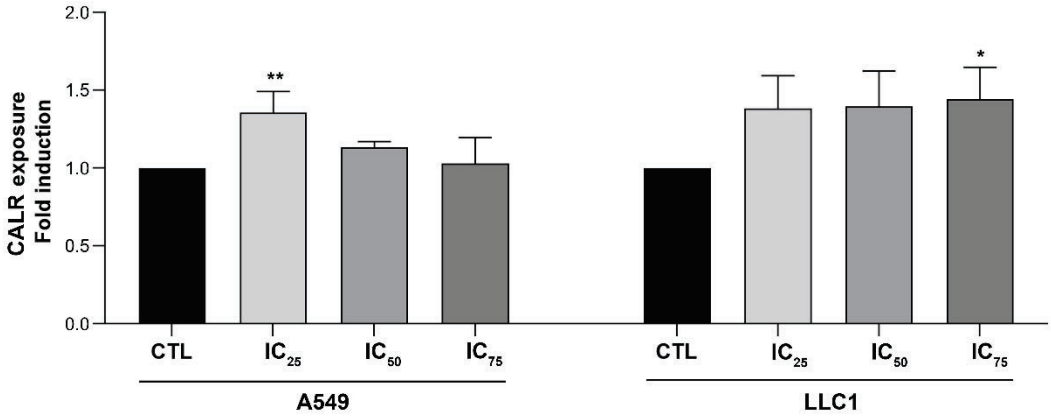

*Figure 54. Calreticulin (CALR) exposure after asenapine maleate (AM) treatment. A549 and LLC1 cells were treated with 25% inhibitory concentration (IC_{25}), half-maximal inhibitory concentration (IC_{50}) and 75% inhibitory concentration (IC_{75}) of AM for 24 h. The surface exposure of CALR was determined by immunofluorescence cytometry among viable (7-Aminoactinomycin D - negative) cells. Bars represent the mean ± SD. Statistically significant results are indicated as *, p-value < 0.05; **, p-value < 0.01; ***, p-value < 0.001. CTL: control.*

ATP release was significantly increased in A549 cells treated with the IC_{75} of AM (Figure 55).

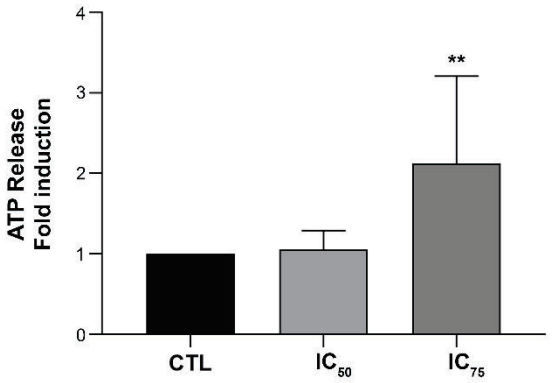

*Figure 55. ATP release after treatment with asenapine maleate (AM). Cells were treated with half-maximal inhibitory concentration (IC_{50}) and 75% inhibitory concentration (IC_{75}) of AM for 24 h. Culture supernatants were collected 24 h after treatment. ATP release was measured with a chemiluminescent assay in A549 cells. Bars represent the mean ± SD. Statistically significant results are indicated as **, p-value < 0.01. CTL, control.*

A similar result was obtained in the case of HMGB1 release, since secretion was the highest when A549 cells were treated with IC_{75} of AM (Figure 56).

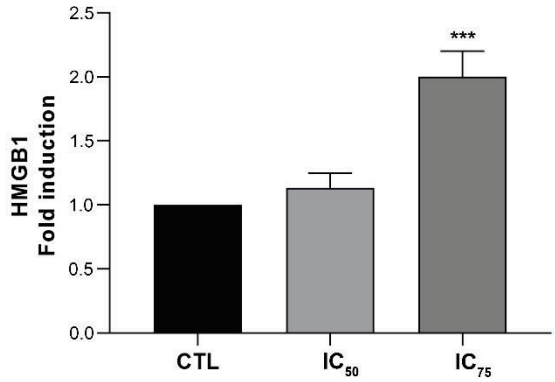

*Figure 56. High-mobility group box 1 (HMGB1) release after asenapine maleate (AM) treatment. Cells were treated with half-maximal inhibitory concentration (IC_{50}) and 75% inhibitory concentration (IC_{75}) of AM for 24 h. HMGB1 release was detected by ELISA in A549 cells. Bars represent the mean ± SD. Statistically significant results are indicated as ***, p-value < 0.001. CTL, control.*

Our results suggest that AM may induce ICD in A549 and LLC1 cells, since it is able to increase DAMPs presence in the cell or their release to the cell environment, leading to a potentially higher activation of the immune response *in vivo* against the tumor cells.

11.4 Preclinical evaluation of the AM monotherapy and combined therapy for tumor sensitization to pro-apoptotic therapies *in vivo*

11.4.1 *In vivo* safety studies of AM

In order to evaluate AM safety *in vivo* and determine the most appropriate dose for the efficacy studies, three different doses of AM (10, 15, 20 mg/kg) or V were administered intraperitoneally to C57BL/6J mice, following a schedule of five consecutive days per week. Although mice lost some weight in the first two days of each cycle, they all recovered and did not show any differences compared to control mice weight at the end of the experiment (Figure 57).

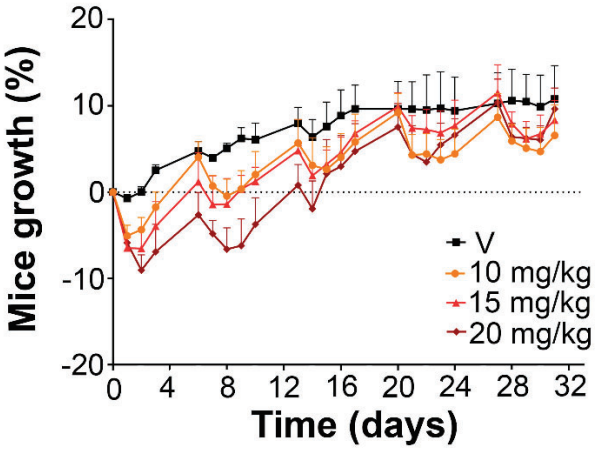

Figure 57. Mice growth monitoring along the safety evaluation of asenapine maleate (AM). Mice weight was monitored during AM treatment (AM doses of 10, 15 and 20 mg/kg and the vehicle (V)) and expressed as the percentage difference from the baseline weight. Results are shown as mean ± SEM.

However, mice showed transient mild secondary effects at the higher doses of AM, e.g. low motility after drug administration, compatible with sedation or somnolence effects typically induced by antipsychotic drugs. On the other hand, vital organs showed no macroscopic differences among all groups. Neither organ weight showed significant changes between groups (Figure 58).

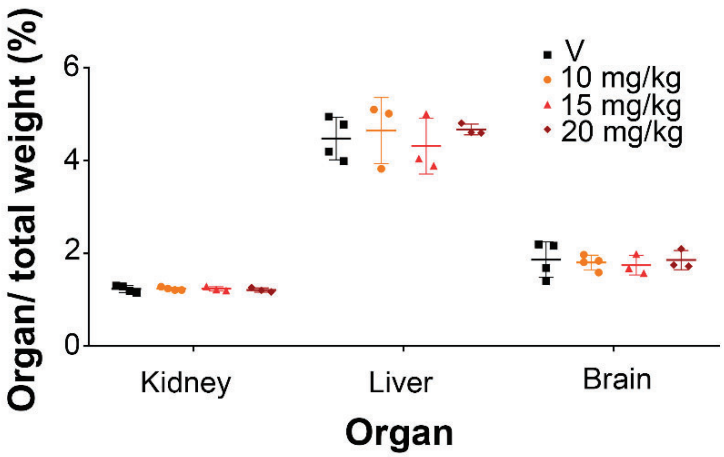

Figure 58. Vital organ's weight at the end of asenapine maleate (AM) safety evaluation. The organ's weight of mice is not altered by AM treatment. After 32 days of treatment with AM (AM doses of 10, 15 and 20 mg/kg) and the vehicle (V), mice were sacrificed and vital organs were isolated and weighed. Organs' weights are represented as a percentage of mice weight. Results are shown as mean ± SD.

Moreover, the alanine aminotransferase (ALT) activity assay showed that AM did not cause significant hepatocellular injury at the tested doses (Figure 59).

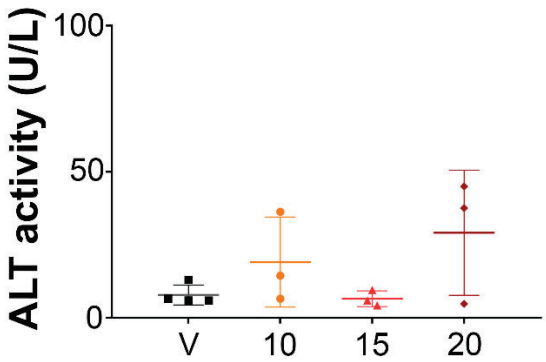

Figure 59. Alanine aminotransferase (ALT) activity after asenapine maleate (AM) treatment in mice. ALT activity was measured using a colorimetric assay kit in blood samples of mice treated with different concentrations of AM (10, 15 and 20 mg/kg) and the vehicle (V). Results are shown as mean ± SD.

At the microscopic level (Figure 60), vital organs (liver, kidney and brain) did not present detectable structural or cellular alterations, indicating that administered doses were well tolerated.

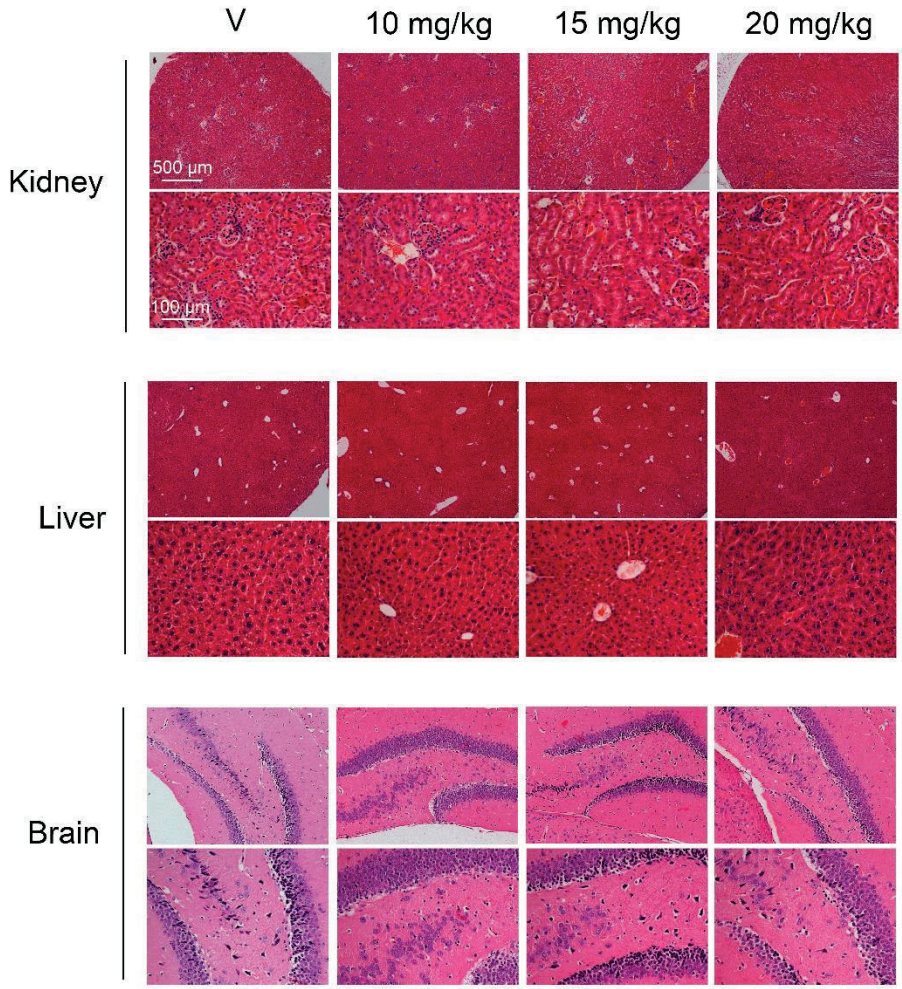

Figure 60. Histological structure of vital organs after asenapine maleate (AM) treatment in mice. Representative microscopic images of mouse liver, kidney and brain stained with H-E for each treatment group (AM at 10, 15 and 20 mg/kg and the vehicle (V) for the control group).

11.4.2 *In vivo* therapeutic efficacy studies

11.4.2.1 Evaluation of antitumor therapeutic effect in ectopic mouse models

We generated a subcutaneous tumor model in mice by inoculating 5 x 10^4 LLC1 cells in the flank of C57BL/6J mice. Once the tumor reached the volume of 40 mm^3, a dose of 10 mg/kg of AM was intraperitoneally administered five consecutive days per week for a total of three weeks. Mice weight evolution of treated mice was similar to the control group (Figure 61).

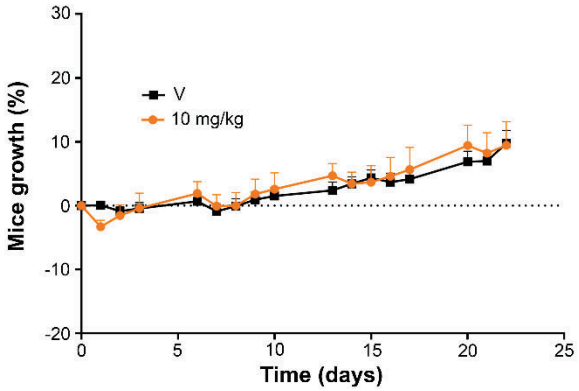

Figure 61. Mice growth monitoring along the therapeutic efficacy study of asenapine maleate (AM). Mice's weight was monitored during treatment with AM (10 mg/kg) and expressed as a percentage difference from the baseline weight. Results are shown as mean ± SEM. V, vehicle.

Interestingly, tumors of AM-treated mice (10 mg/kg) grew slower than the control group (V) (Figure 62A), although the differences were not statistically significant due to high variability in the size of the tumors from the control group.

Observing individually the subjects of the study (Figure 62B and C), it is even more evident that most of the tumors of the control group (Figure 62B) grew faster than the tumors of the treated group (Figure 62C). Moreover, at the end of the study, the mean of the tumor volume was considerably higher in the control group (1461,4 mm^3) than in the treated group (880,1 mm^3). Despite this disparity, the difference is not statistically significant due to the variability of the control group, since some tumors seemed not to grow properly.

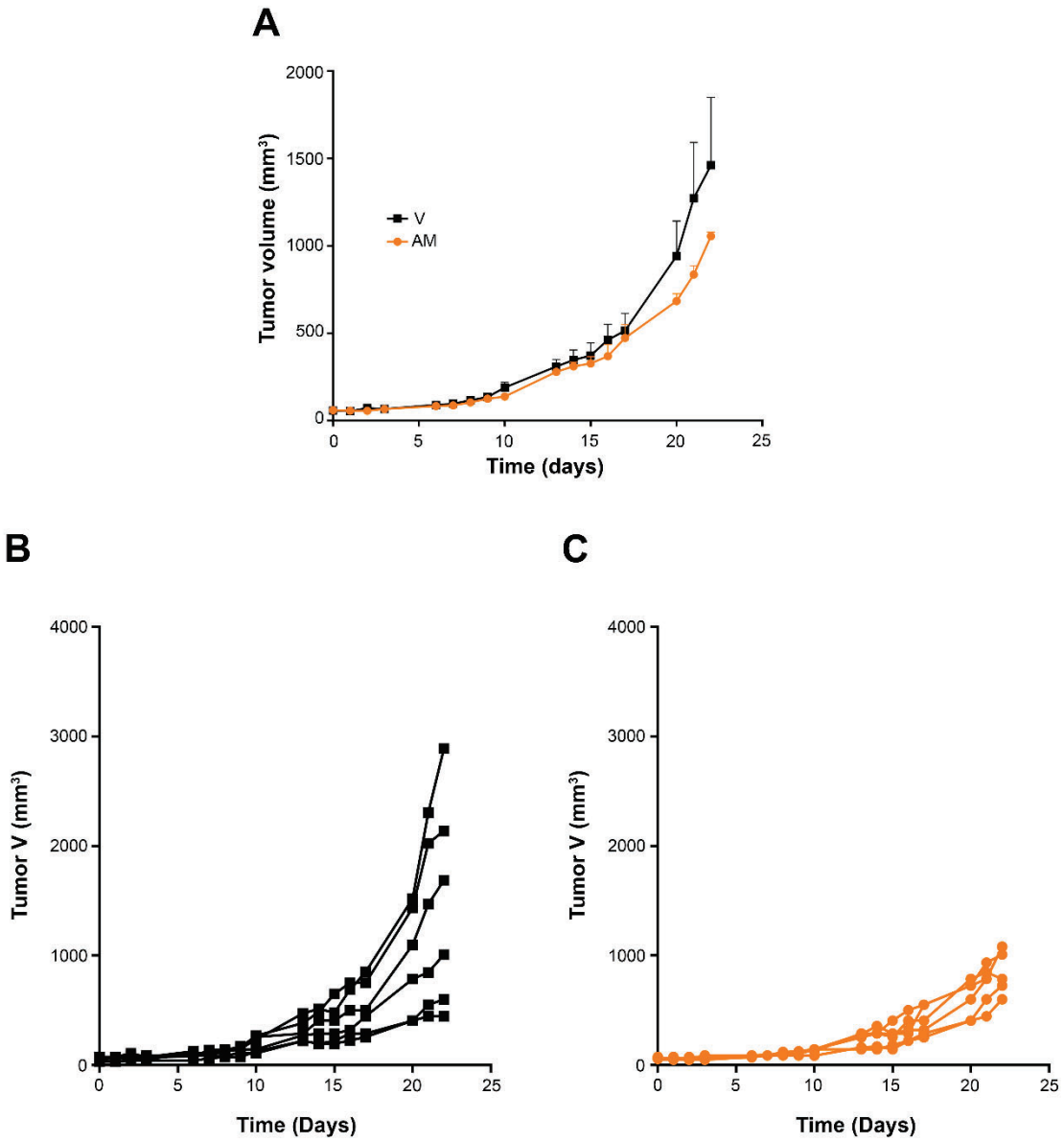

Figure 62. Tumor volume evolution along the therapeutic efficacy study of asenapine maleate (AM). C57BL6 mice were treated with 10 mg/kg of AM 5 days a week. The control group was treated with vehicle (V). We measured tumor volume during the experiment. Results are shown as mean ± SEM (A). Individual values are shown for the control group (B) and the AM-treated group (C).

At the end of the experiment, mice were sacrificed and tumors were isolated. The tumor weight of mice treated with AM was in the range of 800-1000 mg in nearly all mice. However, in the control group, more than half of the animals' tumors weighed around 1500 mg or more, while there were two cases in which tumors remained at 300-500 mg (Figure 63A). Again, the high variability in the control group hinders the analysis of the results in the efficacy assay, because the difference in tumor weights is not considered

statistically significant despite the huge difference between most of the control specimens and the treated mice.

Despite those results, a difference in tumor size between groups can be appreciated macroscopically (Figure 63B), indicating that AM decreases tumor growth in treated mice.

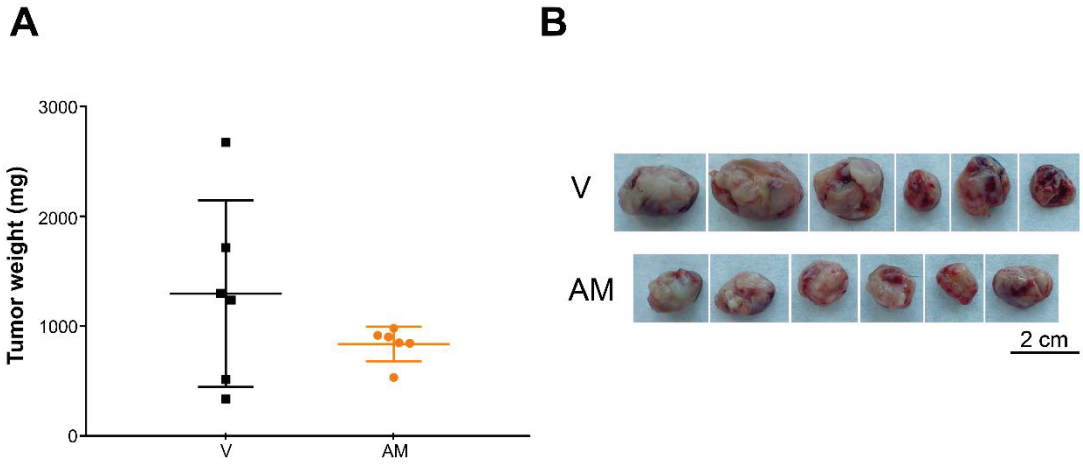

Figure 63. Therapeutic efficacy evaluation of asenapine maleate (AM) treatment. C57BL6 mice were treated with 10 mg/kg of AM 5 days a week. The control group was treated with vehicle (V). At the end of the experiment, tumors were isolated and weighed. Results are shown as mean ± SD (A). Macroscopical images of all tumors are shown (B). Scale bar: 2 cm.

Finally, we confirmed the effect of AM as a survivin inhibitor by evaluating the expression of survivin protein in the tumors, observing that AM reached and efficiently downregulated survivin levels in the tumors (Figure 64).

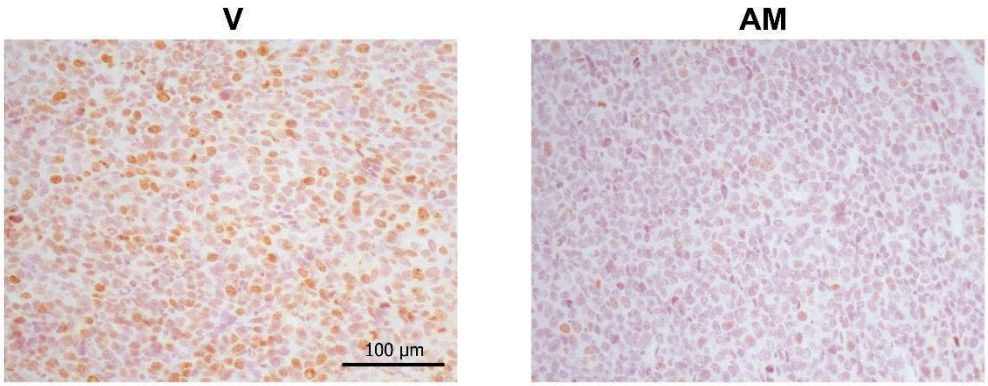

Figure 64. Survivin expression in control (with vehicle (V) administration) and asenapine maleate (AM)-treated tumors. Original magnification: 100x. Scale bar: 100 µm.

11.4.2.1.1 Effect of AM treatment on angiogenesis in an ectopic mouse model

In the assessment of the therapeutic efficacy of AM, we observed a difference in the consistency of the tumors between the treated and the control group. Tumors of AM-treated mice were softer and slightly more viscous than the control group. This, together with the fact that survivin is involved in angiogenic processes such as the proliferation of vascular endothelial cells and the secretion of VEGF, led us to think that AM could be affecting angiogenesis. Thus, the expression of CD31 (a marker for angiogenesis and microvessel density) was analyzed in tumor sections by immunofluorescence (Figure 65A). The percentage of tumor area that was blood vessels was calculated and, although it was not statistically significant, a small difference between the control and the treated group was observed (Figure 65B).

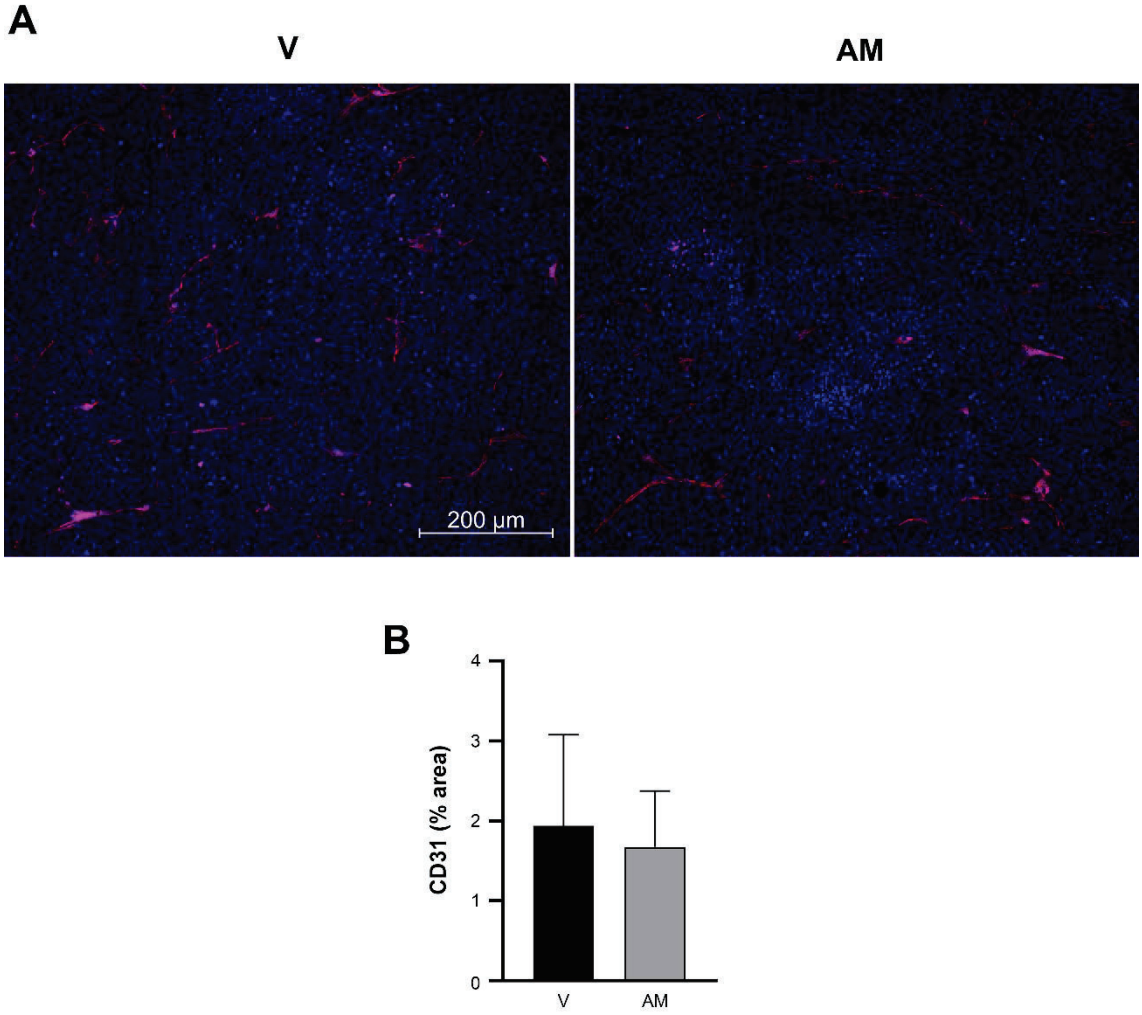

Figure 65. CD31 expression in tumors of control (vehicle (V)) and asenapine maleate (AM)-treated mice. Tumor-bearing mice were treated with AM or the vehicle for 22 days. At the end of the experiment, tumors were isolated and processed for histological study. Immunofluorescence on CD31, a marker of angiogenesis, was performed on these samples (A). The tumor area corresponding to CD31 was quantified and represented as mean ± SD (B). Original magnification: 100x. Scale bar: 200 µm.

11.4.2.2 Therapeutic efficacy study of AM and cisplatin combination

In order to assess the therapeutic efficacy of AM in combination with cisplatin, we used an ectopic lung cancer mice model generated by inoculating 5 x 10^4 LLC1 cells in the flank of each animal. Once the tumor generated in mice reached 40 mm^3, we started with the administration of cisplatin (3 mg/kg days 0, 3 and 6). Then, we administered 5 mg/kg AM in a regimen of five consecutive days per week until the end of the experiment (18 days).

The first week of treatment, mice treated with cisplatin or the combination lost some weight, but they recovered and, by the end of the experiment, mouse weight was similar in all four groups (V, treated with AM, treated with cisplatin and treated with the combination) (Figure 66).

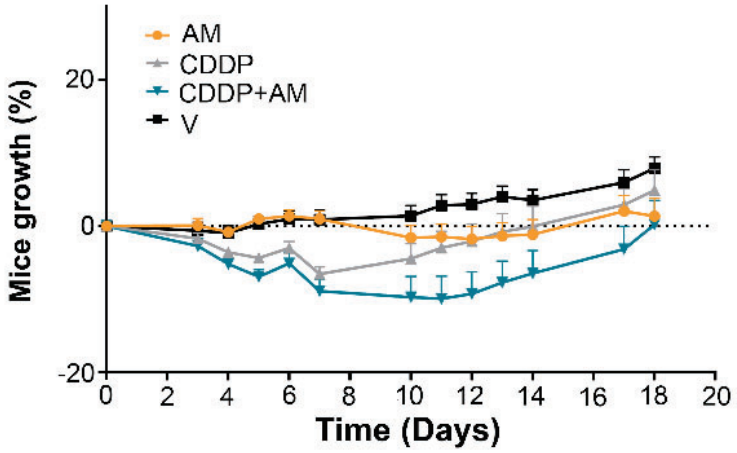

Figure 66. Mice growth monitoring along the therapeutic efficacy evaluation of asenapine maleate (AM) plus cisplatin (CDDP) combination. Mice weight was monitored during treatment with AM (5 mg/kg, five consecutive days per week), cisplatin (3 mg/kg, days 0, 3 and 6) and the combination. The change in mouse weight is expressed as a percentage difference from the initial weight. Results are shown as mean ± SEM. V, vehicle.

Tumors from mice treated with cisplatin or the combination seemed to have slower growth than those in mice treated with the V or AM, with tumors from mice treated with the combination being the ones with the slowest growth (Figure 67A). Moreover, the group treated with the combination presented the lowest tumor weight, with a significant difference compared to the control group (Figure 67B). Isolation of tumors also allowed us to observe macroscopically the difference in size among groups, especially between the control group and the combination one (Figure 67C).

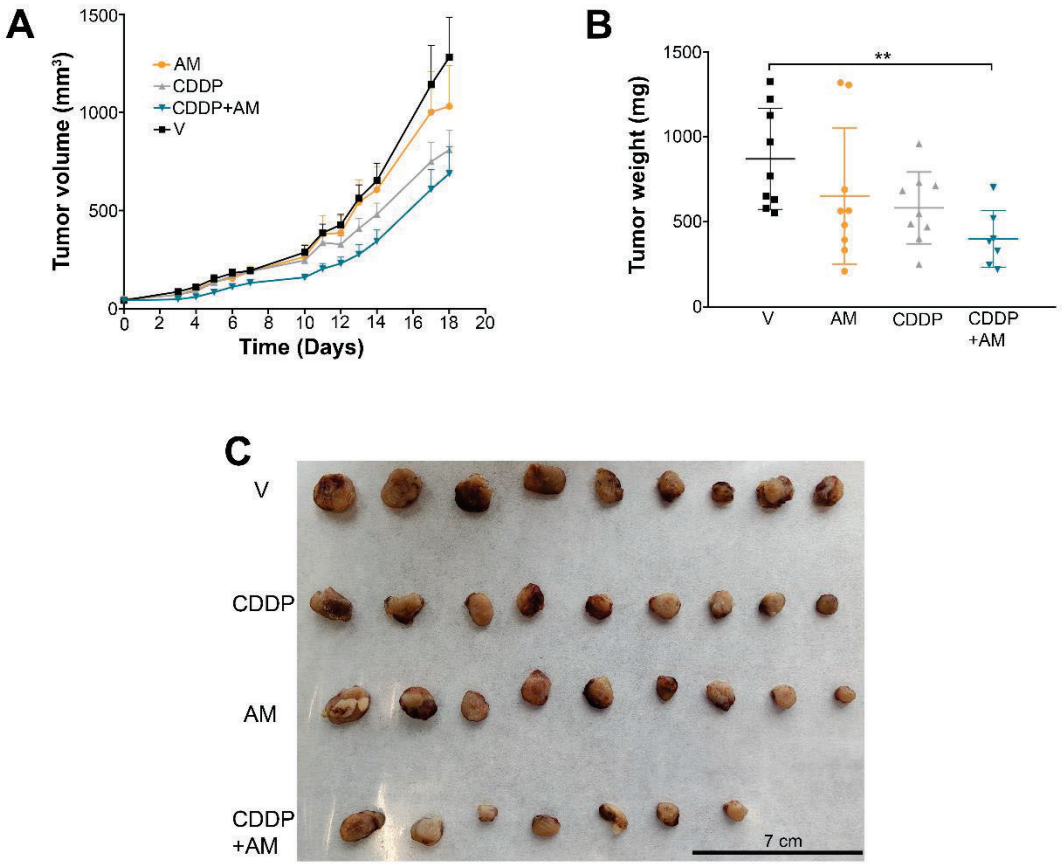

*Figure 67. Therapeutic efficacy evaluation of asenapine maleate (AM) plus cisplatin (CDDP) treatment in mice. Tumor volume was measured during the experiment. Results are shown as mean ± SEM (A). At the end of the therapeutic efficacy assay, tumors were isolated and weighted. Results are shown as mean ± SD (B). Macroscopical images of all tumors are shown (C). Statistically significant results are indicated as **, p-value < 0.01.*

11.4.2.2.1 Analysis of immune infiltration in the tumors of AM-treated mice

In previous experiments, we observed higher levels of DAMPs in cancer cells treated with AM, which suggested the induction of ICD by AM. This fact could stimulate the immune response *in vivo*. To corroborate this hypothesis, we analyzed lymphocyte infiltration by immunohistochemistry techniques in tumors from the previously mentioned *in vivo* experiment. In tumors of mice treated with AM, we observed great levels of necrosis, especially in AM-treated mice tumors, which hindered the labeling of lymphocytes and the analysis of the samples (Figure 68). Thus, a conclusion cannot be obtained from this experiment, since the higher staining in AM-treated tumors corresponds to tumor necrosis.

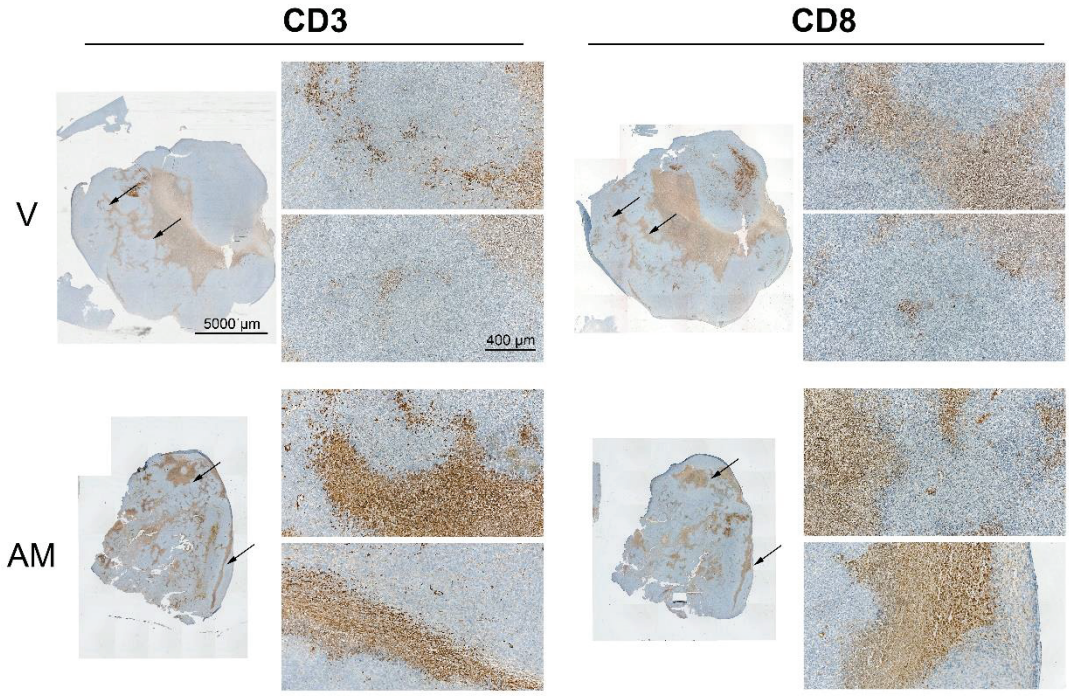

Figure 68. Evaluation of lymphocyte infiltration in tumors after asenapine maleate (AM) treatment in mice. Tumors of LLC1 cells were induced in mice. Once the tumor was palpable, mice were treated with vehicle (V) or AM for 12 days. Then, tumors were collected and were used to evaluate lymphocyte infiltration by immunohistochemistry staining of CD3 and CD8. The stained area does not correspond to lymphocytes but to necrotic tissue. Original magnification: 25x. Scale bars: 5000 and 400 µm.

11.4.2.3 Evaluation of antitumor therapeutic effects in a transgenic mouse model

The efficacy of the combination of AM and CDDP was also tested in a Cre recombinase-controlled (Cre/LoxP) tumor model derived from some somatic cells that are transformed in their natural location. Following this approach, lung cancer was induced in mice with an oncogenic mutation in KRAS (KRASG12D) and stop elements flanked by LoxP sites that avoided the expression of mutant K-RAS until the inhalation of viruses expressing Cre recombinase. The treatment started 13 weeks post-infection. Mice were treated with AM, CDDP or CDDP with AM administered sequentially until the end of the experiment, 36 days after the first administration. There were no significant differences in mice weight among the groups at the end of the experiment, although those treated with CDDP were the ones with the lowest weight (Figure 69).

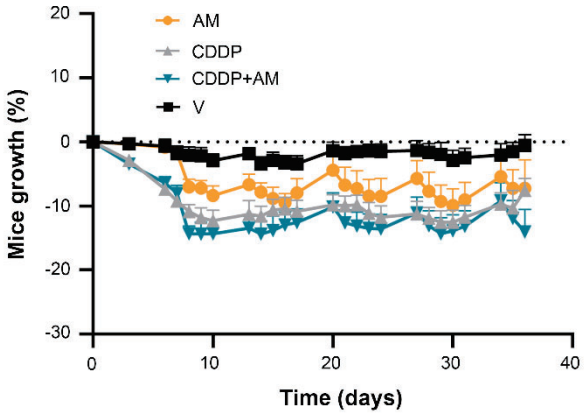

Figure 69. Mice growth monitoring during asenapine maleate (AM) and cisplatin (CDDP) combination treatment. Mice weight was monitored during treatment with AM (5 mg/kg, five consecutive days per week), cisplatin (3 mg/kg days 0, 3 and 6) and the combination. The change in mouse weight is expressed as a percentage difference from the initial weight. Results are shown as mean ± SEM. V, vehicle.

At the end of the experiment, the lungs were isolated and weighed. Lung weight was similar in all cases (Figure 70).

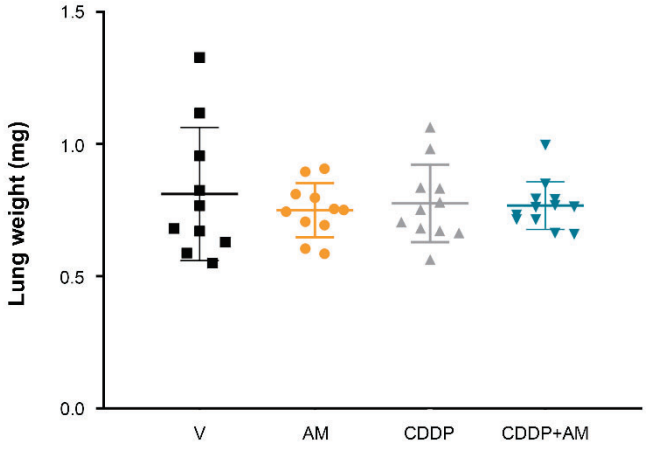

Figure 70. Lung weight after asenapine maleate (AM) and/or cisplatin (CDDP) treatments. At the end of the therapeutic efficacy assay of CDDP and AM combination in the transgenic mice model, the lungs were isolated and weighed. Results are shown as mean ± SD. V, vehicle.

In order to evaluate the effect of the treatments on lung cancer, we processed lungs for histopathological analysis and obtained microscopic images of the lung. Then, we calculated the percentage of area with cells, among which the cancer cells were. Hence, the higher the number of cells, the more advanced lung cancer is. Differences in the tumor area among groups were not detected (Figure 71).

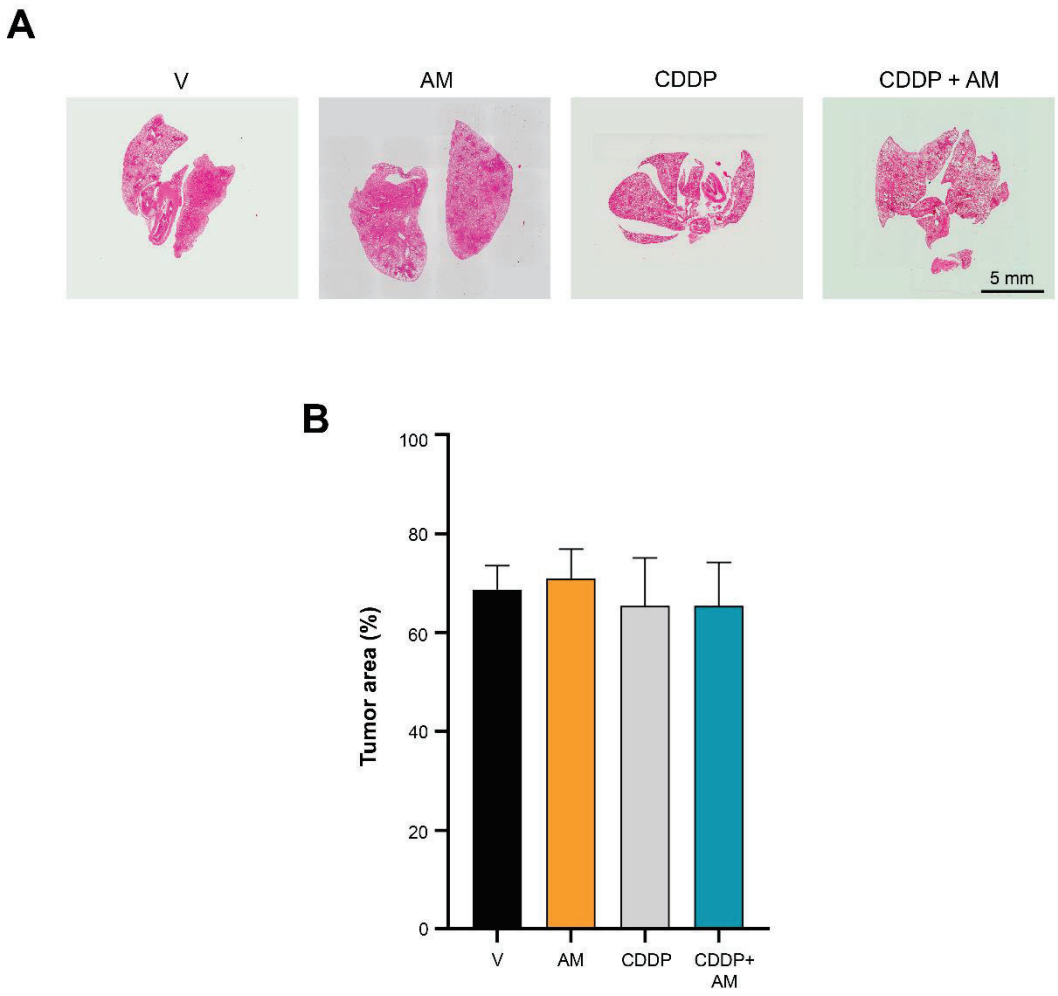

Figure 71. Tumor area quantification in lungs of treated mice. Lung cancer-bearing mice were treated with asenapine maleate (AM) and/or cisplatin (CDDP). At the end of the experiment, lungs were collected and processed for histopathological analysis by hematoxylin-eosin staining. Pictures of the whole lung were obtained and were observed by optical microscopy (A). Finally, the H-E stained area was quantified (B). Results are shown as the mean of the percentage of stained area ± SD. Original magnification: 25x. Scale bar: 5 mm. V, vehicle.

11.4.2.4 Therapeutic efficacy of cisplatin and AM combination in in vivo *experiments in NSG mice*

AM docking experiments were performed using the structure of human survivin. Thus, we decided to test AM and AM plus CDDP therapeutic efficacy in immunodeficient mice (NSG mice), which allowed us to test whether AM treatment could be more efficient against human survivin. To induce subcutaneous tumors of human lung cancer cells, 4 x

10^6 A549 cells were inoculated in each flank of mice. Once the tumors reached 150 mm^3 approximately, CDDP (3 mg/kg) was intraperitoneally administered on days 0, 3 and 6. After the treatment with AM, in the combination group, AM was intraperitoneally administered five consecutive days per week for a total of three weeks. Mice weight evolution was similar in all groups, being the CDDP-treated mice those with the lowest weight (Figure 72).

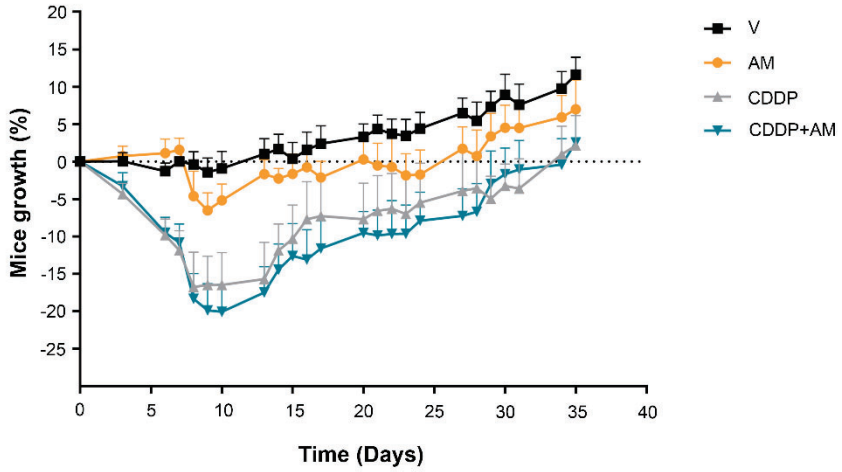

Figure 72. Mice weight after asenapine maleate (AM) and/or cisplatin (CDDP) treatment in NSG mice. Mice weight was monitored during treatment with AM (5 mg/kg, five consecutive days per week), cisplatin (3 mg/kg days 0, 3 and 6) or the combination. The change in mouse weight is expressed as a percentage difference from the initial weight. Results are shown as mean ± SEM. V, vehicle.

In contrast to the control group, tumors of AM-treated mice present a tendency to stabilize their growth, which suggests AM might be impairing tumor growth after only three weeks of treatment (Figure 73A). Moreover, the mean of tumor weights in AM-treated mice is lower than in the control group (Figure 73B). Additionally, they showed less variation than mice with only V administration, being all tumors below 800 mg. Tumor weights of cisplatin-treated mice are significantly lower than in the control group. When cisplatin is combined with AM, although the mean tumor weight is not as small as with cisplatin alone, it is slightly lower than in the control group (Figure 73B). These differences can also be appreciated macroscopically (Figure 73C).

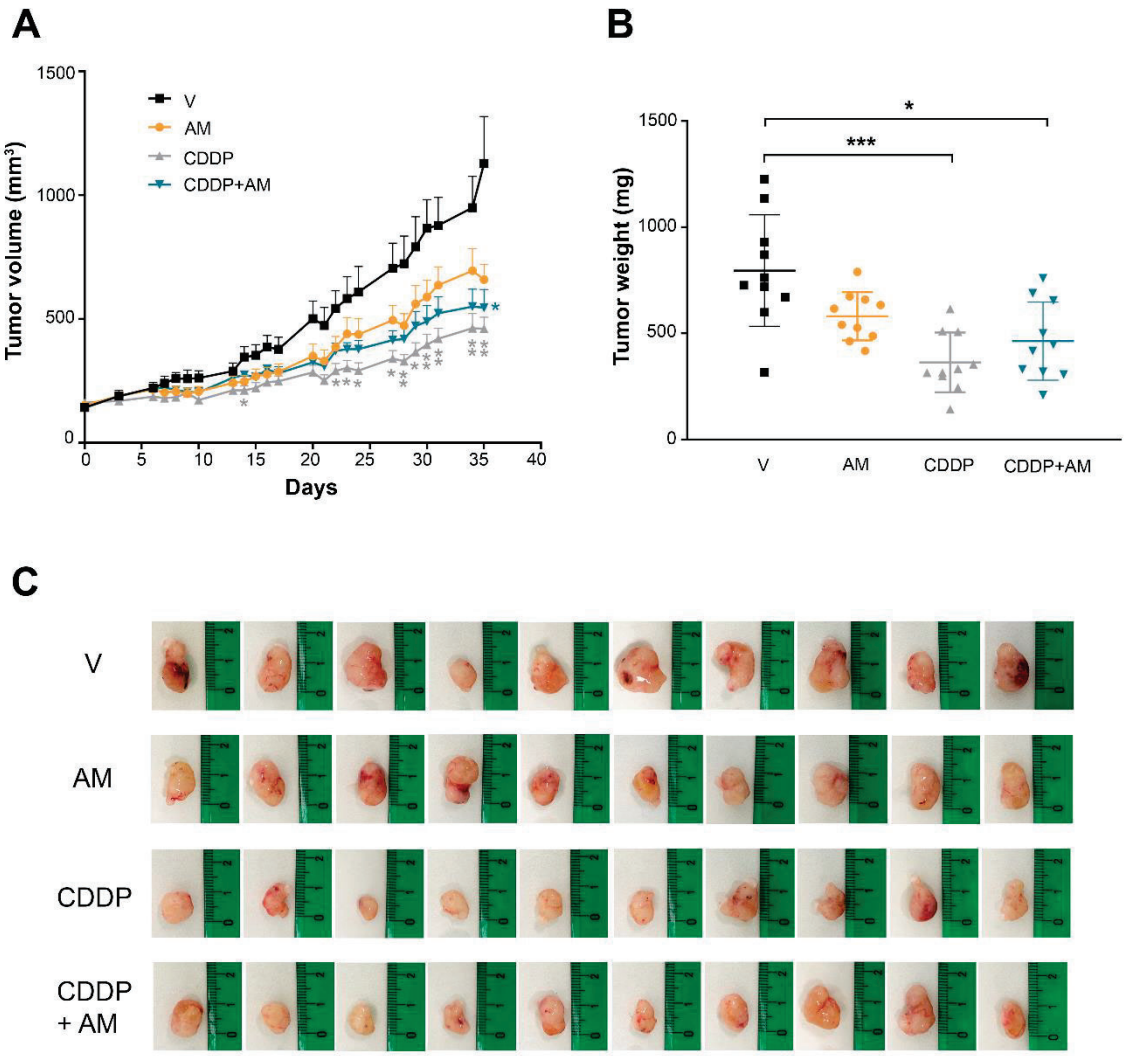

*Figure 73. Evaluation of asenapine maleate (AM) and cisplatin (CDDP) therapeutic efficacy in NSG mice. Tumor volume was measured during the experiment (A) and, at the end, tumors were isolated and weighted (B, C). Results of the tracking of tumor volume are shown as mean ± SEM, while tumor weight data are represented as mean ± SD. V, vehicle. Statistically significant results against control group (V) are indicated as *, p-value < 0.05; ***, p-value < 0.001.*

12 DISCUSSION

Cancer is the main cause of death in the world. In 2022, nearly 19 million people were diagnosed with cancer and almost 10 million died because of it (42). Lung cancer is the type of cancer with the highest number of new cases in 2022. Moreover, 18.7% of cancer-related deaths were attributed to lung cancer in 2022, being the type of cancer with the highest mortality. In economically developed countries, lung cancer mortality has diminished thanks to the awareness of smoking effects, an earlier diagnosis and advanced therapies, such as targeted therapies and immune checkpoint inhibitors (406). Nevertheless, the mortality rate remains very high, so new therapeutic approaches need to be investigated. The evasion of cell death is considered a hallmark of cancer (8) as well as a mechanism of treatment resistance (108), an important obstacle in cancer treatment.

12.1 Survivin selection: value as a molecular target and biomarker in cancer therapeutics

In order to select a suitable therapeutic target for the treatment of lung cancer, we performed a gene expression array in several healthy and pathological patient samples of human squamous cell lung carcinoma tissue. Among other genes, BIRC5, encoding for survivin, was found to be upregulated. Survivin belongs to the IAP family. IAPs have been found to be upregulated in cancer, and their expression is correlated with treatment response and prognosis (156), which makes IAP protein family an **attractive target for cancer treatment**.

Survivin is implicated in the main processes involved cancer transformation, which are dysregulated proliferation and cell death. On the one hand, survivin is needed for the CPC formation, which is crucial for the correct segregation of chromosomes and cytokinesis (175,176). Survivin is also involved in microtubules formation (193). In fact, survivin is enriched at the G_2/M phase of the cell cycle (407). On the other hand, survivin can inhibit apoptosis in a caspase-dependent manner by direct or indirect inhibition of caspases. In the first case, survivin is able to inhibit caspase 3, 7 and 9 by directly binding them (197–199,408) after being released from mitochondria upon cell death stimulus, preventing apoptosis. Survivin can also form a complex with XIAP, increasing its stability

and inhibiting caspases 3, 7 and 9 (186,200). Finally, survivin can also form a complex with HBXIP that binds to procaspase 9 and, as a result, the apoptosome cannot be formed. Additionally, survivin can inhibit caspases indirectly by binding to Smac/DIABLO, inhibiting its proapoptotic function.

In the second case, survivin can also inhibit apoptosis in a caspase-independent manner by interacting with AIF. This interaction hinders AIF translocation to the nucleus to induce DNA fragmentation.

Another fact that makes survivin an interesting therapeutic target is its almost undetectable expression in most normal differentiated tissues. Moreover, although it is expressed in hematopoietic progenitor cells, T lymphocytes, endothelial cells and testes (183), the levels of survivin in cancer cells are much higher (184), which implies that a treatment targeting survivin could specifically have more effect on cancer cells than in healthy cells.

The validation of survivin as a good therapeutic target in cancer has been confirmed by multiple research studies that silenced this protein and observed anticancer effects *in vitro* and *in vivo*. In 2015, Zhang et al generated a survivin-targeted short hairpin RNA (shRNA). The shRNA was transfected into A549 cells, suppressing proliferation and colony formation ability of the cancer cells, as well as inducing apoptosis. They also performed *in vivo* experiments by inoculating A549 cells in nude mice and, once the tumor was formed, they treated them with survivin-targeted shRNA. Results showed that inhibiting survivin with a shRNA hinders tumor growth (409). Shan Liu et al observed a similar result in a 4T1 murine breast cancer model after inhibiting survivin. They administered survivin-targeted siRNA to mice and apoptosis increased in tumor cells, inhibiting tumor growth and metastasis (410). There is also evidence that inhibition of survivin may help to overcome chemotherapy resistance. Treatment with survivin-targeted siRNA followed by chemotherapy sensitized retinoblastoma cells to carboplatin and melphalan, but not the healthy retinal epithelial cells (411). The therapeutic strategy to sensitize tumors to chemotherapy has also been tested *in vivo*. Vivas-Mejia et al. demonstrated that treatment with siRNA against one of the splicing variants of survivin (2B), combined with docetaxel, enhanced the antitumor effect of the chemotherapeutic in an orthotopic murine model of taxane-resistant and non-resistant ovarian cancer

(412). To overcome resistance to paclitaxel in breast cancer, Chen et al. developed a new strategy to co-delivery the chemotherapeutic with survivin-targeted siRNA, and a synergistic inhibitory effect on tumor growth and pulmonary metastasis was observed. Survivin-targeted siRNA has also been combined with Pt (IV) for the treatment of resistant lung cancer model in nude mice, and the results suggest inhibition of survivin together with chemotherapy treatment may reverse cisplatin resistance (413).

In summary, the role of survivin in critical processes for cancer transformation and progression, together with its elevated expression in tumor tissue, establish survivin as a potential therapeutic target. Multiple studies support this hypothesis, demonstrating that survivin inhibition exhibits anticancer effects *in vitro* and *in vivo*.

Furthermore, the importance of survivin expression is reflected in the fact that it has been identified as a **prognosis biomarker in cancer**. This means survivin expression provides information on the likely course of cancer disease in a non-treated patient. Additionally, survivin acts as a predictive marker, helping identify subpopulations of patients more likely to respond to a specific therapeutic approach.

In terms of prognostic relevance, elevated levels of survivin are associated with higher proliferative index and more aggressive and advanced clinicopathologic features. High expression of survivin is also correlated with a higher likelihood of tumor recurrence and impaired disease-free and OS rates.

In lung cancer, a meta-analysis performed in 2021 by Fung et al. found 33 studies that revealed a positive correlation between survivin expression and poor prognosis. Seven studies showed a strong positive correlation between survivin expression and disease recurrence. There was also an association between survivin and T stage, Union for International Cancer Control (UICC) stage, presence of lymph node metastasis and grade of differentiation (414). There is also literature that suggests survivin contributes to carcinogenesis, tumor vascularization, metastasis and treatment resistance (415).

Chen et al. demonstrated that survivin and VEGF are overexpressed in SCLC and are associated with lymph node metastasis. Moreover, survivin expression was significantly coincident with VEGF expression, which indicates a correlation between survivin and vascularization. OS was shorter in the survivin-positive group than in the VEGF-positive

group. They were independent predictive factors of poor prognosis in SCLC patients (416).

In a study, in which they looked at survivin protein and mRNA overexpression, no correlation was found between survival and survivin levels. However, cytoplasmic immunoreactivity was correlated with tumor stage. Survivin mRNA levels were elevated in 96% of carcinomas, with higher levels in squamous cell carcinomas. Cytoplasmic and nuclear immunoreactivity were found in 70% and 80% of tumors (respectively). Both (cytoplasmic and nuclear) were present in 54%. An important finding of this study is that high levels of survivin are detectable in pre-neoplastic lesions such as dysplastic bronchial squamous metaplasia. Although survivin expression has no prognostic implications in these patients, detecting survivin levels may be important in the early diagnosis of cancer or in predicting the effect of some anticancer strategies. The results of this study, which suggest an important role of survivin in the early stages of carcinogenesis, support the idea that survivin is a potential novel target for new therapeutic approaches in lung cancer (417).

In other types of cancer, such as in the case of pancreatic ductal adenocarcinoma (PDAC), elevated levels of survivin in serum and high survivin expression at diagnosis demonstrated poor outcomes (higher invasion and lower rates of OS) (418). Similar results were obtained in gastric cancer, in which an association was found between the expression of survivin and the presence of lymph node metastases, as well as the correlation between the expression of survivin and OS for patients (419). In renal cancer, survivin expression is correlated with lower OS and more advanced clinicopathological features (420). In the case of follicular thyroid carcinoma, there is also a correlation between survivin expression and recurrent disease (420). Survivin expression has been also associated with tumor grade in ovarian carcinoma (421), tumor stage and degree of differentiation of hepatocellular carcinoma (422), clinical stage and tumor grade in cervical cancer (423), tumor stage and cellular differentiation in gallbladder cancer (424) and tumor size and lymph node status in triple-negative breast cancer (425). In the case of esophageal cancer, a meta-analysis revealed that survivin overexpression is associated with poor prognosis. However, correlations with stage, grade of differentiation, lymph node status and metastasis were not found (426,427).

Another important fact of survivin is that it can be studied by using a non-invasive method, since it can be detected in circulating tumor cells (CTCs). In a study of CTCs in NSCLC patients, 44% of patients expressed survivin and it was correlated with cancer stage, poor survival and nodal status (428). Recently, Lu et al. discovered that survivin reduces immune cell infiltration in the circulatory system, because survivin-positive CTCs negatively correlate with lymphocytes in circulation. Additionally, in this study, the OS rate was lower in the high survivin-positive CTC' group of patients (430).

It should be noticed that elevated survivin levels have different impact on tumor prognosis depending on the survivin cellular localization. Qi et al. reported that nuclear levels of survivin impact on OS and lymph node involvement in patients with adenocystic carcinoma and head and neck squamous cell carcinoma (HNSCC) (430). Nuclear survivin also affects tumor recurrences and relapse-free survival in urothelial bladder cancer (431). Moreover, cytoplasmatic expression (not nuclear) of survivin has been associated with poor OS in oral squamous cell carcinoma, while nuclear expression correlates with a higher proliferation rate (432). Nuclear survivin also correlates with poor outcome in gastroenteropancreatic neuroendocrine neoplasms (433) and PDAC (434). Hennings et al. also demonstrated that only cytoplasmatic survivin is linked to biological aggressiveness and prognosis of prostate cancers (435). Although most of the studies show a correlation between high survivin levels and poor survival, other studies also show survivin as a marker of favorable prognosis. For instance, the high cytoplasmatic-to-nuclear ratio of survivin was associated with improved OS in patients with breast cancer (436) or oropharyngeal squamous carcinoma (437). Okada et al. demonstrated an association of survivin nuclear staining associated with a favorable prognosis in gastric cancer. Additionally, nuclear survivin levels were correlated with younger age and lower incidence of vessel cancer invasion (438). Kennedy et al. also found nuclear survivin overexpression as a prognostic indicator of good prognosis in breast cancer (439). Cytoplasmic survivin was found to be associated with a favorable prognostic factor in patients with acute myeloid leukemia, suggesting cytoplasmic survivin is a critical downstream effector of PI3K/AKT pathway that leads to more chemosensitive cells. They suggest that activation of PI3K/AKT leads to accumulation of cytoplasmic survivin in a phosphorylation-dependent manner in two ways: activation of nuclear export signals

that lead to survivin nuclear exclusion or increasing survivin stability at mitosis. In this study, activation of PI3K/AKT/cytosolic survivin was associated with a more proliferative cell fraction and low proportion of G_0 quiescent cells, with overall and relapse-free survival rates over 60%. The more proliferative the cells, the greater the susceptibility to chemotherapy (440).

These reported discrepancies in the role of survivin as a biomarker may be the result of variation of methodologies used to measure survivin levels (protein vs RNA), cohort sizes or focus on specific cellular pools. When survivin expression is assessed through histochemical staining, factors like specificity and concentrations of antibodies, different cut-off points for subgroups identification of patients and different sample processing techniques, can lead to highly variable results.

As for the **predictive relevance of survivin levels**, it has been shown a correlation between elevated levels of survivin with increased risk of recurrence, lymph node metastases and shorter survival in NSCLC, T1 bladder carcinoma, meningiomas, rectal adenocarcinoma and locally advanced prostate cancer treated with conventional radiation therapy or combined chemoradiation (441). Moreover, survivin levels are associated with superior survival rates in patients with locally advanced esophageal cancer and primary oral squamous cell carcinoma after preoperative irradiation or chemoradiation (442).

Some studies suggest survivin plays an important role in treatment resistance in lung cancer. In a clinical assay with stage III NSCLC patients, survivin levels were measured before and after chemo and radiotherapeutic treatment. 88.7 % of the patients expressed survivin in the tumor before the treatment. After the treatment, downregulated survivin and low survivin scores after chemoradiation were associated with a longer time to recurrence and higher OS, suggesting survivin can be involved in cisplatin resistance (443). Another interesting article shows that silencing survivin in vincristine-resistant A549 cells leads to inhibition of cell viability and enhanced apoptosis induced by vincristine treatment. Survivin silencing also re-sensitized A549 cells to methotrexate (444). In esophageal cancer cell lines, overexpression of survivin reduced the percentage of cell death induced by radiation, which indicates survivin could be a

potential predictor to define patients with esophageal squamous carcinoma that would benefit from radiotherapy (330).

CTC survivin expression may also predict OS in metastatic colorectal cancer patients receiving chemotherapy (445). It is also a promising predictor of hepatocarcinoma prognosis and metastasis, since there were higher survivin-positive CTCs in patients than controls and it was associated with stage and degree of differentiation (422). Survivin-positive CTC is also a prognostic factor in bladder cancer (446) and gastric cancer (447).

All of this data underscores the importance of survivin, not only as a therapeutic target, but also as a valuable biomarker. Based on the extensive literature reviewed, we identified survivin as the most optimal target for anticancer treatment among the other upregulated genes found in the gene expression array of lung cancer samples.

12.2 Targeting survivin for cancer treatment

As it has been exposed, survivin is involved in mechanisms that are crucial for cancer and the progression of the disease. Additionally, it is specifically overexpressed in cancer cells, and it is considered an indicator of prognosis as well as a predictive biomarker. All these characteristics make survivin an excellent potential target for anticancer therapy. Therefore, our lab aimed to develop a cancer therapy specifically targeting survivin. The strategies that can be used to target survivin are transcription inhibitors, SMAC mimetics, Hsp90 inhibitors, homodimerization inhibitors and mitotic inhibitors.

The use of **transcription inhibitors** aims to counteract the overexpression of survivin in tumor cells by inhibiting survivin gene promoter or mRNA. These compounds showed good anticancer effect in preclinical studies. In clinical studies, while they demonstrated acceptable tolerance, their efficacy remained modest. Among the survivin transcription inhibitors, YM155 is the most studied compound. YM155 is a small molecule that suppresses the activity of survivin promoter (270,271). It successfully completed phase I and II clinical trials in solid tumors (448–453) and B-cell lymphoma (454,455). It also presented modest activity against NSCLC, with a disease-control rate like other second-line treatments for advanced NSCLC (273). The combination with carboplatin and paclitaxel had a favorable safety profile, but did not demonstrate improvement in response rate in advanced NSCLC (274). Similar results were shown in other types of

cancer. Posterior data showed YM155 damages DNA, being survivin suppression a secondary event, a consequence of transcriptional repression. Hence, YM155 is not a survivin direct inhibitor (276).

The other survivin transcription inhibitor that has reached phase I/II clinical trials is EM-1421 (Terameprocol), showing a good safety profile and partial responses in patients with advanced leukemia, cervical intraepithelial neoplasia and recurrent high-grade glioma (456–458).

Other survivin transcription inhibitors have been tested preclinically with successful results. One example is FL118, a non-selective small molecule inhibitor of survivin, as well as an inhibitor of DDX5 and topoisomerase I (281). FL118 inhibits survivin promoter activity and survivin expression. It also inhibits Mcl-1 and some IAPs (XIAP and c-IAP2), c-Myc and mutant KRAS (280,281). It has great antitumor efficacy without significant toxicity compared to first-line chemotherapeutics (280,459,460).

In this group of survivin transcription inhibitors, we can also find oligonucleotides that bind and degrade survivin mRNA, limiting survivin expression. LY2181308 is an example. It presents a favorable safety profile but mixed clinical outcomes, since it has shown synergistic benefits in patients with refractory or relapsed acute myeloid leukemia when combined with cytarabine and idarubicin (284), but no benefit when administered alone or combined with docetaxel/prednisone in solid tumors (285). A similar result was obtained when combining docetaxel with LY2181308 in a phase II clinical trial of patients with NSCLC (461). SPC3042/EZN-3042 is another antisense oligonucleotide with higher potency that also affects Bcl-2 mRNA. Promising results *in vitro* have been reported (286,287), but the phase I trial was terminated due to dose-limiting toxicity, likely caused by the accumulation of antisense oligonucleotides in the liver (288,462).

Overall, although some survivin transcription inhibitors have advanced to clinical trials, their anticancer effects have been limited and some of them have shown significant adverse effects, such as hepatotoxicity, nephrotoxicity and/or hypersensitivity. This has been attributed to limited survivin silencing *in vivo* and/or off-targets effects.

Another strategy to inhibit survivin is by using survivin **SMAC mimetics**. An example of SMAC mimetic that has reached phase I/II clinical trials is LCL161, which presents good

antineoplasic activity and bioavailability. However, it has shown important side effects, such as an increased risk of infection when combined with paclitaxel or myelosuppression when combined with topotecan (294,295,463). These side effects may be the results of the fact that LCL161 does not only interact with survivin, but also multiple IAPs, like most SMAC mimetics. Another SMAC mimetic that has reached the clinics is birinapant. This compound has undergone multiple phase I/II clinical trials for various cancers, including head and neck squamous cell carcinoma, ovarian cancer, non-Hodgkin lymphoma and leukemias, either as a single agent or in combination with known anticancer drugs. It presents dose-limiting toxicity (464,465) and clinical studies reported the absence of single-agent antitumor activity. In spite of this, birinapant is being preclinically investigated in combination with other therapies (466). Debio1143 is also a SMAC mimetic tested in multiple clinical trials for various types of cancer alone and in combination (238,467,468). The clinical trials have revealed a tolerant toxicity in patients, in contrast with the results in the preclinical evaluation *in vivo*, which reported dose-limiting hepatotoxicity in animals (291).

Other SMAC mimetics that are still in preclinical evaluation are PZ-6-QN, GDC-0152, withanone, piperine and UC-112 and its analogs (182,292,297,301,304,469).

Despite the favorable results of these investigations, the SMAC mimetics therapeutic strategy presents some weaknesses. SMAC mimetics do not only inhibit survivin, but also other IAPs, such as cIAP1/2. The depletion of cIAP1/2 in immune cells can activate an alternative NF-κB pathway, which supports B-cell survival and provides a co-stimulatory signal to dendritic cells and T cells (470). These signals can further enhance immune-modulatory activity, leading to a substantial release of proinflammatory cytokines against cancer cells (471,472). While this process is beneficial for targeting cancer cells, a high-dose SMAC mimetic treatment could lead to systemic toxicity, cytokine release syndrome, or reduced tumor responsiveness to death ligands (473–475).

Finally, another weakness of SMAC mimetics treatment is that cannot be used for treatment of a wide range of tumors since only a small subset of the cells tested have been effectively killed by single-agent SMAC mimetics (476).

Another strategy to inhibit survivin is using **Hsp90 inhibitors**. For example, shepherdin presents a high binding affinity for the ATP pocket of HSP90, leading to the degradation of its client proteins, especially survivin. It has been well tolerated in *in vivo* experiments, with a potent antitumor activity (306). AICAR, which is derived from shepherdin, has also shown antiproliferative and proapoptotic activity (308,477,478). Moreover, synergistic effects with radiotherapy have been reported (479). Despite the good results in preclinical studies, shepherdin and AICAR have not reached the clinics yet.

One more strategy for inhibiting survivin is to employ **mitotic inhibitors**. For example, indinavir is an HIV protease inhibitor that inhibits the interaction of survivin with binding partners (320). A recent phase II clinical trial with indinavir and debulking chemotherapy in elderly patients with Kaposi sarcoma showed a good response, with clinical improvement (480).

Overall, the therapeutic approaches presented so far have shown little improvement over conventional treatments. As we have mentioned above, some have limited efficacy, others exhibit high toxicity, and some suffer from poor bioavailability. Alternative strategies still require further investigation. This is why we chose to explore a promising approach that has not been evaluated in clinical trials yet: targeting **survivin homodimerization.**

By impeding survivin homodimerization, survivin hydrophobic interface in the dimerization site would be exposed, generating instability of the protein and inducing its degradation by the proteasome (309). The degradation of unstable survivin monomers leads to reduced availability of survivin to form the CPC and interact with SMAC/DIABLO, XIAP or caspases. As a result, both the promitotic and the antiapoptotic functions of survivin are compromised. Therefore, the inhibition of survivin homodimerization will not only impair the specific functions performed by survivin homodimers, since it induces the degradation of survivin.

Inhibition of survivin homodimerization would also lead to mitotic aberrations that would result in cell death, because survivin homodimers play a role in microtubule stability. Additionally, there is a short segment of Borealin that interacts with survivin

homodimerization interface (481). Hence, homodimerization interface inhibition may also affect the formation of the CPC complex.

Another advantage of this approach to inhibit survivin is that, unlike other therapeutic approaches previously mentioned (276,281,295,463), inhibitors targeting the homodimerization site are specific to survivin, resulting in fewer off-target effects and reduced toxicity.

There are some survivin homodimerization inhibitors that have already been studied in preclinical studies. One of the first identified homodimerization inhibitors was Abbot 8. It has been used as a reference in this study to identify a more potent anticancer agent, since Abbot 8 anticancer effect was limited due to its low bioavailability (310). Afterward, other dimerization domain inhibitors were reported, such as LLP-3 and LLP-9, which are two compounds that disrupt cell cycle progression and increase cell death. Specifically, they cause defects in the CPC organization and delay mitotic progression primarily due to extended metaphase and anaphase (482). Moreover, LLP-3 has been reported to disrupt the survivin-Ran protein complex in neuroblastoma cells, diminishing the levels of survivin and ran (involved in nucleoplasmic transport of proteins important for cell homeostasis), which are overexpressed in this type of cancer (311). LLP-3 reduces viability, induces apoptosis and inhibits clonogenic and anchorage-independent growth in neuroblastoma cell lines. Additionally, it induces mitochondrial dysfunction and impairs flexibility of energy metabolism by inhibiting oxidative phosphorylation and glycolysis (311,313). Another homodimerization inhibitor is LQZ-7. Other molecules have been derived from this compound. The most recent is LQZ-7F1, which is the most potent. Although these compounds have not reached the clinics yet, they present promising results. LQZ-7F1 has shown induction of spontaneous apoptosis in prostate cancer cells (318). Thus, the inhibition of survivin homodimerization seems a promising therapeutic approach that has not been evaluated in clinical trials yet, so we have selected it for our study.

12.3 Identification of AM as a direct survivin inhibitor

Being survivin homodimerization inhibition the most promising approach to inhibit survivin, we decided to identify molecules with affinity for the homodimerization site of

survivin by computational methods. Specifically, two HTVS were performed on the survivin structure, focused on the homodimerization interface. From more than 8 million compounds screened *in silico*, 16 compounds were identified as highly ranked according to favorable survivin-ligand contacts and electrostatic and shape complementarity. These compounds were subjected to experimental *in vitro* studies. The compound with the highest cytotoxic effect on cancer cells was asenapine. Thus, asenapine was selected as a potential survivin homodimerization inhibitor and was evaluated as an anticancer therapeutic agent.

AM is an FDA-approved drug that is currently used in clinics as a treatment for psychiatric disorders. It presents the advantage that, since it is already approved by the FDA, the preclinical testing, safety assessment and formulation development is already done. Then, the development of the anticancer therapy is faster and more economical. Moreover, it can be easily administered sublingually. Additionally, AM has the ability to penetrate the blood-brain barrier, being a potential therapeutic option for brain cancers.

AM cytotoxic effects were further evaluated in other cell lines, including non-cancer cell lines, being the cancer cells more sensitive to the compound. The efficacy of AM to kill cancer cells varied among the different types of cancer, but the cytotoxic effect was still significant in all the evaluated cancer cell lines. AM was identified as a direct inhibitor of survivin by binding the dimeric interface. The binding of AM to the homodimerization site of survivin was analyzed by SPR, which demonstrated that there is an affinity of AM for survivin. A non-denaturing electrophoresis allowed us to demonstrate that AM disrupted survivin homodimerization, which may induce survivin degradation in cells.

AM forms a H-bond Leu96 of survivin. AM impedes survivin to dimerize and, thus, the hydrophobic interface remains exposed, which can result in protein misfolding and lead to ubiquitin-proteasome-dependent degradation of survivin. This kind of protein degradation is characterized by the joining of 76-aminoacid ubiquitin polypeptide (Ub) to the target protein through reversible isopeptide linkages between the carboxy terminus of ubiquitin and lysine side chains of the target proteins. Ub is recruited by E1 Ub-activating enzyme, then Ub are transferred to the E2 Ub-conjugating enzyme and finally E3 Ub-protein ligases recognize the target protein and attach ubiquitin. The polyubiquitinated protein is finally degraded by the 26S proteasome complex (407).

As for the survivin homodimerization inhibitors that have been already identified, in the case of the small molecules LLP3 and LLP9, they form π-stacking interactions between their aromatic rings and Phe93/Phe101 of survivin. In the case of LQZ-7F1, the small molecule interacts with the dimerization core residues Phe101 and Leu98. Additionally, there are hydrophobic interactions provided by Leu6 and Leu96, as well as a hydrogen bond between the nitrogen of the pyrazine moiety of LQZ-7F1 and Glu94 residue. This binding to the survivin dimeric interface causes the exposure of the hydrophobic dimerization core, which leads to protein misfolding and, thus, degradation in the proteasome, following the same mechanism as AM. Moreover, the small size of the molecule ensures that when LQZ-7F1 is anchored in the hydrophobic pocket, it remains isolated from the surrounding solvent. This suggests that, since AM also presents a small size (unlike LLP3 and LPP9), the same phenomenon could be happening in the interaction between AM and survivin. It is important to highlight that AM offers a significant advantage over these compounds, as it is already FDA-approved, has a well-established safety profile, and is easy to be administered.

12.4 Anticancer effect of AM through induction of apoptosis and disruption of cell cycle

We focused our research on lung cancer because it is the cancer with the highest incidence and mortality worldwide. Thus, we evaluated the effect of AM in squamous cell carcinoma and small cell carcinoma cell lines, apart from the previously evaluated lung adenocarcinoma cell line. The most sensitive cell line was adenocarcinoma, while the small cell carcinoma cell line required higher concentrations of AM to be affected by the drug, although the differences among the IC_{50} of the different cell lines are not significant. However, non-cancer cells were significantly more resistant to AM. This finding correlates with the result of a previous experiment, in which survivin expression was evaluated by Western blot in different lung cancer and non-cancer cell lines. In that Western blot, we observed that all the cancer cell lines evaluated overexpressed survivin compared to non-tumor human lung fibroblast HFL-1, and the expression was similar in all the cancer cell lines evaluated (A549, SW900, H520, DMS53). Moreover, according to the literature, cytoplasmic levels of survivin are also similar in all histological types of

lung cancer (483). Hence, the effects of AM are related to survivin expression, being the cancer cells the ones with the highest survivin levels and the most cytotoxic effects.

The assays performed in 3D cultures of lung adenocarcinoma cells also presented the IC_{50} at a micromolar scale, although the concentration of AM required to affect half of the cell population was significantly higher, probably due to the difficulty of the compound to reach the cells in the center of the spheroid.

The lowest IC_{50} values were obtained in the primary cell cultures derived from the transgenic KRasG12D mice model, which generated NSCLC tumors in the animals. This result suggests that cells derived directly from a tumor are more sensitive to anticancer compounds than established cell lines, which may have acquired resistance characteristics over long-term *in vitro* maintenance.

One of the first line treatments in lung cancer is combined treatment with cisplatin, which has an IC_{50} at 24 h of 20 μM in A549 (484). Although cisplatin presents cytotoxicity in the micromolar range, like AM (40 μM), the specificity of AM for cancer cells may be higher, because the main mechanism of action of cisplatin involves the generation of DNA lesions by interacting with purine bases on DNA, generating the activation of pathways that lead to apoptosis (68). Hence, cisplatin not only affects cancer cells, but also non-cancer cells. This results in one of the challenges of cisplatin, which is its side effects in patients. Contrarily, AM inhibits survivin, which is highly overexpressed in cancer cells compared to healthy cells (183,184). Thus, AM may act more specifically on cancer cells than cisplatin, suggesting a better safety profile than cisplatin in vivo.

Once we studied the effect of AM in cancer cells, we comprehensively explored the mechanism of action of our compound. We demonstrated that AM binds specifically to survivin and not to XIAP, despite the structural similarity of both molecules, since protein levels of the latter were not altered when cancer cells were treated with AM. This result is interesting because a compound that is nonspecific means that hits different off-target proteins, which could be involved in important pathways, not only in cancer cells but also in non-cancer cells, so it could mean higher toxicity of the compound. An example is FL118, whose hematopoietic toxicity may be due to inhibition of topoisomerase I, which is not responsible for the antitumor activity of the drug (485). Moreover, most

SMAC mimetics inhibit not only survivin but all the IAPs, an example is LCL161. LCL161 elevated the risk of infection when combined with paclitaxel (463). Moreover, SMAC mimetics can also induce systemic adverse effects such as cytokine release syndrome (474).

Besides this, there are some compounds that can affect drug transporters in the cells, as in the case of GDC-0152 and UC-112, which have been shown to inhibit ABCB1 and, thus, alter multidrug efflux activities. This can alter the pharmacokinetics and toxicity of different drugs (304,486).

Our study demonstrated that AM impairs the two functions in which survivin is involved in the cell. On the one hand, AM arrested cell cycle in lung cancer cells after 24 h of treatment. In particular, after the treatment with AM, the percentage of cells in G_0/G_1 phase increased, while the percentage of cancer cells in phases S and G_2/M decreased.

In mitosis, the survivin monomer forms part of the CPC and takes part in the destabilization of microtubules that are attached incorrectly to the kinetochore. When there is a lack of tension, resulting from the improper attachment of the CPC to the kinetochore, Aurora B phosphorylates survivin at threonine 117. Then, survivin is released from the centromere and the rest of the CPC is not functional. While the attachment is corrected, survivin is dephosphorylated and it associates again with the CPC complex, and the cell cycle can continue (487). Therefore, it is logical that treatment with AM, a survivin inhibitor, disrupts the cell cycle, consistent with our experimental observations.

Additionally, survivin dimer stabilizes spindle microtubules (178). Inhibition of survivin results in the alteration of microtubules, leading to defective cytokinesis with hyperploidy, multipolar mitotic spindles, and supernumerary centrosomes, finally inducing apoptosis at G_2/M phase (176). This is consistent with the decrease of cells in G_2/M that we observed in our research, which is probably due to apoptosis in this phase. Furthermore, it is possible that after AM treatment, our cancer cells exhibited mitotic aberrations due to destabilized microtubules caused by reduced survivin levels, accumulating these defects and arresting cell cycle in G_0, as we have also observed in our experiments.

Noninvasive cancer therapy aims to maximize tumor cell death and minimize tissue toxicity by targeting cancer specific properties. Inducing apoptosis is a good strategy because evasion of apoptosis is one of the hallmarks of cancer (8). Moreover, unlike other types of cell death, apoptosis does not generate inflammation of the surrounding tissue, avoiding damage of other cells that are not our target (488). We also evaluated the effect of AM on apoptosis and observed that, apart from arresting cell cycle, AM induced the cleavage of caspase-3 and PARP, which corroborates apoptosis induction triggered by AM.

Other investigations support our results. In 2012, Dai et al. generated survivin-deficient hepatocellular carcinoma cells and observed cell cycle arrest and defective mitosis. Moreover, they also identified apoptosis progression by studying caspase-3 expression in the same cells (147). Examples of other anti-survivin drugs that have been demonstrated to affect cell cycle and/or inhibit apoptosis are piperine, which inhibits cell growth and induces apoptosis (299); YM155, which induces apoptosis (270); SPC3042/EZN-3042, which produces cell cycle arrest in the G_2/M phase and apoptosis induction (286,287); and MX-105, which induces apoptosis (182,301). Another survivin inhibitor that binds to the dimer interface of survivin is LLP-3, which reduces the proportion of glioblastoma cells in G_2/M phases and increases G_0/G_1 population, like AM (313). The arrest of the cell cycle at G_0/G_1 in the case of survivin inhibitors that bind to the dimer interface could be attributed to the fact that only survivin homodimers, and not the monomer, have the function of microtubule stability during interphase, impeding a correct mitosis consecution (178).

12.5 Synergistic effect of AM in combination with chemotherapy

The combination of treatments has multiple advantages. Firstly, there are multiple genetic factors and proteins involved in the generation and progression of cancer, as well as epigenetic and environmental factors. Because of that, a therapeutic strategy targeting a specific gene or protein usually leads to unsatisfactory results. Combining therapies enables targeting different factors, which results in improved treatment efficiency, increasing the probability of the therapy's success. Secondly, the conventional monotherapeutic approaches in cancer, especially with chemotherapeutic agents, are non-selective drugs that target proliferating cells, leading to the destruction of healthy

and cancer cells. Thirdly, combining treatments enables a reduction in the dosage of therapies associated with high systemic toxicity, such as chemotherapy. Combined therapies may work in a synergistic or additive manner. In that case, a lower therapeutic dose would be required, meaning less toxicity. Fourthly, constant treatment with a single compound leads to cancer cells to develop strategies to overcome the effects of the drug, which makes the tumor more susceptible to drug resistance. Since combination therapy is more effective, fewer cycles are needed, which results in reduced incidence of resistance. Moreover, one of the therapies may kill the cells that may have survived with the other therapeutic alone. Furthermore, there can be a combination of therapies that target different types of cancer cell populations, eliminating the entire tumor and avoiding remaining cells that could later derive in a relapse. There are drugs that induce cell death, which leads to two key outcomes: first, dendritic cells are stimulated to expose antigens, and second, DAMPs are released into the surrounding environment. That makes cancer cells more visible to the immune system and potentiates the effect of immunotherapy (489–491).

An example of combinatorial drug formulations in targeted therapies is the combination of osimertinib (EGFR-TKI) and bevacizumab (VEGF inhibitor). It is being tested as a first-line strategy in a phase I/II clinical trial (NCT02803203) (492). Moreover, the standard of care in the USA for unresectable locally advanced NSCLC is platinum-based chemotherapy with concurrent radiation therapy followed by consolidation treatment with durvalumab for one year (493,494).

Combinatorial therapy can help to overcome an important handicap with the treatment of brain metastasis. Cytotoxic chemotherapy is unable to cross the blood-brain barrier and penetrate the SNC (495,496). Improvement in treatment with targeted therapy, for example osimertinib and alectinib in adjuvant setting, reduced the risk of CNS disease progression (497,498).

The combination of survivin inhibitors with conventional therapies has shown good results. For example, LLP3 sensitizes colorectal cells to irinotecan in p53-mutated cases (314) and LQZ-7F1 synergizes with docetaxel in inhibiting prostate cancer cells survival (318).

In this project, AM showed synergism with all the chemotherapeutics tested except one, paclitaxel. The chemotherapeutics selected, which are cisplatin, carboplatin, paclitaxel and gemcitabine, were selected for being the most used in the clinics for the treatment of lung cancer. The main mechanism of the antitumor effect of cisplatin is the formation of cisplatin-genomic DNA interstand and intrastand crosslinks by attachment of alkyl groups to DNA bases. This hinders transcription and DNA replication and fragmentation of DNA caused by repairing enzymes, leading to cell death. It also produces mutations by inducing mispairing of the nucleotides (499). It presents severe adverse reactions, including nephrotoxicity and myelosuppression. Some patients are not able to tolerate it (500,501).

Carboplatin is an analog of cisplatin. Like cisplatin, it attaches alkyl groups to the nucleotides, which leads to the formation of monoadducts. DNA fragments when repair enzymes attempt to correct the error. 2% of the activity of carboplatin is due to the DNA-crosslinking from a base on one strand to a base on the other. This avoids the separation of DNA strands for synthesis or transcription. Carboplatin can induce different mutations (502,503). Although they have the same mechanism of action, they differ in the toxicity profile. Cisplatin presents higher rates of nausea, vomiting, nephrotoxicity, ototoxicity. Carboplatin has a higher risk of myelosuppression and neurotoxicity (504). The kinetics of adduct formation differ for different cisplatin analogues, which may influence in the antitumor activity. Cisplatin have higher antitumor activity but carboplatin has higher chemical stability compared to cisplatin (505).

Gemcitabine is a nucleoside analog. Once inside the cancer cells, it is converted by phosphorylation into the active compounds, gemcitabine diphosphate (dFdCDP) and gemcitabine triphosphate (dFdCTP). dFdCTP competes with deoxycytidine triphosphate for incorporation into the DNA. When it is incorporated, chain elongation ends, DNA is fragmented and apoptosis is induced. On the other hand, dFdCDP inhibits ribonucleotide reductase, which is the enzyme responsible for the generation of deoxycytidine. Thus, dFdCDP decreases the competition of dFdCTP for incorporation into DNA (506,507).

Paclitaxel hyperstabilizes microtubules by binding to the β subunit of tubulin, which forms the microtubules, and avoids the disassembling of the structure. This affects important functions of the cells, such as transportation of organelles and vesicles or

mitosis. Moreover, paclitaxel induces apoptosis in cancer cells by binding to Bcl-2, arresting its function (508–510).

A possible explanation to the fact that paclitaxel was the only chemotherapeutic that did not synergize with AM is that survivin is also involved in microtubule stability. If survivin is inhibited, then the stability of microtubule is compromised, but by adding paclitaxel this effect is counterbalanced, since it hyperstabilizes microtubules. The mechanism of action of the other three chemotherapeutics is involved in DNA synthesis and transcription, which complements the induction of apoptosis and arrest of cell cycle induced by AM.

Further investigation into the mechanism of action of AM in combination with cisplatin, the chemotherapeutic agent that demonstrated the most potent synergism, revealed that adding AM to cisplatin treatment enhances apoptosis levels compared to cisplatin monotherapy. This effect could be attributed to multiple mechanisms. Firstly, cisplatin induces apoptosis in dividing cancer cells by hindering DNA replication and inducing DNA fragmentation. 24 h later, the addition of AM arrests cell cycle in the remaining cells, probably by impeding CPC formation and causing microtubule instability which may ultimately lead to apoptosis. Furthermore, AM removes the apoptotic blockade imposed by survivin, thereby restoring and enhancing the apoptosis induced by cisplatin.

12.6 Potential radiosensitization effect of AM

RDT is one of the main therapeutic strategies, being used in over 50% of all cancer patients either alone or, usually, in combination with surgery and chemotherapy. It consists in using high-energy proton radiation to destroy cancer cells and tumor tissue by direct and indirect mechanisms. In the first case, RDT induces single-strand breaks (SSB) and double-strand breaks (DSB) in DNA. This leads to termination of cell division and proliferation or even cell necrosis and apoptosis. In the second case, RDT induces generation of ROS, which generates cellular stress that could alter cellular signaling pathways.

Antitumor activity of RDT depends in big part on the activation of cell death programs activation. Thus, evasion of apoptosis can result in RDT resistance. A strategy to overcome RDT resistance is to antagonize antiapoptotic mechanisms, which would lower

the threshold for RDT-induced cell death. Giagjousiklidis et al. corroborated this fact by showing that Inhibition of XIAP sensitizes pancreatic carcinoma cells for γ-irradiation induced apoptosis, without affecting non-malignant fibroblasts (511).

Radiosensitizers are compounds that, when combined with RDT, have higher antitumor activity that the expected for the additive effect of each modality. Over the last years, small molecules inhibitors of IAP proteins with these characteristics have been developed. For example, it has been shown that two XIAP inhibitors were able to increase the radiosensitivity of glioblastoma cells. Contrarily, those inhibitors did not increase radiotoxicity in non-malignant cells of the central nervous system. This radiosensitization of glioblastoma cells involved increased mitochondrial outer membrane permeabilization, caspase activation and caspase-mediated apoptotic cell death (512). BV6, another small-molecule SMAC mimetic, showed also sensitizing effects of glioblastoma cells for γ-irradiation-mediated apoptosis, requiring NFκB for its proapoptotic effects (513). The SMAC mimetic LBW242 enhance cytotoxic activity of radiotherapy in glioblastoma cell. Moreover, it showed a synergistic suppression of tumor growth in glioblastoma xenograft mouse model when it was combined with RDT and temozolomide (514). 1396-11 and 1396-12 are XIAP antagonists that increase radiosensitivity of pancreatic carcinoma cells and in a subcutaneous xenograft model *in vivo (515)*. Other carcinoma types in which SMAC mimetics increased radiosensitivity are breast carcinoma (516), head and neck squamous cell carcinoma (517), prostate carcinoma (518) and colorectal carcinoma (519,520). In lung cancer, the SMAC mimetic ANTP-SmacN7 fusion peptide radiosensitizes A549 cells by reducing cell clone-forming rate, increasing cytochrome-c, cleaved caspase-8, cleaved caspase-3 and cleaved caspase-9 expression levels, promoting caspase activation and increasing radiation-induced apoptosis. ANTP-SmacN7 increased radiation-induced double-stranded DNA rupture and increased DNA damage (521). Debio 1143, another SMAC mimetic, synergizes with RDT to enhance antitumor immunity by reversing immunosuppressive cell infiltration in the tumor microenvironment. This effect, demonstrated in a lung cancer mouse model, is dependent on TNFα, IFNγ, and CD8+ T cells (467).

Moreover, survivin is downregulated by radiation in normal human endothelial cells. However, this is impaired in malignant cells. In fact, survivin expression is especially

elevated in radio-resistant cells, resulting in the inhibition of RDT-induced apoptosis (522).

Mitotic catastrophe is a response to DNA damage (e.g. induced by radiation) (523). When the damage is severe and cannot be repaired, cells are arrested at G_2, but still some cells attempt to undergo mitosis. Damage DNA is inherited by daughter cells, that will have genomic instability. Mitotic catastrophe triggers apoptosis or necrosis when DNA damage is severe to prevent propagation of genetic aberrations (524). Since survivin is involved in the correct separation of chromatids and microtubule stabilization, the loss of function leads to mitotic problems (mitosis delay, chromosome displacement and cell accumulation in prometaphase) that may induce mitotic catastrophe (525,526). Thus, the persistent expression of survivin may be considered a mechanism of radiation resistance (527).

Previous studies combining survivin inhibition with RDT have yielded promising results. For example, it has been shown that inhibiting survivin by using ribozyme or using a dominant-negative survivin mutant led to the sensitization of melanoma and pancreatic cancer cells to radiation (528,529). In the second case, Asanuma et al. transduced ordinarily radiosensitive MIAPaCa-2 cells with wild-type survivin gene (MS cells). MS cells were less sensitive to RDT than the control. Moreover, radiation-induced activity of caspase was significantly inhibited in MS cells (529).

Overall, radiosensitizing activity of survivin inhibition is multifaceted and seems to involve, caspase-dependent mechanisms (530), caspase-independent mechanisms (269,531), impaired DNA repair, altered cell-cycle distribution and formation of multinucleated cells. All these facts lead to mitotic arrest and cell death.

The encouraging outcomes achieved by inhibiting survivin to enhance RDT response in cancer cells prompted the preclinical evaluation of combining survivin inhibitors with RDT.An example of this therapeutic strategy is the combination of everolimus (mTOR inhibitor) and YM155 (survivin inhibitor) with RDT in renal carcinoma cell lines, which sensitized cells towards radiation as well as tumors toward RDT in xenograft murine RCC models (532).

Given that survivin inhibition enhances radiosensitization in cancer cells and that we identified AM as a survivin inhibitor, we evaluated the response of cancer cells to radiotherapy following treatment with AM. Our experiments revealed that RDT induced DNA damage in lung cancer cells, but this effect was not potentiated when AM was added. However, cell density and morphology were more significantly altered in cells treated with the combination of AM and RDT compared to either treatment alone.

While in terms of apoptosis AM did not show a radiosensitizing effect, in the study of cell cycle we observed that RDT arrests cell cycle at G_2/M while AM arrests cell cycle at G_0/G_1. In the combination of both therapies, the effect on cell cycle is dependent on AM treatment duration. At longer time of exposure to AM treatment, there is a higher percentage of cells at G_0/G_1 cell cycle phase. This may suggest that both treatments may be complementary, each therapy arresting cell cycle at a different phase, inducing a higher decrease in total cell number.

Finally, we observed that the clonogenic ability of lung cancer cells was significantly affected by the combination of AM and RDT. This result is consistent with literature, since treatment with different survivin isoform specific siRNAs (wt, survivin 2B and delta 3) reduces clonogenic survival (533), and the overexpression of WT and survivin-3B protects against irradiation (534).

12.7 AM induces the production of DAMPs, indicators of ICD

One of the obvious goals of anticancer therapy is reducing the number of neoplastic cells. A strategy to achieve so is by inducing cancer cell death, which not only would reduce the number of cancer cells but also would allow the acquisition of antigens by the dendritic cells. Moreover, the DAMPs released would induce an adaptive immune response. For this reason, there is an interest in inducing ICD that would optimize the immune response against the tumor. This is interesting also for the use of immune checkpoints inhibitors (488).

There are multiple IAP inhibitors that induce ICD. ASTX660 (Tolinapant), antagonist of cIAP1/2 and XIAP, in combination with TNFα, induces ICD in HNSCC cell lines. Experiments in mouse models showed that ASTX660 can also enhance radiation-induced ICD. In ex-vivo experiments (tumor cells with TILs) ASTX660 enhanced cytotoxic TIL-

dependent killing, suggesting ASTX660 may enhance antigen presentation on tumor cells (535). It is currently being evaluated in phase II study in T-cell lymphoma patients. In a syngeneic model of T-cell lymphoma, it was able to induce complete tumor regression by activating adaptive and innate immune systems by inducing ICD (536).

Another example is LCL-161, an IAP antagonist that was able to kill pancreatic cancer cells *in vivo* but not *in vitro*. This effect was dependent on dendritic cells and T lymphocytes (535).

Debio 1143, another IAP antagonist, has shown synergistic immunity against tumors when combined with RDT in lung cancer models (467). Debio 1143 also enhances the response to anti-PD-L1 (avelumab) in a mouse model of bladder cancer (537). This combination is in a phase-IIb trial (NCT03270176) for recurrent/metastatic solid tumors. Debio 1143 monotherapy showed increase CD8+ T cell infiltration in HNSCC surgical specimens.

In a recent study, Snacel-Fazy et al. administered GDC-0152, (a SMAC mimetic, to a glioblastoma mouse model and it promoted microglia activation, antigen-presenting function and tumor infiltration (538).

The positive results obtained with these therapeutic strategies led us to evaluate if AM could also potentially induce an enhanced immune response against the tumor. Our study shows AM significantly induces DAMPs in lung cancer cells, which suggests our compound may induce ICD. It would be interesting to study if there is a synergistic effect of AM with anti-PD-L1, such as in the case of Debio 1143.

12.8 AM therapeutic potential as an anticancer agent

After the *in vitro* evaluation, safety and therapeutic efficacy *in vivo* evaluation of AM was performed. Safety experiments showed that doses up to 20 mg/kg were safe in mice, only showing a decrease in animal weight at the first cycles of treatment, which was recovered at the end of the experiment. At the highest doses, mice showed transient mild secondary effects such as decrease in locomotor activity, which is characteristic of antipsychotic drugs. In fact, in male black Swiss mice treated with 0.1 and 0.3 mg/kg of AM (doses significantly lower than the ones used in our study) already presented

reduced activity, increased immobility in the forced-swim test and reduced amphetamine-induced hyperactivity (539). In our case, this effect was transient and animals presented normal behavior after 4 h of AM administration.

Since AM crosses the blood brain barrier, we evaluated potential alterations in the brain, especially in the hippocampus, a neurogenic area (Gonçalves 2016). Additionally, we checked for possible hepatotoxicity since AM is oxidized by CYP1A2, and then glucuronidated via UGT1A4, both enzymes mainly expressed in the liver (540). Finally, kidneys were also evaluated, since 50% of AM is eliminated via urine (402). We concluded from these experiments that none of the vital organs analyzed presented significant alterations by AM in our study.

Despite the maximum dose used in the safety assay (20 mg/kg) did not present a significant toxicity, in the therapeutic efficacy assay of AM monotherapy we selected a lower dose of AM in order to minimize the secondary effects of AM in the CNS. Although there was no statistically significance between the groups due to the high variability in the control group, the difference in tumor size between groups was visibly evident, being the AM-treated mice those with the smallest tumors.

Immunohistochemical assays of survivin showed that AM is able to enter the cells, contrarily to some survivin inhibitors, such as Abbot 8, which effectively inhibits survivin, but has low bioavailability (310).

Apart from the lower tumor size of AM-treated mice compared to the control group, we also observed a different consistency. AM-treated tumors were softer and more viscous than the group treated with the vehicle. This effect of AM together with the fact that survivin is involved in angiogenic processes (541,542) led us to think AM could have an impact on angiogenesis.

Although there were slightly fewer blood vessels in the images of AM-treated tumors than in the control group, the statistical analysis revealed that it was not significant in the analyzed areas. However, the samples of AM-treated mice were hard to analyze because they presented massive necrosis, especially in the center of the tumor. This necrosis, which was importantly more pronounced in AM-treated samples, may be the result of lack of blood flow in the tissue, altogether with the cytotoxic effect of AM. If

this is the case, then the areas of necrosis are those with less blood vessels and the images analyzed in the non-necrotic areas would not be representative. Thus, the higher necrosis in AM-treated samples might be a signal of inhibition of angiogenesis by AM treatment. In fact, the higher necrosis areas in AM-treated samples also difficulted the observation of lymphocyte infiltration in the tumors, since all the necrotic tissue was stained in the immunohistochemistry assays.

Since *in vitro* results showed a strong synergistic interaction between AM and cisplatin, we evaluated the therapeutic efficacy of the combination of AM with cisplatin in an ectopic C57BL/6J mouse model generated by LLC1 cells subcutaneous inoculation. There was a significant difference between the tumor weight of the combination-treated group and the control group. Statistical analysis did not reveal significance compared to cisplatin treated mice, although tumor size of combination-treated animals was smaller than cisplatin-treated mice. This lack of statistical significance is probably due to limitations of the mouse model related with tumor development, since there was an important variability among tumors of non-treated mice.

Lewis lung carcinoma (LLC) model is the only reproducible lung cancer model that is syngeneic, which means it is developed by injecting immunologically compatible cancer cells into immunocompetent mice. The LLC1 cell line is highly tumorigenic and it induces lung metastasis. It is primarily used to evaluate the efficacy of chemotherapeutics *in vivo*. The advantage of this model is that, unlike xenograft models in which human cells are implanted in immunosuppressed mice, the tumor is created in an immunocompetent murine background, so immune and toxicity responses closer to reality can be evaluated (543). The main limitation of this model is that responses to treatment in a complete murine system may not be transferable to humans. Another limitation could be the effect of preparation time and the transfer of LLC1 cells to the animal facilities on cell viability. This may result in varying numbers of viable cells being inoculated, with earlier inoculations containing more living cells, while cells inoculated later may have reduced viability due to suboptimal conditions. Moreover, the main reason for the control variation is the fact that animals are immunocompetent and tumor growth can be affected depending on how the immune system of each animal responds to cancer cell inoculation.

Dorneburg et al. evaluated the effect on tumor growth of S12, another inhibitor of survivin homodimerization, in mice with subcutaneous neuroblastoma xenografts (317). As well as in our experiment, they did not observe significant differences in tumor growth between control and treated group. However, S12-treatment attenuated the hemorrhagic phenotype of tumors, which could be related to the decreased survivin-related vascular integrity (544). This would agree with our observations of an altered consistency and higher necrosis of AM-treated tumors.

Another aspect that should be considered is that in *in vitro* experiments, LLC1 was not the best responding cell line to AM when combined with cisplatin. This, together with the fact that AM is designed to bind to human survivin, and not murine survivin, lead us to evaluate AM therapeutic efficacy in NSG immunodeficient mouse model of lung cancer.

In this *in* vivo assay, we observed lower tumor weight in AM-treated mice. Tumor weight of cisplatin-treated mice was significantly lower compared to the control group. Contrarily to what we expected, the combination of AM and cisplatin did not affect tumor growth more than cisplatin monotherapy, probably due to the pronounced effect of cisplatin alone at the evaluated dose.

Finally, we employed a KRASG12D transgenic mouse model of lung cancer to study the response of *in situ* lung cancer to AM and its combination with cisplatin. Transgenic mice are useful for studying the role of genetic abnormalities in tumor initiation and progression. However, models expressing KRAS transgenes have limitations, such as limited metastasis. Thus, they do not accurately represent adenocarcinoma *in vivo*. One advantage of the Cre/loxP model is the possibility to spatially regulate gene expression and to evaluate the events in lung cancer progression (543,545). In our experiment, neither lung weight nor tumor area were affected by any of the treatments, suggesting that this model may not be the adequate for evaluating the efficacy of these compounds, probably because of the slow progression of lung cancer in this model, which difficult the observation of the cytostatic effects of AM.

12.9 AM potential as a repositioned drug for anticancer therapy

Repositioning is a therapeutic approach in which a current pharmaceutical agent that initially was used for non-cancerous diseases is being used for cancer treatment. This is an efficient strategy because the treatment has already been approved by the regulatory agencies (FDA, EMA), it has already passed drug safety protocols and the pharmacokinetic profile is already known. An example is acetazolamide (pan-carbonic anhydrase inhibitor), used for the treatment of glaucoma, epilepsy and altitude sickness, is now used for cancer (546,547), because cancer cells have high carbonic anhydrase activity. Repurposing can also help to counteract toxicity of conventional monotherapies. For example, the combination can be an agent that kills proliferating cells and a drug that protect normal cells from the first agent (e.g. a cytostatic agent that protect normal cells by arresting cell growth) (490,548),

AM is an antipsychotic indicated for schizophrenia and maniac episodes in bipolar disorder treatment. Our research has demonstrated that this compound has also an antitumoral activity. It is not the only antipsychotic drug with anticancer effects. In fact, several studies have reported that patients treated with antipsychotics have lower cancer incidence of specific cancer types than the general population (549–551). One example of a potential antipsychotic repurposing is trifluoperazine, which induces apoptosis and cell cycle arrest at G_0/G_1 phase in colorectal cancer cells. Moreover, trifluoperazine interacts synergistically with 5-fluorouracil and oxaliplatin (552,553).

In the case of our compound, the binding constant to survivin is in the low micromolar range, while the maximum concentration (C_{max}) in blood of humans with doses used to treat psychosis is in the nanomolar range (554). This is a significant limitation if we aim to repurpose the compound for clinical use in oncology. Pharmacokinetic studies of AM are necessary to determine whether the blood concentration required for its anticancer effects can be achieved within the safety margins of its maximum concentration in humans. Nevertheless, we have demonstrated the antitumor activity of AM *in vivo*, with a tolerable safety profile, which supports its potencial, as well as it may pave the wayfor developing new analogs with improved pharmacokinetic profiles.

An important characteristic of antipsychotics such as AM is their ability to penetrate the blood-brain barrier (BBB), which may allow the use of AM for the treatment of brain tumor cancers or metastases. In this regard, some antipsychotics have been studied for the treatment of glioma. Chlorpromazine in combination with temozolomide was evaluated in a phase II clinical trial as a first-line treatment in glioblastoma patients with unmethylated O^6-methylguanine-DNA methyltransferase (MGMT) gene promoter. This trial reported a good safety profile and longer progression-free survival than expected in these patients (555).

In adults, the benefits obtained by any anticancer treatment outweighs the side effects of the therapy. However, the potential long-term effects of anticancer therapy have a higher impact in children. Moreover, since cancer incidence is much lower in the pediatric population, clinical trials of novel therapeutic strategies have fewer participants (556). Thus, the specific requirements for children make it difficult to find anticancer treatments for the pediatric population. AM is well tolerated in pediatric populations with psychiatric disorders. Hence, its repositioning as an anticancer drug could benefit patients with pediatric tumors with limited available therapeutic options.

Overall, AM is an antipsychotic drug with a great anticancer drug repositioning potential due to its target specificity, the ability to cross the BBB and the fact that pediatric patients may tolerate it, although the development of AM analogs may also be a good strategy to increase its potency, lowering the needed doses to treat cancer patients.

13 CONCLUSIONS

1. Asenapine maleate exhibits cellular toxicity against a variety of human lung cancer cell lines, that are lung adenocarcinoma (A549), squamous cell lung carcinoma (SW900) and small cell lung carcinoma (DMS53), as well as against the murine Lewis lung carcinoma cell line LLC1 and primary lung cancer mouse cultures. Additionally, asenapine maleate shows toxicity towards lung adenocarcinoma spheroids.

2. Asenapine maleate disrupts survivin homodimerization, compromising survivin stability.

3. Asenapine maleate selectively decreases survivin levels in A549 lung adenocarcinoma and U87 MG glioblastoma cells without affecting XIAP protein, another structurally similar member of the inhibitor of apoptosis protein family.

4. The anticancer effect of asenapine maleate is mediated by cell cycle arrest at the G_0/G_1 phase and the induction of apoptosis.

5. Asenapine maleate acts synergistically with cisplatin, carboplatin and gemcitabine, sensitizing A549 lung adenocarcinoma cells to these chemotherapeutic agents.

6. Asenapine maleate potentiates cisplatin-induced apoptosis when administered in combination in lung cancer cells.

7. Pretreatment with asenapine maleate before irradiation induces morphological changes in cancer cells that are indicative of senescence, such as increased cell size and loss of angular shape, as well as an increase in the cell cycle blockade induced by irradiation.

8. Asenapine maleate enhances the impairment of clonogenic ability induced by irradiation in lung adenocarcinoma cells.

9. Asenapine maleate treatment induces the release of damage-associated molecular patterns, which may potentially activate an immune response *in vivo* against tumor cells.

10. Asenapine maleate shows a favorable safety profile in mice at doses below 20 mg/kg, and impairs tumor growth in mouse models.

11. Asenapine maleate enhances cisplatin-induced apoptosis in A549 cells, sensitizing cancer cells to chemotherapy.
12. The combination of cisplatin and asenapine maleate significantly reduces tumor growth in different syngeneic as well as immunocompromised mouse models, paving the way for potential repositioning of this drug and/or the development of novel analogs.

14 BIBLIOGRAPHY

1. National Cancer Institute [Homepage]. Bethesda, MD, USA: National Cancer Institute; [updated 2021 Oct 11; accessed 2024 Oct 25]. What Is Cancer? [12 screens]. Available from: https://www.cancer.gov/about-cancer/understanding/what-is-cancer#definition

2. Nordling CO. Evidence regarding the multiple mutation theory of the cancer-inducing mechanism. Acta Genet Stat Med. 1955;5(2):93–104.

3. Riva L, Pandiri AR, Li YR, Droop A, Hewinson J, Quail MA, et al. The mutational signature profile of known and suspected human carcinogens in mice. Nat Genet. 2020;52(11):1189–97.

4. Soto AM, Sonnenschein C. The tissue organization field theory of cancer: a testable replacement for the somatic mutation theory. Bioessays. 2011;33(5):332–40.

5. Tomasetti C, Li L, Vogelstein B. Stem cell divisions, somatic mutations, cancer etiology, and cancer prevention. Science. 2017;355(6331):1330–4.

6. Zhu L, Finkelstein D, Gao C, Shi L, Wang Y, López-Terrada D, et al. Multi-organ Mapping of Cancer Risk. Cell. 2016;166(5):1132-1146.e7.

7. Jassim A, Rahrmann EP, Simons BD, Gilbertson RJ. Cancers make their own luck: theories of cancer origins. Nat Rev Cancer. 2023;23(10):710–24.

8. Hanahan D. Hallmarks of Cancer: New Dimensions. Cancer Discov. 2022;12(1):31–46.

9. Du Z, Lovly CM. Mechanisms of receptor tyrosine kinase activation in cancer. Mol Cancer. 2018;17(1):58.

10. Biffi G, Tuveson DA. Diversity and Biology of Cancer-Associated Fibroblasts. Physiol Rev. 2021;101(1):147–76.

11. Cheng N, Chytil A, Shyr Y, Joly A, Moses HL. Transforming growth factor-beta signaling-deficient fibroblasts enhance hepatocyte growth factor signaling in mammary carcinoma cells to promote scattering and invasion. Mol Cancer Res. 2008;6(10):1521–33.

12. Valverde JR, Alonso J, Palacios I, Pestaña Á. RB1 gene mutation up-date, a meta-analysis based on 932 reported mutations available in a searchable database. BMC Genet. 2005;6:53.

13. Levine AJ. p53: 800 million years of evolution and 40 years of discovery. Nat Rev Cancer. 2020;20(8):471–80.

14. Chiasson-MacKenzie C, Morris ZS, Baca Q, Morris B, Coker JK, Mirchev R, et al. NF2/Merlin mediates contact-dependent inhibition of EGFR mobility and internalization via cortical actomyosin. J Cell Biol. 2015;211(2):391–405.

15. Kim NW, Piatyszek MA, Prowse KR, Harley CB, West MD, Ho PLC, et al. Specific association of human telomerase activity with immortal cells and cancer. Science. 1994;266(5193):2011–5.

16. Roake CM, Artandi SE. Regulation of human telomerase in homeostasis and disease. Nat Rev Mol Cell Biol. 2020;21(7):384–97.

17. Moshe DL, Baghaie L, Leroy F, Skapinker E, Szewczuk MR. Metamorphic Effect of Angiogenic Switch in Tumor Development: Conundrum of Tumor Angiogenesis Toward Progression and Metastatic Potential. Biomedicines. 2023;11(8):2142.

18. Gerstberger S, Jiang Q, Ganesh K. Metastasis. Cell. 2023;186(8):1564–79.

19. Padmanaban V, Krol I, Suhail Y, Szczerba BM, Aceto N, Bader JS, et al. E-cadherin is required for metastasis in multiple models of breast cancer. Nature. 2019;573(7774):439–44.

20. Wang M, Ren D, Guo W, Huang S, Wang Z, Li Q, et al. N-cadherin promotes epithelial-mesenchymal transition and cancer stem cell-like traits via ErbB signaling in prostate cancer cells. Int J Oncol. 2016;48(2):595–606.

21. Luo Y, Yu T, Zhang Q, Fu Q, Hu Y, Xiang M, et al. Upregulated N-cadherin expression is associated with poor prognosis in epithelial-derived solid tumours: A meta-analysis. Eur J Clin Invest. 2018;48(4):e12903.

22. Martínez-Reyes I, Chandel NS. Cancer metabolism: looking forward. Nat Rev Cancer. 2021;21(10):669–80.

23. Schiliro C, Firestein BL. Mechanisms of Metabolic Reprogramming in Cancer Cells Supporting Enhanced Growth and Proliferation. Cells. 2021;10(5):1056.

24. Sonveaux P, Végran F, Schroeder T, Wergin MC, Verrax J, Rabbani ZN, et al. Targeting lactate-fueled respiration selectively kills hypoxic tumor cells in mice. J Clin Invest. 2008;118(12):3930–42.

25. Jhunjhunwala S, Hammer C, Delamarre L. Antigen presentation in cancer: insights into tumour immunogenicity and immune evasion. Nat Rev Cancer. 2021;21(5):298–312.

26. Yuan S, Norgard RJ, Stanger BZ. Cellular Plasticity in Cancer. Cancer Discov. 2019;9(7):837–51.

27. Faget D V., Ren Q, Stewart SA. Unmasking senescence: context-dependent effects of SASP in cancer. Nat Rev Cancer. 2019;19(8):439–53.

28. Wang B, Kohli J, Demaria M. Senescent Cells in Cancer Therapy: Friends or Foes? Trends Cancer. 2020;6(10):838–57.

29. Li H, Zimmerman SE, Weyemi U. Genomic instability and metabolism in cancer. Int Rev Cell Mol Biol. 2021;364:241–65.

30. Andor N, Maley CC, Ji HP. Genomic instability in cancer: Teetering on the limit of tolerance. Cancer Res. 2017;77(9):2179-85.

31. Jurkovicova D, Neophytou CM, Gašparović AČ, Gonçalves AC. DNA Damage Response in Cancer Therapy and Resistance: Challenges and Opportunities. Int J Mol Sci. 2022;23(23): 14672.

32. Pilié PG, Tang C, Mills GB, Yap TA. State-of-the-art strategies for targeting the DNA damage response in cancer. Nat Rev Clin Oncol. 2019;16(2):81-104.

33. Maciejowski J, De Lange T. Telomeres in cancer: tumour suppression and genome instability. Nat Rev Mol Cell Biol. 2017;18(3):175–86.

34. Denk D, Greten FR. Inflammation: the incubator of the tumor microenvironment. Trends Cancer. 2022;8(11):901–14.

35. Rodriguez-Meira A, Norfo R, Wen S, Chédeville AL, Rahman H, O'Sullivan J, et al. Single-cell multi-omics identifies chronic inflammation as a driver of TP53-mutant leukemic evolution. Nature Genetics. 2023;55(9):1531–41.

36. Srinivas US, Tan BWQ, Vellayappan BA, Jeyasekharan AD. ROS and the DNA damage response in cancer. Redox Biol. 2018;25:101084.

37. Bitman-Lotan E, Orian A. Nuclear organization and regulation of the differentiated state. Cell Mol Life Sci. 2021;78(7):3141–58.

38. Zeng Y, Chen T. DNA Methylation Reprogramming during Mammalian Development. Genes (Basel). 2019;10(4):257.

39. Sheflin AM, Whitney AK, Weir TL. Cancer-Promoting Effects of Microbial Dysbiosis. Curr Oncol Rep. 2014;16(10):406.

40. Pereira-Marques J, Ferreira RM, Pinto-Ribeiro I, Figueiredo C. Helicobacter pylori Infection, the Gastric Microbiome and Gastric Cancer. Adv Exp Med Biol. 2019;1149:195–210.

41. Mager LF, Burkhard R, Pett N, Cooke NCA, Brown K, Ramay H, et al. Microbiome-derived inosine modulates response to checkpoint inhibitor immunotherapy. Science. 2020;369(6510):1481–9.

42. Global Cancer Observatory [Homepage]. Lyon, France: International Agency for Research on Cancer; [updated 2024 8 Feb; accessed 2024 Oct 25]. Cancer Today [1 screen]. Available from: https://gco.iarc.fr/en

43. Choi HK, Mazzone PJ. Lung Cancer Screening. Med Clin North Am. 2022;106(6):1041–53.

44. Ye J, Liu H, Xu ZL, Zheng L, Liu RY. Identification of a multidimensional transcriptome prognostic signature for lung adenocarcinoma. J Clin Lab Anal. 2019;33(9):e22990.

45. Harris JE. Cigarette smoking among successive birth cohorts of men and women in the United States during 1900-80. J Natl Cancer Inst. 1983;71(3):473–9.

46. Kim AS, Ko HJ, Kwon JH, Lee JM. Exposure to Secondhand Smoke and Risk of Cancer in Never Smokers: A Meta-Analysis of Epidemiologic Studies. Int J Environ Res Public Health. 2018;15(9): 1981.

47. Öberg M, Jaakkola MS, Woodward A, Peruga A, Prüss-Ustün A. Worldwide burden of disease from exposure to second-hand smoke: a retrospective analysis of data from 192 countries. Lancet. 2011;377(9760):139–46.

48. Feliu A, Filippidis FT, Joossens L, Fong GT, Vardavas CI, Baena A, et al. Impact of tobacco control policies on smoking prevalence and quit ratios in 27 European Union countries from 2006 to 2014. Tob Control. 2019;28(1):101–9.

49. Huang J, Deng Y, Tin MS, Lok V, Ngai CH, Zhang L, et al. Distribution, Risk Factors, and Temporal Trends for Lung Cancer Incidence and Mortality: A Global Analysis. Chest. 2022;161(4):1101–11.

50. American Cancer Society [Homepage]. Atlanta, GA, USA:American Cancer Society;[updated 2024 Jan 29; accessed 2024 Oct 26]. Lung Cancer Risk Factors [7 screens]. Available from: https://www.cancer.org/cancer/types/lung-cancer/causes-risks-prevention/risk-factors.html

51. Howlader N, Forjaz G, Mooradian MJ, Meza R, Kong CY, Cronin KA, et al. The Effect of Advances in Lung-Cancer Treatment on Population Mortality. N Engl J Med. 2020;383(7):640–9.

52. Cancer Research UK [Homepage]. London, UK: Cancer Research UK; [accessed 2024 Oct 26]. Lung cancer statistics [5 screens]. Available from: https://www.cancerresearchuk.org/health-professional/cancer-statistics/statistics-by-cancer-type/lung-cancer#heading-One

53. Luo Q, Yu XQ, Wade S, Caruana M, Pesola F, Canfell K, et al. Lung cancer mortality in Australia: Projected outcomes to 2040. Lung Cancer. 2018;125:68–76.

54. Zhang J, Basu P, Emery JD, IJzerman MJ, Bray F. Lung cancer statistics in the United States: a reflection on the impact of cancer control. Ann Cancer Epidemiol. 2022;6(0):2.

55. Kris MG, Mitsudomi T, Peters S. Adjuvant therapies in stages I–III epidermal growth factor receptor-mutated lung cancer: Current and future perspectives. Transl Lung Cancer Res. 2023;12(4):824–36.

56. Knight SB, Crosbie PA, Balata H, Chudziak J, Hussell T, Dive C. Progress and prospects of early detection in lung cancer. Open Biol. 2017;7(9):170070.

57. Travis WD, Rekhtman N, Riley GJ, Geisinger KR, Asamura H, Brambilla E, et al. Pathologic diagnosis of advanced lung cancer based on small biopsies and cytology: a paradigm shift. J Thorac Oncol. 2010;5(4):411–4.

58. Nooreldeen R, Bach H. Current and Future Development in Lung Cancer Diagnosis. Int J Mol Sci. 2021;22(16):8661.

59. Nicholson AG, Tsao MS, Beasley MB, Borczuk AC, Brambilla E, Cooper WA, et al. The 2021 WHO Classification of Lung Tumors: Impact of Advances Since 2015. J Thorac Oncol. 2022;17(3):362–87.

60. Patel AS, Yoo S, Kong R, Sato T, Sinha A, Karam S, et al. Prototypical oncogene family Myc defines unappreciated distinct lineage states of small cell lung cancer. Sci Adv. 2021;7(5):eabc2578.

61. Zugazagoitia J, Paz-Ares L. Extensive-Stage Small-Cell Lung Cancer: First-Line and Second-Line Treatment Options. J Clin Oncol. 2022;40(6):671–80.

62. Wang M, Herbst RS, Boshoff C. Toward personalized treatment approaches for non-small-cell lung cancer. Nat Med. 2021;27(8):1345–56.

63. Pao W, Girard N. New driver mutations in non-small-cell lung cancer. Lancet Oncol. 2011;12(2):175–80.

64. Hoy H, Lynch T, Beck M. Surgical Treatment of Lung Cancer. Crit Care Nurs Clin North Am. 2019;31(3):303–13.

65. Eberhardt WEE, De Ruysscher D, Weder W, Le Péchoux C, De Leyn P, Hoffmann H, et al. 2nd ESMO Consensus Conference in Lung Cancer: locally advanced stage III non-small-cell lung cancer. Ann Oncol. 2015;26(8):1573–88.

66. Vinod SK, Hau E. Radiotherapy treatment for lung cancer: Current status and future directions. Respirology. 2020;25 Suppl 2(S2):61–71.

67. Lee SH. Chemotherapy for Lung Cancer in the Era of Personalized Medicine. Tuberc Respir Dis (Seoul). 2019;82(3):179–89.

68. Ghosh S. Cisplatin: The first metal based anticancer drug. Bioorg Chem. 2019;88:102925.

69. Hendriks LE, Kerr KM, Menis J, Mok TS, Nestle U, Passaro A, et al. Non-oncogene-addicted metastatic non-small-cell lung cancer: ESMO Clinical Practice Guideline for diagnosis, treatment and follow-up. Ann Oncol. 2023;34(4):358–76.

70. Boumahdi S, de Sauvage FJ. The great escape: tumour cell plasticity in resistance to targeted therapy. Nat Rev Drug Discov. 2020;19(1):39–56.

71. Lee CK, Brown C, Gralla RJ, Hirsh V, Thongprasert S, Tsai CM, et al. Impact of EGFR inhibitor in non-small cell lung cancer on progression-free and overall survival: a meta-analysis. J Natl Cancer Inst. 2013;105(9):595–605.

72. Soria JC, Ohe Y, Vansteenkiste J, Reungwetwattana T, Chewaskulyong B, Lee KH, et al. Osimertinib in Untreated EGFR-Mutated Advanced Non-Small-Cell Lung Cancer. N Engl J Med. 2018;378(2):113–25.

73. Mok TS, Cheng Y, Zhou X, Lee KH, Nakagawa K, Niho S, et al. Improvement in Overall Survival in a Randomized Study That Compared Dacomitinib With Gefitinib in Patients With Advanced Non-Small-Cell Lung Cancer and EGFR-Activating Mutations. J Clin Oncol. 2018;36(22):2244–50.

74. Ruiz-Cordero R, Devine WP. Targeted Therapy and Checkpoint Immunotherapy in Lung Cancer. Surg Pathol Clin. 2020 Mar 1;13(1):17–33.

75. Novello S, Kowalski DM, Luft A, Gümüş M, Vicente D, Mazières J, et al. Pembrolizumab Plus Chemotherapy in Squamous Non-Small-Cell Lung Cancer: 5-Year Update of the Phase III KEYNOTE-407 Study. J Clin Oncol. 2023;41(11):1999–2006.

76. Paz-Ares L, Luft A, Vicente D, Tafreshi A, Gümüş M, Mazières J, et al. Pembrolizumab plus Chemotherapy for Squamous Non-Small-Cell Lung Cancer. N Engl J Med. 2018;379(21):2040–51.

77. Boyer M, Şendur MAN, Rodríguez-Abreu D, Park K, Lee DH, Çiçin I, et al. Pembrolizumab Plus Ipilimumab or Placebo for Metastatic Non-Small-Cell Lung Cancer With PD-L1 Tumor Proportion Score ≥ 50%: Randomized, Double-Blind Phase III KEYNOTE-598 Study. J Clin Oncol. 2021;39(21):2327–38.

78. Niu J, Maurice-Dror C, Lee DH, Kim DW, Nagrial A, Voskoboynik M, et al. First-in-human phase 1 study of the anti-TIGIT antibody vibostolimab as monotherapy or with pembrolizumab for advanced solid tumors, including non-small-cell lung cancer. Ann Oncol. 2022;33(2):169–80.

79. Dingemans AMC, Früh M, Ardizzoni A, Besse B, Faivre-Finn C, Hendriks LE, et al. Small-cell lung cancer: ESMO Clinical Practice Guidelines for diagnosis, treatment and follow-up. Annals of Oncology. 2021;32(7):839–53.

80. Stahel R, Thatcher N, Früh M, Le Péchoux C, Postmus PE, Sorensen JB, et al. 1st ESMO Consensus Conference in lung cancer; Lugano 2010: small-cell lung cancer. Ann Oncol. 2011;22(9):1973–80.

81. O'Brien MER, Ciuleanu TE, Tsekov H, Shparyk Y, Čučeviá B, Juhasz G, et al. Phase III trial comparing supportive care alone with supportive care with oral topotecan in patients with relapsed small-cell lung cancer. J Clin Oncol. 2006;24(34):5441–7.

82. Evans WK, Osoba D, Feld R, Shepherd FA, Bazos MJ, DeBoer G. Etoposide (VP-16) and cisplatin: an effective treatment for relapse in small-cell lung cancer. J Clin Oncol. 1985;3(1):65–71.

83. Leal JFM, Martínez-Díez M, García-Hernández V, Moneo V, Domingo A, Bueren-Calabuig JA, et al. PM01183, a new DNA minor groove covalent binder with potent in vitro and in vivo anti-tumour activity. Br J Pharmacol. 2010;161(5):1099–110.

84. Masuda N, Fukuoka M, Kusunoki Y, Motsui K, Takifuji N, Kudoh S, et al. CPT-11: a new derivative of camptothecin for the treatment of refractory or relapsed small-cell lung cancer. J Clin Oncol. 1992;10(8):1225–9.

85. Yamamoto N, Tsurutani J, Yoshimura N, Asai G, Moriyama A, Nakagawa K, et al. Phase II study of weekly paclitaxel for relapsed and refractory small cell lung cancer. 2006;26(1B):777-81.

86. Pietanza MC, Kadota K, Huberman K, Sima CS, Fiore JJ, Sumner DK, et al. Phase II trial of temozolomide in patients with relapsed sensitive or refractory small cell lung cancer, with assessment of methylguanine-DNA methyltransferase as a potential biomarker. Clin Cancer Res. 2012;18(4):1138–45.

87. Ginsberg RJ, Rubinstein L V. Randomized trial of lobectomy versus limited resection for T1 N0 non-small cell lung cancer. Ann Thorac Surg. 1995;60(3):615–23.

88. Shi Y, Wu S, Ma S, Lyu Y, Xu H, Deng L, et al. Comparison Between Wedge Resection and Lobectomy/Segmentectomy for Early-Stage Non-small Cell Lung Cancer: A Bayesian Meta-analysis and Systematic Review. Ann Surg Oncol. 2022;29(3):1868–79.

89. Kodama K, Higashiyama M, Okami J, Tokunaga T, Imamura F, Nakayama T, et al. Oncologic Outcomes of Segmentectomy Versus Lobectomy for Clinical T1a N0 M0 Non-Small Cell Lung Cancer. Ann Thorac Surg. 2016;101(2):504–11.

90. Salah S, Tanvetyanon Tawee T, Abbasi S. Metastatectomy for extra-cranial extra-adrenal non-small cell lung cancer solitary metastases: systematic review and analysis of reported cases. Lung Cancer. 2012;75(1):9–14.

91. Garon EB, Hellmann MD, Rizvi NA, Carcereny E, Leighl NB, Ahn MJ, et al. Five-Year Overall Survival for Patients With Advanced Non–Small-Cell Lung Cancer Treated With Pembrolizumab: Results From the Phase I KEYNOTE-001 Study. J Clin Oncol. 2019;37(28):2518–27.

92. Doroshow DB, Bhalla S, Beasley MB, Sholl LM, Kerr KM, Gnjatic S, et al. PD-L1 as a biomarker of response to immune-checkpoint inhibitors. Nat Rev Clin Oncol. 2021;18(6):345–62.

93. Paijens ST, Vledder A, de Bruyn M, Nijman HW. Tumor-infiltrating lymphocytes in the immunotherapy era. Cell Mol Immunol. 2020;18(4):842-859.

94. Schumacher TN, Schreiber RD. Neoantigens in cancer immunotherapy. Science. 2015;348(6230):69–74.

95. Marabelle A, Fakih M, Lopez J, Shah M, Shapira-Frommer R, Nakagawa K, et al. Association of tumour mutational burden with outcomes in patients with advanced solid tumours treated with pembrolizumab: prospective biomarker analysis of the multicohort, open-label, phase 2 KEYNOTE-158 study. Lancet Oncol. 2020;21(10):1353–65.

96. Morgensztern D, Campo MJ, Dahlberg SE, Doebele RC, Garon E, Gerber DE, et al. Molecularly targeted therapies in non-small-cell lung cancer annual update 2014. J Thorac Oncol. 2015;10(1 Suppl 1):S1–63.

97. Duma N, Santana-Davila R, Molina JR. Non-Small Cell Lung Cancer: Epidemiology, Screening, Diagnosis, and Treatment. Mayo Clin Proc. 2019;94(8):1623–40.

98. Jänne PA, Yang JCH, Kim DW, Planchard D, Ohe Y, Ramalingam SS, et al. AZD9291 in EGFR inhibitor-resistant non-small-cell lung cancer. N Engl J Med. 2015;372(18):1689–99.

99. Bean J, Brennan C, Shih JY, Riely G, Viale A, Wang L, et al. MET amplification occurs with or without T790M mutations in EGFR mutant lung tumors with acquired resistance to gefitinib or erlotinib. Proc Natl Acad Sci U S A. 2007;104(52):20932–7.

100. Engelman JA, Zejnullahu K, Mitsudomi T, Song Y, Hyland C, Joon OP, et al. MET amplification leads to gefitinib resistance in lung cancer by activating ERBB3 signaling. Science. 2007;316(5827):1039–43.

101. Hendriks LE, Kerr KM, Menis J, Mok TS, Nestle U, Passaro A, et al. Oncogene-addicted metastatic non-small-cell lung cancer: ESMO Clinical Practice Guideline for diagnosis, treatment and follow-up. Ann Oncol. 2023;34(4):339–57.

102. Vasan N, Baselga J, Hyman DM. A view on drug resistance in cancer. Nature. 2019;575(7782):299–309.

103. Holohan C, Van Schaeybroeck S, Longley DB, Johnston PG. Cancer drug resistance: an evolving paradigm. Nat Rev Cancer. 2013;13(10):714–26.

104. Ramos A, Sadeghi S, Tabatabaeian H. Battling Chemoresistance in Cancer: Root Causes and Strategies to Uproot Them. Int J Mol Sci. 2021;22(17):9451.

105. Kuo MT, Chen HHW, Song IS, Savaraj N, Ishikawa T. The roles of copper transporters in cisplatin resistance. Cancer Metastasis Rev. 2007 Mar;26(1):71–83.

106. Li ZH, Qiu MZ, Zeng ZL, Luo HY, Wu WJ, Wang F, et al. Copper-transporting P-type adenosine triphosphatase (ATP7A) is associated with platinum-resistance in non-small cell lung cancer (NSCLC). J Transl Med. 2012;10:21.

107. Lv P, Man S, Xie L, Ma L, Gao W. Pathogenesis and therapeutic strategy in platinum resistance lung cancer. Biochim Biophys Acta Rev Cancer. 2021;1876(1):188577.

108. Haider T, Pandey V, Banjare N, Gupta PN, Soni V. Drug resistance in cancer: mechanisms and tackling strategies. Pharmacol Rep. 2020;72(5):1125–51.

109. Xu Y, Jiang T, Wu C, Zhang Y. CircAKT3 inhibits glycolysis balance in lung cancer cells by regulating miR-516b-5p/STAT3 to inhibit cisplatin sensitivity. Biotechnol Lett. 2020;42(7):1123–35.

110. Chen HHW, Yan JJ, Chen WC, Kuo MT, Lai YH, Lai WW, et al. Predictive and prognostic value of human copper transporter 1 (hCtr1) in patients with stage III non-small-cell lung cancer receiving first-line platinum-based doublet chemotherapy. Lung Cancer. 2012;75(2):228–34. Available from: https://pubmed.ncbi.nlm.nih.gov/21788094/

111. Meijer C, Mulder NH, Timmer-Bosscha H, Sluiter WJ, Meersma GJ, de Vries EG. Relationship of cellular glutathione to the cytotoxicity and resistance of seven platinum compounds. Cancer Res. 1992;52(24):6885–9.

112. Kawato Y, Aonuma M, Hirota Y, Kuga H, Sato K. Intracellular roles of SN-38, a metabolite of the camptothecin derivative CPT-11, in the antitumor effect of CPT-11. Cancer Res. 1991;51(16):4187–91.

113. Satar NA, Fakiruddin KS, Lim MN, Mok PL, Zakaria N, Fakharuzi NA, et al. Novel triple positive markers identified in human non small cell lung cancer cell line with chemotherapy-resistant and putative cancer stem cell characteristics. Oncol Rep. 2018;40(2):669–81.

114. Jing X, Yang F, Shao C, Wei K, Xie M, Shen H, et al. Role of hypoxia in cancer therapy by regulating the tumor microenvironment. Mol Cancer. 2019;18(1):157.

115. Roma-Rodrigues C, Mendes R, Baptista P V., Fernandes AR. Targeting Tumor Microenvironment for Cancer Therapy. Int J Mol Sci. 2019;20(4):840.

116. Shin DH, Choi YJ, Park JW. SIRT1 and AMPK mediate hypoxia-induced resistance of non-small cell lung cancers to cisplatin and doxorubicin. Cancer Res. 2014;74(1):298–308.

117. Wang J, Tian L, Khan MN, Zhang L, Chen Q, Zhao Y, et al. Ginsenoside Rg3 sensitizes hypoxic lung cancer cells to cisplatin via blocking of NF-κB mediated epithelial-mesenchymal transition and stemness. Cancer Lett. 2018;415:73–85.

118. He Y, Xie H, Yu P, Jiang S, Wei L. FOXC2 promotes epithelial-mesenchymal transition and cisplatin resistance of non-small cell lung cancer cells. Cancer Chemother Pharmacol. 2018;82(6):1049–59.

119. Ashrafizadeh M, Zarrabi A, Hushmandi K, Kalantari M, Mohammadinejad R, Javaheri T, et al. Association of the Epithelial-Mesenchymal Transition (EMT) with Cisplatin Resistance. Int J Mol Sci. 2020;21(11):1–46.

120. Saleh R, Elkord E. Acquired resistance to cancer immunotherapy: Role of tumor-mediated immunosuppression. Semin Cancer Biol. 2020;65:13–27.

121. Pistritto G, Trisciuoglio D, Ceci C, Alessia Garufi, D'Orazi G. Apoptosis as anticancer mechanism: function and dysfunction of its modulators and targeted therapeutic strategies. Aging. 2016;8(4):603–19.

122. Tang D, Kang R, Berghe T Vanden, Vandenabeele P, Kroemer G. The molecular machinery of regulated cell death. Cell Res. 2019;29(5):347–64.

123. D'Arcy MS. Cell death: a review of the major forms of apoptosis, necrosis and autophagy. Cell Biol Int. 2019;43(6):582–92.

124. Wang X, Hua P, He C, Chen M. Non-apoptotic cell death-based cancer therapy: Molecular mechanism, pharmacological modulators, and nanomedicine. Acta Pharm Sin B. 2022;12(9):3567.

125. Peng F, Liao M, Qin R, Zhu S, Peng C, Fu L, et al. Regulated cell death (RCD) in cancer: key pathways and targeted therapies. Signal Transduct Target Ther. 2022;7(1):286.

126. Durgan J, Florey O. Cancer cell cannibalism: Multiple triggers emerge for entosis. Biochim Biophys Acta Mol Cell Res. 2018;1865(6):831–41.

127. Brinkmann V, Reichard U, Goosmann C, Fauler B, Uhlemann Y, Weiss DS, et al. Neutrophil extracellular traps kill bacteria. Science. 2004;303(5663):1532–5.

128. Aits S, Jäättelä M. Lysosomal cell death at a glance. J Cell Sci. 2013;126(9):1905–12.

129. Chen F, Kang R, Liu J, Tang D. Mechanisms of alkaliptosis. Front Cell Dev Biol. 2023;11:1213995.

130. Song X, Zhu S, Xie Y, Liu J, Sun L, Zeng D, et al. JTC801 Induces pH-dependent Death Specifically in Cancer Cells and Slows Growth of Tumors in Mice. Gastroenterology. 2018;154(5):1480–93.

131. Holze C, Michaudel C, MacKowiak C, Haas DA, Benda C, Hubel P, et al. Oxeiptosis, a ROS-induced caspase-independent apoptosis-like cell-death pathway. Nat Immunol. 2018;19(2):130–40.

132. Kroemer G, Galassi C, Zitvogel L, Galluzzi L. Immunogenic cell stress and death. Nat Immunol. 2022;23(4):487–500.

133. Krysko D V., Garg AD, Kaczmarek A, Krysko O, Agostinis P, Vandenabeele P. Immunogenic cell death and DAMPs in cancer therapy. Nat Rev Cancer. 2012 ;12(12):860–75.

134. Galluzzi L, Buqué A, Kepp O, Zitvogel L, Kroemer G. Immunogenic cell death in cancer and infectious disease. Nat Rev Immunol. 2017;17(2):97–111.

135. de Oca RM, Alavi AS, Vitali N, Bhattacharya S, Blackwell C, Patel K, et al. Belantamab Mafodotin (GSK2857916) Drives Immunogenic Cell Death and Immune-mediated Antitumor Responses In Vivo. Mol Cancer Ther. 2021;20(10):1941–55.

136. Kepp O, Zitvogel L, Kroemer G. Lurbinectedin: an FDA-approved inducer of immunogenic cell death for the treatment of small-cell lung cancer. Oncoimmunology. 2020;9(1):286.

137. Borys S, Khozmi R, Kranc W, Bryja A, Dyszkiewicz-Konwińska M, Jeseta M, et al. Recent findings of the types of programmed cell death. Adv Cell Biol. 2017 Mar 1;5(1):43–9.

138. Ketelut-Carneiro N, Fitzgerald KA. Apoptosis, Pyroptosis, and Necroptosis-Oh My! The Many Ways a Cell Can Die. J Mol Biol. 2022;434(4): 167378.

139. Bertheloot D, Latz E, Franklin BS. Necroptosis, pyroptosis and apoptosis: an intricate game of cell death. Cell Mol Immunol. 2021;18(5):1106–21.

140. Brenner D, Mak TW. Mitochondrial cell death effectors. Curr Opin Cell Biol. 2009;21(6):871–7.

141. Liu X, Kim CN, Yang J, Jemmerson R, Wang X. Induction of apoptotic program in cell-free extracts: requirement for dATP and cytochrome c. Cell. 1996;86(1):147–57.

142. Cain K, Brown DG, Langlais C, Cohen GM. Caspase activation involves the formation of the aposome, a large (approximately 700 kDa) caspase-activating complex. J Biol Chem. 1999;274(32):22686–92.

143. Acehan D, Jiang X, Morgan DG, Heuser JE, Wang X, Akey CW. Three-dimensional structure of the apoptosome: implications for assembly, procaspase-9 binding, and activation. Mol Cell. 2002;9(2):423–32.

144. Czabotar PE, Garcia-Saez AJ. Mechanisms of BCL-2 family proteins in mitochondrial apoptosis. Nat Rev Mol Cell Biol. 2023;24(10):732–48.

145. Kvansakul M, Yang H, Fairlie WD, Czabotar PE, Fischer SF, Perugini MA, et al. Vaccinia virus anti-apoptotic F1L is a novel Bcl-2-like domain-swapped dimer that binds a highly selective subset of BH3-containing death ligands. Cell Death Differ. 2008;15(10):1564–71.

146. Wang Y, Tjandra N. Structural insights of tBid, the caspase-8-activated Bid, and its BH3 domain. J Biol Chem. 2013;288(50):35840–51.

147. Dai H, Smith A, Meng XW, Schneider PA, Pang YP, Kaufmann SH. Transient binding of an activator BH3 domain to the Bak BH3-binding groove initiates Bak oligomerization. J Cell Biol. 2011;194(1):39–48.

148. Sattler M, Liang H, Nettesheim D, Meadows RP, Harlan JE, Eberstadt M, et al. Structure of Bcl-xL-Bak peptide complex: recognition between regulators of apoptosis. Science. 1997;275(5302):983–6.

149. Vandenabeele P, Bultynck G, Savvides SN. Pore-forming proteins as drivers of membrane permeabilization in cell death pathways. Nat Rev Mol Cell Biol. 2023;24(5):312–33.

150. Suzuki M, Youle RJ, Tjandra N. Structure of Bax: coregulation of dimer formation and intracellular localization. Cell. 2000;103(4):645–54.

151. Lazarou M, Stojanovski D, Frazier AE, Kotevski A, Dewson G, Craigen WJ, et al. Inhibition of Bak activation by VDAC2 is dependent on the Bak transmembrane anchor. J Biol Chem. 2010;285(47):36876–83.

152. Enari M, Sakahira H, Yokoyama H, Okawa K, Iwamatsu A, Nagata S. A caspase-activated DNase that degrades DNA during apoptosis, and its inhibitor ICAD. Nature. 1998;391(6662):43–50.

153. Segawa K, Kurata S, Yanagihashi Y, Brummelkamp TR, Matsuda F, Nagata S. Caspase-mediated cleavage of phospholipid flippase for apoptotic phosphatidylserine exposure. Science. 2014;344(6188):1164–8.

154. Sebbagh M, Renvoizé C, Hamelin J, Riché N, Bertoglio J, Bréard J. Caspase-3-mediated cleavage of ROCK I induces MLC phosphorylation and apoptotic membrane blebbing. Nat Cell Biol. 2001;3(4):346–52.

155. Van De Craen M, Declercq W, Van Den Brande I, Fiers W, Vandenabeele P. The proteolytic procaspase activation network: an in vitro analysis. Cell Death Differ. 1999;6(11):1117–24.

156. Kumar S, Fairmichael C, Longley DB, Turkington RC. The Multiple Roles of the IAP Super-family in cancer. Pharmacol Ther. 2020;214: 107610.

157. Samuel T, Welsh K, Lober T, Togo SH, Zapata JM, Reed JC. Distinct BIR domains of cIAP1 mediate binding to and ubiquitination of tumor necrosis factor receptor-associated factor 2 and second mitochondrial activator of caspases. J Biol Chem. 2006;281(2):1080–90.

158. Vaux DL, Silke J. IAPs, RINGs and ubiquitylation. Nat Rev Mol Cell Biol. 2005;6(4):287–97.

159. Gyrd-Hansen M, Darding M, Miasari M, Santoro MM, Zender L, Xue W, et al. IAPs contain an evolutionarily conserved ubiquitin-binding domain that regulates NF-kappaB as well as cell survival and oncogenesis. Nat Cell Biol. 2008;10(11):1309–17.

160. Bartke T, Pohl C, Pyrowolakis G, Jentsch S. Dual role of BRUCE as an antiapoptotic IAP and a chimeric E2/E3 ubiquitin ligase. Mol Cell. 2004;14(6):801–11.

161. Liang J, Zhao W, Tong P, Li P, Zhao Y, Li H, et al. Comprehensive molecular characterization of inhibitors of apoptosis proteins (IAPs) for therapeutic targeting in cancer. BMC Med Genomics. 2020;13(1):7.

162. Lopez J, John SW, Tenev T, Rautureau GJP, Hinds MG, Francalanci F, et al. CARD-mediated autoinhibition of cIAP1's E3 ligase activity suppresses cell proliferation and migration. Mol Cell. 2011;42(5):569–83.

163. Imoto I, Yang ZQ, Pimkhaokham A, Tsuda H, Shimada Y, Ohki M, et al. Identification of cIAP1 as a candidate target gene within an amplicon at 11q22 in esophageal squamous cell carcinomas. Cancer Res. 2001;61(18):6629–34.

164. Imoto I, Tsuda H, Hirasawa A, Miura M, Sakamoto M, Hirohashi S, et al. Expression of cIAP1, a target for 11q22 amplification, correlates with resistance of cervical cancers to radiotherapy. Cancer Res. 2002;62(17):4860–6.

165. Liu G, Yuan X, Zeng Z, Tunici P, Ng H, Abdulkadir IR, et al. Analysis of gene expression and chemoresistance of CD133+ cancer stem cells in glioblastoma. Mol Cancer. 2006;5:67.

166. Franklin MC, Kadkhodayan S, Ackerly H, Alexandru D, Distefano MD, Elliott LO, et al. Structure and function analysis of peptide antagonists of melanoma inhibitor of apoptosis (ML-IAP). Biochemistry. 2003;42(27):8223–31.

167. Vucic D, Deshayes K, Ackerly H, Pisabarro MT, Kadkhodayan S, Fairbrother WJ, et al. SMAC negatively regulates the anti-apoptotic activity of melanoma inhibitor of apoptosis (ML-IAP). J Biol Chem. 2002;277(14):12275–9.

168. Oost TK, Sun C, Armstrong RC, Al-Assaad AS, Betz SF, Deckwerth TL, et al. Discovery of potent antagonists of the antiapoptotic protein XIAP for the treatment of cancer. J Med Chem. 2004;47(18):4417–26.

169. Sun H, Nikolovska-Coleska Z, Lu J, Meagher JL, Yang CY, Qiu S, et al. Design, synthesis, and characterization of a potent, nonpeptide, cell-permeable, bivalent Smac mimetic that concurrently targets both the BIR2 and BIR3 domains in XIAP. J Am Chem Soc. 2007;129(49):15279–94.

170. Estornes Y, Bertrand MJM. IAPs, regulators of innate immunity and inflammation. Semin Cell Dev Biol. 2015;39:106–14.

171. Zarnegar BJ, Wang Y, Mahoney DJ, Dempsey PW, Cheung HH, He J, et al. Noncanonical NF-kappaB activation requires coordinated assembly of a regulatory complex of the adaptors cIAP1, cIAP2, TRAF2 and TRAF3 and the kinase NIK. Nat Immunol. 2008;9(12):1371–8.

172. Dougan M, Dougan S, Slisz J, Firestone B, Vanneman M, Draganov D, et al. IAP inhibitors enhance co-stimulation to promote tumor immunity. J Exp Med. 2010;207(10):2195–206.

173. Beug ST, Beauregard CE, Healy C, Sanda T, St-Jean M, Chabot J, et al. Smac mimetics synergize with immune checkpoint inhibitors to promote tumour immunity against glioblastoma. Nat Commun. 2017;8:14278.

174. Calarco JA. “Cryptic” exons reveal some of their secrets. Elife. 2013;2:e00476.

175. Chantalat L, Skoufias DA, Kleman JP, Jung B, Dideberg O, Margolis RL. Crystal structure of human survivin reveals a bow tie-shaped dimer with two unusual alpha-helical extensions. Mol Cell. 2000;6(1):183–9.

176. Li F, Altieri DC. Transcriptional analysis of human survivin gene expression. Biochem J. 1999;344(2):305–11.

177. Verdecia MA, Huang HK, Dutil E, Kaiser DA, Hunter T, Noel JP. Structure of the human anti-apoptotic protein survivin reveals a dimeric arrangement. Nat Struct Biol. 2000;7(7):602–8.

178. Pavlyukov MS, Antipova N V., Balashova M V., Vinogradova T V., Kopantzev EP, Shakhparonov MI. Survivin monomer plays an essential role in apoptosis regulation. J Biol Chem. 2011;286(26):23296–307.

179. Martínez-García D, Manero-Rupérez N, Quesada R, Korrodi-Gregório L, Soto-Cerrato V. Therapeutic strategies involving survivin inhibition in cancer. Med Res Rev. 2019;39(3):887–909.

180. Sah NK, Seniya C. Survivin splice variants and their diagnostic significance. Tumour Biol. 2015;36(9):6623–31.

181. Li F. Role of survivin and its splice variants in tumorigenesis. Br J Cancer. 2005;92(2):212–6.

182. Albadari N, Li W. Survivin Small Molecules Inhibitors: Recent Advances and Challenges. Molecules. 2023;28(3):1376.

183. Fukuda S, Pelus LM. Survivin, a cancer target with an emerging role in normal adult tissues. Mol Cancer Ther. 2006;5(5):1087–98.

184. Kanwar JR, Kamalapuram SK, Kanwar RK. Survivin signaling in clinical oncology: a multifaceted dragon. Med Res Rev. 2013;33(4):765–89.

185. Li F, Yang J, Ramnath N, Javle MM, Tan D. Nuclear or cytoplasmic expression of survivin: what is the significance? Int J Cancer. 2005;114(4):509–12.

186. Dohi T, Beltrami E, Wall NR, Plescia J, Altieri DC. Mitochondrial survivin inhibits apoptosis and promotes tumorigenesis. J Clin Invest. 2004;114(8):1117–27.

187. Garg H, Suri P, Gupta JC, Talwar GP, Dubey S. Survivin: a unique target for tumor therapy. Cancer Cell Int. 2016;16(1):49.

188. Wheatley SP, Altieri DC. Survivin at a glance. J Cell Sci. 2019;132(7):jcs223826.

189. Altieri DC. Validating survivin as a cancer therapeutic target. Nat Rev Cancer. 2003;3(1):46–54.

190. Kitagawa M, Lee SH. The chromosomal passenger complex (CPC) as a key orchestrator of orderly mitotic exit and cytokinesis. Front Cell Dev Biol. 2015;3:14.

191. Jeyaprakash AA, Klein UR, Lindner D, Ebert J, Nigg EA, Conti E. Structure of a Survivin-Borealin-INCENP core complex reveals how chromosomal passengers travel together. Cell. 2007;131(2):271–85.

192. Athanasoula KC, Gogas H, Polonifi K, Vaiopoulos AG, Polyzos A, Mantzourani M. Survivin beyond physiology: orchestration of multistep carcinogenesis and therapeutic potentials. Cancer Lett. 2014;347(2):175–82.

193. Rosa J, Canovas P, Islam A, Altieri DC, Doxsey SJ. Survivin modulates microtubule dynamics and nucleation throughout the cell cycle. Mol Biol Cell. 2006;17(3):1483–93.

194. Giodini A, Kallio MJ, Wall NR, Gorbsky GJ, Tognin S, Marchisio PC, et al. Regulation of microtubule stability and mitotic progression by survivin. Cancer Res. 2002;62(9):2462–7.

195. Babkoff A, Cohen-Kfir E, Aharon H, Ronen D, Rosenberg M, Wiener R, et al. A direct interaction between survivin and myosin II is required for cytokinesis. J Cell Sci. 2019;132(14):jcs233130.

196. Andonegui-Elguera MA, Cáceres-Gutiérrez RE, López-Saavedra A, Cisneros-Soberanis F, Justo-Garrido M, Díaz-Chávez J, et al. The Roles of Histone Post-Translational Modifications in the Formation and Function of a Mitotic Chromosome. Int J Mol Sci. 2022;23(15):8704.

197. Shin S, Sung BJ, Cho YS, Kim HJ, Ha NC, Hwang JI, et al. An anti-apoptotic protein human survivin is a direct inhibitor of caspase-3 and -7. Biochemistry. 2001;40(4):1117–23.

198. Fang X long, Cao X ping, Xiao J, Hu Y, Chen M, Raza HK, et al. Overview of role of survivin in cancer: expression, regulation, functions, and its potential as a therapeutic target. J Drug Target. 2024;32(3):223–40.

199. Sarvagalla S, Lin TY, Kondapuram SK, Cheung CHA, Coumar MS. Survivin - caspase protein-protein interaction: Experimental evidence and computational investigations to decipher the hotspot residues for drug targeting. J Mol Struct. 2021;1229:129619.

200. Eckelman BP, Salvesen GS. The human anti-apoptotic proteins cIAP1 and cIAP2 bind but do not inhibit caspases. J Biol Chem. 2006;281(6):3254–60.

201. Arora V, Cheung HH, Plenchette S, Micali OC, Liston P, Korneluk RG. Degradation of survivin by the X-linked inhibitor of apoptosis (XIAP)-XAF1 complex. J Biol Chem. 2007;282(36):26202–9.

202. Mehrotra S, Languino LR, Raskett CM, Mercurio AM, Dohi T, Altieri DC. IAP regulation of metastasis. Cancer Cell. 2010;17(1):53–64.

203. Marusawa H, Matsuzawa S ichi, Welsh K, Zou H, Armstrong R, Tamm I, et al. HBXIP functions as a cofactor of survivin in apoptosis suppression. EMBO J. 2003;22(11):2729–40.

204. Song Z, Yao X, Wu M. Direct interaction between survivin and Smac/DIABLO is essential for the anti-apoptotic activity of survivin during taxol-induced apoptosis. J Biol Chem. 2003;278(25):23130–40.

205. Ceballos-Cancino G, Espinosa M, Maldonado V, Melendez-Zajgla J. Regulation of mitochondrial Smac/DIABLO-selective release by survivin. Oncogene. 2007;26(54):7569–75.

206. Liu T, Brouha B, Grossman D. Rapid induction of mitochondrial events and caspase-independent apoptosis in Survivin-targeted melanoma cells. Oncogene. 2004;23(1):39–48.

207. Asanuma K, Tsuji N, Endoh T, Yagihashi A, Watanabe N. Survivin enhances Fas ligand expression via up-regulation of specificity protein 1-mediated gene transcription in colon cancer cells. J Immunol. 2004;172(6):3922–9.

208. Chen J, Jin S, Tahir SK, Zhang H, Liu X, Sarthy A V., et al. Survivin enhances Aurora-B kinase activity and localizes Aurora-B in human cells. J Biol Chem. 2003;278(1):486–90.

209. Park MH, Kim SY, Kim YJ, Chung YH. ALS2CR7 (CDK15) attenuates TRAIL induced apoptosis by inducing phosphorylation of survivin Thr34. Biochem Biophys Res Commun. 2014;450(1):129–34.

210. Lyu H, Huang J, He Z, Liu B. Epigenetic mechanism of survivin dysregulation in human cancer. Sci China Life Sci. 2018;61(7):808–14.

211. Mityaev M V., Kopantzev EP, Buzdin AA, Vinogradova T V., Sverdlov ED. Functional significance of a putative sp1 transcription factor binding site in the survivin gene promoter. Biochemistry. 2008;73(11):1183–91.

212. Chen Y, Wang X, Li W, Zhang H, Zhao C, Li Y, et al. Sp1 upregulates survivin expression in adenocarcinoma of lung cell line A549. Anat Rec. 2011;294(5):774–80.

213. Estève PO, Chin HG, Pradhan S. Human maintenance DNA (cytosine-5)-methyltransferase and p53 modulate expression of p53-repressed promoters. Proc Natl Acad Sci U S A. 2005;102(4):1000–5.

214. Nakano J, Huang CL, Liu D, Ueno M, Sumitomo S, Yokomise H. Survivin gene expression is negatively regulated by the p53 tumor suppressor gene in non-small cell lung cancer. Int J Oncol. 2005;27(5):1215–21.

215. Wang Z, Fukuda S, Pelus LM. Survivin regulates the p53 tumor suppressor gene family. Oncogene. 2004;23(49):8146–53.

216. Mirza A, McGuirk M, Hockenberry TN, Wu Q, Ashar H, Black S, et al. Human survivin is negatively regulated by wild-type p53 and participates in p53-dependent apoptotic pathway. Oncogene. 2002;21(17):2613–22.

217. Papanikolaou V, Iliopoulos D, Dimou I, Dubos S, Kappas C, Kitsiou-Tzeli S, et al. Survivin regulation by HER2 through NF-κB and c-myc in irradiated breast cancer cells. J Cell Mol Med. 2011;15(7):1542–50.

218. Wagner M, Schmelz K, Dörken B, Tamm I. Transcriptional regulation of human survivin by early growth response (Egr)-1 transcription factor. Int J Cancer. 2008;122(6):1278–87.

219. Gashler A, Sukhatme VP. Early growth response protein 1 (Egr-1): prototype of a zinc-finger family of transcription factors. Prog Nucleic Acid Res Mol Biol. 1995;50(C):191–224.

220. Nair P, Muthukkumar S, Sells SF, Han SS, Sukhatme VP, Rangnekar VM. Early growth response-1-dependent apoptosis is mediated by p53. J Biol Chem. 1997;272(32):20131–8.

221. Levkovitz Y, Baraban JM. A dominant negative Egr inhibitor blocks nerve growth factor-induced neurite outgrowth by suppressing c-Jun activation: role of an Egr/c-Jun complex. J Neurosci. 2002;22(10):3845–54.

222. Jiang Y, Saavedra HI, Holloway MP, Leone G, Altura RA. Aberrant regulation of survivin by the RB/E2F family of proteins. J Biol Chem. 2004 Sep 24;279(39):40511–20.

223. Fang X long, Cao X ping, Xiao J, Hu Y, Chen M, Raza HK, et al. Overview of role of survivin in cancer: expression, regulation, functions, and its potential as a therapeutic target. J Drug Target. 2024;32(3):223–40.

224. Huang J, Lyu H, Wang J, Liu B. MicroRNA regulation and therapeutic targeting of survivin in cancer. 2014;5(1):20–31.

225. Subramanian C, McCallister R, Cohen MS. Multi-genomic analysis of 260 adrenocortical cancer patient tumors identifies novel network BIRC5-hsa-miR-335-5p-PAX8-AS1 strongly associated with poor survival. Surgery. 2023;173(1):43–51.

226. Ou D, Wu Y, Liu J, Lao X, Zhang S, Liao G. miRNA-335 and miRNA-182 affect the occurrence of tongue squamous cell carcinoma by targeting survivin. Oncol Lett. 2016;12(4):2531–7.

227. Chen X, Duan N, Zhang C, Zhang W. Survivin and Tumorigenesis: Molecular Mechanisms and Therapeutic Strategies. J Cancer. 2016;7(3):314–23.

228. Zhu ZB, Makhija SK, Lu B, Wang M, Kaliberova L, Liu B, et al. Transcriptional targeting of tumors with a novel tumor-specific survivin promoter. Cancer Gene Ther. 2004;11(4):256–62.

229. Yang L, Cao Z, Li F, Post DE, Van Meir EG, Zhong H, et al. Tumor-specific gene expression using the survivin promoter is further increased by hypoxia. Gene Ther. 2004;11(15):1215–23.

230. Barrett RMA, Colnaghi R, Wheatley SP. Threonine 48 in the BIR domain of survivin is critical to its mitotic and anti-apoptotic activities and can be phosphorylated by CK2 in vitro. Cell Cycle. 2011;10(3):538–48.

231. Wheatley SP, Barrett RM, Andrews PD, Medema RH, Morley SJ, Swedlow JR, et al. Phosphorylation by aurora-B negatively regulates survivin function during mitosis. Cell Cycle. 2007;6(10):1220–30.

232. Dohi T, Xia F, Altieri DC. Compartmentalized phosphorylation of IAP by protein kinase A regulates cytoprotection. Mol Cell. 2007;27(1):17–28.

233. Chu Y, Yao PY, Wang W, Wang D, Wang Z, Zhang L, et al. Aurora B kinase activation requires survivin priming phosphorylation by PLK1. J Mol Cell Biol. 2011;3(4):260–7.

234. Altieri DC. Survivin - The inconvenient IAP. Semin Cell Dev Biol. 2015;39:91–6.

235. Wang H, Holloway MP, Ma L, Cooper ZA, Riolo M, Samkari A, et al. Acetylation directs survivin nuclear localization to repress STAT3 oncogenic activity. J Biol Chem. 2010;285(46):36129–37.

236. Altieri DC. New wirings in the survivin networks. Oncogene. 2008;27(48):6276–84.

237. Vong QP, Cao K, Li HY, Iglesias PA, Zheng Y. Chromosome alignment and segregation regulated by ubiquitination of survivin. Science. 2005;310(5753):1499–504.

238. Kondapuram SK, Ramachandran HK, Arya H, Coumar MS. Targeting survivin for cancer therapy: Strategies, small molecule inhibitors and vaccine based therapeutics in development. Life Sci. 2023;335:122260.

239. Martínez-Sifuentes MA, Bassol-Mayagoitia S, Nava-Hernández MP, Ruiz-Flores P, Ramos-Treviño J, Haro-Santa Cruz J, et al. Survivin in Breast Cancer: A Review. Genet Test Mol Biomarkers. 2022;26(9):411–21.

240. Gasowska-Bajger B, Gasowska-Bodnar A, Knapp P, Bodnar L. Prognostic Significance of Survivin Expression in Patients with Ovarian Carcinoma: A Meta-Analysis. J Clin Med. 2021;10(4):1–15.

241. Mahmoudian-Sani MR, Alghasi A, Saeedi-Boroujeni A, Jalali A, Jamshidi M, Khodadadi A. Survivin as a diagnostic and therapeutic marker for thyroid cancer. Pathol Res Pract. 2019;215(4):619–25.

242. Uhlén M, Fagerberg L, Hallström BM, Lindskog C, Oksvold P, Mardinoglu A, et al. Proteomics. Tissue-based map of the human proteome. Science. 2015;347(6220):1260419.

243. The Human Protein Atlas [Homepage]. Stockholm, Sweden: The Human Protein Atlas; [accessed 2024 Oct 31]. BIRC5 [4 screens]. Available from: https://www.proteinatlas.org/ENSG00000089685-BIRC5

244. Velculescu VE, Madden SL, Zhang L, Lash AE, Yu J, Rago C, et al. Analysis of human transcriptomes. Nat Genet. 1999;23(4):387–8.

245. Siffroi-Fernandez S, Dulong S, Li XM, Filipski E, Grećhez-Cassiau A, Peteri-Bruñback B, et al. Functional genomics identify Birc5/survivin as a candidate gene involved in the chronotoxicity of cyclin-dependent kinase inhibitors. Cell Cycle. 2014;13(6):984–91.

246. Antonacopoulou AG, Floratou K, Bravou V, Kottorou A, Dimitrakopoulos FI, Marousi S, et al. The survivin -31 snp in human colorectal cancer correlates with survivin splice variant expression and improved overall survival. Cellular oncology. 2011;34(4):381–91.

247. Bogdanovic L, Lazic M, Bogdanovic J, Soldatovic I, Nikolic N, Radunovic M, et al. Polymorphisms of survivin -31 G/C gene are associated with risk of urothelial carcinoma in Serbian population. Journal of BUON. 2017;22(1):270–7.

248. Weng CJ, Hsieh YH, Chen MK, Tsai CM, Lin CW, Yang SF. Survivin SNP-carcinogen interactions in oral cancer. J Dent Res. 2012;91(4):358–63.

249. Kostić M, Nikolić N, Ilić B, Čarkić J, Milenković S, Vukadinović M. Analysis of polymorphism in the survivin gene promoter as a potential risk factor for head and neck cancers development. Srp Arh Celok Lek. 2013;141(5–6):304–7.

250. Bayram S, Akkiz H, Bekar A, Akgöllü E. The association between the survivin -31G/C promoter polymorphism and hepatocellular carcinoma risk in a Turkish population. Cancer Epidemiol. 2011;35(6):555–9.

251. Hagenbuchner J, Kuznetsov A V., Obexer P, Ausserlechner MJ. BIRC5/Survivin enhances aerobic glycolysis and drug resistance by altered regulation of the mitochondrial fusion/fission machinery. Oncogene. 2013;32(40):4748–57.

252. Cheung CHA, Cheng LT, Chang KY, Chen HH, Chang JY. Investigations of survivin: the past, present and future. Front Biosci. 2011;16(3):952–61.

253. Fernández JG, Rodríguez DA, Valenzuela M, Calderon C, Urzúa U, Munroe D, et al. Survivin expression promotes VEGF-induced tumor angiogenesis via PI3K/Akt enhanced β-catenin/Tcf-Lef dependent transcription. Mol Cancer. 2014;13(1):209.

254. Humphry NJ, Wheatley SP. Survivin inhibits excessive autophagy in cancer cells but does so independently of its interaction with LC3. Biol Open. 2018;7(10):bio037374.

255. Zhang L, Zhang W, Wang YF, Liu B, Zhang WF, Zhao YF, et al. Dual induction of apoptotic and autophagic cell death by targeting survivin in head neck squamous cell carcinoma. Cell Death Dis. 2015;6(5):e1771.

256. Li F, Ambrosini G, Chu EY, Plescia J, Tognin S, Marchisio PC, et al. Control of apoptosis and mitotic spindle checkpoint by survivin. Nature. 1998;396(6711):580–4.

257. Zaffaroni N, Pennati M, Colella G, Perego P, Supino R, Gatti L, et al. Expression of the anti-apoptotic gene survivin correlates with taxol resistance in human ovarian cancer. Cell Mol Life Sci. 2002;59(8):1406–12.

258. Zhang M, Mukherjee N, Bermudez RS, Latham DE, Delaney MA, Zietman AL, et al. Adenovirus-mediated inhibition of survivin expression sensitizes human prostate cancer cells to paclitaxel in vitro and in vivo. Prostate. 2005;64(3):293–302.

259. Ling X, Bernacki RJ, Brattain MG, Li F. Induction of survivin expression by taxol (paclitaxel) is an early event, which is independent of taxol-mediated G2/M arrest. J Biol Chem. 2004;279(15):15196–203.

260. Gerber HP, McMurtrey A, Kowalski J, Yan M, Keyt BA, Dixit V, et al. Vascular endothelial growth factor regulates endothelial cell survival through the phosphatidylinositol 3'-kinase/Akt signal transduction pathway. Requirement for Flk-1/KDR activation. J Biol Chem. 1998;273(46):30336–43.

261. Tran J, Rak J, Sheehan C, Saibil SD, Lacasse E, Korneluk RG, et al. Marked induction of the IAP family antiapoptotic proteins survivin and XIAP by VEGF in vascular endothelial cells. Biochem Biophys Res Commun. 1999;264(3):781–8.

262. Tran J, Master Z, Yu JL, Rak J, Dumont DJ, Kerbel RS. A role for survivin in chemoresistance of endothelial cells mediated by VEGF. Proc Natl Acad Sci U S A. 2002;99(7):4349–54.

263. Nomura T, Yamasaki M, Nomura Y, Mimata H. Expression of the inhibitors of apoptosis proteins in cisplatin-resistant prostate cancer cells. Oncol Rep. 2005;14(4):993–7.

264. Van Geelen CMM, De Vries EGE, De Jong S. Lessons from TRAIL-resistance mechanisms in colorectal cancer cells: paving the road to patient-tailored therapy. Drug Resist Updat. 2004;7(6):345–58.

265. Tirrò E, Consoli ML, Massimino M, Manzella L, Frasca F, Sciacca L, et al. Altered expression of c-IAP1, survivin, and Smac contributes to chemotherapy resistance in thyroid cancer cells. Cancer Res. 2006;66(8):4263–72.

266. Wang L, Zhang GM, Feng ZH. Down-regulation of survivin expression reversed multidrug resistance in adriamycin-resistant HL-60/ADR cell line. Acta Pharmacol Sin. 2003;24(12):1235–40.

267. Zhang M, Latham DE, Delaney MA, Chakravarti A. Survivin mediates resistance to antiandrogen therapy in prostate cancer. Oncogene. 2005;24(15):2474–82.

268. Asanuma K, Moriai R, Yajima T, Yagihashi A, Yamada M, Kobayashi D, et al. Survivin as a radioresistance factor in pancreatic cancer. Jpn J Cancer Res. 2000;91(11):1204–9.

269. Rödel F, Hoffmann J, Distel L, Herrmann M, Noisternig T, Papadopoulos T, et al. Survivin as a radioresistance factor, and prognostic and therapeutic target for radiotherapy in rectal cancer. Cancer Res. 2005;65(11):4881–7.

270. Nakahara T, Takeuchi M, Kinoyama I, Minematsu T, Shirasuna K, Matsuhisa A, et al. YM155, a novel small-molecule survivin suppressant, induces regression

of established human hormone-refractory prostate tumor xenografts. Cancer Res. 2007;67(17):8014–21.

271. Nakahara T, Kita A, Yamanaka K, Mori M, Amino N, Takeuchi M, et al. Broad spectrum and potent antitumor activities of YM155, a novel small-molecule survivin suppressant, in a wide variety of human cancer cell lines and xenograft models. Cancer Sci. 2011;102(3):614–21.

272. Tolcher AW, Mita A, Lewis LD, Garrett CR, Till E, Daud AI, et al. Phase I and pharmacokinetic study of YM155, a small-molecule inhibitor of survivin. J Clin Oncol. 2008;26(32):5198–203.

273. Giaccone G, Zatloukal P, Roubec J, Floor K, Musil J, Kuta M, et al. Multicenter phase II trial of YM155, a small-molecule suppressor of survivin, in patients with advanced, refractory, non-small-cell lung cancer. J Clin Oncol. 2009;27(27):4481–6.

274. Kelly RJ, Thomas A, Rajan A, Chun G, Lopez-Chavez A, Szabo E, et al. A phase I/II study of sepantronium bromide (YM155, survivin suppressor) with paclitaxel and carboplatin in patients with advanced non-small-cell lung cancer. Ann Oncol. 2013;24(10):2601–6.

275. Tang H, Shao H, Yu C, Hou J. Mcl-1 downregulation by YM155 contributes to its synergistic anti-tumor activities with ABT-263. Biochem Pharmacol. 2011;82(9):1066–72.

276. Glaros TG, Stockwin LH, Mullendore ME, Smith B, Morrison BL, Newton DL. The “survivin suppressants” NSC 80467 and YM155 induce a DNA damage response. Cancer Chemother Pharmacol. 2012;70(1):207–12.

277. Na YS, Yang SJ, Kim SM, Jung KA, Moon JH, Shin JS, et al. YM155 induces EGFR suppression in pancreatic cancer cells. PLoS One. 2012;7(6):e38625.

278. Hong M, Ren MQ, Silva J, Paul A, Wilson WD, Schroeder C, et al. YM155 inhibits topoisomerase function. Anticancer Drugs. 2017;28(2):142–52.

279. Mackay RP, Weinberger PM, Copland JA, Mahdavian E, Xu Q. YM155 Induces DNA Damage and Cell Death in Anaplastic Thyroid Cancer Cells by Inhibiting DNA Topoisomerase IIα at the ATP-Binding Site. Mol Cancer Ther. 2022;21(6):925–35.

280. Ling X, Cao S, Cheng Q, Keefe JT, Rustum YM, Li F. A novel small molecule FL118 that selectively inhibits survivin, Mcl-1, XIAP and cIAP2 in a p53-independent manner, shows superior antitumor activity. PLoS One. 2012;7(9):e45571.

281. Ling X, Wu W, Aljahdali IAM, Liao J, Santha S, Fountzilas C, et al. FL118, acting as a “molecular glue degrader”, binds to dephosphorylates and degrades the oncoprotein DDX5 (p68) to control c-Myc, survivin and mutant Kras against

colorectal and pancreatic cancer with high efficacy. Clin Transl Med. 2022;12(5):e881.

282. Li F, Fountzilas C, Puzanov I, Attwood KM, Morrison C, Ling X. Multiple functions of the DEAD-box RNA helicase, DDX5 (p68), make DDX5 a superior oncogenic biomarker and target for targeted cancer therapy. Am J Cancer Res. 2021;11(10):5190–213.

283. Carrasco RA, Stamm NB, Marcusson E, Sandusky G, Iversen P, Patel BKR. Antisense inhibition of survivin expression as a cancer therapeutic. Mol Cancer Ther. 2011;10(2):221–32.

284. Erba HP, Sayar H, Juckett M, Lahn M, Andre V, Callies S, et al. Safety and pharmacokinetics of the antisense oligonucleotide (ASO) LY2181308 as a single-agent or in combination with idarubicin and cytarabine in patients with refractory or relapsed acute myeloid leukemia (AML). Invest New Drugs. 2013;31(4):1023–34.

285. Wiechno P, Somer BG, Mellado B, Chłosta PL, Cervera Grau JM, Castellano D, et al. A randomised phase 2 study combining LY2181308 sodium (survivin antisense oligonucleotide) with first-line docetaxel/prednisone in patients with castration-resistant prostate cancer. Eur Urol. 2014;65(3):516–20.

286. Hansen JB, Fisker N, Westergaard M, Kjærulff LS, Hansen HF, Thrue CA, et al. SPC3042: a proapoptotic survivin inhibitor. Mol Cancer Ther. 2008;7(9):2736–45.

287. Sapra P, Wang M, Bandaru R, Zhao H, Greenberger LM, Horak ID. Down-modulation of survivin expression and inhibition of tumor growth in vivo by EZN-3042, a locked nucleic acid antisense oligonucleotide. Nucleosides Nucleotides Nucleic Acids. 2010;29(2):97–112.

288. Raetz EA, Morrison D, Romanos-Sirakis E, Gaynon P, Sposto R, Bhojwani D, et al. A phase I study of EZN-3042, a novel survivin messenger ribonucleic acid (mRNA) antagonist, administered in combination with chemotherapy in children with relapsed acute lymphoblastic leukemia (ALL): a report from the therapeutic advances in childhood leukemia and lymphoma (TACL) consortium. J Pediatr Hematol Oncol. 2014;36(6):458–63.

289. Cruz RQ, Morais CM, Cardoso AM, Silva SG, Vale ML, Marques EF, et al. Enhancing glioblastoma cell sensitivity to chemotherapeutics: A strategy involving survivin gene silencing mediated by gemini surfactant-based complexes. Eur J Pharm Biopharm. 2016;104:7–18.

290. Lyu H, Wang S, Huang J, Wang B, He Z, Liu B. Survivin-targeting miR-542-3p overcomes HER3 signaling-induced chemoresistance and enhances the antitumor activity of paclitaxel against HER2-overexpressing breast cancer. Cancer Lett. 2018;420:97–108.

291. Morrish E, Brumatti G, Silke J. Future Therapeutic Directions for Smac-Mimetics. Cells. 2020;9(2):406.

292. Park SH, Shin I, Park SH, Kim ND, Shin I. An Inhibitor of the Interaction of Survivin with Smac in Mitochondria Promotes Apoptosis. Chem Asian J. 2019;14(22):4035–41.

293. Flygare JA, Beresini M, Budha N, Chan H, Chan IT, Cheeti S, et al. Discovery of a potent small-molecule antagonist of inhibitor of apoptosis (IAP) proteins and clinical candidate for the treatment of cancer (GDC-0152). J Med Chem. 2012;55(9):4101–13.

294. Chang YC, Cheung CHA. An Updated Review of Smac Mimetics, LCL161, Birinapant, and GDC-0152 in Cancer Treatment. Applied Sciences. 2021;11(1):335.

295. Johnson ML, Patel MR, Aljumaily R, Jones SF, Burris, HA, Spigel DR. A Phase Ib Dose-Escalation Study of LCL161 Plus Oral Topotecan for Patients With Relapsed/Refractory Small Cell Lung Cancer and Select Gynecologic Malignancies. Oncologist. 2023;28(7):640-e559.

296. Wadegaonkar VP, Wadegaonkar PA. Withanone as an inhibitor of survivin: a potential drug candidate for cancer therapy. J Biotechnol. 2013;168(2):229–33.

297. Widodo N, Priyandoko D, Shah N, Wadhwa R, Kaul SC. Selective killing of cancer cells by Ashwagandha leaf extract and its component Withanone involves ROS signaling. PLoS One. 2010;5(10):e13536.

298. Sattarinezhad E, Bordbar AK, Fani N. Virtual screening of Piperine analogs as Survivin inhibitors and their molecular interaction analysis by using consensus docking, MD simulation, MMPB/GBSA and alanine scanning techniques. J Biomol Struct Dyn. 2017;35(8):1824–32.

299. Yaffe PB, Power Coombs MR, Doucette CD, Walsh M, Hoskin DW. Piperine, an alkaloid from black pepper, inhibits growth of human colon cancer cells via G1 arrest and apoptosis triggered by endoplasmic reticulum stress. Mol Carcinog. 2015;54(10):1070–85.

300. Wang J, Li W. Discovery of novel second mitochondria-derived activator of caspase mimetics as selective inhibitor of apoptosis protein inhibitors. J Pharmacol Exp Ther. 2014;349(2):319–29.

301. Zhao G, Wang Q, Wu Z, Tian X, Yan H, Wang B, et al. Ovarian Primary and Metastatic Tumors Suppressed by Survivin Knockout or a Novel Survivin Inhibitor. Mol Cancer Ther. 2019;18(12):2233–45.

302. Karthika C, Sureshkumar R, Zehravi M, Akter R, Ali F, Ramproshad S, et al. Multidrug Resistance in Cancer Cells: Focus on a Possible Strategy Plan to Address Colon Carcinoma Cells. Life (Basel). 2022;12(6):811.

303. Amawi H, Sim HM, Tiwari AK, Ambudkar S V., Shukla S. ABC Transporter-Mediated Multidrug-Resistant Cancer. Adv Exp Med Biol. 2019;1141:549–80.

304. Lei ZN, Albadari N, Teng QX, Rahman H, Wang JQ, Wu Z, et al. ABCB1-dependent collateral sensitivity of multidrug-resistant colorectal cancer cells to the survivin inhibitor MX106-4C. Drug Resist Updat. 2024;73:101065.

305. Fortugno P, Beltrami E, Plescia J, Fontana J, Pradhan D, Marchisio PC, et al. Regulation of survivin function by Hsp90. Proc Natl Acad Sci U S A. 2003;100(24):13791–6.

306. Plescia J, Salz W, Xia F, Pennati M, Zaffaroni N, Daidone MG, et al. Rational design of shepherdin, a novel anticancer agent. Cancer Cell. 2005;7(5):457–68.

307. Venkatesan N, Kanwar JR, Deepa PR, Navaneethakrishnan S, Joseph C, Krishnakumar S. Targeting HSP90/Survivin using a cell permeable structure based peptido-mimetic shepherdin in retinoblastoma. Chem Biol Interact. 2016;252:141–9.

308. Meli M, Pennati M, Curto M, Daidone MG, Plescia J, Toba S, et al. Small-molecule targeting of heat shock protein 90 chaperone function: rational identification of a new anticancer lead. J Med Chem. 2006;49(26):7721–30.

309. Kubota H. Quality control against misfolded proteins in the cytosol: a network for cell survival. J Biochem. 2009;146(5):609–16.

310. Wendt MD, Sun C, Kunzer A, Sauer D, Sarris K, Hoff E, et al. Discovery of a novel small molecule binding site of human survivin. Bioorg Med Chem Lett. 2007;17(11):3122–9.

311. Galiger C, Zohora FT, Dorneburg C, Tews D, Debatin KM, Beltinger C. The survivin-ran inhibitor LLP-3 decreases oxidative phosphorylation, glycolysis and growth of neuroblastoma cells. BMC Cancer. 2023;23(1):1148.

312. Xia F, Canovas PM, Guadagno TM, Altieri DC. A survivin-ran complex regulates spindle formation in tumor cells. Mol Cell Biol. 2008;28(17):5299–311.

313. Guvenc H, Pavlyukov MS, Joshi K, Kurt H, Banasavadi-Siddegowda YK, Mao P, et al. Impairment of Glioma Stem Cell Survival and Growth by a Novel Inhibitor for Survivin–Ran Protein Complex. Clin Cancer Res. 2012;19(3):631-42.

314. Steigerwald C, Rasenberger B, Christmann M, Tomicic MT. Sensitization of colorectal cancer cells to irinotecan by the Survivin inhibitor LLP3 depends on

XAF1 proficiency in the context of mutated p53. Arch Toxicol. 2018;92(8):2645–8.

315. Qi J, Dong Z, Liu J, Peery RC, Zhang S, Liu JY, et al. Effective Targeting of the Survivin Dimerization Interface with Small-Molecule Inhibitors. Cancer Res. 2016;76(2):453–62.

316. Peery R, Kyei-Baffour K, Dong Z, Liu J, De Andrade Horn P, Dai M, et al. Synthesis and Identification of a Novel Lead Targeting Survivin Dimerization for Proteasome-Dependent Degradation. J Med Chem. 2020;63(13):7243–51.

317. Dorneburg C, Galiger C, Stadler GL, Westhoff MA, Rasche V, Barth TFE, et al. Inhibition of Survivin Homodimerization Decreases Neuroblastoma Cell Growth. Cancers (Basel). 2023;15(24):5775.

318. Peery R, Cui Q, Kyei-Baffour K, Josephraj S, Huang C, Dong Z, et al. A novel survivin dimerization inhibitor without a labile hydrazone linker induces spontaneous apoptosis and synergizes with docetaxel in prostate cancer cells. Bioorg Med Chem. 2022;65:116761.

319. Altieri DC. The case for survivin as a regulator of microtubule dynamics and cell-death decisions. Curr Opin Cell Biol. 2006;18(6):609–15.

320. Sarvagalla S, Cheung CHA, Tsai JY, Hsieh HP, Coumar MS. Disruption of protein–protein interactions: hot spot detection, structure-based virtual screening and in vitro testing for the anti-cancer drug target – survivin. RSC Adv. 2016;6(38):31947–59.

321. Berezov A, Cai Z, Freudenberg JA, Zhang H, Cheng X, Thompson T, et al. Disabling the mitotic spindle and tumor growth by targeting a cavity-induced allosteric site of survivin. Oncogene. 2012;31(15):1938–48.

322. Li F, Aljahdali I, Ling X. Cancer therapeutics using survivin BIRC5 as a target: what can we do after over two decades of study? J Exp Clin Cancer Res. 2019;38(1):368.

323. Brun SN, Markant SL, Esparza LA, Garcia G, Terry D, Huang JM, et al. Survivin as a therapeutic target in Sonic hedgehog-driven medulloblastoma. Oncogene. 2015;34(29):3770–9.

324. Anandharaj A, Cinghu S, Park WY. Rapamycin-mediated mTOR inhibition attenuates survivin and sensitizes glioblastoma cells to radiation therapy. Acta Biochim Biophys Sin (Shanghai). 2011;43(4):292–300.

325. Guha M, Plescia J, Leav I, Li J, Languino LR, Altieri DC. Endogenous tumor suppression mediated by PTEN involves survivin gene silencing. Cancer Res. 2009;69(12):4954–8.

326. Li W, Wang H, Kuang CY, Zhu JK, Yu Y, Qin ZX, et al. An essential role for the Id1/PI3K/Akt/NFkB/survivin signalling pathway in promoting the proliferation

of endothelial progenitor cells in vitro. Mol Cell Biochem. 2012;363(1–2):135–45.

327. Khan Z, Khan AA, Yadav H, Prasad GBKS, Bisen PS. Survivin, a molecular target for therapeutic interventions in squamous cell carcinoma. Cell Mol Biol Lett. 2017;22:8.

328. Peng XH, Karna P, Cao Z, Jiang BH, Zhou M, Yang L. Cross-talk between epidermal growth factor receptor and hypoxia-inducible factor-1alpha signal pathways increases resistance to apoptosis by up-regulating survivin gene expression. J Biol Chem. 2006;281(36):25903–14.

329. Xia W, Bisi J, Strum J, Liu L, Carrick K, Graham KM, et al. Regulation of survivin by ErbB2 signaling: therapeutic implications for ErbB2-overexpressing breast cancers. Cancer Res. 2006;66(3):1640–7.

330. Zhu H, Wang Q, Hu C, Zhang W, Quan L, Liu M, et al. High expression of survivin predicts poor prognosis in esophageal squamous cell carcinoma following radiotherapy. Tumour Biol. 2011;32(6):1147–53.

331. Zhou C, Qiu L, Sun Y, Helaley S, Wanebo H, Kouttab N, et al. Inhibition of EGFR/PI3K/AKT cell survival pathway promotes TSA's effect on cell death and migration in human ovarian cancer cells - PubMed. Int J Oncol. 2006;29(1):269–78.

332. Hakonen E, Ustinov J, Palgi J, Miettinen PJ, Otonkoski T. EGFR signaling promotes β-cell proliferation and survivin expression during pregnancy. PLoS One. 2014;9(4):e93651.

333. Belyanskaya LL, Hopkins-Donaldson S, Kurtz S, Simões-Wüst AP, Yousefi S, Simon HU, et al. Cisplatin activates Akt in small cell lung cancer cells and attenuates apoptosis by survivin upregulation. Int J Cancer. 2005;117(5):755–63.

334. Roca H, Varsos Z, Pienta KJ. CCL2 protects prostate cancer PC3 cells from autophagic death via phosphatidylinositol 3-kinase/AKT-dependent survivin up-regulation. J Biol Chem. 2008;283(36):25057–73.

335. Siddiqa A, Long LM, Li L, Marciniak RA, Kazhdan I. Expression of HER-2 in MCF-7 breast cancer cells modulates anti-apoptotic proteins Survivin and Bcl-2 via the extracellular signal-related kinase (ERK) and phosphoinositide-3 kinase (PI3K) signalling pathways. BMC Cancer. 2008;8:129.

336. Wang J, Yang L, Yang J, Kuropatwinski K, Wang W, Liu XQ, et al. Transforming growth factor beta induces apoptosis through repressing the phosphoinositide 3-kinase/AKT/survivin pathway in colon cancer cells. Cancer Res. 2008;68(9):3152–60.

337. Sommer KW, Schamberger CJ, Schmidt GE, Sasgary S, Cerni C. Inhibitor of apoptosis protein (IAP) survivin is upregulated by oncogenic c-H-Ras. Oncogene. 2003;22(27):4266–80.

338. Lauder SN, Smart K, Kersemans V, Allen D, Scott J, Pires A, et al. Enhanced antitumor immunity through sequential targeting of PI3Kδ and LAG3. J Immunother Cancer. 2020;8(2):e000693.

339. Wei Y, Ke W, Lu Z, Ren Y. PI3K δ inhibitor PI-3065 induces apoptosis in hepatocellular carcinoma cells by targeting survivin. Chem Biol Interact. 2023;371:110343.

340. Wang SP, Hsu YP, Chang CJ, Chan YC, Chen CH, Wang RH, et al. A novel EGFR inhibitor suppresses survivin expression and tumor growth in human gefitinib-resistant EGFR-wild type and -T790M non-small cell lung cancer. Biochem Pharmacol. 2021;193:114792.

341. Agarwal E, Chaudhuri A, Leiphrakpam PD, Haferbier KL, Brattain MG, Chowdhury S. Akt inhibitor MK-2206 promotes anti-tumor activity and cell death by modulation of AIF and Ezrin in colorectal cancer. BMC Cancer. 2014;14:145.

342. Strömberg T, Dimberg A, Hammarberg A, Carlson K, Österborg A, Nilsson K, et al. Rapamycin sensitizes multiple myeloma cells to apoptosis induced by dexamethasone. Blood. 2004;103(8):3138–47.

343. Zhu L, Fukuda S, Cordis G, Das DK, Maulik N. Anti-apoptotic protein survivin plays a significant role in tubular morphogenesis of human coronary arteriolar endothelial cells by hypoxic preconditioning. FEBS Lett. 2001;508(3):369–74.

344. Lin J, Hsiao PW, Chiu TH, Chao JI. Combination of cyclooxygenase-2 inhibitors and oxaliplatin increases the growth inhibition and death in human colon cancer cells. Biochem Pharmacol. 2005;70(5):658–67.

345. Yu ZW, Zhang N, Jiang CY, Wu SX, Feng XY, Feng XY. Exploring the genes involved in biosynthesis of dihydroquercetin and dihydromyricetin in Ampelopsis grossedentata. Sci Rep. 2021;11(1):15596.

346. Hwang KE, Na KS, Park DS, Choi KH, Kim BR, Shim H, et al. Apoptotic induction by simvastatin in human lung cancer A549 cells via Akt signaling dependent down-regulation of survivin. Invest New Drugs. 2011;29(5):945–52.

347. Tang C, Luo H, Luo D, Yang H, Zhou X. Src homology phosphotyrosyl phosphatase 2 mediates cisplatin-related drug resistance by inhibiting apoptosis and activating the Ras/PI3K/Akt1/survivin pathway in lung cancer cells. Oncol Rep. 2018;39(2):611–8.

348. Jin Q, Feng L, Behrens C, Bekele BN, Wistuba II, Hong WK, et al. Implication of AMP-activated protein kinase and Akt-regulated survivin in lung cancer chemopreventive activities of deguelin. Cancer Res. 2007;67(24):11630–9.

349. Luo Z, Chen W, Wu W, Luo W, Zhu T, Guo G, et al. Metformin promotes survivin degradation through AMPK/PKA/GSK-3β-axis in non-small cell lung cancer. J Cell Biochem. 2019;120(7):11890–9.

350. Chang YX, Lin YF, Chen CL, Huang MS, Hsiao M, Liang PH. Chaperonin-Containing TCP-1 Promotes Cancer Chemoresistance and Metastasis through the AKT-GSK3β-β-Catenin and XIAP-Survivin Pathways. Cancers (Basel). 2020;12(12):1–25.

351. Rawlings JS, Rosler KM, Harrison DA. The JAK/STAT signaling pathway. J Cell Sci. 2004;117(Pt 8):1281–3.

352. Yu H, Jove R. The STATs of cancer--new molecular targets come of age. Nat Rev Cancer. 2004;4(2):97–105.

353. Gritsko T, Williams A, Turkson J, Kaneko S, Bowman T, Huang M, et al. Persistent activation of stat3 signaling induces survivin gene expression and confers resistance to apoptosis in human breast cancer cells. Clin Cancer Res. 2006;12(1):11–9.

354. Stella S, Tirrò E, Conte E, Stagno F, Di Raimondo F, Manzella L, et al. Suppression of survivin induced by a BCR-ABL/JAK2/STAT3 pathway sensitizes imatinib-resistant CML cells to different cytotoxic drugs. Mol Cancer Ther. 2013;12(6):1085–98.

355. Aoki Y, Feldman GM, Tosato G. Inhibition of STAT3 signaling induces apoptosis and decreases survivin expression in primary effusion lymphoma. Blood. 2003;101(4):1535–42.

356. Raut PK, Lee HS, Joo SH, Chun KS. Thymoquinone induces oxidative stress-mediated apoptosis through downregulation of Jak2/STAT3 signaling pathway in human melanoma cells. Food Chem Toxicol. 2021;157:112604.

357. Duan Z, Bradner JE, Greenberg E, Levine R, Foster R, Mahoney J, et al. SD-1029 inhibits signal transducer and activator of transcription 3 nuclear translocation. Clin Cancer Res. 2006;12(22):6844–52.

358. Wang H qin, Jin J jun, Wang J. Arctigenin enhances chemosensitivity to cisplatin in human nonsmall lung cancer H460 cells through downregulation of survivin expression. J Biochem Mol Toxicol. 2014;28(1):39–45.

359. Srirangam A, Milani M, Mitra R, Guo Z, Rodriguez M, Kathuria H, et al. The human immunodeficiency virus protease inhibitor ritonavir inhibits lung cancer cells, in part, by inhibition of survivin. J Thorac Oncol. 2011;6(4):661–70.

360. Martínez-García D, Pérez-Hernández M, Korrodi-Gregório L, Quesada R, Ramos R, Baixeras N, et al. The Natural-Based Antitumor Compound T21 Decreases Survivin Levels through Potent STAT3 Inhibition in Lung Cancer Models. Biomolecules. 2019;9(8):361.

361. Burotto M, Chiou VL, Lee JM, Kohn EC. The MAPK pathway across different malignancies: a new perspective. Cancer. 2014;120(22):3446–56.

362. Bahar ME, Kim HJ, Kim DR. Targeting the RAS/RAF/MAPK pathway for cancer therapy: from mechanism to clinical studies. Signal Transduct Target Ther. 2023;8(1):455.

363. Wang H, Gambosova K, Cooper ZA, Holloway MP, Kassai A, Izquierdo D, et al. EGF regulates survivin stability through the Raf-1/ERK pathway in insulin-secreting pancreatic β-cells. BMC Mol Biol. 2010;11:66.

364. Carter BZ, Mak DH, Schober WD, Cabreira-Hansen M, Beran M, McQueen T, et al. Regulation of survivin expression through Bcr-Abl/MAPK cascade: targeting survivin overcomes imatinib resistance and increases imatinib sensitivity in imatinib-responsive CML cells. Blood. 2006;107(4):1555–63.

365. O'Connor DS, Grossman D, Plescia J, Li F, Zhang H, Villa A, et al. Regulation of apoptosis at cell division by p34cdc2 phosphorylation of survivin. Proc Natl Acad Sci U S A. 2000;97(24):13103–7.

366. Mobahat M, Narendran A, Riabowol K. Survivin as a preferential target for cancer therapy. Int J Mol Sci. 2014;15(2):2494–516.

367. Kang X, Chen H, Zhou Z, Tu S, Cui B, Li Y, et al. Targeting Cyclin-Dependent Kinase 1 Induces Apoptosis and Cell Cycle Arrest of Activated Hepatic Stellate Cells. Adv Biol. 2024;8(3):e2300403.

368. Wall NR, O'Connor DS, Plescia J, Pommier Y, Altieri DC. Suppression of survivin phosphorylation on Thr34 by flavopiridol enhances tumor cell apoptosis. Cancer Res. 2003;63(1):230–5.

369. Bible KC, Peethambaram PP, Oberg AL, Maples W, Groteluschen DL, Boente M, et al. A phase 2 trial of flavopiridol (Alvocidib) and cisplatin in platin-resistant ovarian and primary peritoneal carcinoma: MC0261. Gynecol Oncol. 2012;127(1):55–62.

370. Pennati M, Campbell AJ, Curto M, Binda M, Cheng YZ, Wang LZ, et al. Potentiation of paclitaxel-induced apoptosis by the novel cyclin-dependent kinase inhibitor NU6140: a possible role for survivin down-regulation. Mol Cancer Ther. 2005;4(9):1328–37.

371. Hsiao CJ, Hsiao G, Chen WL, Wang SW, Chiang CP, Liu LY, et al. Cephalochromin induces G0/G1 cell cycle arrest and apoptosis in A549 human non-small-cell

lung cancer cells by inflicting mitochondrial disruption. J Nat Prod. 2014;77(4):758–65.

372. Oh TI, Lee YM, Nam TJ, Ko YS, Mah S, Kim J, et al. Fascaplysin Exerts Anti-Cancer Effects through the Downregulation of Survivin and HIF-1α and Inhibition of VEGFR2 and TRKA. Int J Mol Sci. 2017;18(10):2074.

373. Cuadrado A, Nebreda AR. Mechanisms and functions of p38 MAPK signalling. Biochem J. 2010;429(3):403–17.

374. Sato A, Mizobuchi Y, Nakajima K, Shono K, Fujihara T, Kageji T, et al. Blocking COX-2 induces apoptosis and inhibits cell proliferation via the Akt/survivin- and Akt/ID3 pathway in low-grade-glioma. J Neurooncol. 2017;132(2):231–8.

375. Liu HF, Hu HC, Chao JI. Oxaliplatin down-regulates survivin by p38 MAP kinase and proteasome in human colon cancer cells. Chem Biol Interact. 2010;188(3):535–45.

376. Rauch A, Carlstedt A, Emmerich C, Mustafa AHM, Göder A, Knauer SK, et al. Survivin antagonizes chemotherapy-induced cell death of colorectal cancer cells. Oncotarget. 2018;9(45):27835–50.

377. Colak S, ten Dijke P. Targeting TGF-β Signaling in Cancer. Trends Cancer. 2017;3(1):56–71.

378. Chowdhury S, Howell GM, Rajput A, Teggart CA, Brattain LE, Weber HR, et al. Identification of a novel TGFβ/PKA signaling transduceome in mediating control of cell survival and metastasis in colon cancer. PLoS One. 2011;6(5):e19335.

379. Marwitz S, Turkowski K, Nitschkowski D, Weigert A, Brandenburg J, Reiling N, et al. The Multi-Modal Effect of the Anti-fibrotic Drug Pirfenidone on NSCLC. Front Oncol. 2020;9:1550.

380. You L, He B, Xu Z, Uematsu K, Mazieres J, Mikami I, et al. Inhibition of Wnt-2-mediated signaling induces programmed cell death in non-small-cell lung cancer cells. Oncogene. 2004;23(36):6170–4.

381. Kim PJ, Plescia J, Clevers H, Fearon ER, Altieri DC. Survivin and molecular pathogenesis of colorectal cancer. Lancet. 2003;362(9379):205–9.

382. Zhu H, Zhang G, Wang Y, Xu N, He S, Zhang W, et al. Inhibition of ErbB2 by Herceptin reduces survivin expression via the ErbB2-beta-catenin/TCF4-survivin pathway in ErbB2-overexpressed breast cancer cells. Cancer Sci. 2010;101(5):1156–62.

383. Emami KH, Nguyen C, Ma H, Kim DH, Jeong KW, Eguchi M, et al. A small molecule inhibitor of beta-catenin/CREB-binding protein transcription [corrected]. Proc Natl Acad Sci U S A. 2004;101(34):12682–7.

384. Or CHR, Huang CW, Chang CC, Lai YC, Chen YJ, Chang CC. Obatoclax, a Pan-BCL-2 Inhibitor, Downregulates Survivin to Induce Apoptosis in Human Colorectal Carcinoma Cells Via Suppressing WNT/β-catenin Signaling. Int J Mol Sci. 2020;21(5):1773.

385. Li L, Tang P, Li S, Qin X, Yang H, Wu C, et al. Notch signaling pathway networks in cancer metastasis: a new target for cancer therapy. Med Oncol. 2017;34(10):180.

386. Palazzo E, Morandi P, Lotti R, Saltari A, Truzzi F, Schnebert S, et al. Notch Cooperates with Survivin to Maintain Stemness and to Stimulate Proliferation in Human Keratinocytes during Ageing. Int J Mol Sci. 2015;16(11):26291–302.

387. Chen Y, Li D, Liu H, Xu H, Zheng H, Qian F, et al. Notch-1 signaling facilitates survivin expression in human non-small cell lung cancer cells. Cancer Biol Ther. 2011;11(1):14–21.

388. Liu R, Mitchell DA. Survivin as an immunotherapeutic target for adult and pediatric malignant brain tumors. Cancer Immunol Immunother. 2010;59(2):183–93.

389. Hirohashi Y, Torigoe T, Maeda A, Nabeta Y, Kamiguchi K, Sato T, et al. An HLA-A24-restricted cytotoxic T lymphocyte epitope of a tumor-associated protein, survivin. Clinical cancer research. 2002;8(6):1731–9.

390. Tsuruma T, Iwayama Y, Ohmura T, Katsuramaki T, Hata F, Furuhata T, et al. Clinical and immunological evaluation of anti-apoptosis protein, survivin-derived peptide vaccine in phase I clinical study for patients with advanced or recurrent breast cancer. J Transl Med. 2008;6:24.

391. Villella JA, Wilson MK, Berinstein NL, Brown J, Lheureux S, Butler MO, et al. Safety, immunogenicity, and clinical activity of the immunotherapeutic vaccine, DPX-Survivac, in a Phase 1/1b trial of women with ovarian, fallopian tube, or peritoneal cancer. Journal of Clinical Oncology. 2015;33:3072.

392. National Library of Medicine [Homepage]. Bethesda, MD, USA: National Institutes of Health; [updated 2024 Aug 5; accessed 2024 Nov 4]. Multiple Myeloma Trial of Orally Administered Salmonella Based Survivin Vaccine [15 screens]. Available from: https://www.clinicaltrials.gov/study/NCT03762291?term=NCT03762291&rank=1

393. Li Y, Lu W, Yang J, Edwards M, Jiang S. Survivin as a biological biomarker for diagnosis and therapy. Expert Opin Biol Ther. 2021;21(11):1429–41.

394. Jin MZ, Jin WL. The updated landscape of tumor microenvironment and drug repurposing. Signal Transduct Target Ther. 2020;5(1):166.

395. Pushpakom S, Iorio F, Eyers PA, Escott KJ, Hopper S, Wells A, et al. Drug repurposing: progress, challenges and recommendations. Nat Rev Drug Discov. 2019;18(1):41–58.

396. Dalwadi SM, Hunt A, Bonnen MD, Ghebre YT. Computational approaches for drug repurposing in oncology: untapped opportunity for high value innovation. Front Oncol. 2023;13:1198284.

397. Irwin JJ, Sterling T, Mysinger MM, Bolstad ES, Coleman RG. ZINC: a free tool to discover chemistry for biology. J Chem Inf Model. 2012;52(7):1757–68.

398. Wishart DS, Knox C, Guo AC, Shrivastava S, Hassanali M, Stothard P, et al. DrugBank: a comprehensive resource for in silico drug discovery and exploration. Nucleic Acids Res. 2006;34(Database issue).

399. National Center for Biotechnology Information [Homepage]. Bethesda, MD, USA: National Library of Medicine; [accessed 2024 Nov 5]. Asenapine Maleate [31 screens]. Available from: https://pubchem.ncbi.nlm.nih.gov/compound/6917875

400. European Medicines Agency [Homepage]. Amsterdam, Netherlands: European Medicines Agency; [updated 2022 Dec 7; accessed 2024 Nov 5]. Sycrest (8 screens). Available from: https://www.ema.europa.eu/en/medicines/human/EPAR/sycrest

401. Drugs.com [Homepage]. New York, NY: Drugs.com; [accessed 2024 Nov 5]. Asenapine Side Effects: Common, Severe, Long Term [8 screens]. Available from: https://www.drugs.com/sfx/asenapine-side-effects.html

402. DrugBank [Homepage]. London, Canada: DrugBank Online; [accessed 2024 Nov 5]. Asenapine: Uses, Interactions, Mechanism of Action [26 screens]. Available from: https://go.drugbank.com/drugs/DB06216

403. Niedzialkowska E, Wang F, Porebski PJ, Minor W, Higgins JMG, Stukenberga PT. A Highlights from MBoC Selection: Molecular basis for phosphospecific recognition of histone H3 tails by Survivin paralogues at inner centromeres. Mol Biol Cell. 2012;23(8):1457.

404. Le Guilloux V, Schmidtke P, Tuffery P. Fpocket: an open source platform for ligand pocket detection. BMC Bioinformatics. 2009;10:168.

405. Office of Research of Boston University [Homepage]. Boston, MA: Boston University; [updated 2024 May 3; accessed 2024 Dec 13]. Sample Size Calculations (IACUC) [11 screens]. Available from: https://www.bu.edu/research/forms-policies/iacuc-sample-size-calculations/

406. Leiter A, Veluswamy RR, Wisnivesky JP. The global burden of lung cancer: current status and future trends. Nature Reviews Clinical Oncology 2023 20:9. 2023;20(9):624–39.

407. Zhao J, Tenev T, Martins LM, Downward J, Lemoine NR. The ubiquitin-proteasome pathway regulates survivin degradation in a cell cycle-dependent manner. J Cell Sci. 2000;113 Pt 23(23):4363–71.

408. Tamm I, Wang Y, Sausville E, Scudiero DA, Vigna N, Oltersdorft T, et al. IAP-family protein survivin inhibits caspase activity and apoptosis induced by Fas (CD95), Bax, caspases, and anticancer drugs. Cancer Res. 1998;58(23):5315–20.

409. Zhang K, Zhang K, Li Y, Liu W, Gao X. Silencing survivin expression inhibits the tumor growth of non-small-cell lung cancer cells in vitro and in vivo. Mol Med Rep. 2015;11(1):639–44.

410. Liu S, Huang W, Jin MJ, Fan B, Xia GM, Gao ZG. Inhibition of murine breast cancer growth and metastasis by survivin-targeted siRNA using disulfide cross-linked linear PEI. Eur J Pharm Sci. 2016;82:171–82.

411. Passos Gibson V, Derbali RM, Phan HT, Tahiri H, Allen C, Hardy P, et al. Survivin silencing improved the cytotoxicity of carboplatin and melphalan in Y79 and primary retinoblastoma cells. Int J Pharm. 2020;589:119824.

412. Vivas-Mejia PE, Rodriguez-Aguayo C, Han HD, Shahzad MMK, Valiyeva F, Shibayama M, et al. Silencing survivin splice variant 2B leads to antitumor activity in taxane--resistant ovarian cancer. Clin Cancer Res. 2011;17(11):3716–26.

413. Ma S, Li X, Ran M, Ji M, Gou J, Yin T, et al. Fabricating nanoparticles co-loaded with survivin siRNA and Pt(IV) prodrug for the treatment of platinum-resistant lung cancer. Int J Pharm. 2021;601:120577.

414. Fung S, Knoefel WT, Krieg A. Clinicopathological and Prognostic Significance of Inhibitor of Apoptosis Protein (IAP) Family Members in Lung Cancer: A Meta-Analysis. Cancers (Basel). 2021;13(16):4098.

415. Pachimatla AG, Fenstermaker R, Ciesielski M, Yendamuri S. Survivin in lung cancer: a potential target for therapy and prevention—a narrative review. Transl Lung Cancer Res. 2024;13(2):362–74.

416. Chen P, Zhu J, Liu DY, Li HY, Xu N, Hou M. Over-expression of survivin and VEGF in small-cell lung cancer may predict the poorer prognosis. Med Oncol. 2014;31(1):775.

417. Falleni M, Pellegrini C, Marchetti A, Oprandi B, Buttitta F, Barassi F, et al. Survivin gene expression in early-stage non-small cell lung cancer. J Pathol. 2003;200(5):620–6.

418. Dong H, Qian D, Wang Y, Meng L, Chen D, Ji X, et al. Survivin expression and serum levels in pancreatic cancer. World J Surg Oncol. 2015;13:189.

419. Krieg A, Baseras B, Tomczak M, Verde PE, Stoecklein NH, Knoefel WT. Role of survivin as prognostic and clinicopathological marker in gastric cancer: a meta-analysis. Mol Biol Rep. 2013;40(9):5501–11.

420. Werner TA, Dizdar L, Nolten I, Riemer JC, Mersch S, Schütte SC, et al. Survivin and XIAP - two potential biological targets in follicular thyroid carcinoma. Sci Rep. 2017;7(1):11383.

421. He X, Yang K, Wang H, Chen X, Wu H, Yao L, et al. Expression and clinical significance of survivin in ovarian cancer: A meta-analysis. PLoS One. 2018;13(5):e0194463.

422. Yu J, Wang Z, Zhang H, Wang Y, Li DQ. Survivin-positive circulating tumor cells as a marker for metastasis of hepatocellular carcinoma. World J Gastroenterol. 2021;27(43):7546–62.

423. Liu HQ, Wang YH, Wang LL, Hao M. P16INK4A and survivin: Diagnostic and prognostic markers in cervical intraepithelial neoplasia and cervical squamous cell carcinoma. Exp Mol Pathol. 2015;99(1):44–9.

424. Nigam J, Chandra A, Kazmi HR, Singh A, Gupta V, Parmar D, et al. Expression of serum survivin protein in diagnosis and prognosis of gallbladder cancer: a comparative study. Med Oncol. 2014;31(9):1–5.

425. Zhang M, Zhang X, Zhao S, Wang Y, Di W, Zhao G, et al. Prognostic value of survivin and EGFR protein expression in triple-negative breast cancer (TNBC) patients. Target Oncol. 2014;9(4):349–57.

426. Xia H, Chen S, Huang H, Ma H. Survivin over-expression is correlated with a poor prognosis in esophageal cancer patients. Clin Chim Acta. 2015;446:82–5.

427. Li C, Li Z, Zhu M, Zhao T, Chen L, Ji W, et al. Clinicopathological and prognostic significance of survivin over-expression in patients with esophageal squamous cell carcinoma: a meta-analysis. PLoS One. 2012;7(9):e44764.

428. Yie S mian, Lou B, Ye S rong, He X, Cao M, Xie K, et al. Clinical significance of detecting survivin-expressing circulating cancer cells in patients with non-small cell lung cancer. Lung Cancer. 2009;63(2):284–90.

429. Lu J, Tang H, Chen L, Huang N, Hu G, Li C, et al. Association of survivin positive circulating tumor cell levels with immune escape and prognosis of osteosarcoma. J Cancer Res Clin Oncol. 2023;149(15):13741–51.

430. Qi G, Kudo Y, Ando T, Tsunematsu T, Shimizu N, Siriwardena SBSM, et al. Nuclear Survivin expression is correlated with malignant behaviors of head and neck cancer together with Aurora-B. Oral Oncol. 2010;46(4):263–70.

431. Skagias L, Politi E, Karameris A, Sambaziotis D, Archondakis A, Ntinis A, et al. Survivin expression as a strong indicator of recurrence in urothelial bladder cancer. Predictive value of nuclear versus cytoplasmic staining. Anticancer Res. 2009;29(10):4163–7.

432. Troiano G, Guida A, Aquino G, Botti G, Losito NS, Papagerakis S, et al. Integrative Histologic and Bioinformatics Analysis of BIRC5/Survivin Expression in Oral Squamous Cell Carcinoma. Int J Mol Sci. 2018;19(9):2664.

433. Krieg S, Roderburg C, Fung S, Luedde T, Knoefel WT, Krieg A. Nuclear survivin is a prognosticator in gastroenteropancreatic neuroendocrine neoplasms: a meta-analysis. J Cancer Res Clin Oncol. 2022;148(9):2235–46.

434. Zhou L, Lu J, Liang ZY, Zhou WX, Yuan D, Li BQ, et al. High nuclear Survivin expression as a poor prognostic marker in pancreatic ductal adenocarcinoma. J Surg Oncol. 2018;118(7):1115–21.

435. Hennigs JK, Minner S, Tennstedt P, Löser R, Huland H, Klose H, et al. Subcellular Compartmentalization of Survivin is Associated with Biological Aggressiveness and Prognosis in Prostate Cancer. Sci Rep. 2020;10(1):3250.

436. Rexhepaj E, Jirstrom K, O'Connor DP, O'Brien SL, Landberg G, Duffy MJ, et al. Validation of cytoplasmic-to-nuclear ratio of survivin as an indicator of improved prognosis in breast cancer. BMC Cancer. 2010;10:639.

437. Engels K, Knauer SK, Metzler D, Simf C, Struschka O, Bier C, et al. Dynamic intracellular survivin in oral squamous cell carcinoma: underlying molecular mechanism and potential as an early prognostic marker. J Pathol. 2007;211(5):532–40.

438. Okada E, Murai Y, Matsui K, Isizawa S, Cheng C, Masuda M, et al. Survivin expression in tumor cell nuclei is predictive of a favorable prognosis in gastric cancer patients. Cancer Lett. 2001;163(1):109–16.

439. Kennedy SM, O'Driscoll L, Purcell R, Fitz-Simons N, McDermott EW, Hill AD, et al. Prognostic importance of survivin in breast cancer. Br J Cancer. 2003;88(7):1077–83.

440. Serrano-López J, Serrano J, Figueroa V, Torres-Gomez A, Tabares S, Casaño J, et al. Cytoplasmic localization of wild-type survivin is associated with constitutive activation of the PI3K/Akt signaling pathway and represents a favorable prognostic factor in patients with acute myeloid leukemia. Haematologica. 2013;98(12):1877–85.

441. Rodel F, Sprenger T, Kaina B, Liersch T, Rodel C, Fulda S, et al. Survivin as a prognostic/predictive marker and molecular target in cancer therapy. Curr Med Chem. 2012;19(22):3679–88.

442. Warnecke-Eberz U, Hokita S, Xi H, Higashi H, Baldus SE, Metzger R, et al. Overexpression of survivin mRNA is associated with a favorable prognosis following neoadjuvant radiochemotherapy in esophageal cancer. Oncol Rep. 2005;13(6):1241–6.

443. Cho HJ, Kim HR, Park YS, Kim YH, Kim DK, Park S Il. Prognostic value of survivin expression in stage III non-small cell lung cancer patients treated with platinum-based therapy. Surg Oncol. 2015;24(4):329–34.

444. Zhou C, Zhu Y, Lu B, Zhao W, Zhao X. Survivin expression modulates the sensitivity of A549 lung cancer cells resistance to vincristine. Oncol Lett. 2018;16(4):5466–72.

445. Ning Y, Hanna DL, Zhang W, Mendez A, Yang D, El-Khoueiry R, et al. Cytokeratin-20 and Survivin-Expressing Circulating Tumor Cells Predict Survival in Metastatic Colorectal Cancer Patients by a Combined Immunomagnetic qRT-PCR Approach. Mol Cancer Ther. 2015;14(10):2401–8.

446. Gradilone A, Petracca A, Nicolazzo C, Gianni W, Cortesi E, Naso G, et al. Prognostic significance of survivin-expressing circulating tumour cells in T1G3 bladder cancer. BJU Int. 2010;106(5):710–5.

447. Bertazza L, Mocellin S, Marchet A, Pilati P, Gabrieli J, Scalerta R, et al. Survivin gene levels in the peripheral blood of patients with gastric cancer independently predict survival. J Transl Med. 2009;7:111.

448. Satoh T, Okamoto I, Miyazaki M, Morinaga R, Tsuya A, Hasegawa Y, et al. Phase I study of YM155, a novel survivin suppressant, in patients with advanced solid tumors. Clin Cancer Res. 2009;15(11):3872–80.

449. Clemens MR, Gladkov OA, Gartner E, Vladimirov V, Crown J, Steinberg J, et al. Phase II, multicenter, open-label, randomized study of YM155 plus docetaxel as first-line treatment in patients with HER2-negative metastatic breast cancer. Breast Cancer Res Treat. 2015;149(1):171–9.

450. Lewis KD, Samlowski W, Ward J, Catlett J, Cranmer L, Kirkwood J, et al. A multi-center phase II evaluation of the small molecule survivin suppressor YM155 in patients with unresectable stage III or IV melanoma. Invest New Drugs. 2011;29(1):161–6.

451. Tolcher AW, Quinn DI, Ferrari A, Ahmann F, Giaccone G, Drake T, et al. A phase II study of YM155, a novel small-molecule suppressor of survivin, in castration-resistant taxane-pretreated prostate cancer. Ann Oncol. 2012;23(4):968–73.

452. Shimizu T, Nishio K, Sakai K, Okamoto I, Okamoto K, Takeda M, et al. Phase I safety and pharmacokinetic study of YM155, a potent selective survivin inhibitor, in combination with erlotinib in patients with EGFR TKI refractory

advanced non-small cell lung cancer. Cancer Chemother Pharmacol. 2020;86(2):211–9.

453. Kudchadkar R, Ernst S, Chmielowski B, Redman BG, Steinberg J, Keating A, et al. A phase 2, multicenter, open-label study of sepantronium bromide (YM155) plus docetaxel in patients with stage III (unresectable) or stage IV melanoma. Cancer Med. 2015;4(5):643–50.

454. Cheson BD, Bartlett NL, Vose JM, Lopez-Hernandez A, Seiz AL, Keating AT, et al. A phase II study of the survivin suppressant YM155 in patients with refractory diffuse large B-cell lymphoma. Cancer. 2012;118(12):3128–34.

455. Papadopoulos KP, Lopez-Jimenez J, Smith SE, Steinberg J, Keating A, Sasse C, et al. A multicenter phase II study of sepantronium bromide (YM155) plus rituximab in patients with relapsed aggressive B-cell Non-Hodgkin lymphoma. Leuk Lymphoma. 2016;57(8):1848–55.

456. Tibes R, McDonagh KT, Lekakis L, Bogenberger JM, Kim S, Frazer N, et al. Phase I study of the novel Cdc2/CDK1 and AKT inhibitor terameprocol in patients with advanced leukemias. Invest New Drugs. 2015;33(2):389–96.

457. Khanna N, Dalby R, Tan M, Arnold S, Stern J, Frazer N. Phase I/II clinical safety studies of terameprocol vaginal ointment. Gynecol Oncol. 2007;107(3):554–62.

458. Grossman SA, Ye X, Peereboom D, Rosenfeld MR, Mikkelsen T, Supko JG, et al. Phase I study of terameprocol in patients with recurrent high-grade glioma. Neuro Oncol. 2012;14(4):511–7.

459. Fan G, Luo X, Shi Y, Wang Y, Ji L, Gong Y, et al. FL118: A potential bladder cancer therapeutic compound targeting H2A.X identified through library screening. Bioorg Chem. 2024;153:107802.

460. Takeda K, Ohta S, Nagao M, Kobayashi E, Tago K, Funakoshi-Tago M. FL118 Is a Potent Therapeutic Agent against Chronic Myeloid Leukemia Resistant to BCR-ABL Inhibitors through Targeting RNA Helicase DDX5. Int J Mol Sci. 2024;25(7):3693.

461. Natale R, Blackhall F, Kowalski D, Ramlau R, Bepler G, Grossi F, et al. Evaluation of antitumor activity using change in tumor size of the survivin antisense oligonucleotide LY2181308 in combination with docetaxel for second-line treatment of patients with non-small-cell lung cancer: a randomized open-label phase II study. J Thorac Oncol. 2014;9(11):1704–8.

462. Alhamadani F, Zhang K, Parikh R, Wu H, Rasmussen TP, Bahal R, et al. Adverse Drug Reactions and Toxicity of the Food and Drug Administration-Approved Antisense Oligonucleotide Drugs. Drug Metab Dispos. 2022;50(6):879–87.

463. Morita S, Minami H, Mitsuma A, Toyoda M, Kiyota N, Ando Y. A phase I study of LCL161, a novel oral pan-inhibitor of apoptosis protein (IAP) antagonist, in Japanese patients with advanced solid tumors. Asia Pac J Clin Oncol. 2022;18(5):e427–34.

464. Condon SM, Mitsuuchi Y, Deng Y, Laporte MG, Rippin SR, Haimowitz T, et al. Birinapant, a smac-mimetic with improved tolerability for the treatment of solid tumors and hematological malignancies. J Med Chem. 2014;57(9):3666–77.

465. Amaravadi RK, Schilder RJ, Martin LP, Levin M, Graham MA, Weng DE, et al. A Phase I Study of the SMAC-Mimetic Birinapant in Adults with Refractory Solid Tumors or Lymphoma. Mol Cancer Ther. 2015;14(11):2569–75.

466. Zhang W, Sun S, Zhu W, Meng D, Hu W, Yang S, et al. Birinapant Reshapes the Tumor Immunopeptidome and Enhances Antigen Presentation. Int J Mol Sci. 2024;25(7):3660.

467. Tao Z, McCall NS, Wiedemann N, Vuagniaux G, Yuan Z, Lu B. SMAC Mimetic Debio 1143 and Ablative Radiation Therapy Synergize to Enhance Antitumor Immunity against Lung Cancer. Clin Cancer Res. 2019;25(3):1113–24.

468. Sun XS, Tao Y, Le Tourneau C, Pointreau Y, Sire C, Kaminsky MC, et al. Debio 1143 and high-dose cisplatin chemoradiotherapy in high-risk locoregionally advanced squamous cell carcinoma of the head and neck: a double-blind, multicentre, randomised, phase 2 study. Lancet Oncol. 2020;21(9):1173–87.

469. Zadorozhna M, Tataranni T, Mangieri D. Piperine: role in prevention and progression of cancer. Mol Biol Rep. 2019;46(5):5617–29.

470. Dougan SK, Dougan M. Regulation of innate and adaptive antitumor immunity by IAP antagonists. Immunotherapy. 2018;10(9):787–96.

471. Mo X, Tang C, Niu Q, Ma T, Du Y, Fu H. HTiP: High-Throughput Immunomodulator Phenotypic Screening Platform to Reveal IAP Antagonists as Anti-cancer Immune Enhancers. Cell Chem Biol. 2019;26(3):331-339.e3.

472. Beug ST, Tang VA, LaCasse EC, Cheung HH, Beauregard CE, Brun J, et al. Smac mimetics and innate immune stimuli synergize to promote tumor death. Nat Biotechnol. 2014;32(2):182–90.

473. Rettinger E, Glatthaar A, Abhari BA, Oelsner S, Pfirrmann V, Huenecke S, et al. SMAC Mimetic BV6 Enables Sensitization of Resistant Tumor Cells but also Affects Cytokine-Induced Killer (CIK) Cells: A Potential Challenge for Combination Therapy. Front Pediatr. 2014;2:75.

474. Infante JR, Dees EC, Olszanski AJ, Dhuria S V., Sen S, Cameron S, et al. Phase I dose-escalation study of LCL161, an oral inhibitor of apoptosis proteins

inhibitor, in patients with advanced solid tumors. J Clin Oncol. 2014;32(28):3103–10.

475. Zhao XY, Wang XY, Wei QY, Xu YM, Lau ATY. Potency and Selectivity of SMAC/DIABLO Mimetics in Solid Tumor Therapy. Cells. 2020;9(4):1012.

476. Petersen SL, Wang L, Yalcin-Chin A, Li L, Peyton M, Minna J, et al. Autocrine TNFalpha signaling renders human cancer cells susceptible to Smac-mimetic-induced apoptosis. Cancer Cell. 2007;12(5):445–56.

477. Su CC, Hsieh KL, Liu PL, Yeh HC, Huang SP, Fang SH, et al. AICAR Induces Apoptosis and Inhibits Migration and Invasion in Prostate Cancer Cells Through an AMPK/mTOR-Dependent Pathway. Int J Mol Sci. 2019;20(7):1647.

478. Tripathi V, Jaiswal P, Assaiya A, Kumar J, Parmar HS. Anti-cancer Effects of 5-Aminoimidazole-4-Carboxamide-1-β-D-Ribofuranoside (AICAR) on Triple-negative Breast Cancer (TNBC) Cells: Mitochondrial Modulation as an Underlying Mechanism. Curr Cancer Drug Targets. 2022;22(3):245–56.

479. Rae C, Mairs RJ. AMPK activation by AICAR sensitizes prostate cancer cells to radiotherapy. Oncotarget. 2019;10(7):749–59.

480. Sgadari C, Scoppio B, Picconi O, Tripiciano A, Gaiani FM, Francavilla V, et al. Clinical Efficacy of the HIV Protease Inhibitor Indinavir in Combination with Chemotherapy for Advanced Classic Kaposi Sarcoma Treatment: A Single-Arm, Phase II Trial in the Elderly. Cancer research communications. 2024;4(8):2112–22.

481. Bourhis E, Hymowitz SG, Cochran AG. The mitotic regulator survivin binds as a monomer to its functional interactor borealin. Journal of Biological Chemistry. 2007;282(48):35018–23.

482. Chettiar SN, Cooley J V., Park IH, Bhasin D, Chakravarti A, Li PK, et al. Design, synthesis and biological studies of survivin dimerization modulators that prolong mitotic cycle. Bioorg Med Chem Lett. 2013;23(19):5429–33.

483. Hirano H, Maeda H, Yamaguchi T, Yokota S, Mori M, Sakoda S. Survivin expression in lung cancer: Association with smoking, histological types and pathological stages. Oncol Lett. 2015;10(3):1456–62.

484. Genomics of Drug Sensitivity in Cancer [Homepage]. Cambridge, MA, USA: Genomics of Drug Sensitivity in Cancer; [accessed 2024 Dec 21]. Cisplatin [4 screens]. Available from: https://www.cancerrxgene.org/compound/Cisplatin/1005/by-tissue?tissue=LUAD

485. Li F, Ling X, Harris DL, Liao J, Wang Y, Westover D, et al. Topoisomerase I (Top1): a major target of FL118 for its antitumor efficacy or mainly involved in its side effects of hematopoietic toxicity? Am J Cancer Res. 2017;7(2):370-382.

486. Lin IL, Lin YT, Chang YC, Kondapuram SK, Lin KH, Chen PC, et al. The SMAC mimetic GDC-0152 is a direct ABCB1-ATPase activity modulator and BIRC5 expression suppressor in cancer cells. Toxicol Appl Pharmacol. 2024;485:116888.

487. Delacour-Larose M, Thi MNH, Dimitrov S, Molla A. Role of survivin phosphorylation by aurora B in mitosis. Cell Cycle. 2007;6(15):1878-85.

488. Hänggi K, Ruffell B. Cell death, therapeutics, and the immune response in cancer. Trends Cancer. 2023;9(5):381–96.

489. Bhatia K, Bhumika, Das A. Combinatorial drug therapy in cancer - New insights. Life Sci. 2020;258:118134.

490. Mokhtari RB, Homayouni TS, Baluch N, Morgatskaya E, Kumar S, Das B, et al. Combination therapy in combating cancer. Oncotarget. 2017;8(23):38022–43.

491. Al-Lazikani B, Banerji U, Workman P. Combinatorial drug therapy for cancer in the post-genomic era. Nat Biotechnol. 2012;30(7):679–92.

492. Remon J, Steuer CE, Ramalingam SS, Felip E. Osimertinib and other third-generation EGFR TKI in EGFR-mutant NSCLC patients. Ann Oncol. 2018;29(suppl_1):i20–7.

493. Remon J, Soria JC, Peters S. Early and locally advanced non-small-cell lung cancer: an update of the ESMO Clinical Practice Guidelines focusing on diagnosis, staging, systemic and local therapy. Ann Oncol. 2021;32(12):1637–42.

494. Riely GJ, Wood DE, Ettinger DS, Aisner DL, Akerley W, Bauman JR, et al. Non-Small Cell Lung Cancer, Version 4.2024, NCCN Clinical Practice Guidelines in Oncology. J Natl Compr Canc Netw. 2024;22(4):249–74.

495. Van Den Bent MJ. The role of chemotherapy in brain metastases. Eur J Cancer. 2003;39(15):2114–20.

496. Kadry H, Noorani B, Cucullo L. A blood-brain barrier overview on structure, function, impairment, and biomarkers of integrity. Fluids Barriers CNS. 2020;17(1):69.

497. Tsuboi M, Herbst RS, John T, Kato T, Majem M, Grohé C, et al. Overall Survival with Osimertinib in Resected EGFR-Mutated NSCLC. N Engl J Med. 2023;389(2):137–47.

498. Wu YL, Dziadziuszko R, Ahn JS, Barlesi F, Nishio M, Lee DH, et al. Alectinib in Resected ALK-Positive Non-Small-Cell Lung Cancer. N Engl J Med. 2024;390(14):1265–76.

499. DrugBank [Homepage]. London, Canada: DrugBank Online; [accessed 2024 Dec 21]. Cisplatin: Uses, Interactions, Mechanism of Action [36 screens]. Available from: https://go.drugbank.com/drugs/DB00515

500. Campbell AB, Kalman SM, Jacobs C. Plasma platinum levels: relationship to cisplatin dose and nephrotoxicity. Cancer Treat Rep. 1983;67(2):169–72.

501. Matsui K, Masuda N, Uchida Y, Fukuoka M, Negoro S, Yana T, et al. Determinants of myelosuppression in the treatment of non-small cell lung cancer with cisplatin-containing chemotherapy. Jpn J Cancer Res. 1996;87(7):781–6.

502. Povirk LF, Shuker DE. DNA damage and mutagenesis induced by nitrogen mustards. Mutat Res. 1994;318(3):205–26.

503. DrugBank [Homepage]. London, Canada: DrugBank Online; [accessed 2024 Dec 21]. Carboplatin: Uses, Interactions, Mechanism of Actionp [42 screens]. Available from: https://go.drugbank.com/drugs/DB00958

504. de Castria TB, da Silva EMK, Gois AFT, Riera R. Cisplatin versus carboplatin in combination with third-generation drugs for advanced non-small cell lung cancer. Cochrane Database Syst Rev. 2013;2013(8):CD009256.

505. van der Vijgh WJF. Clinical pharmacokinetics of carboplatin. Clin Pharmacokinet. 1991;21(4):242–61.

506. DrugBank [Homepage]. London, Canada: DrugBank Online; [accessed 2024 Dec 21]. Gemcitabine: Uses, Interactions, Mechanism of Action [30 screens]. Available from: https://go.drugbank.com/drugs/DB00441

507. Mini E, Nobili S, Caciagli B, Landini I, Mazzei T. Cellular pharmacology of gemcitabine. Ann Oncol. 2006;17 (Suppl 5):v7-12.

508. DrugBank [Homepage]. London, Canada: DrugBank Online; [accessed 2024 Dec 21]]. Paclitaxel: Uses, Interactions, Mechanism of Action [42 screens]. Available from: https://go.drugbank.com/drugs/DB01229

509. Ferlini C, Cicchillitti L, Raspaglio G, Bartollino S, Cimitan S, Bertucci C, et al. Paclitaxel directly binds to Bcl-2 and functionally mimics activity of Nur77. Cancer Res. 2009;69(17):6906–14.

510. Zhu L, Chen L. Progress in research on paclitaxel and tumor immunotherapy. Cell Mol Biol Lett. 2019;24:40.

511. Giagkousiklidis S, Vellanki SH, Debatin KM, Fulda S. Sensitization of pancreatic carcinoma cells for gamma-irradiation-induced apoptosis by XIAP inhibition. Oncogene. 2007;26(49):7006–16.

512. Vellanki SHK, Grabrucker A, Liebau S, Proepper C, Eramo A, Braun V, et al. Small-molecule XIAP inhibitors enhance gamma-irradiation-induced apoptosis in glioblastoma. Neoplasia. 2009;11(8):743–52.

513. Berger R, Jennewein C, Marschall V, Karl S, Cristofanon S, Wagner L, et al. NF-κB is required for Smac mimetic-mediated sensitization of glioblastoma cells for γ-irradiation-induced apoptosis. Mol Cancer Ther. 2011;10(10):1867–75.

514. Ziegler DS, Keating J, Kesari S, Fast EM, Zawel L, Ramakrishna N, et al. A small-molecule IAP inhibitor overcomes resistance to cytotoxic therapies in malignant gliomas in vitro and in vivo. Neuro Oncol. 2011;13(8):820–9.

515. Karikari CA, Roy I, Tryggestad E, Feldmann G, Pinilla C, Welsh K, et al. Targeting the apoptotic machinery in pancreatic cancers using small-molecule antagonists of the X-linked inhibitor of apoptosis protein. Mol Cancer Ther. 2007;6(3):957–66.

516. Yang D, Zhao Y, Li AY, Wang S, Wang G, Sun Y. Smac-mimetic compound SM-164 induces radiosensitization in breast cancer cells through activation of caspases and induction of apoptosis. Breast Cancer Res Treat. 2012;133(1):189–99.

517. Yang J, McEachern D, Li W, Davis MA, Li H, Morgan MA, et al. Radiosensitization of head and neck squamous cell carcinoma by a SMAC-mimetic compound, SM-164, requires activation of caspases. Mol Cancer Ther. 2011;10(4):658–69.

518. Dai Y, Liu M, Tang W, Desano J, Burstein E, Davis M, et al. Molecularly targeted radiosensitization of human prostate cancer by modulating inhibitor of apoptosis. Clin Cancer Res. 2008;14(23):7701–10.

519. Huerta S, Gao X, Livingston EH, Kapur P, Sun H, Anthony T. In vitro and in vivo radiosensitization of colorectal cancer HT-29 cells by the smac mimetic JP-1201. Surgery. 2010;148(2):346–53.

520. Fulda S. Targeting IAP proteins in combination with radiotherapy. Radiat Oncol. 2015;10:105.

521. Zhang R, Sun H, Wang H, Zhang W, Geng K, Liu Q, et al. ANTP-SmacN7 fusion peptide-induced radiosensitization in A549 cells and its potential mechanisms. Thorac Cancer. 2020;11(5):1271–9.

522. Lu B, Mu Y, Cao C, Zeng F, Schneider S, Tan J, et al. Survivin as a therapeutic target for radiation sensitization in lung cancer. Cancer Res. 2004;64(8):2840–5.

523. Sia J, Szmyd R, Hau E, Gee HE. Molecular Mechanisms of Radiation-Induced Cancer Cell Death: A Primer. Front Cell Dev Biol. 2020;8:41.

524. Vakifahmetoglu H, Olsson M, Zhivotovsky B. Death through a tragedy: mitotic catastrophe. Cell Death Differ. 2008;15(7):1153–62.

525. Vader G, Kauw JJW, Medema RH, Lens SMA. Survivin mediates targeting of the chromosomal passenger complex to the centromere and midbody. EMBO Rep. 2006;7(1):85–92.

526. Mita AC, Mita MM, Nawrocki ST, Giles FJ. Survivin: key regulator of mitosis and apoptosis and novel target for cancer therapeutics. Clin Cancer Res. 2008;14(16):5000–5.

527. Rödel C, Haas J, Groth A, Grabenbauer GG, Sauer R, Rödel F. Spontaneous and radiation-induced apoptosis in colorectal carcinoma cells with different intrinsic radiosensitivities: Survivin as a radioresistance factor. Int J Radiat Oncol Biol Phys. 2003;55(5):1341–7.

528. Pennati M, Binda M, Colella G, Folini M, Citti L, Villa R, et al. Radiosensitization of human melanoma cells by ribozyme-mediated inhibition of survivin expression. J Invest Dermatol. 2003;120(4):648–54.

529. Asanuma K, Kobayashi D, Furuya D, Tsuji N, Yagihashi A, Watanabe N. A role for survivin in radioresistance of pancreatic cancer cells. Jpn J Cancer Res. 2002;93(9):1057–62.

530. Kami K, Doi R, Koizumi M, Toyoda E, Mori T, Ito D, et al. Downregulation of survivin by siRNA diminishes radioresistance of pancreatic cancer cells. Surgery. 2005;138(2):299–305.

531. Chakravarti A, Zhai GG, Zhang M, Malhotra R, Latham DE, Delaney MA, et al. Survivin enhances radiation resistance in primary human glioblastoma cells via caspase-independent mechanisms. Oncogene. 2004;23(45):7494–506.

532. Rachamala HK, Madamsetty VS, Angom RS, Nakka NM, Dutta SK, Wang E, et al. Targeting mTOR and survivin concurrently potentiates radiation therapy in renal cell carcinoma by suppressing DNA damage repair and amplifying mitotic catastrophe. J Exp Clin Cancer Res. 2024;43(1):159.

533. Kappler M, Rot S, Taubert H, Greither T, Bartel F, Dellas K, et al. The effects of knockdown of wild-type survivin, survivin-2B or survivin-delta3 on the radiosensitization in a soft tissue sarcoma cells in vitro under different oxygen conditions. Cancer Gene Ther. 2007;14(12):994–1001.

534. Knauer SK, Bier C, Schlag P, Fritzmann J, Dietmaier W, Rödel F, et al. The survivin isoform survivin-3B is cytoprotective and can function as a chromosomal passenger complex protein. Cell cycle. 2007;6(12):1502–9.

535. Ye W, Gunti S, Allen CT, Hong Y, Clavijo PE, Van Waes C, et al. ASTX660, an antagonist of cIAP1/2 and XIAP, increases antigen processing machinery and

can enhance radiation-induced immunogenic cell death in preclinical models of head and neck cancer. Oncoimmunology. 2020;9(1):1710398.

536. Ferrari N, Ward G, Gewinner C, Davis MP, Jueliger S, Saini H, et al. Antagonism of inhibitors of apoptosis proteins reveals a novel, immune response-based therapeutic approach for T-cell lymphoma. Blood Adv. 2021;5(20):4003–16.

537. Vermeer DW, Coppock JD, Zeng E, Lee KM, Spanos WC, Onken MD, et al. Metastatic model of HPV+ oropharyngeal squamous cell carcinoma demonstrates heterogeneity in tumor metastasis. Oncotarget. 2016;7(17):24194–207.

538. Snacel-Fazy E, Soubéran A, Grange M, Joseph K, Colin C, Morando P, et al. SMAC mimetic drives microglia phenotype and glioblastoma immune microenvironment. Cell Death Dis. 2024;15(9):676.

539. Ene HM, Kara NZ, Einat H. The effects of the atypical antipsychotic asenapine in a strain-specific battery of tests for mania-like behaviors. Behavioural pharmacology. 2015;26(4):331–7.

540. Nakamura A, Nakajima M, Yamanaka H, Fujiwara R, Yokoi T. Expression of UGT1A and UGT2B mRNA in human normal tissues and various cell lines. Drug Metab Dispos. 2008;36(8):1461–4.

541. Li S, Yang Y, Ding Y, Tang X, Sun Z. Impacts of survivin and caspase-3 on apoptosis and angiogenesis in oral cancer. Oncol Lett. 2017;14(3):3774–9.

542. Li Z, Ren W, Zeng Q, Chen S, Zhang M, Zhao Y, et al. Effects of survivin on angiogenesis in vivo and in vitro. Am J Transl Res. 2016;8(2):270–83.

543. Kellar A, Egan C, Morris D. Preclinical Murine Models for Lung Cancer: Clinical Trial Applications. Biomed Res Int. 2015;2015:621324.

544. Zwerts F, Lupu F, De Vriese A, Pollefeyt S, Moons L, Altura RA, et al. Lack of endothelial cell survivin causes embryonic defects in angiogenesis, cardiogenesis, and neural tube closure. Blood. 2007;109(11):4742–52.

545. Arnal-Estapé A, Foggetti G, Starrett JH, Nguyen DX, Politi K. Preclinical Models for the Study of Lung Cancer Pathogenesis and Therapy Development. Cold Spring Harb Perspect Med. 2021;11(12):a037820.

546. Mokhtari RB, Kumar S, Islam SS, Yazdanpanah M, Adeli K, Cutz E, et al. Combination of carbonic anhydrase inhibitor, acetazolamide, and sulforaphane, reduces the viability and growth of bronchial carcinoid cell lines. BMC Cancer. 2013;13:378.

547. Islam SS, Mokhtari RB, Akbari P, Hatina J, Yeger H, Farhat WA. Simultaneous Targeting of Bladder Tumor Growth, Survival, and Epithelial-to-Mesenchymal Transition with a Novel Therapeutic Combination of Acetazolamide (AZ) and Sulforaphane (SFN). Target Oncol. 2016;11(2):209–27.

548. Blagosklonny M V. A new science-business paradigm in anticancer drug development. Trends Biotechnol. 2003;21(3):103–6.

549. Mortensen PB. The incidence of cancer in schizophrenic patients. J Epidemiol Community Health (1978). 1989;43(1):43–7.

550. Dalton SO, Mellemkjær L, Thomassen L, Mortensen PB, Johansen C. Risk for cancer in a cohort of patients hospitalized for schizophrenia in Denmark, 1969-1993. Schizophr Res. 2005;75(2–3):315–24.

551. Grinshpoon A, Barchana M, Ponizovsky A, Lipshitz I, Nahon D, Tal O, et al. Cancer in schizophrenia: is the risk higher or lower? Schizophr Res. 2005;73(2–3):333–41.

552. Avendaño-Félix M, Aguilar-Medina M, Bermudez M, Lizárraga-Verdugo E, López-Camarillo C, Ramos-Payán R. Refocusing the Use of Psychiatric Drugs for Treatment of Gastrointestinal Cancers. Front Oncol. 2020;10:1452.

553. Lianos GD, Alexiou GA, Rausei S, Galani V, Mitsis M, Kyritsis AP. Repurposing antipsychotic drugs for cancer treatment: current evidence and future perspectives. Expert Rev Anticancer Ther. 2022;22(2):131–4.

554. Dogterom P, Riesenberg R, de Greef R, Dennie J, Johnson M, Reddy VP, et al. Asenapine pharmacokinetics and tolerability in a pediatric population. Drug Des Devel Ther. 2018;12:2677–93.

555. Pace A, Lombardi G, Villani V, Benincasa D, Abbruzzese C, Cestonaro I, et al. Efficacy and safety of chlorpromazine as an adjuvant therapy for glioblastoma in patients with unmethylated MGMT gene promoter: RACTAC, a phase II multicenter trial. Front Oncol. 2023;13:1320710.

556. Kattner P, Strobel H, Khoshnevis N, Grunert M, Bartholomae S, Pruss M, et al. Compare and contrast: pediatric cancer versus adult malignancies. Cancer Metastasis Rev. 2019;38(4):673–82.

15 ANNEX

Biomedicine & Pharmacotherapy 182 (2025) 117756

Contents lists available at ScienceDirect

Biomedicine & Pharmacotherapy

journal homepage: www.elsevier.com/locate/biopha

Identification of the atypical antipsychotic Asenapine as a direct survivin inhibitor with anticancer properties and sensitizing effects to conventional therapies

Cristina Benítez-García [a,b], David Martínez-García [a,b], Martin Kotev [c], Marta Pérez-Hernández [a,b], Yvonne Westermaier [c], Lucía Díaz [c], Luis Korrodi-Gregório [a], Pere Fontova [a,d], Ana Aurora Torres [a,b], Ricardo Pérez-Tomás [a], María García-Valverde [d], Roberto Quesada [d], Robert Soliva [c], Vanessa Soto-Cerrato [a,b,*]

[a] Department of Pathology and Experimental Therapeutics, Faculty of Medicine and Health Sciences, Universitat de Barcelona, Barcelona, Spain
[b] Molecular Signaling, Oncobell Program, Institut d'Investigació Biomèdica de Bellvitge (IDIBELL), L'Hospitalet de Llobregat, Spain
[c] Nostrum Biodiscovery, Av. de Josep Tarradellas, 8-10, Barcelona E-08029, Spain
[d] Department of Chemistry, Universidad de Burgos, Burgos, Spain

ARTICLE INFO

Keywords:
Survivin inhibitor
Drug repositioning
Treatment sensitization
Inhibitor of apoptosis proteins
Combination treatment
Lung cancer

ABSTRACT

Therapy resistance in human cancers is a major limitation in Clinical Oncology. In this regard, overexpression of anti-apoptotic proteins, such as survivin, has been described in several tumors, contributing to this clinical issue. Survivin has a dual role in key cellular functions, inducing cell cycle progression and inhibiting apoptosis; thus, survivin is an attractive target for cancer therapy. Therefore, we focused on identifying and validating a novel specific, directly binding survivin inhibitor for cancer treatment and tumor sensitization to conventional pro-apoptotic therapies. In this work, we conducted a structure-based high-throughput virtual screening at the survivin homodimerization domain. Asenapine Maleate (AM), an approved drug for central nervous system diseases, was identified as a direct binder of the survivin homodimerization domain and it significantly affected cell viability of lung, colon, and brain cancer cell lines. Direct interaction of AM to survivin protein was corroborated by surface plasmon resonance and a specific survivin protein decrease was observed in cancer cells, compared to other inhibitors of apoptosis proteins. Therapeutic *in vivo* studies showed an impairment of tumor growth in AM-treated mice. Finally, a synergistic anticancer effect was detected *in vitro* when combined with different conventional chemotherapies, and *in vivo* studies showed higher antitumor effects when combined with cisplatin. Altogether, our results identify AM as a specific direct binding inhibitor of survivin, showing anticancer properties *in vitro* and *in vivo* and sensitizing effects when combined with cisplatin, opening the possibility of repositioning this approved drug for cancer treatment.

1. Introduction

Resistance to conventional therapies is responsible for most of the cancer-related deaths. In this regard, evasion of apoptosis is one of the most predominant mechanisms of treatment resistance in human cancers, and overexpression of anti-apoptotic proteins, such as survivin, has been described in several tumors, contributing to this clinical issue [35].

Survivin (encoded by BIRC5; Baculoviral Inhibitor of Apoptosis Repeat-Containing 5) is the smallest protein (16.5 kDa) of the Inhibitor of Apoptosis Protein (IAP) family. IAPs inhibit apoptosis and their dysregulation leads to cancer development and drug resistance [43]. Survivin has key roles in apoptosis inhibition and cell cycle progression [2,53]. As a monomer, survivin exerts its anti-apoptotic activity in the cytoplasm, usually by interacting with other IAPs to inhibit caspases [33]. It can also form homodimers, which are mainly involved in promoting the mitotic activity in the nucleus [40]. Besides its anti-apoptotic and pro-mitotic functions, it has also been demonstrated that there are survivin isoforms able to promote angiogenesis by upregulating VEGF expression and promoting endothelial cell proliferation (S. [28]; Z. [27]). Moreover, survivin is also involved in enhancing metastasis [11,

* Correspondence to: C/Feixa Llarga s/n, Pavelló de Govern, 5002, L'Hospitalet de Llobregat, Barcelona 08907, Spain.
E-mail address: vsoto@ub.edu (V. Soto-Cerrato).

https://doi.org/10.1016/j.biopha.2024.117756
Received 7 October 2024; Received in revised form 27 November 2024; Accepted 10 December 2024
Available online 17 December 2024

8] and regulating cancer stem cell physiology [15].

Survivin overexpression is negatively correlated with tumor prognosis, it is thus considered a biomarker of patient clinical outcome and drug resistance in many cancers [13,30,31,44]. Moreover, survivin is abundantly expressed in most cancer malignancies, whereas it is almost undetectable in most normal differentiated tissues. Garg et al., [12]. Altogether, these findings make survivin a good anticancer target, for which several survivin inhibitors have been developed [32]. The main strategies that have been studied for targeting survivin are transcription inhibitors, SMAC mimetics, Hsp90 inhibitors, homodimerization inhibitors and mitotic inhibitors. Different treatments based on some of these therapeutic approaches have reached clinical trials. That is the case of YM155 [23,39,47] and EM-1421 [14,22,50], two small molecules that inhibit survivin transcription. The oligonucleotide LY2181308 is another example of survivin transcription inhibitor that has been evaluated in clinical trials [54,9]. LCL161, birinapant, and Debio1143 are SMAC mimetics that have progressed through phase I/II clinical trials [20,36,7]. Finally, indinavir is a mitotic inhibitor that has shown good results in a recent clinical trial [46]. Some of these strategies have shown limited efficacy and/or dose-limiting toxicity (such as LY2181308, YM155 or LCL161) that has been attributed to deficiencies in complete and selective inhibition of survivin in patients and due to off-target effects. Moreover, the optimal therapeutic effect of survivin inhibitors is expected to be achieved in combination with other drugs, since survivin inhibitors sensitize cancer cells to apoptosis. In fact, there are studies demonstrating the synergy of combining survivin inhibitors with chemotherapy or radiotherapy to enhance the apoptotic effect of these therapies and to overcome resistance in cancer patients [4,6]. The fact is that, although survivin is a key target in cancer research due to its expression pattern and multiple key biological functions, we still do not have an effective survivin-specific anticancer agent available, hence more direct and specific inhibitors should be developed [53].

In this work, we aim to identify a novel survivin inhibitor with a different mode of action than the previously assessed compounds in the clinics, that is, an inhibitor that directly and selectively binds to the survivin homodimerization domain to exert its anticancer effects. For this purpose, we performed a structure-based high-throughput virtual screening (HTVS). After identifying and validating the best survivin inhibitor candidate, we evaluated its potential anticancer properties, investigated the mechanism of action of the compound alone and in combination with conventional chemotherapeutics, and assessed the safety and efficacy profiles of the drug in *in vivo* cancer mouse models.

2. Materials and methods

2.1. High-throughput virtual screening

A druggability analysis was carried out on the PDB structures 2QFA [19] and 3UEC [38] using fpocket [25]. The DrugBank database (version of 2015) and the ZINC database of 'lead' compounds, composed of 8 M ligands, were prepared using the default settings of LigPrep [Schrödinger Release 2018–1: LigPrep, Schrödinger, LLC, New York, NY, 2018]. 2QFA and 3UED were prepared using the default settings of Maestro's PrepWizard [Schrödinger Release 2018–1: Maestro, Schrödinger, LLC, New York, NY, 2018]. HTVS was carried out with Glide at the SP level on a grid centered around Phe13 for both crystal structures. The 200 top-scored docking poses from each database were visually inspected and prioritized according to favorable survivin-ligand contacts and electrostatic and shape complementarity.

2.2. Compounds

Asenapine (MedChem Express, HY-10121) or Asenapine Maleate (AM) (MedChemExpress, HY-11100) were dissolved in dimethyl sulfoxide (DMSO, Sigma-Aldrich, St. Louis, USA). Subsequent solutions for biological assays were made in media for *in vitro* experiments (1 % DMSO v/v) or in phosphate-buffered saline (PBS) with 7.5 % DMSO and 0.8 % Tween20 for *in vivo* experiments. The chemotherapeutics used for the combination assays were cisplatin (Accord, Barcelona, Spain), carboplatin (TCI, Tokyo, Japan) and gemcitabine (SUN pharma, Goregaon, Mumbai). Promazine (1032472060), stanozolol (1025149306), ampicillin (1025470147), baclofen (1032119993), raloxifene (1032471356), and naphazoline (1032472098) were supplied by MedChemExpress (Monmouth Junction, NJ, USA). Amb1987219, Amb9684524, and Amb9615334 were supplied by Ambinter (Orleans, France). 15567877, 16122246, 48253418, 49138141 and 93921014 were supplied by Chembridge (San Diego, CA, USA). 1-acetyl-N-(5-chloro-3-(4-(2-chloro-5-(trifluoromethyl)phenyl)-5-cyano-6-oxo-1,6-dihydropyridin-2-yl)-2-hydroxybenzyl)-N-methylpiperidine-4-carboxamide (MM87 or compound Abbot 23b as described in [52]) was re-synthesized in-house and used as a reference compound.

2.3. Cell line and culture conditions

A549 (human epithelial lung adenocarcinoma), SW620 (human colon carcinoma), U87 MG (human glioblastoma), MCF10A (non-tumorigenic human breast cell line), RD (pediatric human rhabdomyosarcoma), HFL-1 (human fibroblast from the lung) and LLC1 (mouse Lewis lung carcinoma cell line) cell lines were obtained from the American Type Culture Collection (ATCC, Manassas, VA, USA). LAN-1 (human neuroblastoma bone marrow metastasis) cell line was obtained from the European Collection of Authenticated Cell Cultures (ECACC, Salisbury, UK).

A549, SW620, U87 MG, and LLC1 cell lines were maintained in DMEM (Biological Industries, Beit Haemek, Israel) supplemented with 100 U/mL penicillin, 100 μg/mL streptomycin, and 2 mM L-glutamine, all from Biological Industries, and 10 % fetal bovine serum (FBS). MCF10A cells were cultured in DMEM/F12 1:1 medium (Biological Industries) supplemented with the already mentioned factors (100 U/mL penicillin, 100 μg/mL streptomycin and 2 mM L-glutamine) as well as 5 % horse serum (Gibco, Paisley, UK), 100 ng/mL cholera toxin (Calbiochem, San Diego, CA, USA), 0.5 μg/mL hydrocortisone, 20 ng/mL epidermal growth factor, and 10 μg/mL human insulin (all from Sigma-Aldrich Chemical Co., Saint Louis, MO, USA). LAN-1 and RD cell lines were cultured in RPMI (Biological Industries) with 100 U/mL penicillin, 100 μg/mL streptomycin, 2 mM L-glutamine, and 10 % FBS. HFL-1 cells were cultured in HAM-F12 (Biological Industries) with 100 U/mL penicillin, 100 μg/mL streptomycin, 2 mM L-glutamine, 1 % non-essential amino acids solution (NEAA, Biological Industries), and 10 % FBS. All cell lines were maintained in 5 % CO_2 and 37 ºC conditions. Cells were cultured between passage 10 and 25 and were routinely tested for mycoplasma contamination.

2.4. Viability assays

To perform these assays, cells (1×10^5 cells/well) were seeded in 96-well microtiter plates and were incubated for 24 h to allow for cell attaching. For single-point cell viability assays, A549 and SW620 cells were treated for 24 h with selected FDA-approved drugs (5 and 20 μM) and small molecules (5 and 50 μM) from available chemical libraries (Supplementary Figure 1) that showed potential binding to survivin protein in the HTVS and docking studies. We also obtained dose-response curves of AM to calculate the inhibitory concentration (IC) of 25 %, 50 %, and 75 % of cell populations in different cell lines. For this purpose, cells were treated for 24 h with AM in a concentration range of 0.8–100 μM. Two different approaches were performed. For combination experiments, after 24 h of seeding, cells were treated with AM, cisplatin, carboplatin, or gemcitabine in monotherapy, or with AM plus cisplatin, carboplatin or gemcitabine simultaneously. Second, the sequential combination treatment was performed by adding cisplatin (to A549 and LLC1 cells) and 24 h later, AM was added. The concentrations of chemotherapeutics were 0.013–0.1 mg/mL for cisplatin, 0.063–1 mg/

mL for carboplatin, and 0.25–4 mg/mL for gemcitabine, combined with the corresponding IC of 50 % of the cell population (IC_{50}) of AM depending on the cell line used. DMSO was used as negative control at a concentration of 1 % (v/v).

In all experiments, 10 μM of 3-(4,5-dimethylthiazol-2-yl)-2,5-diphenyltetrazolium bromide (MTT, Sigma-Aldrich) diluted in 1x PBS was added to each well after treatment and incubated at 37 ºC for an additional 2 h. Then, we removed the medium and dissolved the MTT formazan precipitates in 100 μL of DMSO. Absorbance was read on a Multiskan™ multiwell plate reader (Thermo Fisher Scientific Inc., Waltham, MA, USA) at 570 nm. For each condition, at least three independent experiments were performed (in duplicate or triplicate). Cell viability was expressed as a percentage of control cells, and data are shown as the mean value ± S.D. The IC_{25}, IC_{50}, and IC_{75} values were calculated with GraphPad Prism™ 8 software (Graph Pad Software, San Diego, CA, USA).

In the combination experiments, the Compusyn software was used to generate the combination index (CI), which is defined as the sum of the ratios of the dose of the combination (D1, D2) required to produce a determined percentage of efficacy (x) divided by the dose of the drug alone needed for the same effect (Dx1, Dx2) (Formula 1).

$$CI = \frac{D1}{Dx1} + \frac{D2}{Dx2}$$

Formula 1. Combination Index (CI) calculation. D1 and D2 correspond to the doses of drug 1 or drug 2 that produce x percentage of effect in combination. Dx1 and Dx2 are the doses of each drug alone required to produce x percentage of effect.

Depending on the value of CI, we distinguish different types of interaction, being $CI < 1$ synergism, $CI = 1$ additive effect, and $CI > 1$ antagonism.

2.5. Surface plasmon resonance assay (SPR)

SPR assays were designed to monitor the interaction between survivin (Calmodulin tag; Abcam87202) bound to the chip and the compounds AM and Abbot23b (as analytes). Abbott23b was used as a positive control. Survivin was immobilized following the Biacore T200 protocol on a sensor chip CM5 (GE Healthcare BioSciences AB) coated with a carboxymethylated dextran matrix that allows a covalent protein attachment by amine coupling. Survivin is tagged with calmodulin; thus, we also immobilized the calmodulin (Abcam78694) ligand alone in the reference channel. A pH scouting was performed before immobilization to determine the optimal pH to pre-concentrate the ligand on the matrix. The ligand was diluted to 1 μM in 10 mM acetate buffers pH 4 and 4.25, and injected during 180 s with a flow of 5 μL/min on an unmodified sensor chip. Then, the surface was regenerated with 50 mM NaOH to ensure no ligand remained bound to the surface. Once the optimum pH was selected, the surface of the sensor chip was activated with a 1:1 mixture of 1-ethyl-3-(3-dimethylaminopropyl)-carbodiimide (EDC) and N-hydroxy succinimide (NHS) to form reactive ester groups on the surface. Subsequently, survivin protein was diluted to 0.05 μg/μL in 10 mM acetate buffer pH 4.25 and immobilized in flow-cell 2 up to 1600 response units (RU). Similarly, calmodulin protein was diluted to 0.05 μg/μL in 10 mM acetate buffer with pH 4 and immobilized in flow-cell 1 up to 1300 RU. The immobilized ligand level was previously calculated according to the relative molecular weights of survivin and the analytes and the maximum binding capacity of the surface with a theoretical R_{max} (maximal response) of 50 RU. Once the immobilization was performed, an ethanolamine solution was injected to deactivate the remaining reactive groups of the surface.

Compounds were stored as a stock solution in 100 % DMSO at −20 ºC. The compounds were diluted with running buffer, 1X HBS-P (HEPES-buffered saline 0.005 % P20) 5 % DMSO, at concentrations ranging from 0.012 μM to 40 μM. Afterward, samples were injected in duplicates in both channels at 30 μL/min flow for 90 s and dissociated within 300 s. Moreover, a solvent correction with carefully prepared DMSO reference solutions ranging from 4.5 % to 5.8 % was run to adjust measured sample responses due to solvent effects on the bulk refractive index variations.

Experiments were performed with the instrument temperature (flow cell, sensor chip, and sample compartment temperature) set to 25 ºC. For affinity evaluation, the Biacore™ T200 evaluation software 2.0 was used to subtract the reference and blank data, correct the solvent, and fit the curve, using the 1:1 Langmuir model.

2.6. Immunoblot analysis

For the non-denaturing electrophoresis, 1 μg of purified survivin (Abcam) was incubated in PBS with DMSO or with different concentrations of AM (50, 200 or 500 μM). Then, the samples were mixed with an equal volume of sample buffer (0.5 M Tris pH 8, 20 % glycerol, 0.005 % bromophenol blue, 2 % Triton X-100, 100 mM DTT) for 30 min at room temperature (RT). After centrifugation at 11000 g for 10 min, the supernatants were separated by electrophoresis in a non-denaturing PAGE of 15 % polyacrylamide and transferred to the PVDF membrane. Results were obtained from three independent experiments.

To determine the molecular mechanism of action of AM, A549 and U87 MG cells were seeded at 1×10^5 cells/mL. After 24 h, cells were treated with DMSO (control) or AM (IC_{50}) for 24 h. In the combination experiments, cisplatin (IC_{50}) was added after 24 h of seeding, whereas AM (IC_{50}) was incorporated on the next day for an additional 24 h. Dead cells from culture supernatants were collected and lysed with attached cells using ice-cold lysis buffer containing 0.1 % SDS, 1 % NP-40, 0.5 % sodium deoxycholate, 50 mmol/L sodium fluoride, 40 mmol/L β-glycerophosphate, 200 μmol/L sodium orthovanadate, 1 mmol/L phenylmethyl sulfonyl fluoride (all from Sigma-Aldrich), and protease inhibitor cocktail (Roche Diagnostics). Lysate was sonicated, followed by centrifugation at 16000 g for 15 min at 4 ºC. The supernatant was collected and the protein concentration was determined by BCA protein assay (Pierce™, Thermo Fisher Scientific) following the manufacturer's instructions. 40 μg of protein extracts were separated in 15 % SDS-polyacrylamide gel electrophoresis and transferred to the PVDF membrane. Membranes were then incubated with the following primary antibodies overnight at 4 ºC: anti-cleaved caspase 3 (#9664, lot. 22), anti-GAPDH (#2118, lot. 14), anti-PARP (#9542, lot. 15), and anti-survivin (#2808, lot. 15) from Cell Signaling Technology (Danvers, MA, USA) and anti-X-linked inhibitor of apoptosis protein (XIAP, sc-55550, lot. I2016) and p53 (sc-6243, lot. L1714), both from Santa Cruz Biotechnology (Dallas, TX, USA).

On the next day, after washing with TRIS-buffered saline-Tween 20 0.1 % (TBS-T), membranes were incubated with horseradish peroxidase (HRP) conjugated secondary antibodies for 1 h at RT, goat anti-mouse IgG-HRP (62–6520, lot. XB337870, Thermo Fisher Scientific) and goat anti-rabbit IgG-HRP (7074P2, lot. 26, Cell Signaling Technology). Images were captured on an Image Quant LAS 500 (GE Healthcare) using ECL™ Western blotting detection reagent (Amersham, GE Healthcare, Buckinghamshire, UK). Band densitometries were retrieved using the Image J software (v1.53t, National Institutes of Health, Bethesda, MD, USA) and Image Studio™ Lite software (v.5.2., LICOR Biosciences, Lincoln, Nebraska, USA). GAPDH was used as the gel loading control. The results shown are representative of Western blot data analysis obtained from at least three independent experiments.

2.7. Flow cytometry

To study the effect of AM on the cell cycle, 1.25×10^5 cells/mL were seeded in 6-well plates and, 24 h later, cells were treated with DMSO or AM (IC_{50}). Three independent experiments were performed to obtain the results.

To analyze combination therapy effects on apoptosis, A549 cells at 1×10^5 cells/mL were seeded in 6-well plates. After 24 h, cells were

treated with DMSO, AM (IC_{50}), cisplatin (0.03 mg/mL) or the combination (cisplatin plus AM) for 48 h, and Muse Annexin V & Death Cell Kit™ (Luminex Corporation, Austin, TX, USA) was used. For the cell cycle assay, 1.25×10^5 cells/mL were seeded. 24 h later, cells were treated with DMSO, AM (IC_{50}), cisplatin (0.03 mg/mL), and the combination of AM (IC_{50}) plus cisplatin (0.03 mg/mL) for 24 h. Muse™ Cell Cycle Kit (EMD Millipore, Burlington, MA, USA) was employed following the manufacturer's instructions. All analyses were performed using Muse™ Cell Analyzer and 10,000 events were acquired. The findings were obtained from four independent experiments.

A549 and LLC1 cells (1×10^5 cells/mL) were seeded in 6-well plates to study calreticulin (CALR) exposure on cellular membranes. After 24 h, cells were treated with AM at concentrations corresponding to AM IC_{25}, IC_{50} and IC_{75} for 24 h. On the next day, cells were collected and incubated for 1 h at RT with CALR PE-conjugated monoclonal antibody (Enzo Life Sciences Inc., Farmingdale, NY, USA. ADI-SPA-601PE-F, lot. 09072110; 1:70). Then, cells were washed and resuspended in 1X PBS for flow cytometry analysis. Death cells were labeled with 7-Aminoactinomycin viability staining solution (eBioscience™, Thermo Fisher Scientific). Flow cytometry was completed using a FACS Canto II™ (BD Biosciences, Franklin Lakes, NJ, USA) taking 10,000 events for each condition. The mean fluorescence intensity of PE-CALR was analyzed by BD FACSDiva™ Software. The findings were derived from four independent experiments.

2.8. HMGB1 and ATP release determination

A549 (5×10^4 cells/mL) cells were seeded in a 6-well plate. After 48 h, we treated cells with AM for 24 h at concentrations corresponding to AM IC_{25}, IC_{50}, and IC_{75} in A549 cells. Cell culture supernatant was collected and stored at −80 ºC. High mobility group box-1 (HMGB1) release was assessed in cell culture supernatants with HMGB1 express ELISA (#30164033, TECAN, Hamburg, Germany) according to the manufacturer's instructions. Microplate reader FLUOstar® Omega (BMG Labtech, Mornington, VIC, Australia) was used to measure plate absorbance. ATP release was determined in cell culture supernatants with RealTime-Glo™ Extracellular ATP Assay (Promega, Madison, WI, USA). The ATP-derived luminescent signal was detected on multi-mode microplate reader FLUOstar® Omega in five reading cycles of 1 min duration. Seven independent replicates were performed.

2.9. Animal studies

All animal studies were carried out in accordance with EU Directive 2010/63/EU for animal experiments and protocols were approved by the Local Ethics Committee (Generalitat de Catalunya) under protocol number 10928. For the AM safety evaluation assay, ten-week-old C57BL6 mice (both sexes) were randomized into four groups (4 mice/group): vehicle (7.5 % DMSO and 0.8 % Tween-20 in PBS), 10, 15, and 20 mg/kg AM. The treatment was intraperitoneally injected once daily on a 5-days-on/2-days-off schedule for 31 days. Body weight was recorded daily until the end of the treatment. Once mice were sacrificed, blood, liver, kidneys, spleen, and brain were collected and weighed. Organs were fixed in 4 % paraformaldehyde (PFA) at 4 ºC for 24 h. Then, the samples were processed for hematoxylin and eosin (H/E) staining and analyzed under the microscope (Nikon Europe BV, Badhoevedorp, The Netherlands).

For AM and AM plus cisplatin therapeutic efficacy assays performed in C57BL/6 mice (n = 6 and n = 9 mice/group respectively, 8–12-week-old, both sexes), a subcutaneous model was used and 100 μL of 5×10^4 LLC1 cells in PBS:Corning® Matrigel® (Cultek, Spain) (1:1) were inoculated into the right flank of isoflurane-anesthetized mice. We started the treatment when the tumors were palpable. For the AM monotherapy assay, tumor-bearing mice were separated into 2 groups and treated with vehicle or 10 mg/kg AM. The treatment was intraperitoneally administered once daily on a 5-days-on/2-days-off schedule for 22 days.

The AM monotherapy efficacy assay was also conducted in NSG mice (Mouse Lab, Idibell, Barcelona, Spain). 4×10^6 A549 cells in PBS: Corning® Matrigel® (Cultek, Spain) (1:1) were inoculated subcutaneously in each flank of the animals (n = 5 mice/group, 8–12-week-old, both sexes). Tumor-bearing mice were separated into 2 groups and treated with vehicle or 5 mg/kg of AM. The treatment was intraperitoneally administered once daily on a 5-days-on/2-days-off schedule for 20 days.

For the combination assay, mice were randomized into four groups: vehicle, 5 mg/kg AM, 3 mg/kg cisplatin, and the combination of AM plus cisplatin (5 mg/kg and 3 mg/kg, respectively). Cisplatin was administered on days 0, 3, and 6 of treatment. All the treatments were intraperitoneally administered. Once cisplatin administration was finished, we started with daily doses of AM (5-days-on/2-days-off schedule). This experiment finished 18 days after the first drug administration.

In all *in vivo* experiments, body weight and tumor volume were daily recorded. Tumor volume was calculated by the following formula: ($width^2$ x length)/2. Mice were sacrificed and tumors were collected, weighed and photographed. Tumors were fixed in 4 % PFA at 4 ºC. After 24 h, samples were paraffin-embedded and cut into 5 μm sections and were processed for H/E staining and immunohistochemistry.

For immunohistochemistry, after sample deparaffination and antigen retrieval (in 10 mmol/L sodium citrate buffer with 0.05 % Tween-20 in the microwave at sub-boiling temperature, 95–98 ºC, for 20 min) slides were washed twice with distilled H_2O (dH_2O) for 5 min each time. Endogenous peroxidase was blocked by incubation in 3 % H_2O_2 for 5 min at RT followed by two washing steps for 5 min, with dH_2O and PBS, respectively. Slides were blocked with normal goat serum in a 1:30 dilution for 1 h at RT and incubated with anti-survivin antibody (#2808, lot. 15, Cell Signaling) diluted 1:200 in PBS overnight at 4 ºC in a wet chamber. Afterward, slides were washed three times in PBS 0.1 % Tween-20 for 5 min each and incubated with biotin-conjugated secondary antibody (#711–066–152, lot. 151061, The Jackson Laboratory, Bar Harbor, Maine, USA) at 1:200 dilution in PBS 0.1 % Tween-20 for 1 h at RT. Later, we added streptavidin coupled with HRP (#016–030–084, lot. 152266, The Jackson Laboratory) at 1:250 dilution in PBS for 20 min, at RT. Then, slides were washed three times with PBS for 5 min each and the signal was developed by incubation with DAB (3,3′-diaminobenzidine) (#D8001, Sigma) for 10 min at RT. Finally, slides were washed for 5 min with dH_2O, counterstained with Hematoxylin (#A3865, PanReac AppliChem, Barcelona, Spain), dehydrated, and mounted with DPX (#100579, Merck, Madrid, Spain). Samples were observed in a Nikon Eclipse E800 microscope and images were taken.

2.10. Statistical and data mining analysis

For the statistical analysis of Western Blot, cytometry, and MTT assay data, one-way ANOVA with *post-hoc* Tukey analysis was carried out using the GraphPad Prism 8 software when more than two groups were compared, whereas t-Student analysis was performed when only two groups were compared. The *in vivo* results were analyzed with GraphPad Prism 8 using the nonparametric Mann-Whitney U-test. Statistically significant differences, $p < 0.05$, $p < 0.01$, $p < 0.001$, and $p < 0.0001$, are represented by * , * *, * ** , * ** * respectively.

3. Results

3.1. In silico identification of molecules potentially binding to survivin and characterization of the binding mode

To identify suitable molecules targeting survivin, we ran two HTVS on two publicly available survivin structures focusing on the homodimerization interface. Our druggability analysis revealed varying druggability scores in the two structures due to the flipping of Phe93. This phenylalanine is found in the up conformation in the PDB structure

3UED, while it is in the down conformation in 2QFA, burying its side-chain and creating a deeper cavity on the surface, increasing its susceptibility to binding small molecules.

For the structure-based virtual screening we used commercially available compounds (Zinc database [18]) and also FDA-approved and experimental drugs (as found in DrugBank, version 2015 [55]). More than 8 M compounds were screened *in silico*, and 16 compounds (seven FDA-approved drugs and nine small molecules from commercial catalogs) were identified as highly ranked, passing all our in-house filters. These compounds were selected for experimental *in vitro* studies (Supplementary Figure 1).

Biological testing revealed promising results for some molecules, especially for Asenapine. SPR and cell viability experiments (see below) confirmed its binding to survivin and anticancer activity, prompting a closer look at its binding mode and careful study of its potential interactions with the target.

The two possible isomers of Asenapine (the drug is administered as a mixture) were re-docked into 2QFA using the same parameters as for the virtual screen, and it was found that the plus (Figs. 1A and 1C) and the minus isomers (Figs. 1B and 1D) had similar binding modes in the Phe13-'down' conformation, as found in the chromosome passenger complex. These isomers feature a charge-assisted H-bond between the protonated tertiary nitrogen of the drug and the backbone carbonyl oxygen of Leu96. Hydrophobic packing of the two phenyl rings of the butterfly-shaped tetracycle against Leu6, Leu14, Trp10, Phe13, Leu98, and Phe101 is observed for both, resulting in an extensive contact area between Asenapine and survivin. Depending on the isomer, the chlorine atom is predicted to be solvent-exposed (plus isomer, Fig. 1C) or buried (minus isomer, Fig. 1D).

3.2. Evaluation of in vitro anticancer properties

After having identified compounds showing promising results in the HTVS as potential survivin binders, we wanted to check whether these molecules could reach survivin and inhibit it in cellular assays. Thus, to measure the potential inhibitory effect of the selected compounds on tumor cell proliferation, we performed a cell viability MTT assay at different concentrations (5 and 20 μM for FDA-approved molecules; 5 and 50 μM for small-molecules from chemical libraries) in lung adenocarcinoma A549 and colorectal cancer SW620 cells, both cell lines being representatives of the cancers with the highest incidence (Supplementary Figure 1, Supplementary Figure 2). After 24 h of treatment, Asenapine showed the most potent cytotoxic effect in both cell lines among all compounds tested in the screening (Supplementary Figure 1A and C). Asenapine is an antipsychotic drug identified by our HTVS as a compound potentially binding to the survivin homodimerization domain, revealing its potential as an anticancer agent (Supplementary Figure 1 A and C). Conversely, the already described survivin dimer binding molecule Abbot23b (MM87) [52] did neither decrease the cell viability of A549 nor SW620 at tested concentrations, probably due to limited cell permeability. Furthermore, Asenapine showed a limited cytotoxic effect on non-tumor human lung fibroblasts HFL-1, highlighting that cancer cells are significantly more sensitive to Asenapine cytotoxic effects than non-cancer cells (Fig. 2A).

To evaluate the potential repositioning of this drug for cancer treatment, we evaluated the sensitivity of cancer cells to formulated Asenapine (AM, Fig. 2B) in A549 and SW620 cells at different concentrations (0.8–100 μM) for 24 h. Moreover, since AM can easily cross the blood-brain barrier, we also considered evaluating the cytotoxic effect of AM on the glioblastoma cell line U87 MG, for its potential application in the treatment of brain cancers or brain metastasis. Besides, we tested the compound in two pediatric cancer cell lines (RD and LAN-1), which have no current successful clinical treatment. We also tested the compound in LLC1 murine lung cancer cells, as these are the cells used in the *in vivo* lung cancer model for the assessment of AM therapeutic efficacy in this study (Fig. 2C). Altogether, although formulated AM showed slightly less potent effects than the active ingredient alone, it still maintains significant anticancer effects in all the evaluated cancer cell lines, as shown by the obtained IC_{50} values (Fig. 2 and Supplementary Table 1). These results support the potential use of AM as a future chemotherapeutic drug beyond its antipsychotic properties.

3.3. Validation of survivin binding through Surface Plasmon Resonance (SPR)

After selecting AM as the drug with the most potent anticancer effect,

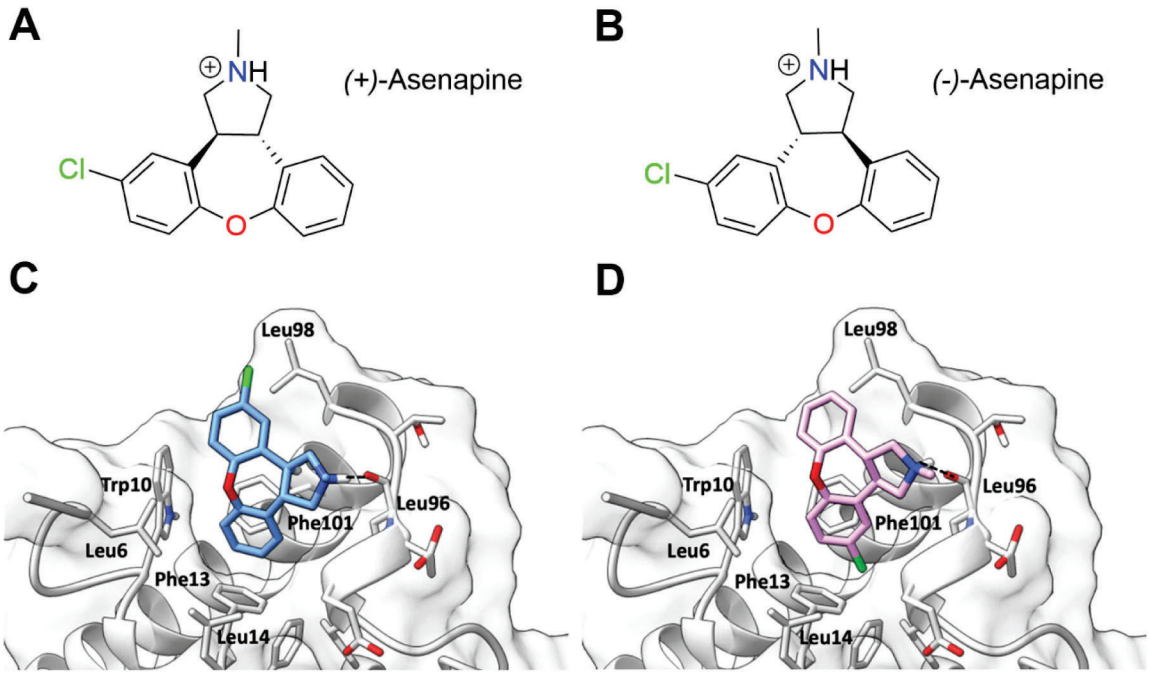

Fig. 1. Structures and docking poses of (+)-Asenapine (A and C) and (-)-Asenapine (B and D) at the dimerization interface of survivin (apo X-ray structure of the chromosome passenger complex; PDB identifier: 2QFA).

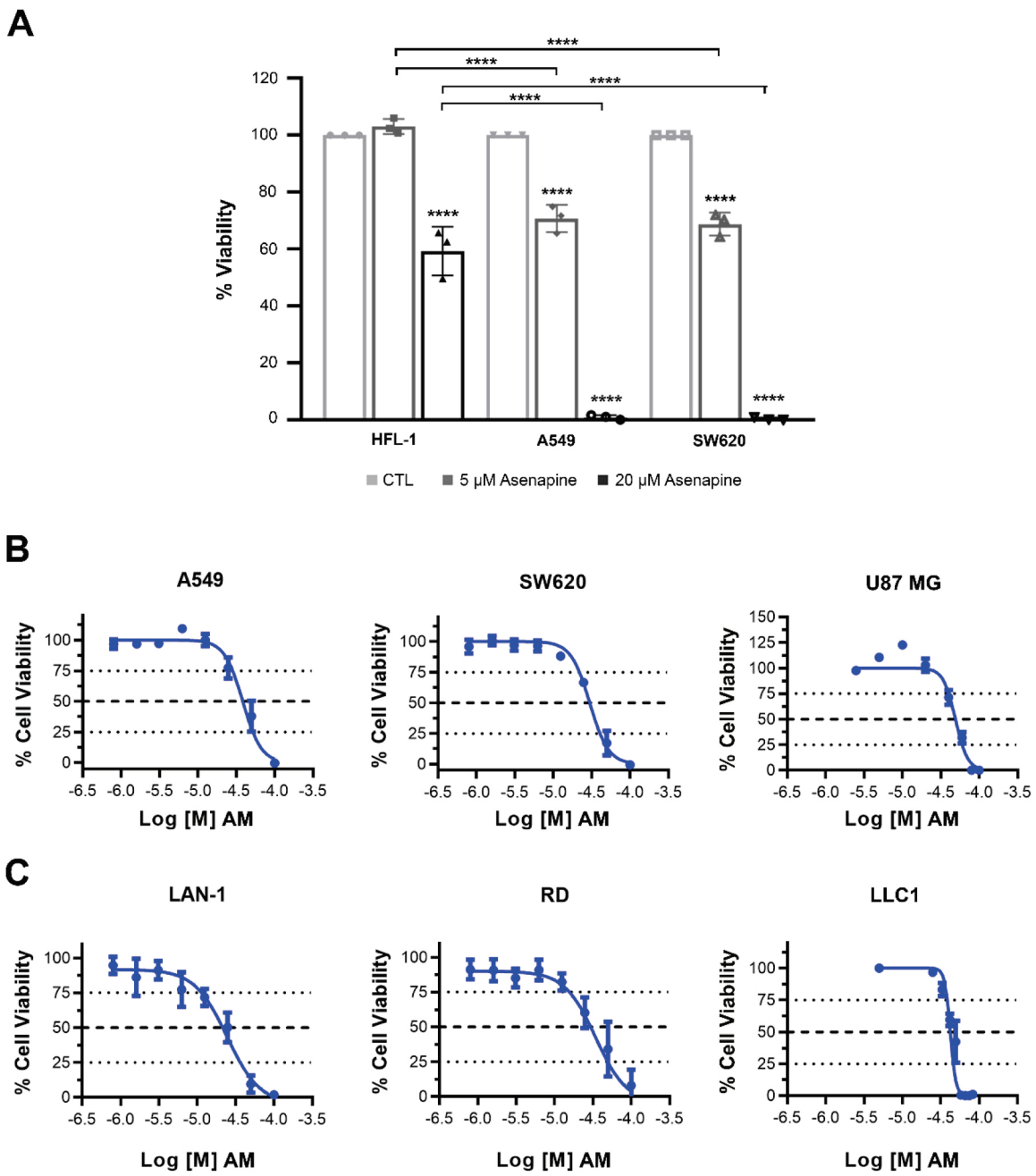

Fig. 2. Effect of Asenapine and AM on cell viability. MTT cell viability assay was performed after 24 h of treatment with Asenapine at 5 and 20 μM in HFL-1 (non-tumor human lung fibroblast), A549 (human lung adenocarcinoma), and SW620 (human colon adenocarcinoma) cell lines (A). Dose-response MTT cell viability assay after 24 h of treatment with AM at concentrations ranging from 0.8 to 100 μM in A549, SW620, U87 MG (glioblastoma), LAN-1 (pediatric neuroblastoma) and RD (pediatric sarcoma) human cancer cell lines, as well as in murine cancer cell line LLC1 (Lewis lung carcinoma) (B, C). Results were obtained from at least three independent experiments. Data are shown as mean ± SD. Statistically significant results are indicated as * ** *, p-value < 0.0001.

we corroborated and characterized the direct interaction between survivin and AM further by SPR. This real-time protein-ligand interaction analysis allows for evaluating the specificity of binding, potency, and kinetics. We first immobilized the recombinant protein survivin on a sensor surface. Survivin was tagged with calmodulin, which was also immobilized on another sensor surface as a reference channel. Next, the analytes AM and Abbott23b were injected onto the sensor surface at concentrations ranging from 0.012 to 40 μM. Abbott23B was used as a positive control due to its described high capacity to interact with the dimer interface of survivin [52]. Changes in SPR response, expressed in RU, showed the association and dissociation curves corresponding to the interactions between survivin and the analytes AM and Abbott23b, respectively (Fig. 3A), resulting in the affinity curves (Fig. 3B).

From these curves, we obtained a KD of 25.72 μM for AM, which was slightly higher than the KD obtained for Abbott23b (4.11 μM). It is important to mention that small molecules like AM have fewer potential binding sites on proteins than larger molecules. Therefore, the values obtained may reflect a high affinity of AM for survivin, supporting the complexation of AM with survivin.

Since our computational studies identified AM as a potential survivin inhibitor that binds to its dimerization domain, we evaluated the ability of AM to dissociate survivin homodimers *in vitro*, observing a clear ability to disrupt the homodimer, which may compromise survivin stability inducing its degradation in cells (Fig. 3C and D).

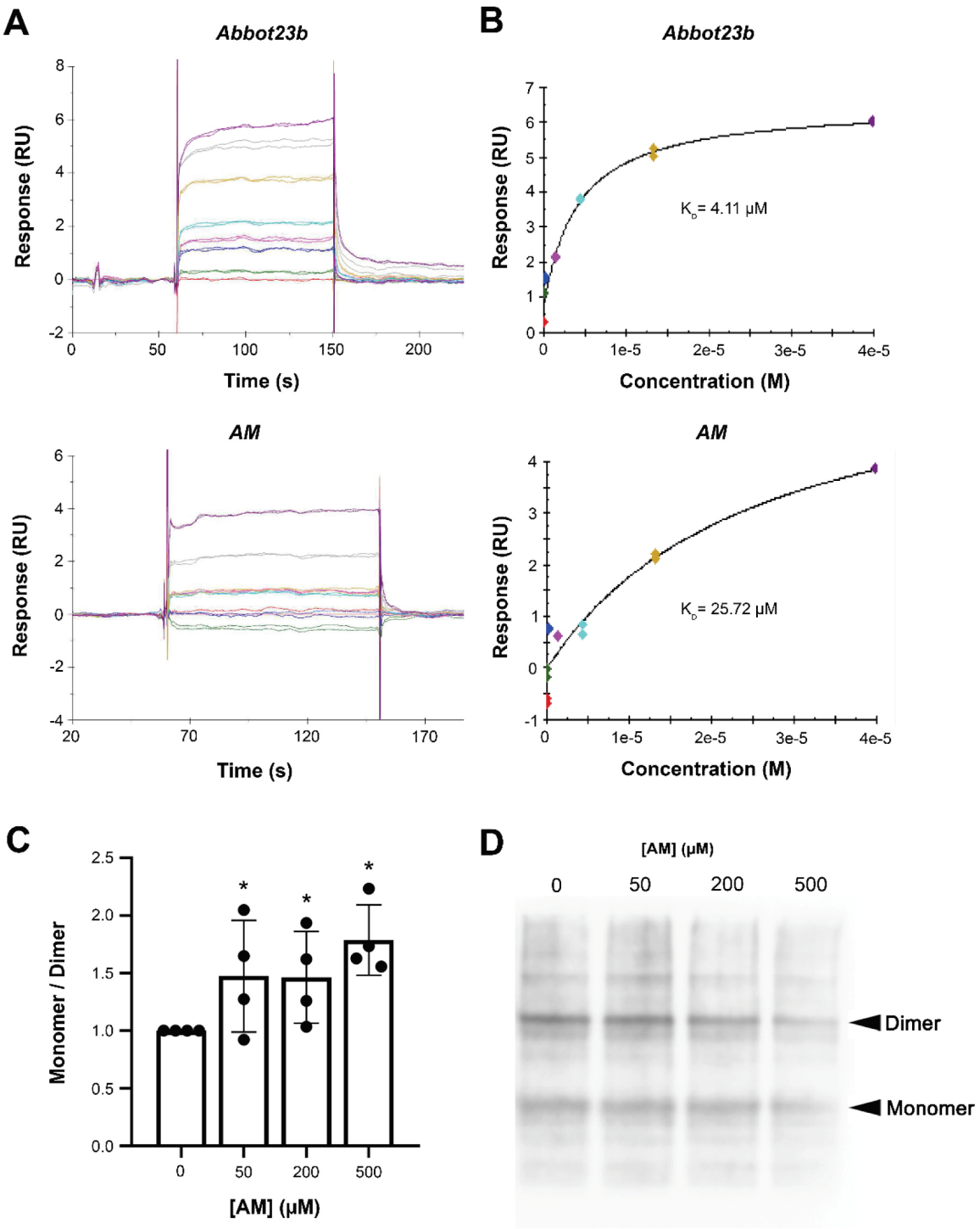

Fig. 3. AM binds to survivin. SPR-derived association and dissociation curves for binding of Abbot23b and AM (concentrations ranging from 0.012 to 40 µM) to immobilized calmodulin-tagged survivin (A). Affinity curves (B). Non-denaturing electrophoresis was conducted to test the ability of AM to dissociate purified survivin homodimers at concentrations of 50, 200 and 500 µM (C, D). Results were obtained from at least three independent experiments. Bars represent the mean ± SD. Statistically significant results are indicated as * , p-value < 0.05. RU: Response units; (M): molar concentration. (K_D): binding constant.

3.4. Mechanism of action of AM

After validating AM binding to survivin, its specificity and mechanism of action were evaluated *in vitro*. A549 and U87 MG cells were treated with AM at their IC_{50} for 24 h to investigate a possible cellular inhibitory effect on survivin. AM was able to significantly decrease survivin protein levels (Fig. 4A). Expression levels of XIAP, another IAP protein structurally related to survivin, did not show significant differences between AM-treated and non-treated cells, indicating that AM specifically downregulates survivin levels.

Regarding the observed AM-induced cell viability decrease, we evaluated whether it was due to cell cycle arrest and/or cell death induction. Given that survivin exerts a pro-mitotic activity, we evaluated the effect of AM on cell cycle progression in A549 cells. Treatment of A549 by AM at 24 h showed a clear and significant cell cycle arrest, compared to control cells (Fig. 4B). Notably, AM was able to decrease

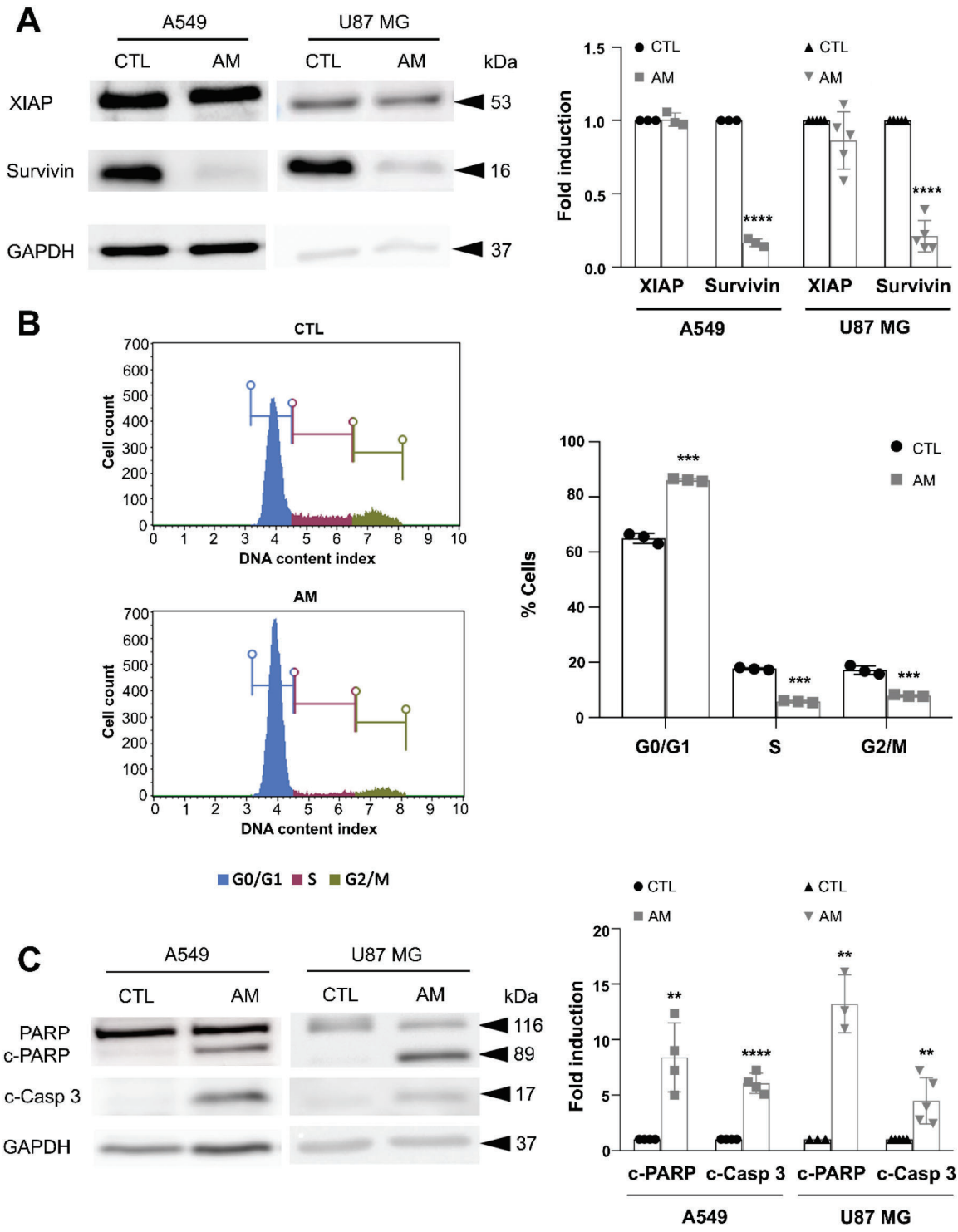

Fig. 4. AM decreases survivin levels in vitro, impairs the cell cycle and promotes apoptosis. After 24 h of treatment with the IC_{50} concentration of AM, the expression of survivin and XIAP was analyzed by Western Blot analysis in A549 and U87 MG cell lines (A). AM effect on cell cycle was analyzed in the A549 cell line after 24 h of treatment with AM at IC_{50} concentration by flow cytometry (B). AM effect on the expression of apoptotic proteins in A549 and U87 MG cells previously treated with the IC_{50} of AM for 24 h was measured by Western Blot (C). Protein levels were normalized with their respective loading controls. Results were obtained from at least three independent experiments. Bars represent the mean ± SD. CTL: control. Statistically significant results are indicated as * *, p-value < 0.01; * ** , p-value < 0.001; * ** *, p-value < 0.0001.

the percentage of cells in both S and G2/M phases and increase it in the G0/G1 phase. However, as survivin can elicit an anti-apoptotic function, we evaluated whether AM triggers apoptosis in A549 and U87 MG cells. Our results show a significant cleavage of PARP-1 and caspase 3 after 24 h of AM treatment in both cell lines, corroborating apoptotic induction (Fig. 4C). Finally, immunogenic cell death (ICD) was also analyzed to evaluate whether AM could induce an adaptive immune response against dying or stressed cells that release damage-associated molecular patterns (DAMPs). Therefore, we measured the exposure and release of DAMPs (CALR; ATP; HMGB1) in cells treated with AM to

evaluate the potential induction of ICD by this compound (Fig. 5). AM significantly increased CALR exposure, the most characteristic signal of ICD, in A549 cells treated with the IC_{25} concentration of AM for 24 h. In LLC1 cells (also used in further *in vivo* experiments), we observed a significant increase in CALR exposure at IC_{75} concentration. ATP and HMGB1 secretion were significantly increased in A549 cells treated with the IC_{75} concentration of AM. Our results suggest that AM may induce ICD in A549 and LLC1 cells, because it can increase externalization and release of DAMPs, leading to an expected potential stronger activation of immune response *in vivo*.

Altogether, AM was able to specifically inhibit survivin levels as well as to promote cell cycle arrest, activate apoptosis, and trigger ICD.

3.5. In vivo safety evaluation

To evaluate AM safety *in vivo* and determine the optimal dose for efficacy studies, three different doses of AM (10, 15, and 20 mg/kg) or vehicle were administered intraperitoneally to C57BL/6 mice, following a schedule of five consecutive days per week. Although mice lost some weight during the first two days of each cycle, they all recovered and did not show any differences compared to the control mice's weights at the end of the experiment (Fig. 6A). However, mice showed transient mild secondary effects at higher doses, such as low motility after drug administration, compatible with sedation or somnolence effects typically induced by antipsychotic drugs (i.e. Asenapine). Vital organs did not present macroscopic differences when comparing all groups and no significant organ weight changes were detected among groups (Fig. 6B). Moreover, the alanine aminotransferase (ALT) activity assay showed that AM did not cause hepatocellular injury at the tested doses (Fig. 6C). At the microscopic level (Fig. 6D), vital organs (liver, kidney, and brain) did not present detectable structural alterations, indicating that administered doses are well tolerated.

3.6. In vivo therapeutic efficacy evaluation

We generated a subcutaneous tumor model in mice by inoculating 5×10^4 LLC1 cells in the flank of C57BL/6 mice. Once the tumor reached the volume of 40 mm^3, AM was intraperitoneally administered over 5 consecutive days per week for three weeks. The weight evolution of treated mice was similar to the control group (Fig. 7A). On the other hand, tumors of treated mice grew slower and weighed less than those in the non-treated control group (Fig. 7B, C, and G), suggesting that AM impairs tumor growth at 10 mg/kg. Moreover, we confirmed the effect of AM on survivin by evaluating the expression of survivin in the tumors, observing that AM reached and efficiently downregulated survivin levels in the tumors (Fig. 7H).

To corroborate AM anticancer effects in human cancer cells, subcutaneous tumors of A549 cells were induced in immunodeficient NSG mice. 4×10^6 A549 cells were inoculated in each flank of the mice. Once the tumors reached approximately 150 mm^3, AM was intraperitoneally administered for 5 consecutive days per week for a total of 3 weeks. Mice weight evolution was similar in treated and non-treated groups (Fig. 7D). Tumors in AM-treated mice grew slower than those of control mice, suggesting AM impairs tumor growth after only three weeks of

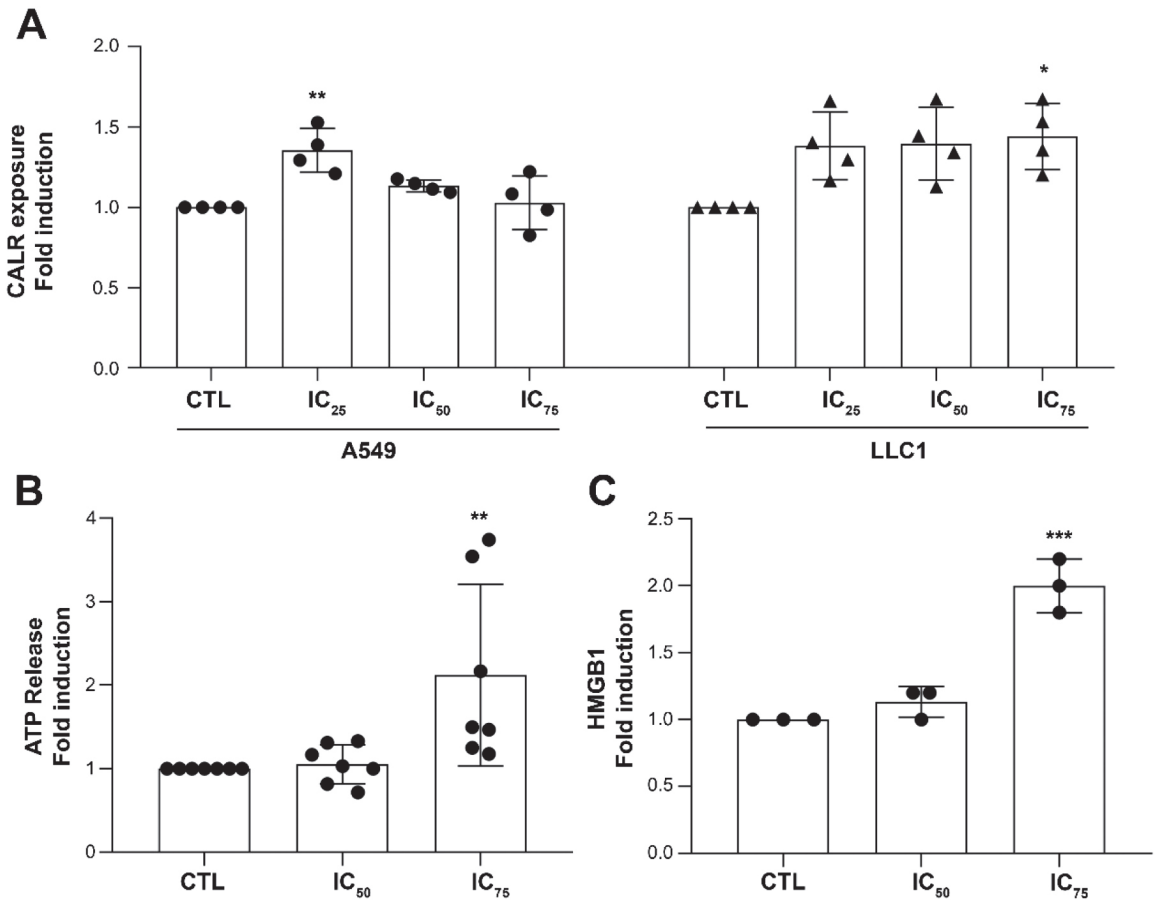

Fig. 5. AM-induced immunogenic cell death in A549 cells. Cells were treated with IC_{25}, IC_{50}, and IC_{75} concentrations of AM for 24 h. The surface exposure of CALR was determined by immunofluorescence cytometry among viable (7-Aminoactinomycin D - negative) cells (A). Culture supernatants were collected 24 h after treatment. ATP release was measured with a chemiluminescent assay in A549 cells (B). HMGB1 secretion was detected by ELISA in A549 cells (C). Results were obtained from at least three independent experiments. Bars represent the mean ± SD. Statistically significant results are indicated as * , p-value < 0.05; * *, p-value < 0.01; * ** , p-value < 0.001. CTL: control.

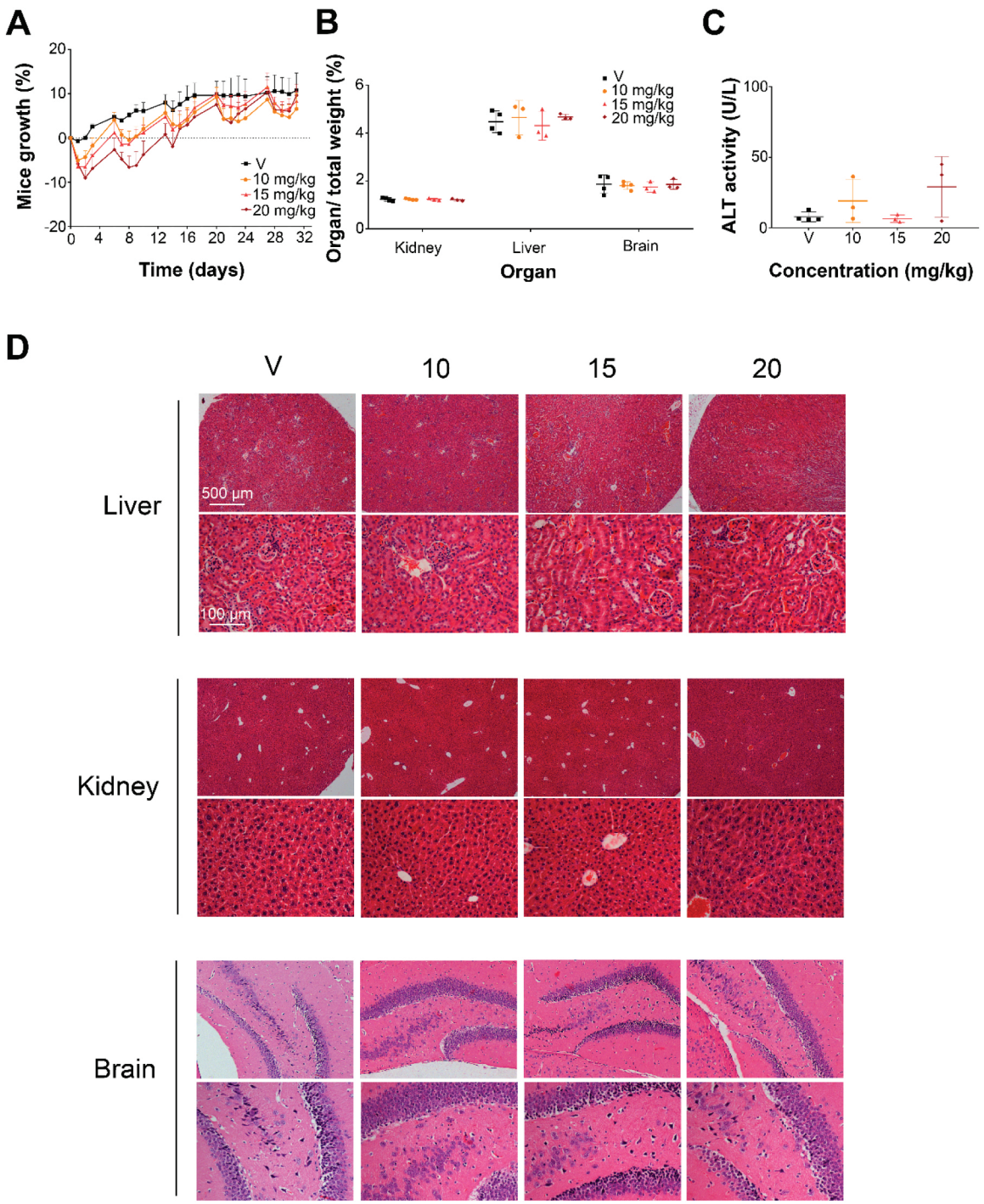

Fig. 6. In vivo safety study of AM. Mice were treated with 10, 15 and 20 mg/kg of AM for five consecutive days per week. The control group was treated with vehicle (V). Mice weights were monitored during treatment and are represented as a percentage of the weight difference with respect to the initial weight (A). Organs were weighed and represented as a percentage of the mice's weights. Results are shown as mean ± SD (B). Alanine aminotransferase (ALT) activity was measured using a colorimetric assay kit. Results are shown as mean ± SEM. (C). Representative microscopic images of the liver, kidney, and brain stained with Hematoxylin/Eosin (D).

treatment (Fig. 7E). Moreover, the tumor weight of AM-treated mice showed statistically significant differences compared to control tumors, supporting the anticancer therapeutic effect of the AM treatment (Fig. 7F).

3.7. Assessment of in vitro AM effects in combination with current chemotherapy

Our *in vivo* and *in vitro* experiments suggested that AM induces an effect diminishing tumor growth. This led us to investigate whether AM could exert a possible sensitization of cancer cells to conventional chemotherapy. Thus, to test the efficacy of AM combined with chemotherapy, we treated A549 cells with the IC_{50} concentration of AM and different concentrations of some of the most used conventional lung cancer chemotherapeutics: cisplatin, carboplatin, and gemcitabine. The IC_{50} concentration of the chemotherapeutic agent plus AM was significantly lower than monotherapy in all three combinations (Fig. 8A). We analyzed these data with the Compusyn software to elucidate the

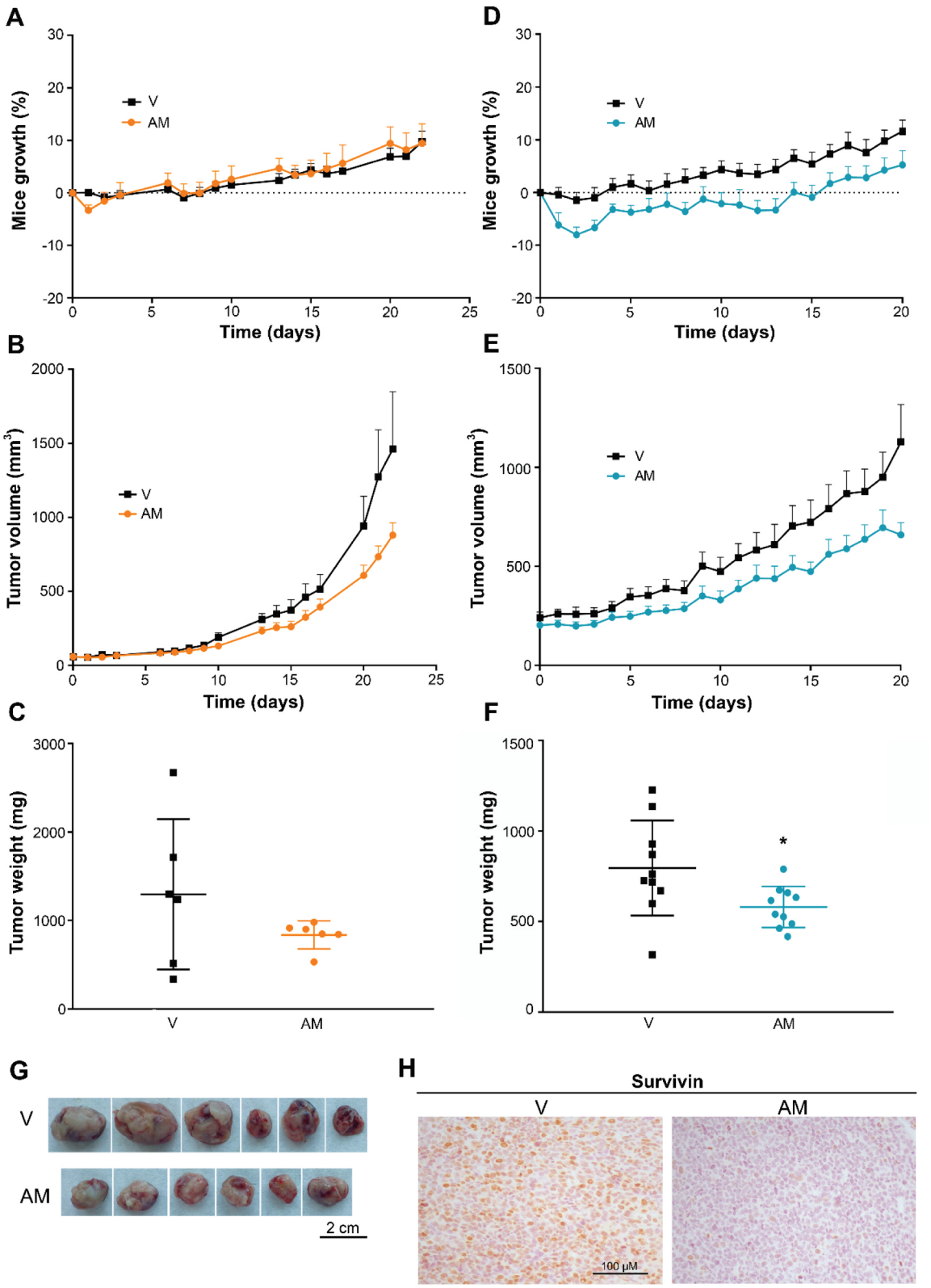

Fig. 7. In vivo efficacy study of AM in C57BL6 (A-C, G, H) and NSG mice (D-F). In the efficacy study with C57BL6 mice, animals were treated with 10 mg/kg of AM for 5 days per week. In the case of NSG mice, the dose of AM was 5 mg/kg for 5 days per week. In both experiments, the control group was treated with vehicle (V). Mice weights were monitored during treatment and represented as a weight difference, in percentage, with respect to initial weight (A, D). Tumor volume was measured during the experiment (B, E) and tumors were isolated and weighed (C, F) Results are shown as mean ± SEM (A-B and D-E) and mean ± SD (C and F). Tumors isolated from C57BL/6 mice (G). Immunohistochemistry of survivin in control (V) and AM-treated tumors of C57BL/6 mice (H).

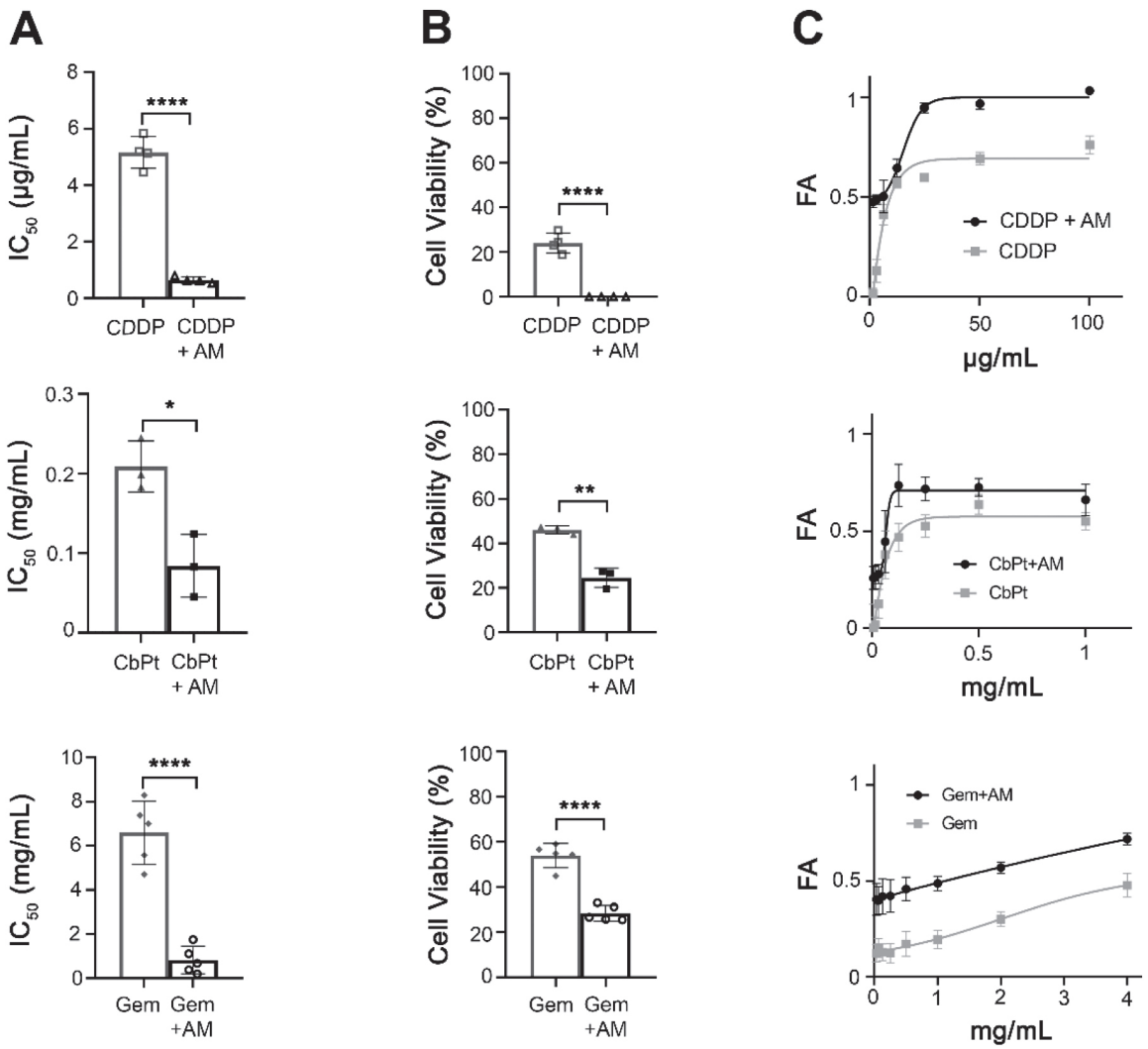

Fig. 8. Combination treatment of AM plus chemotherapeutic agents. Dose-response MTT cell viability assays treating A549 cells for 24 h with the IC_{50} concentration of AM and one chemotherapeutic: cisplatin (CDDP, concentration range of 13–100 µg/mL), carboplatin (CbPt, concentration range of 0.063–1 mg/mL) or gemcitabine (Gem, concentration range of 0.25–4 mg/mL). IC_{50} concentration of the chemotherapeutic agent alone versus the IC_{50} concentration of its combination with AM (A). Cell viability at the dose at which more synergism is shown in cells treated with chemotherapeutic monotherapy versus the combination with AM (B). Graphs representing the cell fraction affected (FA) for each condition (C). Results were obtained from at least three independent experiments. Data are shown as mean ± SD. Statistically significant results are indicated as * , p-value < 0.05; * *, p-value < 0.01; * ** *, p-value < 0.0001.

possible interaction between the chemotherapeutics and AM. We obtained combination Index (CI) below 1 in the three combinations, which correlates with additive or synergistic effects (Supplementary Table 2). For carboplatin and gemcitabine, there is a moderate synergism when combined with AM (0.7 <CI<0.85), whereas there is a stronger synergistic effect when combining AM with cisplatin (CI<0.7). To validate this finding, we selected the dose of each chemotherapeutic agent at which more synergism was observed with AM according to the CI, and compared cell viability at that dose in cells treated with the chemotherapeutic agent alone versus the combination with AM. At the same dose as the chemotherapeutic agent alone, the cell viability percentage was considerably inferior when cells were treated with the combination (Fig. 8B), confirming the Compusyn analysis. Moreover, the cellular fraction affected (FA) at different doses was much higher when cells were treated with the combination than with the chemotherapeutics alone (Fig. 8C).

Altogether, our data show that there is a synergistic effect when combining AM with any of the three conventional chemotherapeutics used in our study. This effect is especially stronger when we combine AM with cisplatin.

To elucidate the molecular mechanism of action of the AM and cisplatin combination, A549 cells were treated with the IC_{50} concentration of cisplatin and the IC_{50} concentration of AM was added after 24 h. Cytometry assays showed that apoptosis is significantly enhanced when AM is combined with cisplatin in comparison to cells treated with cisplatin alone (Fig. 9A and C), while cell cycle arrest is observed with AM monotherapy (Fig. 9B and D). To further investigate the mechanism of action, we evaluated the expression of proteins involved in apoptosis (PARP and Caspase-3) and observed that cells treated with the combination had significantly higher expression of both cleaved PARP and cleaved caspase-3 compared to cisplatin monotherapy. p53 expression is induced in cells treated with cisplatin alone and in those treated with the combination. Survivin expression was also evaluated to corroborate the effects of AM on its target (Fig. 9E). Altogether, these results suggest that AM enhances cisplatin's ability to induce apoptosis in A549 cells, while cell cycle arrest is not enhanced by the combination treatment.

3.8. *In vivo evaluation of the combination therapy*

We used the ectopic subcutaneous mouse model to assess the *in vivo*

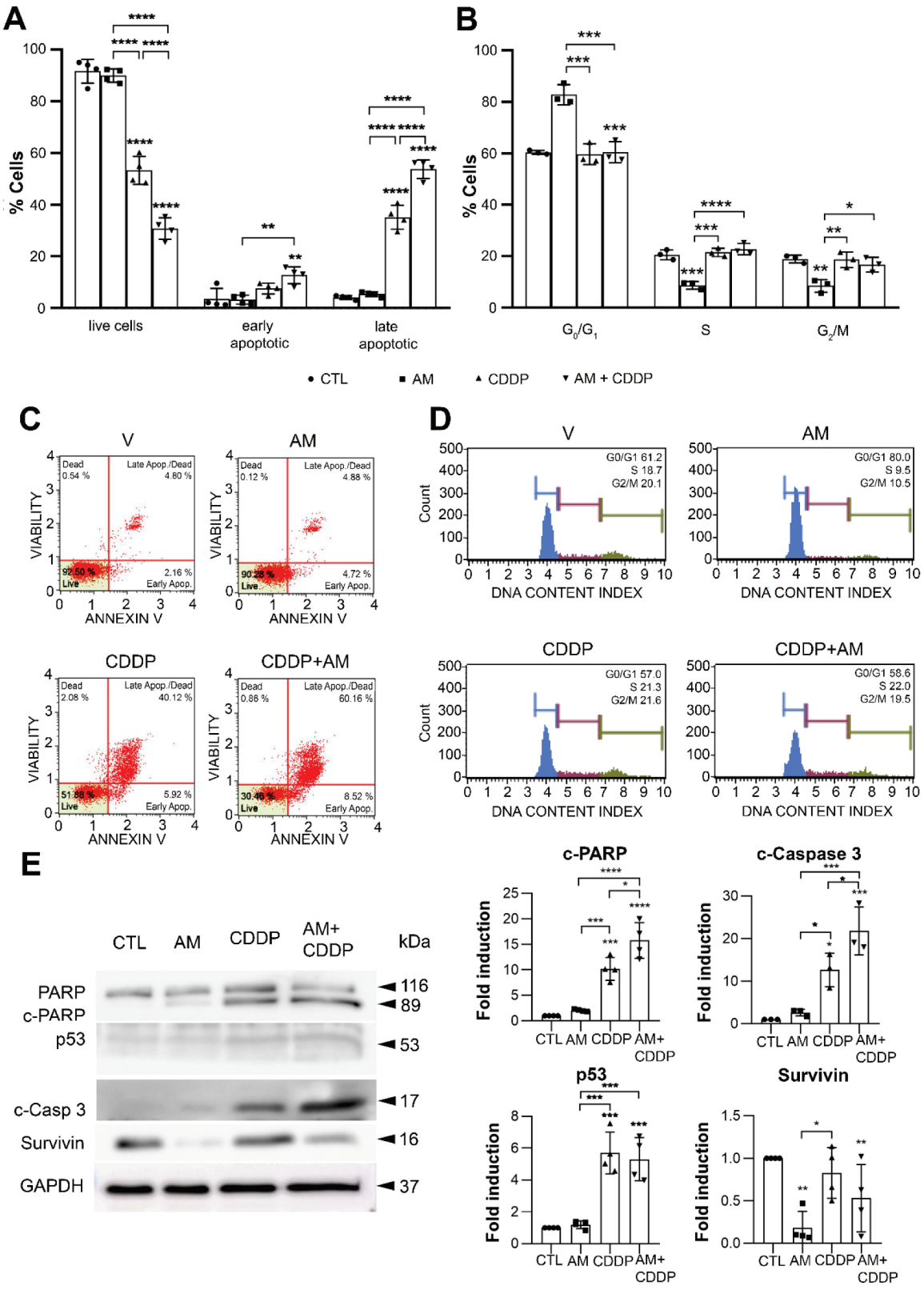

Fig. 9. The combination of cisplatin and AM increases apoptosis induction. A549 cells were treated with the IC_{50} concentration of cisplatin and, after 24 h, with the IC_{50} concentration of AM. The percentage of cell populations (Live: Annexin-/7AAD-; Early apoptosis: Annexin+/7AAD-; Late apoptosis/dead: Annexin+/7AAD+) and cells in each cell cycle phase were measured using flow cytometry (A and B). Representative cytometry graphs are shown (C and D, respectively). Results were obtained from at least three independent experiments. Bars represent the mean ± SD. Expression of apoptotic proteins in A549 cells previously treated with the IC_{50} concentration of cisplatin and AM (E). Protein levels were normalized with their respective loading controls. Statistically significant results are indicated as * , p-value < 0.05; * *, p-value < 0.01; * ** , p-value < 0.001; * ** *, p-value < 0.0001.

therapeutic efficacy of AM in combination with cisplatin. Once the tumor generated in mice reached 40 mm^3, we started with the administration of cisplatin (3 mg/kg days 0, 3, and 6). Then, we administered 5 mg/kg AM in a regimen of five days per week until the end of the experiment (18 days). In the first week of treatment, mice treated with cisplatin or the combination lost some weight, but they recovered it and by the end of the experiment mice weights were similar in all four groups (vehicle, treated with AM, treated with cisplatin, and treated with the combination) (Fig. 10A). Tumors from mice treated with cisplatin or the combination seemed to have grown slower than those from mice treated with the vehicle or AM, being tumors treated with the combination the ones showing the slowest growth (Fig. 10B). Moreover, the group treated with the combination presented the lowest tumor weight, with a significant difference compared to the control group (Fig. 10C). Isolation of tumors also allowed us to macroscopically observe the size difference among groups, especially between the control and the combination groups (Fig. 10D).

4. Discussion

Drug resistance in cancer treatment is a phenomenon in which cancer cells can tolerate pharmacological treatments. It is responsible for most cancer relapses and up to 90 % of mortality of cancer patients is attributed to drug resistance [51]. Multiple mechanisms lead to anticancer drug resistance, being cell death inhibition through the overexpression of anti-apoptotic proteins one of them [35]. Survivin is the smallest member of the IAP family. It is involved in both cell cycle promotion and apoptosis inhibition. Moreover, its low expression in normal tissue and overexpression in cancer malignancies makes survivin an ideal target for cancer therapy [32].

Among the different approaches targeting survivin, we can find oligonucleotides such as LY2181308, as well as molecules that impair gene transcription such as YM155. Moreover, interacting with the Second Mitochondria-derived Activator of Caspases (SMAC) binding site led to the development of several SMAC mimetics with anticancer activities and sensitizing effects [10], but systemic toxicities, like the cytokine release syndrome, have been detected [17]. Nevertheless, targeting the survivin homodimerization interface has been less explored and it is expected to show better results due to its specificity targeting survivin, irrespective of other IAPs.

We performed a docking-based HTVS at the homodimerization site of survivin, which led us to discover 16 drugs with high potency for survivin. After an *in vitro* evaluation of their effects on cell viability, we identified Asenapine as the drug with the highest cytotoxic effect on cancer cells and a high potency for the survivin dimerization domain. Related computational methodologies have been useful in the discovery or optimization of several marketed drugs such as imatinib, zanamivir, nelfinavir, and erdafitinib [1].

Asenapine is already used in humans as an antipsychotic agent. It is an antagonist of serotonin, dopamine, noradrenaline, and histamine. AM is sublingually administrated in cases of central nervous system disorders, such as schizophrenia and manic episodes associated with bipolar disorders [49]. Our experiments showed that AM is more cytotoxic in cancer cells than in non-cancer cells. Moreover, AM shows a more detrimental effect on cancer cell viability than Abbot23b, a survivin inhibitor that also binds to the dimer interface. The latter compound was not progressed to clinical trials, presumably due to unfavorable physicochemical properties [52]. Binding assays suggest that AM can dissociate survivin homodimers, and induces survivin degradation in cells. Other inhibitors that disrupt survivin

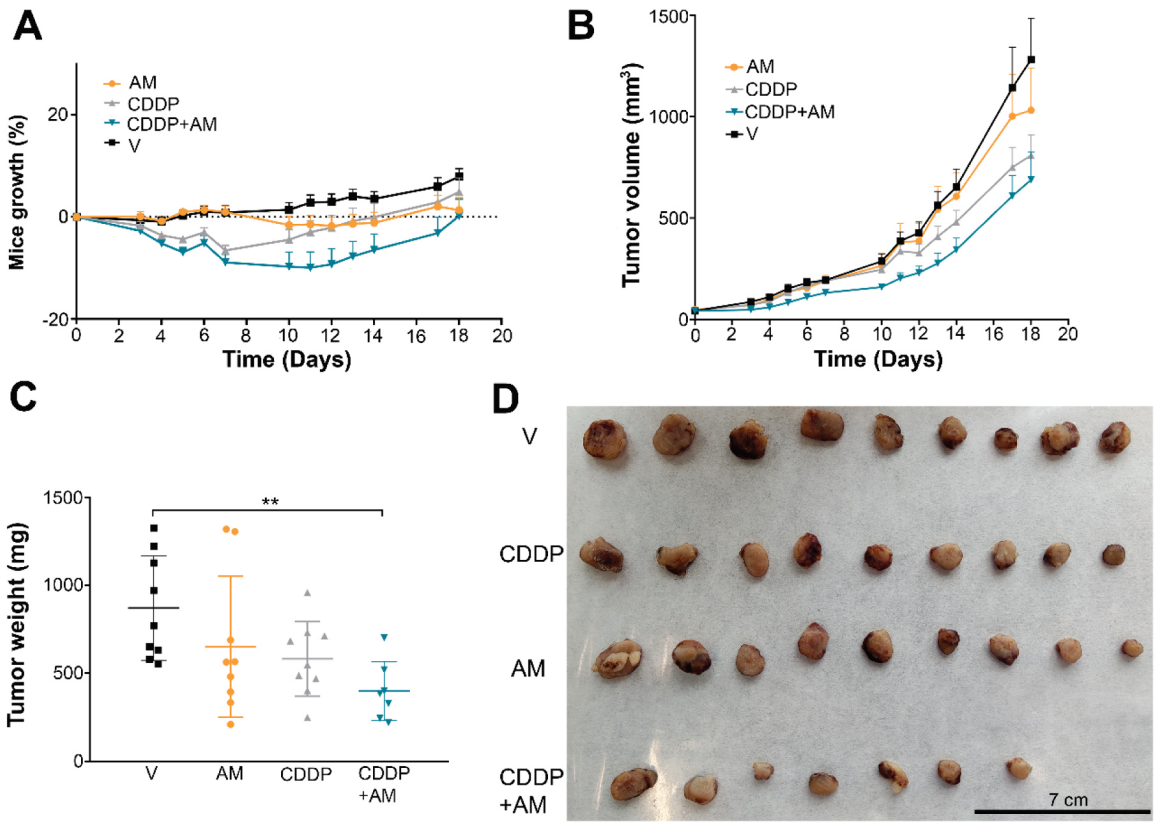

Fig. 10. In vivo efficacy study of AM and cisplatin combination. Mice were treated with 3 mg/kg of cisplatin on days 0, 3 and 6 and then mice were treated with 5 mg/kg of AM 5 days per week until the day of the sacrifice. The control group was treated with vehicle (V). Mice's weights were monitored during treatment and represented as a weight difference, in percentage, with respect to initial weight (A). Tumor volume was measured during the experiment (B) and tumors were isolated and weighed (C, D). Results are shown as mean ± SEM in the case of mice growth and tumor volume and as mean ± SD in the case of tumor weight.

homodimerization and show promising preclinical anticancer results are the experimental compounds LLP3 and LQZ-7F1 [15,41,48]. Moreover, direct inhibitors of survivin are expected to be more potent in cancer therapy than those that affect survivin transcriptional regulation (e.g. YM155) [42].

Survivin is involved in the alignment of chromosomes during prometaphase and is part of the chromosomal passenger complex [21, 26,5]. Survivin also modulates microtubule dynamics in multiple cell cycle phases [45] and has a crucial role in cytokinesis by delineating the cleavage plane [3]. AM effects observed on the cell cycle support these data since we have observed that inhibiting survivin with AM promotes a significant cell cycle arrest.

XIAP, another member of the IAP family, inhibits caspase-3, −7 and −9 [16]. Survivin can bind to SMAC, a negative regulator of XIAP. Hence, survivin promotes XIAP inhibition of caspases, which are crucial pro-apoptotic proteins. Moreover, XIAP and survivin can bind and form a complex that stabilizes both of them and synergistically inhibits caspase-9. Besides, survivin may modulate caspase-independent apoptosis by regulating nuclear translocation of apoptosis-inducing factor (AIF) [29,53]. All this data is consistent with our results, showing that a survivin inhibitor such as AM can activate apoptosis.

Furthermore, AM increases DAMPs in the tumor environment. This may lead to a higher activation of immune response *in vivo* and, thus, induction of ICD, as seen for paclitaxel [24]. The link between survivin levels and tumor immune cell infiltration is known [56], therefore, a synergy with the ICD triggered by AM in survivin-overexpressing cancer cells may exist.

Furthermore, *in vivo* experiments in mice showed that doses of AM under 20 mg/kg, administered intraperitoneally over five days per week, were not toxic. Mice presented transient low motility after drug administration, which is compatible with the most common adverse effect of AM in the clinics: somnolence, hypoesthesia, and dizziness [37]. The therapeutic efficacy assays suggest that AM impairs tumor growth in vivo. To find an optimal therapeutic strategy for patients, we combined AM with conventional chemotherapeutic agents, with cisplatin being the one that showed the highest synergism with AM. The study of the mechanism of action indicates that AM enhances the ability of cisplatin to induce apoptosis in A549 cells. Regarding the *in vivo* experiments, the combination of cisplatin and AM significantly reduced tumor growth in an ectopic mouse lung cancer model. Thus, the strategy of combining homodimerization domain survivin inhibitors with conventional chemotherapeutic agents seems promising. These results may pave the way for AM repositioning and developing more potent analogues based on AM. Other survivin inhibitors, such as the small molecule YM155, also suppressed tumor growth in combination with cisplatin in *in vivo* experiments in ovarian cancer [34] and hepatoblastoma [57].

5. Conclusions

In this work, we have identified through HTVS the antipsychotic drug Asenapine as a novel direct survivin inhibitor that binds to the homodimerization domain and shows anticancer properties. We have evidenced its anticancer effects *in vitro* as well as *in vivo*, particularly in combination with the chemotherapeutic drug cisplatin. These results may pave the way to new therapeutic strategies using Asenapine, or AM analogs, as survivin inhibitors in cancer treatment, especially in combination with other conventional chemotherapeutics.

Ethics approval statement

This study was approved by the Local Animal Experimentation Ethics Committee (Generalitat de Catalunya, protocol number 10928).

Funding statement

This research has been funded by Instituto de Salud Carlos III (Grant PI22/00256 and PI18/00441), co-funded by the European Regional Development Fund ERDF. This work has also been partially funded by Consejería de Educación de la Junta de Castilla y León and European Regional Development Fund (ERDF) (project BU067P20), the European Union's Horizon 2020 research and innovation program (BioExcel-3 101093290) and the PTQ-PTQ-16-08333 (M.K.), PTQ-2018-009992 (Y. W.) and PTQ-2018-009991 (L. D.) (Ayuda Torres Quevedo, Ministerio de Ciencia e Innovación).

CRediT authorship contribution statement

Luis Korrodi-Gregório: Writing – review & editing, Software, Methodology, Investigation, Formal analysis, Data curation. **Lucía Díaz:** Writing – review & editing, Writing – original draft, Validation, Supervision, Software, Formal analysis, Data curation. **Ana Aurora Torres:** Writing – review & editing, Methodology, Investigation, Formal analysis. **Pere Fontova:** Writing – review & editing, Writing – original draft, Software, Methodology, Investigation, Formal analysis. **María García-Valverde:** Writing – review & editing, Resources, Methodology. **Ricardo Pérez-Tomás:** Writing – review & editing, Supervision, Funding acquisition. **Robert Soliva:** Writing – review & editing, Validation, Supervision, Software, Resources, Project administration, Funding acquisition, Formal analysis, Conceptualization. **David Martínez-García:** Writing – review & editing, Software, Methodology, Investigation, Formal analysis, Data curation. **Cristina Benítez-García:** Writing – review & editing, Writing – original draft, Software, Methodology, Investigation, Formal analysis. **Roberto Quesada:** Writing – review & editing, Supervision, Resources, Funding acquisition, Conceptualization. **Marta Pérez-Hernández:** Writing – review & editing, Software, Methodology, Investigation, Formal analysis. **Vanessa Soto-Cerrato:** Writing – review & editing, Writing – original draft, Validation, Supervision, Resources, Project administration, Methodology, Funding acquisition, Formal analysis, Data curation, Conceptualization. **Martin Kotev:** Writing – review & editing, Software, Methodology, Investigation, Formal analysis. **Yvonne Westermaier:** Writing – review & editing, Writing – original draft, Software, Resources, Methodology, Investigation, Formal analysis.

Declaration of Competing Interest

The authors declare that they have no known competing financial interests or personal relationships that could have appeared to influence the work reported in this paper

Vanessa Soto-Cerrato and other co-authors had patent #PCT/EP2022/071374 pending to none **(no longer in force).**

Co-author currently employed by Nostrum Biodiscovery (**as mentioned in her affiliation**): LD Co-author previously employed by Nostrum Biodiscovery (**as mentioned in her/his affiliation**): YW, RS.

Therefore, there are no conflict of interests. If there are other authors, they declare that they have no known competing financial interests or personal relationships that could have appeared to influence the work reported in this paper

Acknowledgments

Authors thank Dr. Silvia Barceló-Batllori (Molecular Interactions Unit, IDIBELL) and Eva Sánchez (Department of Pathology and Experimental Therapeutics, Universitat of Barcelona) for technical assistance. We thank the Biology-Bellvitge Unit from Scientific and Technological Centers (CCiTUB), Universitat de Barcelona, and their staff for their support and advice. We also thank Dr. Jaume Mora (Sant Joan de Deu Hospital, Barcelona, Spain) for kindly providing some relevant materials. The authors also thank the CERCA Program, Generalitat de

Catalunya, for institutional support.

Appendix A. Supporting information

Supplementary data associated with this article can be found in the online version at doi:10.1016/j.biopha.2024.117756.

References

[1] A. Abdolmaleki, F. Shiri, J.B. Ghasemi, Use of Molecular Docking as a Decision-Making Tool in Drug Discovery. In Molecular Docking for Computer-Aided Drug Design: Fundamentals, Techniques, Resources and Applications, Academic Press, 2021, pp. 229–243, https://doi.org/10.1016/B978-0-12-822312-3.00010-2.

[2] D.C. Altieri, Survivin, versatile modulation of cell division and apoptosis in cancer, Oncogene 22 (53) (2003) 8581–8589, https://doi.org/10.1038/SJ.ONC.1207113.

[3] A. Babkoff, E. Cohen-Kfir, H. Aharon, D. Ronen, M. Rosenberg, R. Wiener, S. Ravid, A direct interaction between survivin and myosin II is required for cytokinesis, J. Cell Sci. 132 (14) (2019), https://doi.org/10.1242/JCS.233130.

[4] K.C. Bible, P.P. Peethambaram, A.L. Oberg, W. Maples, D.L. Groteluschen, M. Boente, J.K. Burton, L.C. Gomez Dahl, J.D. Tibodeau, C.R. Isham, J.L. Maguire, V. Shridhar, A.K. Kukla, K.J. Voll, M.J. Mauer, A.D. Colevas, J. Wright, L.A. Doyle, C. Erlichman, North Central Cancer Treatment Group (NCCTG), A phase 2 trial of flavopiridol (Alvocidib) and cisplatin in platin-resistant ovarian and primary peritoneal carcinoma: MC0261, Gynecol. Oncol. 127 (1) (2012) 55–62, https://doi.org/10.1016/j.ygyno.2012.05.030.

[5] A. Carvalho, M. Carmena, C. Sambade, W.C. Earnshaw, S.P. Wheatley, Survivin is required for stable checkpoint activation in taxol-treated HeLa cells, J. Cell Sci. 116 (Pt 14) (2003) 2987–2998, https://doi.org/10.1242/JCS.00612.

[6] A.M. Castro-Gamero, K.S. Borges, D.A. Moreno, V.K. Suazo, M.M. Fujinami, R. De Paula Gomes Queiroz, H.F. De Oliveira, C.G. Carlotti, C.A. Scrideli, L.G. Tone, Tetra-O-methyl nordihydroguaiaretic acid, an inhibitor of Sp1-mediated survivin transcription, induces apoptosis and acts synergistically with chemo-radiotherapy in glioblastoma cells, Investig. N. Drugs 31 (4) (2013) 858–870, https://doi.org/10.1007/S10637-012-9917-4.

[7] Y.C. Chang, C.H.A. Cheung, An updated review of smac mimetics, LCL161, birinapant, and GDC-0152 in cancer treatment, Appl. Sci. 11 (1) (2021) 335, https://doi.org/10.3390/APP11010335.

[8] X.Y. Chu, L.B. Chen, J.H. Wang, Q.S. Su, J.R. Yang, Y. Lin, L.J. Xue, X.B. Liu, X. B. Mo, Overexpression of survivin is correlated with increased invasion and metastasis of colorectal cancer, J. Surg. Oncol. 105 (6) (2012) 520–528, https://doi.org/10.1002/jso.22134.

[9] H.P. Erba, H. Sayar, M. Juckett, M. Lahn, V. Andre, S. Callies, S. Schmidt, S. Kadam, J.T. Brandt, D. Van Bockstaele, M. Andreeff, Safety and pharmacokinetics of the antisense oligonucleotide (ASO) LY2181308 as a single-agent or in combination with idarubicin and cytarabine in patients with refractory or relapsed acute myeloid leukemia (AML), Investig. N. Drugs 31 (4) (2013) 1023–1034, https://doi.org/10.1007/S10637-013-9935-X.

[10] S. Fulda, Promises and challenges of smac mimetics as cancer therapeutics, Clin. Cancer Res. Off. J. Am. Assoc. Cancer Res. 21 (22) (2015) 5030–5036, https://doi.org/10.1158/1078-0432.CCR-15-0365.

[11] N.R. Galloway, K.F. Ball, T. Stiff, N.R. Wall, Yin Yang 1 (YY1): regulation of survivin and its role in invasion and metastasis, Crit. Rev. Oncog. 22 (1–2) (2017) 23–36, https://doi.org/10.1615/CritRevOncog.2017020836.

[12] H. Garg, P. Suri, J.C. Gupta, G.P. Talwar, S. Dubey, Survivin: a unique target for tumor therapy, Cancer Cell Int. 16 (1) (2016), https://doi.org/10.1186/S12935-016-0326-1.

[13] B. Gasowska-Bajger, A. Gasowska-Bodnar, P. Knapp, L. Bodnar, Prognostic significance of survivin expression in patients with ovarian carcinoma: a meta-analysis, J. Clin. Med. 10 (4) (2021) 1–15, https://doi.org/10.3390/JCM10040879.

[14] S.A. Grossman, X. Ye, D. Peereboom, M.R. Rosenfeld, T. Mikkelsen, J.G. Supko, S. Desideri, Phase I study of terameprocol in patients with recurrent high-grade glioma, Neuro-Oncol. 14 (4) (2012) 511–517, https://doi.org/10.1093/NEUONC/NOR230.

[15] H. Guvenc, M.S. Pavlyukov, K. Joshi, H. Kurt, Y.K. Banasavadi-Siddegowda, P. Mao, C. Hong, R. Yamada, C.H. Kwon, D. Bhasin, S. Chettiar, G. Kitange, I. H. Park, J.N. Sarkaria, C. Li, M.I. Shakhparonov, I. Nakano, Impairment of glioma stem cell survival and growth by a novel inhibitor for Survivin-Ran protein complex, Clin. Cancer Res.: Off. J. Am. Assoc. Cancer Res. 19 (3) (2013) 631–642, https://doi.org/10.1158/1078-0432.CCR-12-0647.

[16] M. Hanifeh, F. Ataei, XIAP as a multifaceted molecule in cellular signaling, Apoptosis: Int. J. Program. Cell Death 27 (7–8) (2022) 441–453, https://doi.org/10.1007/S10495-022-01734-Z.

[17] J.R. Infante, E.C. Dees, A.J. Olszanski, S.V. Dhuria, S. Sen, S. Cameron, R.B. Cohen, Phase I dose-escalation study of LCL161, an oral inhibitor of apoptosis proteins inhibitor, in patients with advanced solid tumors, J. Clin. Oncol. Off. J. Am. Soc. Clin. Oncol. 32 (28) (2014) 3103–3110, https://doi.org/10.1200/JCO.2013.52.3993.

[18] J.J. Irwin, T. Sterling, M.M. Mysinger, E.S. Bolstad, R.G. Coleman, ZINC: a free tool to discover chemistry for biology, J. Chem. Inf. Model. 52 (7) (2012) 1757–1768, https://doi.org/10.1021/CI3001277.

[19] A.A. Jeyaprakash, U.R. Klein, D. Lindner, J. Ebert, E.A. Nigg, E. Conti, Structure of a Survivin-Borealin-INCENP core complex reveals how chromosomal passengers travel together, Cell 131 (2) (2007) 271–285, https://doi.org/10.1016/J.CELL.2007.07.045.

[20] M.L. Johnson, M.R. Patel, R. Aljumaily, S.F. Jones, H.A. Burris, D.R. Spigel, A phase Ib dose-escalation study of LCL161 plus oral topotecan for patients with relapsed/refractory small cell lung cancer and select gynecologic malignancies, Oncologist 28 (7) (2023), https://doi.org/10.1093/ONCOLO/OYAD029.

[21] A.E. Kelly, C. Ghenoiu, J.Z. Xue, C. Zierhut, H. Kimura, H. Funabiki, Survivin reads phosphorylated histone H3 threonine 3 to activate the mitotic kinase Aurora B, Science 330 (6001) (2010) 235–239, https://doi.org/10.1126/SCIENCE.1189505.

[22] N. Khanna, R. Dalby, M. Tan, S. Arnold, J. Stern, N. Frazer, Phase I/II clinical safety studies of terameprocol vaginal ointment, Gynecol. Oncol. 107 (3) (2007) 554–562, https://doi.org/10.1016/J.YGYNO.2007.08.074.

[23] R. Kudchadkar, S. Ernst, B. Chmielowski, B.G. Redman, J. Steinberg, A. Keating, F. Jie, C. Chen, R. Gonzalez, J. Weber, A phase 2, multicenter, open-label study of sepantronium bromide (YM155) plus docetaxel in patients with stage III (unresectable) or stage IV melanoma, Cancer Med. 4 (5) (2015) 643–650, https://doi.org/10.1002/CAM4.363.

[24] T.S. Lau, L.K.Y. Chan, G.C.W. Man, C.H. Wong, J.H.S. Lee, S.F. Yim, T.H. Cheung, I. A. McNeish, J. Kwong, Paclitaxel induces immunogenic cell death in ovarian cancer via TLR4/IKK2/SNARE-dependent exocytosis, Cancer Immunol. Res. 8 (8) (2020) 1099–1111, https://doi.org/10.1158/2326-6066.CIR-19-0616.

[25] V. Le Guilloux, P. Schmidtke, P. Tuffery, Fpocket: an open source platform for ligand pocket detection, BMC Bioinforma. 10 (2009), https://doi.org/10.1186/1471-2105-10-168.

[26] S.M.A. Lens, R.M.F. Wolthuis, R. Klompmaker, J. Kauw, R. Agami, T. Brummelkamp, G. Kops, R.H. Medema, Survivin is required for a sustained spindle checkpoint arrest in response to lack of tension, EMBO J. 22 (12) (2003) 2934–2947, https://doi.org/10.1093/EMBOJ/CDG307.

[27] Z. Li, W. Ren, Q. Zeng, S. Chen, M. Zhang, Y. Zhao, J. Cheng, X. Wang, Effects of survivin on angiogenesis in vivo and in vitro, Am. J. Transl. Res. 8 (2) (2016) 270–283.

[28] S. Li, Y. Yang, Y. Ding, X. Tang, Z. Sun, Impacts of survivin and caspase-3 on apoptosis and angiogenesis in oral cancer, Oncol. Lett. 14 (3) (2017) 3774, https://doi.org/10.3892/OL.2017.6626.

[29] T. Liu, D. Biddle, A.N. Hanks, B. Brouha, H. Yan, R.M. Lee, S.A. Leachman, D. Grossman, Activation of dual apoptotic pathways in human melanocytes and protection by survivin, J. Invest. Dermatol. 126 (10) (2006) 2247, https://doi.org/10.1038/SJ.JID.5700381.

[30] M.R. Mahmoudian-Sani, A. Alghasi, A. Saeedi-Boroujeni, A. Jalali, M. Jamshidi, A. Khodadadi, Survivin as a diagnostic and therapeutic marker for thyroid cancer, Pathol. Res. Pract. 215 (4) (2019) 619–625, https://doi.org/10.1016/J.PRP.2019.01.025.

[31] V. Margulis, Y. Lotan, S.F. Shariat, Survivin: a promising biomarker for detection and prognosis of bladder cancer, World J. Urol. 26 (1) (2008) 59–65, https://doi.org/10.1007/S00345-007-0219-Y.

[32] D. Martínez-García, N. Manero-Rupérez, R. Quesada, L. Korrodi-Gregório, V. Soto-Cerrato, Therapeutic strategies involving survivin inhibition in cancer, Med. Res. Rev. 39 (3) (2019) 887–909, https://doi.org/10.1002/MED.21547.

[33] H. Marusawa, S. ichi Matsuzawa, K. Welsh, H. Zou, R. Armstrong, I. Tamm, J. C. Reed, HBXIP functions as a cofactor of survivin in apoptosis suppression, EMBO J. 22 (11) (2003) 2729–2740, https://doi.org/10.1093/EMBOJ/CDG263.

[34] R. Mir, E. Stanzani, F. Martinez-Soler, A. Villanueva, A. Vidal, E. Condom, J. Ponce, J. Gil, A. Tortosa, P. Giménez-Bonafé, YM155 sensitizes ovarian cancer cells to cisplatin inducing apoptosis and tumor regression, Gynecol. Oncol. 132 (1) (2014) 211–220, https://doi.org/10.1016/J.YGYNO.2013.11.013.

[35] R.M. Mohammad, I. Muqbil, L. Lowe, C. Yedjou, H.Y. Hsu, L.T. Lin, M.D. Siegelin, C. Fimognari, N.B. Kumar, Q.P. Dou, H. Yang, A.K. Samadi, G.L. Russo, C. Spagnuolo, S.K. Ray, M. Chakrabarti, J.D. Morre, H.M. Coley, K. Honoki, A. S. Azmi, Broad targeting of resistance to apoptosis in cancer, Semin. Cancer Biol. 35 (0) (2015) S78, https://doi.org/10.1016/J.SEMCANCER.2015.03.001.

[36] S. Morita, H. Minami, A. Mitsuma, M. Toyoda, N. Kiyota, Y. Ando, A phase I study of LCL161, a novel oral pan-inhibitor of apoptosis protein (IAP) antagonist, in Japanese patients with advanced solid tumors. Asia-Pacific, J. Clin. Oncol. 18 (5) (2022) e427–e434, https://doi.org/10.1111/AJCO.13744.

[37] M. Musselman, J. Faden, L. Citrome, Asenapine: an atypical antipsychotic with atypical formulations, 204512532110352, Ther. Adv. Psychopharmacol. 11 (2021), https://doi.org/10.1177/20451253211035269.

[38] E. Niedzialkowska, F. Wang, P.J. Porebski, W. Minor, J.M.G. Higgins, P. T. Stukenberga, A highlights from MBoC selection: molecular basis for phosphospecific recognition of histone H3 tails by survivin paralogues at inner centromeres, Mol. Biol. Cell 23 (8) (2012) 1457, https://doi.org/10.1091/MBC.E11-11-0904.

[39] K.P. Papadopoulos, J. Lopez-Jimenez, S.E. Smith, J. Steinberg, A. Keating, C. Sasse, F. Jie, A. Thyss, A multicenter phase II study of sepantronium bromide (YM155) plus rituximab in patients with relapsed aggressive B-cell Non-Hodgkin lymphoma, Leuk. Lymphoma 57 (8) (2016) 1848–1855, https://doi.org/10.3109/10428194.2015.1113275.

[40] M.S. Pavlyukov, N.V. Antipova, M.V. Balashova, T.V. Vinogradova, E.P. Kopantzev, M.I. Shakhparonov, Survivin monomer plays an essential role in apoptosis regulation, J. Biol. Chem. 286 (26) (2011) 23296–23307, https://doi.org/10.1074/JBC.M111.237586.

[41] R. Peery, Q. Cui, K. Kyei-Baffour, S. Josephraj, C. Huang, Z. Dong, M. Dai, J. T. Zhang, J.Y. Liu, A novel survivin dimerization inhibitor without a labile hydrazone linker induces spontaneous apoptosis and synergizes with docetaxel in prostate cancer cells, Bioorg. Med. Chem. 65 (2022), https://doi.org/10.1016/J.BMC.2022.116761.

[42] J. Qi, Z. Dong, J. Liu, R.C. Peery, S. Zhang, J.Y. Liu, J.T. Zhang, Effective targeting of the survivin dimerization interface with small-molecule inhibitors, Cancer Res. 76 (2) (2016) 453–462, https://doi.org/10.1158/0008-5472.CAN-15-1874.
[43] R. Rathore, J.E. McCallum, E. Varghese, A.M. Florea, D. Büsselberg, Overcoming chemotherapy drug resistance by targeting inhibitors of apoptosis proteins (IAPs), Apoptosis 22 (7) (2017) 898–919, https://doi.org/10.1007/s10495-017-1375-1.
[44] F. Rodel, T. Sprenger, B. Kaina, T. Liersch, C. Rodel, S. Fulda, S. Hehlgans, Survivin as a prognostic/predictive marker and molecular target in cancer therapy, Curr. Med. Chem. 19 (22) (2012) 3679–3688, https://doi.org/10.2174/092986712801661040.
[45] J. Rosa, P. Canovas, A. Islam, D.C. Altieri, S.J. Doxsey, Survivin modulates microtubule dynamics and nucleation throughout the cell cycle, Mol. Biol. Cell 17 (3) (2006) 1483, https://doi.org/10.1091/MBC.E05-08-0723.
[46] C. Sgadari, B. Scoppio, O. Picconi, A. Tripiciano, F.M. Gaiani, V. Francavilla, A. Arancio, M. Campagna, C. Palladino, S. Moretti, P. Monini, L. Brambilla, B. Ensoli, Clinical efficacy of the HIV protease inhibitor indinavir in combination with chemotherapy for advanced classic kaposi sarcoma treatment: a single-arm, phase ii trial in the elderly, Cancer Res. Commun. 4 (8) (2024) 2112–2122, https://doi.org/10.1158/2767-9764.CRC-24-0102.
[47] T. Shimizu, K. Nishio, K. Sakai, I. Okamoto, K. Okamoto, M. Takeda, M. Morishita, K. Nakagawa, Phase I safety and pharmacokinetic study of YM155, a potent selective survivin inhibitor, in combination with erlotinib in patients with EGFR TKI refractory advanced non-small cell lung cancer, Cancer Chemother. Pharmacol. 86 (2) (2020) 211–219, https://doi.org/10.1007/S00280-020-04112-1.
[48] C. Steigerwald, B. Rasenberger, M. Christmann, M.T. Tomicic, Sensitization of colorectal cancer cells to irinotecan by the Survivin inhibitor LLP3 depends on XAF1 proficiency in the context of mutated p53, Arch. Toxicol. 92 (8) (2018) 2645–2648, https://doi.org/10.1007/S00204-018-2240-X.
[49] Sycrest European Medicines Agency. (n.d.). Retrieved September 19, 2023, from ⟨https://www.ema.europa.eu/en/medicines/human/EPAR/sycrest⟩.
[50] R. Tibes, K.T. McDonagh, L. Lekakis, J.M. Bogenberger, S. Kim, N. Frazer, S. Mohrland, D. Bassett, R. Garcia, K. Schroeder, V. Shanmugam, J. Carpten, R. T. Hagelstrom, C. Beaudry, D. Von Hoff, T.C. Shea, Phase I study of the novel Cdc2/CDK1 and AKT inhibitor terameprocol in patients with advanced leukemias, Investig. N. Drugs 33 (2) (2015) 389–396, https://doi.org/10.1007/S10637-014-0198-Y.
[51] X. Wang, H. Zhang, X. Chen, Drug resistance and combating drug resistance in cancer, Cancer Drug Resist. 2 (2) (2019) 141, https://doi.org/10.20517/CDR.2019.10.
[52] M.D. Wendt, C. Sun, A. Kunzer, D. Sauer, K. Sarris, E. Hoff, L. Yu, D.G. Nettesheim, J. Chen, S. Jin, K.M. Comess, Y. Fan, S.N. Anderson, B. Isaac, E.T. Olejniczak, P. J. Hajduk, S.H. Rosenberg, S.W. Elmore, Discovery of a novel small molecule binding site of human survivin, Bioorg. Med. Chem. Lett. 17 (11) (2007) 3122–3129, https://doi.org/10.1016/J.BMCL.2007.03.042.
[53] S.P. Wheatley, D.C. Altieri, Survivin at a glance, J. Cell Sci. 132 (7) (2019), https://doi.org/10.1242/JCS.223826.
[54] P. Wiechno, B.G. Somer, B. Mellado, P.L. Chłosta, J.M. Cervera Grau, D. Castellano, C. Reuter, M. Stöckle, J. Kamradt, J. Pikiel, I. Durán, S. Wedel, S. Callies, V. André, K. Hurt, J. Brown, M. Lahn, B. Heinrich, A randomised phase 2 study combining LY2181308 sodium (survivin antisense oligonucleotide) with first-line docetaxel/prednisone in patients with castration-resistant prostate cancer, Eur. Urol. 65 (3) (2014) 516–520, https://doi.org/10.1016/J.EURURO.2013.10.039.
[55] D.S. Wishart, C. Knox, A.C. Guo, S. Shrivastava, M. Hassanali, P. Stothard, Z. Chang, J. Woolsey, DrugBank: a comprehensive resource for in silico drug discovery and exploration (Database issue), Nucleic Acids Res. 34 (2006), https://doi.org/10.1093/NAR/GKJ067.
[56] L. Xu, W. Yu, H. Xiao, K. Lin, BIRC5 is a prognostic biomarker associated with tumor immune cell infiltration, Sci. Rep. 11 (1) (2021), https://doi.org/10.1038/S41598-020-79736-7.
[57] Y. Yu, X. Zhao, Y. Zhang, Y. Kang, J. Wang, Y. Liu, Antitumor activity of YM155, a selective survivin suppressant, in combination with cisplatin in hepatoblastoma, Oncol. Rep. 34 (1) (2015) 407–414, https://doi.org/10.3892/OR.2015.3947.